NASA TECHNICAL MEMORANDUM

NASA TM X-1268

NASA TM X-1268

HIGH-VACUUM TECHNOLOGY, TESTING, AND MEASUREMENT MEETING - JUNE 8-9, 1965

COMPILATION OF PAPERS

Lewis Research Center
Cleveland, Ohio

NATIONAL AERONAUTICS AND SPACE ADMINISTRATION • WASHINGTON, D. C. • AUGUST 1966

NASA TM X-1268

HIGH-VACUUM TECHNOLOGY, TESTING, AND MEASUREMENT MEETING - JUNE 8-9, 1965

COMPILATION OF PAPERS

Lewis Research Center
Cleveland, Ohio

NATIONAL AERONAUTICS AND SPACE ADMINISTRATION

For sale by the Clearinghouse for Federal Scientific and Technical Information
Springfield, Virginia 22151 – Price $6.00

CONTENTS

Chairman's Summary

Mason T. Charak
NASA Headquarters

The overall purpose for this meeting, sponsored by the Office of Advanced Research and Technology, was to exchange and review technical information on NASA's in-house and contract efforts in high-vacuum simulation, experimentation and measurement. Specific objectives were: To identify current and planned research and technology programs; to describe new developments in vacuum facilities and diagnostic instrumentation; to discuss testing techniques and experiences including safety aspects; and to highlight problems requiring attention.

Attendance at this meeting was limited to representatives of NASA Centers and Headquarters so that informal and open discussions could occur. These proceedings are the written record of the papers presented and thus furnish a good cross section of vacuum technology activities in NASA. For many reasons, not all of NASA's work associated with high vacuum was discussed; for example, there is considerable activity in the materials research area involving basic vacuum effects which were not reported.

In general, the papers and related discussions showed that NASA's vacuum programs are growing rapidly. Increasing numbers of engineers, scientists, and technicians—involved in research, technological, and operational problems - are using more and more vacuum facilities for tests. However, to complement the experimental program, additional theoretical studies are required to insure a better understanding of basic vacuum properties and effects.

To guide possible future meetings in vacuum technology, the consensus was that concurrent specialist groups in such areas as mass spectrometry, man-rating, etc. should also meet.

By: James B. Stephens
JPL

Space Simulators and Facility Engineering

A. Space Molecular Sink Research Laboratory

1. Cryogenic Quartz Crystal Microbalance

A quartz crystal vibrating in a thickness shear mode as illustrated in Fig. 1 is frequency sensitive in a linear fashion to changes in mass and can thus measure the rate at which a molecular flux condenses upon its surface at a particular temperature. Devices based upon this principle have been used in the Facilities Research Group in the following manner.

A 5 MC $\pm$ 1KC, 0.500 in. dia., beveled quartz crystal, A-T cut at 39° 49' $\pm$ 15", mounted on an untinned standard HC-6 spring clip base, Fig. 2, was high temperature soldered at a liquid nitrogen cooled, reservoir fed, holder as shown in Fig. 3. The low capacatance (100pf) leads are fed through a flange to a 5 MC vacuum tube oscillator, Fig. 4, (International Crystal Company, Model FO-11, Cat. No. 200-130) which is mounted adjacent to the flange. The leads are restrained to prevent mechanical vibration since a change of .10 pf will cause a spurious frequency shift of 1 cps.

A standard 100 MC electronic counter, digital-to-analog converter, and strip chart recorder are used to monitor and record the output of the oscillator. A manual or automatic stepping R-F switch is used when multiple crystals are monitored. All oscillators should remain on to avoid warm-up transients.

Sensitivities as high as 1 x 10^{-10} gm/cm^2 (a gas monolayer is approximately 10^{-8} gm/cm^2) can be achieved by operating the crystal at the

temperature at which changes in temperature produce small changes in frequency (turnover point). The turnover point of a crystal can be adjusted by the angle at which it is cut (39^{o} 49' for a crystal mounted on the liquid nitrogen cooled holder of Fig. 3). Figure 5 roughly plots the temperature of turnover vs. the angle of cut.

Cryogenic quartz crystal microbalances (CQCM) can be used to obtain an absolute measure of the time rate of change of the mass per unit area of a condensing molecular flux. The four crystals mounted on a holder, Fig. 3, were used to calibrate a space molecular sink simulator molecular trap array configuration(Ref. SPS 37-30 Vol. IV).

The molecular trap calibration instrument simultaneously monitors with two exposed cryo-cut crystals the condensible molecular flux (H_2O) eminating from a temperature controlled diffuser (small porous sphere in Fig. 3) and the reflected condensible flux from the moltrap array. An unexposed cryo-cut crystal and an unexposed room temperature-cut crystal are used to monitor the temperature stability of the holder.

Two crystals mounted on the bottom of the liquid nitrogen cold trap, Fig. 6, were used to monitor oil backstreaming of diffusion pumps and turbo-molecular-impact pumps. One crystal was exposed to the condensible flux and an unexposed crystal was used to monitor the temperature stability of the cold trap since filling transients took over an hour to stabilize.

A combination of a liquid helium cooled CQCM and a 300^{o}K room temperature-cut quartz crystal microbalance can be used to monitor the performance of a titanium sublimation pump. The warm crystal monitors the titanium sublimation rate and the CQCM monitors the outgassing rate of the test item. With qualitative data from a residual gas analyzer, optimum use may be made of the titanium sublimated.

Operation of quartz crystals off their turnover points provides a very sensitive, repeatable, fast but non-linear cryogenic thermometer which can be used to monitor cryopump temperatures as well as crystal holder temperatures.

This condensible molecular flux detector will prove very useful in understanding spacecraft contaminant migration and surface effect phenomenon problems.

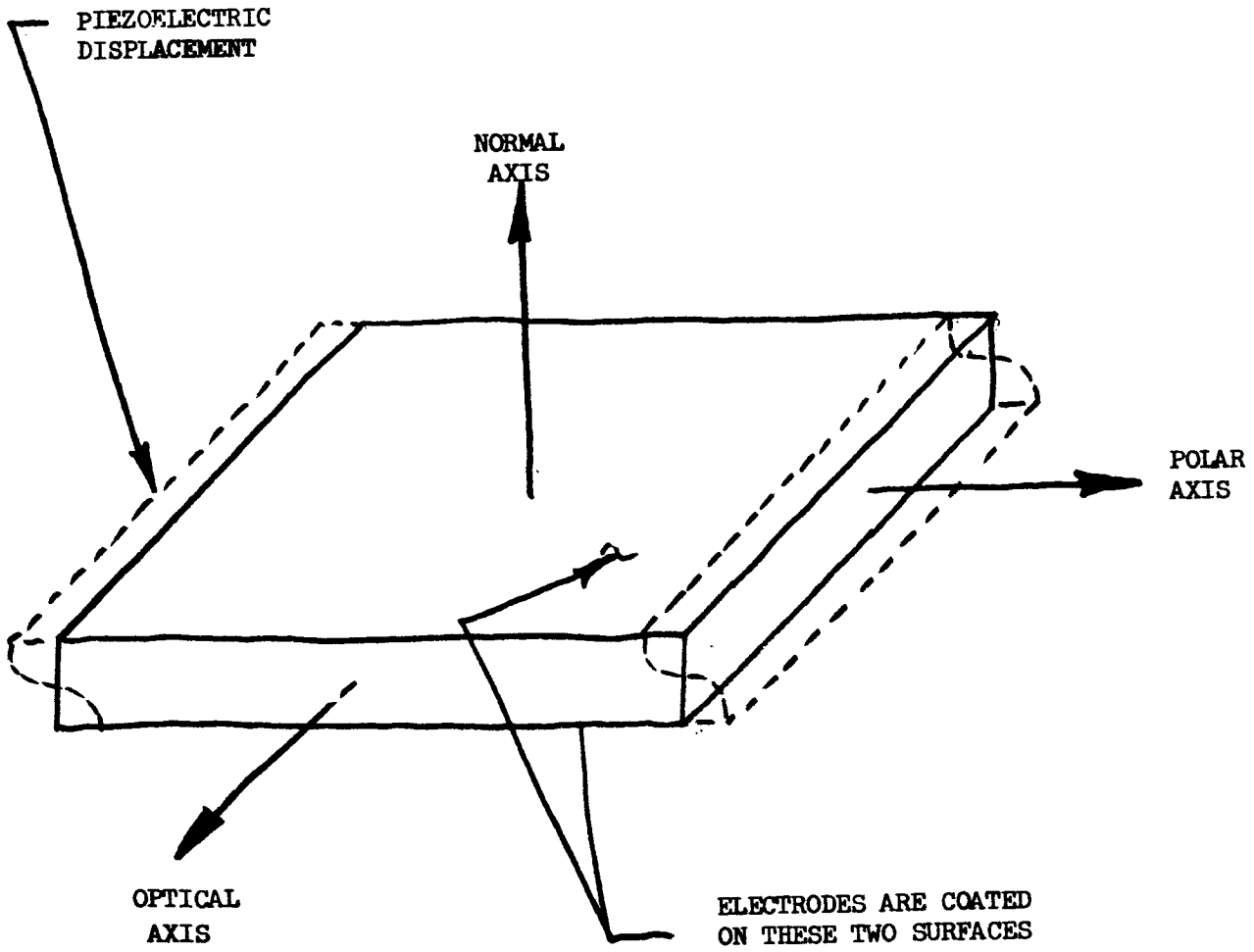

QUARTZ CRYSTAL VIBRATING IN A THICKNESS SHEAR MODE

FIG. 1

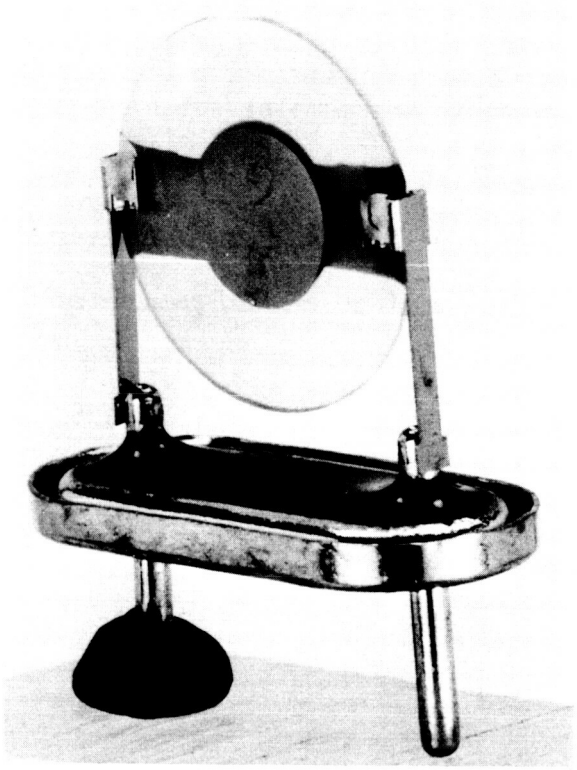

Figure 2.- Quartz Crystal.

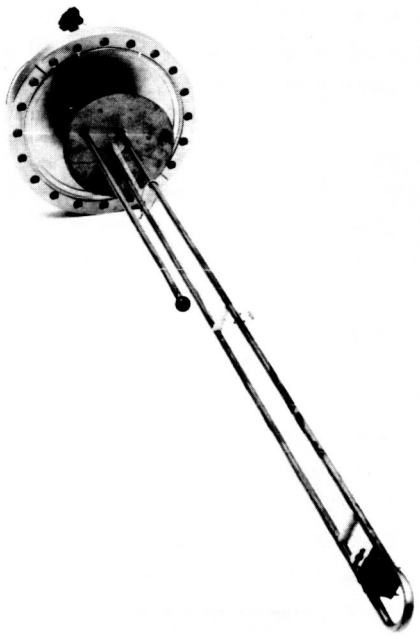

Figure 3.- Molecular Trap Calibrator.

Figure 4.- 5 MC Oscillator.

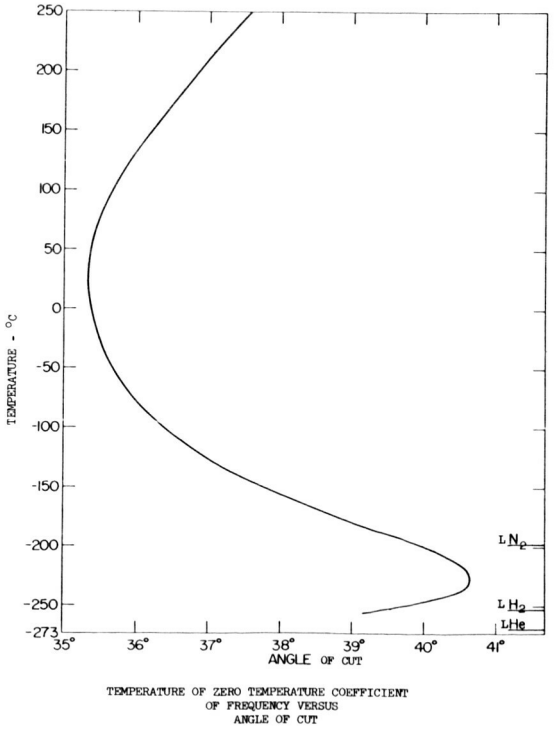

TEMPERATURE OF ZERO TEMPERATURE COEFFICIENT
OF FREQUENCY VERSUS
ANGLE OF CUT

Figure 5.

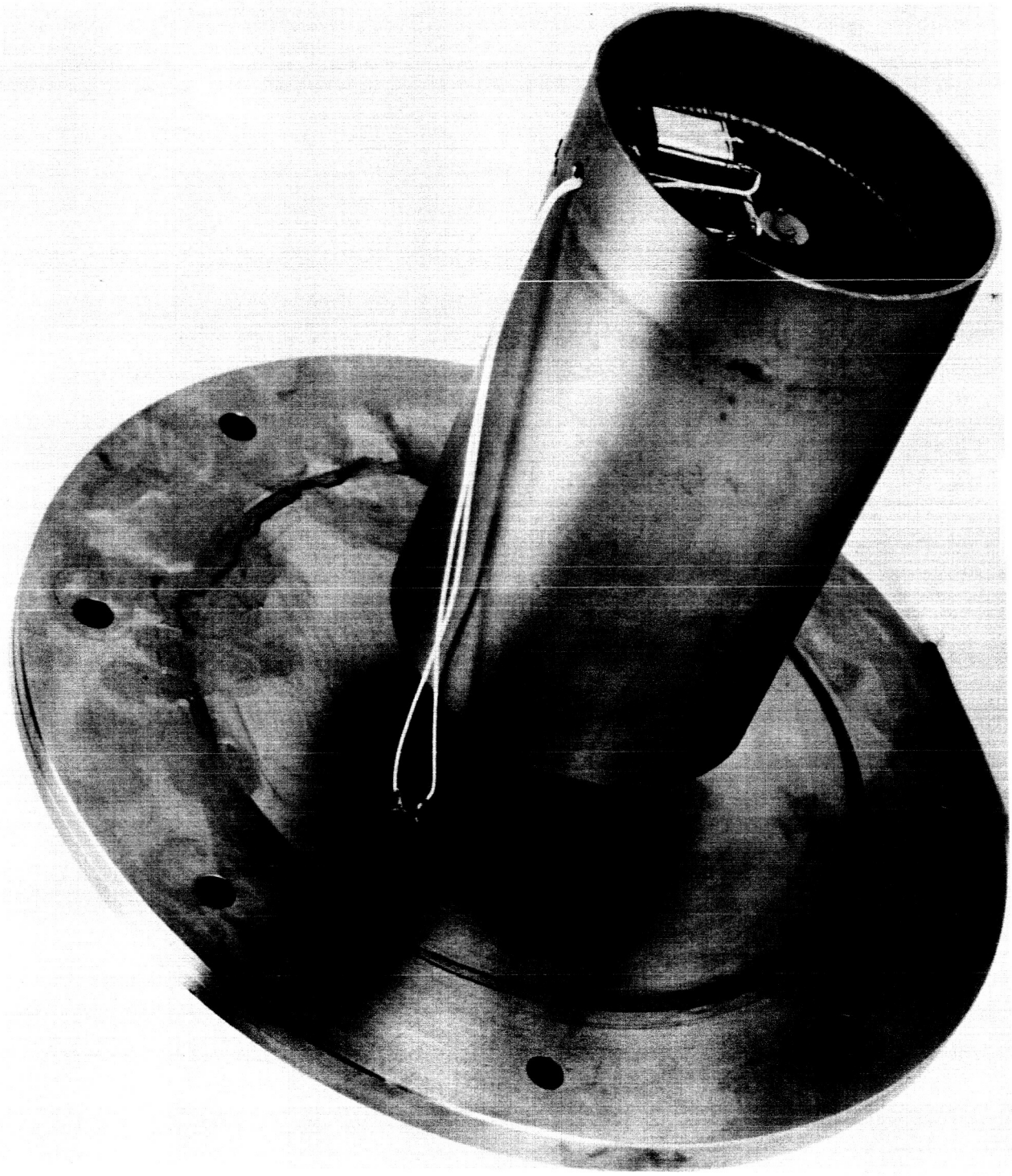

Figure 6.- Oil Backstreaming Monitor.

TECHNIQUES FOR SIMULATING THE SPACE VACUUM ENVIRONMENT

BY: William F. Hardgrove, GSFC

Introduction

The complexity of our present spacecraft experiments and the long range planning for future thermal vacuum space simulation requirements, establish the basis for the vacuum research task to be achieved under our Advanced Research and Technology program. The principal objective of the task is to establish test criteria and simulation methods that will govern the vacuum environment necessary for adequate testing of spacecraft systems, subsystems, components, and materials.

The development of thermal vacuum test criteria and simulation methods requires that one have a capability for the creation, measurement and analysis of a contamination-free ultrahigh vacuum. To achieve this capability we have divided our present work into three major categories:

1. The creation of ultrahigh vacuum.
2. Contamination measurement and control.
3. Residual gas analysis.

Ultrahigh Vacuum

One of our approaches to the creation of ultrahigh vacuum incorporates the cryosorption technique. The initial work has been well reported and I will not burden you with the details here. However, to bring you up-to-date with our present position using molecular sieve material bonded to cryogenic plates, I need to outline what has been accomplished. I will describe the vacuum unit as I proceed, but basically what we want to accomplish with the system is to provide the advantages of cryogenic pumping while possessing a reserved pumping capacity for the so-called noncondensable gases at ultrahigh vacuum. To make such a system economically attractive it is advantageous to operate at as high a cryopanel temperature as possible. We believe that the use of a cryosorption array with a conventionally cryopumped vacuum system provides these desirable features.

To utilize the cryosorption technique, we have designed and written specifications for a cryopump-cryosorption unit to be integrated into an existing simulator at Goddard. The cryopump-cryosorption array will be inserted into the test volume of the existing space simulator as shown in Figure 1. The volume between the outer two vessels is evacuated by a conventional vacuum system. The intermediate chamber is cooled with liquid nitrogen to reduce the heat load on the walls of the inner chamber that are cooled to 20°K by gaseous helium. The internal cryogenic and cryosorption arrays are presently being fabricated and will be integrated into the Goddard facility under a performance type contract. The hardware is nearly completed and is scheduled for delivery to Goddard late in July with installation and checkout to be completed in the following 30 days.

During the period being consumed by the process of getting the complete cryosorption unit fabricated and installed, we have obtained some preliminary data and operating experience using the bonded zeolite cryosorption panels. The general arrangement of the array is shown in Figure 2. The zeolite is bonded to the bottom of the cryosorption panel. The adsorbent panel is shielded by the gaseous helium cooled chevron baffle and the liquid nitrogen cooled shield and radiation baffle. The liquid helium capability shown in Figure 2 is a design feature intended for use in future experimentation for capture of helium molecules but has nothing to do with the present work with cryosorption.

Our experience with this array has not been nearly as spectacular as we had expected it would be. Data from the tests conducted with this particular array indicated that there were thermal short circuits in the system that prevented a uniform temperature distribution on the surface of the adsorbent bed (Figure 3). The non-uniformity of temperature in conjunction with an operating temperature level above 20°K due to poor heat transfer prevented pumping speed measurements for hydrogen below 10^{-8} torr. Figure 4 shows the vacuum levels obtained at the various stages of pumpdown. The electronic indications from the vacuum gauges, which were cold cathode devices, placed the ultimate vacuum obtained with this configuration between the low 10^{-11} and high 10^{-12} torr region.

We have redesigned the entire array and it is presently being fabricated in Goddard's Experimental Fabrication and Engineering Division. The unit is scheduled for installation and checkout during the month of July. Experimentation with the array will continue until the complete cryopumping-cryosorption system is ready for installation. At that time this unit will be adapted to one of our routine testing space simulators.

It is quite obvious that we are confronted with all of the difficulties one encounters with the measurement and analysis of the vacua at ultrahigh vacuum conditions. The initial vacuum gauging for the experimentation phases will include several of the various standard cold cathode gauges. At the present time we are using residual gas analysers in conjunction with our vacuum gauges. The restrictions imposed by the present instrumentation include the difficulty of sensing the environment of the test volume directly. We will use a quadrupole analyser in future experiments to eliminate the tubulation effect imposed by our present instruments.

We recently tried to secure vacuum gauge calibration services for the instruments to be used in the space simulators over the range of 10^{-3} to 10^{-14} torr. The result was non-response to the Invitation for Bid, but it did result in the submission of several proposals to fabricate calibration systems for use over the range of 10^{-3} to approximately 10^{-11} torr.

Contamination-Measurement and Control

The nature of the experiments on the more complex spacecraft create an ever-increasing concern for sources of contamination that could have a deleterious effect on the performance of the spacecraft. For example, the optics in the observatory type spacecraft and solar paddle power sources could be particularly sensitive to different forms of contamination. There must also be a concern for contamination in the space simulators that house the intricate systems for solar simulation. Vacuum pumping systems such as cryosorption are dependent on clean surfaces for maximum effectiveness. Because of this there is a reluctance to use

the zeolite panels in conjunction with an oil diffusion pumped system. The initial work with the cryosorption technique will, however, be accomplished using an oil diffusion pump. The reason for doing this is to evaluate the problems that may be associated with increasing the vacuum pumping capacity and reducing the contamination level of the first generation of space simulators by incorporating the cryosorption technique.

As there will be requirements for an oil contamination-free environment for some experimentation, there are two approaches being developed to achieve this condition. One is to have an all cryogenic system whereby we will rough out the test volume with sorption type pumps and then use cryopumping with cryosorption down to ultimate vacuum. The other method is to use ionic pumping in combination with titanium sublimation. A 3000 liter per second ion pump has been purchased and is presently being installed at Goddard prior to performance testing. The ion pump was designed to be compatible with the existing cryosorption pumped experimental chamber. The pump is a triode unit with high temperature electrical bakeout. Titanium sublimators can be added to the basic ion pump without further modification.

Contamination measurement and control is being incorporated into our space environment simulators for all spacecraft testing. The objective is to develop contamination detectors and methods for collecting contaminants during test of typical spacecraft.

Our experience has shown that contamination of the test volume of space simulators is cumulative in that one cannot entirely remove all the residual contamination from one test run to the next. For example, we know of no way to completely remove DC 704 pump fluid from the metal surfaces of the test space. The use of recommended cleaners such as trichlorethylene, acetone, Freon T.F., etc., seem to only spread the oil film thinner over a greater area. Essentially, once a facility that cannot be baked out is contaminated, all one can do under ambient conditions is to chase the oil from place to place. To alleviate this problem as much as possible, test space cleaning methods

are being investigated along with operating procedures to reduce contamination originating from the test space walls and the test item.

Preliminary samples of contaminants have been gathered under actual test conditions and infrared spectral analysis has been completed to demonstrate the feasibility of this approach. Design and construction of cold condenser plates to act as molecular traps to collect the gross contaminant load are being completed. In addition to this in-house effort, Goddard is supporting contract work that is basically a cleanliness improvement program for space simulation facilities.

We are also conducting residual gas analysis experiments to perfect the application of mass spectrometers for spacecraft test and evaluation purposes. This effort has resulted in a program to develop a reliable procedure to obtain mass spectra of typical materials used in space chambers and in construction of spacecraft. Residual gas analysers have been attached to vacuum systems and sample runs have been made. Vacuum mass spectra data will be coded for computer handling. This work should result in a data system and computer program to gather raw spectral data from test chambers and, by automatic comparison with a catalogue of spectra, will identify the materials contributing to the gas load.

Conclusion

I have described the areas of vacuum technology, and some of the experimentation we are planning under the Advanced Research Technology program.

As we approach fiscal year 1966 we are expecting that all the necessary hardware will soon be installed and the ultrahigh vacuum research chamber will become operational. After pumping capacity and basic data are established, controlled experiments will be initiated and vacuum test requirements will be explored.

Cooperative experimentation will be done in conjunction with other groups on critical materials such as spacecraft thermal coatings, exposed bearing elements, and other

surface phenomena dependent experiments. Greater emphasis will be placed on perfecting instrumentation to detect the effect of the environment during these experiments. Application of an improved spectrometer will be investigated to establish its utility as a vacuum gauge and gas analyser at extremely low pressure. The results of tests on typical spacecraft equipment will be analyzed to relate the time-temperature-pressure dependence of data. This should provide a basis for the duration and level of vacuum tests for spacecraft equipment.

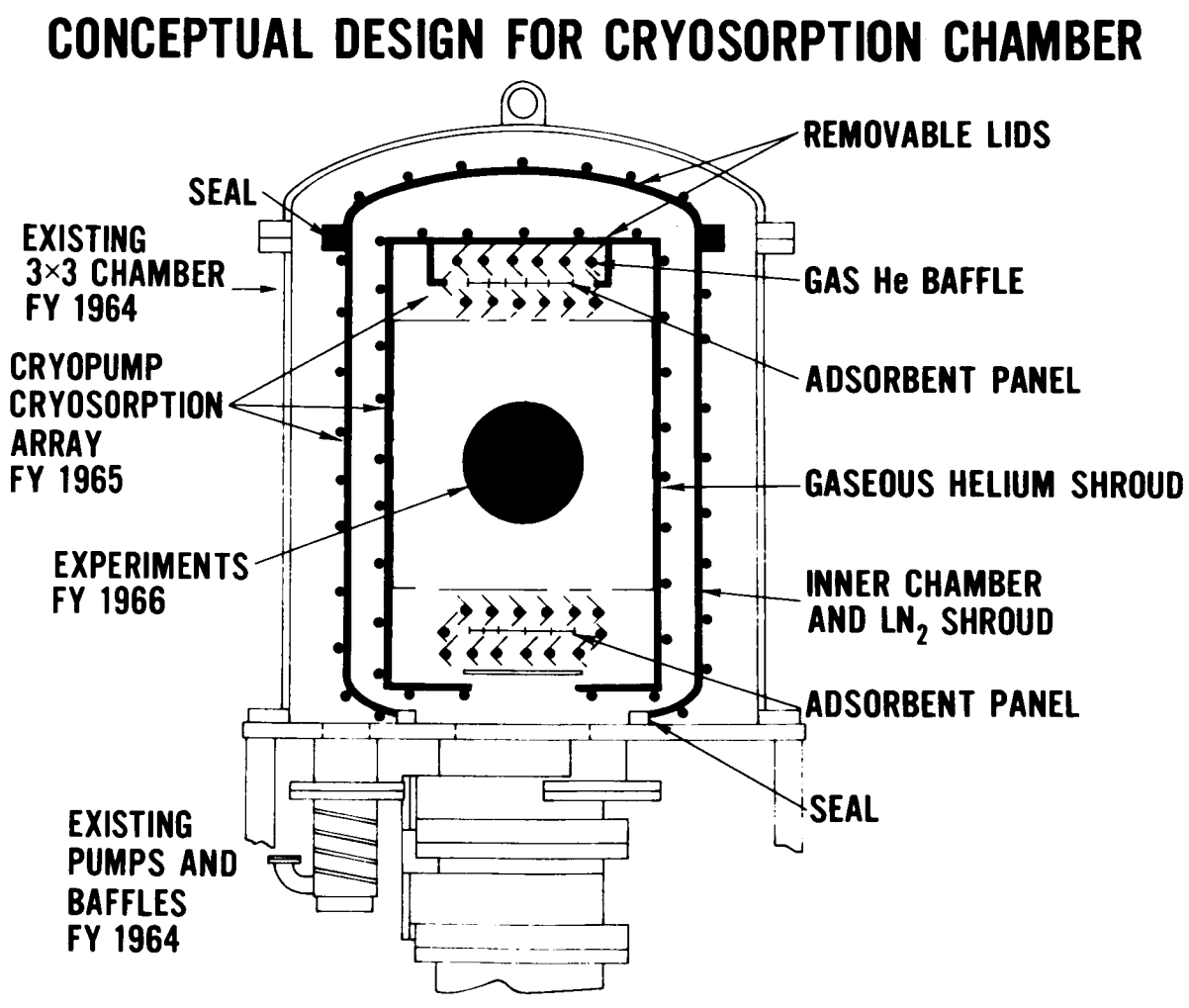

Figure 1.

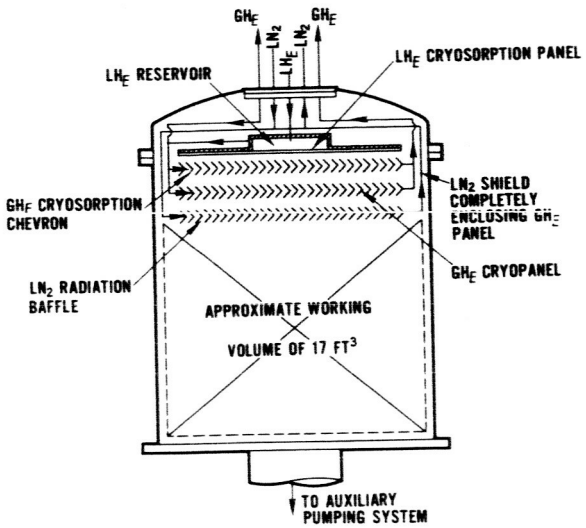

Figure 2

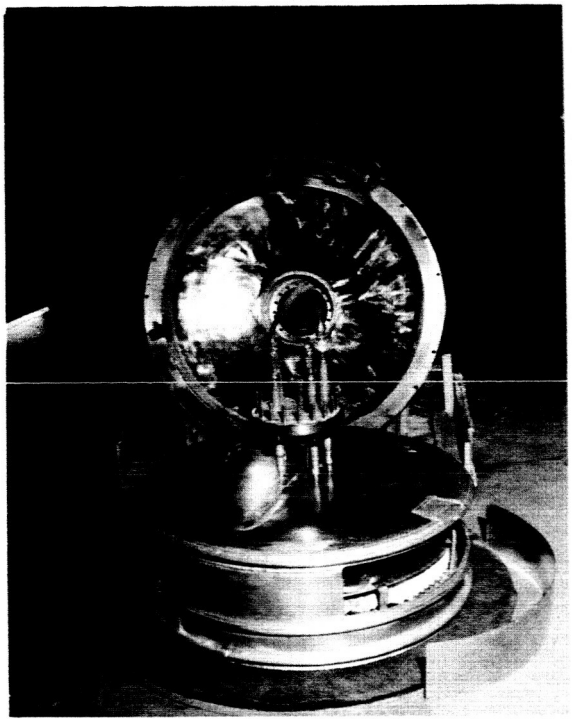

Figure 3

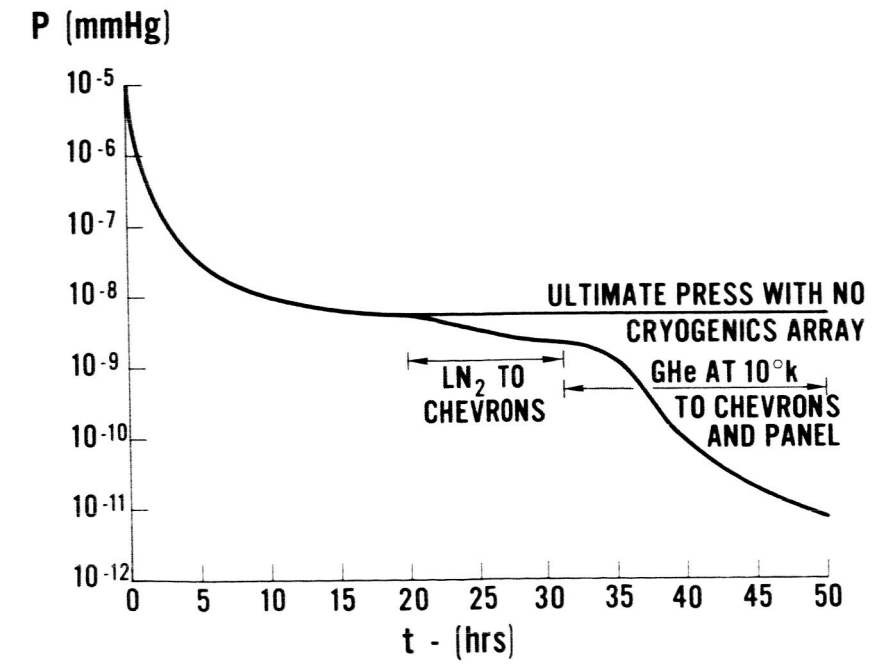

Figure 4

AN ULTRAHIGH VACUUM RESEARCH FACILITY

By James M. Bradford

NASA Langley Research Center

The design criteria and basic features of the 150-cubic-foot Space Vacuum Facility to be constructed at the Langley Research Center of the NASA were delineated at the 1963 High Vacuum Technology Review and Planning Meeting held at NASA Headquarters. Since that time the facility has progressed toward completion and it is the purpose here to give a report on the current status of the facility.

The system design is shown in figure 1. As you can see, the system is basically a triple-walled system. The outer chamber is a conventional stainless-steel vacuum system approximately 7.5 feet in diameter and 12 feet long with a full opening door at one end for access into the chamber. All of the vacuum seals on the outer chamber are crushed metal "O" rings except for the full opening door which is an elastomer "O" ring. The inner chamber is made of embossed paneling and in operation liquid nitrogen flows in the channels formed by the embossing. The inner chamber is a cylinder 6.5 feet in diameter and 8.5 feet long and is essentially vacuum tight. The space between the inner and outer chambers is pumped by a 20-inch diffusion pump. The space inside the inner chamber wall is pumped by four 35-inch diffusion pumps. Inside the inner chamber is located the helium panel. This panel is also made of the embossed paneling and in this instance liquid helium is circulated through the channels formed by the embossing. The helium panel is a cylinder approximately 5.5 feet in diameter and 7 feet long. The inside surfaces of the helium panel are coated in order to increase the absorptivity of this surface. Liquid helium for the liquid helium panel is provided by a large-capacity helium liquefier which is part of the facility.

A view of the completed facility is shown in figure 2. In it you can see the outer chamber and the door. The diffusion pumps and associated cold traps are located below the floor shown here. The control console is shown in the left part of the figure. On the control console are located the various controls necessary for the operation of the vacuum system and its associated helium liquefier. The piping shown in the center of the figure is the liquid nitrogen line to and from the inner chamber wall.

Figure 3 shows a view of the facility with the inner chamber wall installed and with the door of the inner chamber wall removed. You can see in this figure that the door does open fully to allow complete access to the interior of the vacuum vessel. The model supports are also shown in this figure. Attached to the model supports are heaters which were used in some of the acceptance tests.

In figure 4 are outlined some of the capabilities of the vacuum facility that we have measured during the acceptance tests. The normal chamber configuration is with the inner chamber and helium panel installed. In this

configuration the test volume is 150 cubic feet and the pressure attained so far is something less than 8×10^{-11} torr. A thermal load of 1.4 kW can be removed at temperatures below 5.2° K in this configuration. With the helium panel removed the test volume is 300 cubic feet and the pressure attainable is 5×10^{-10} torr. A thermal load of 10 kW can be removed at temperatures below -300° F in this mode. With the inner chamber removed the test volume is 400 cubic feet and the pressure attainable is 2×10^{-8} torr. In this configuration there are no provisions for the removal of any thermal load. You can see that the vacuum facility has flexibility and can be used in many different configurations.

At the present time the facility is essentially complete with 11 of the 12 acceptance tests having been successfully completed. The facility is scheduled for complete acceptance in the summer of 1965.

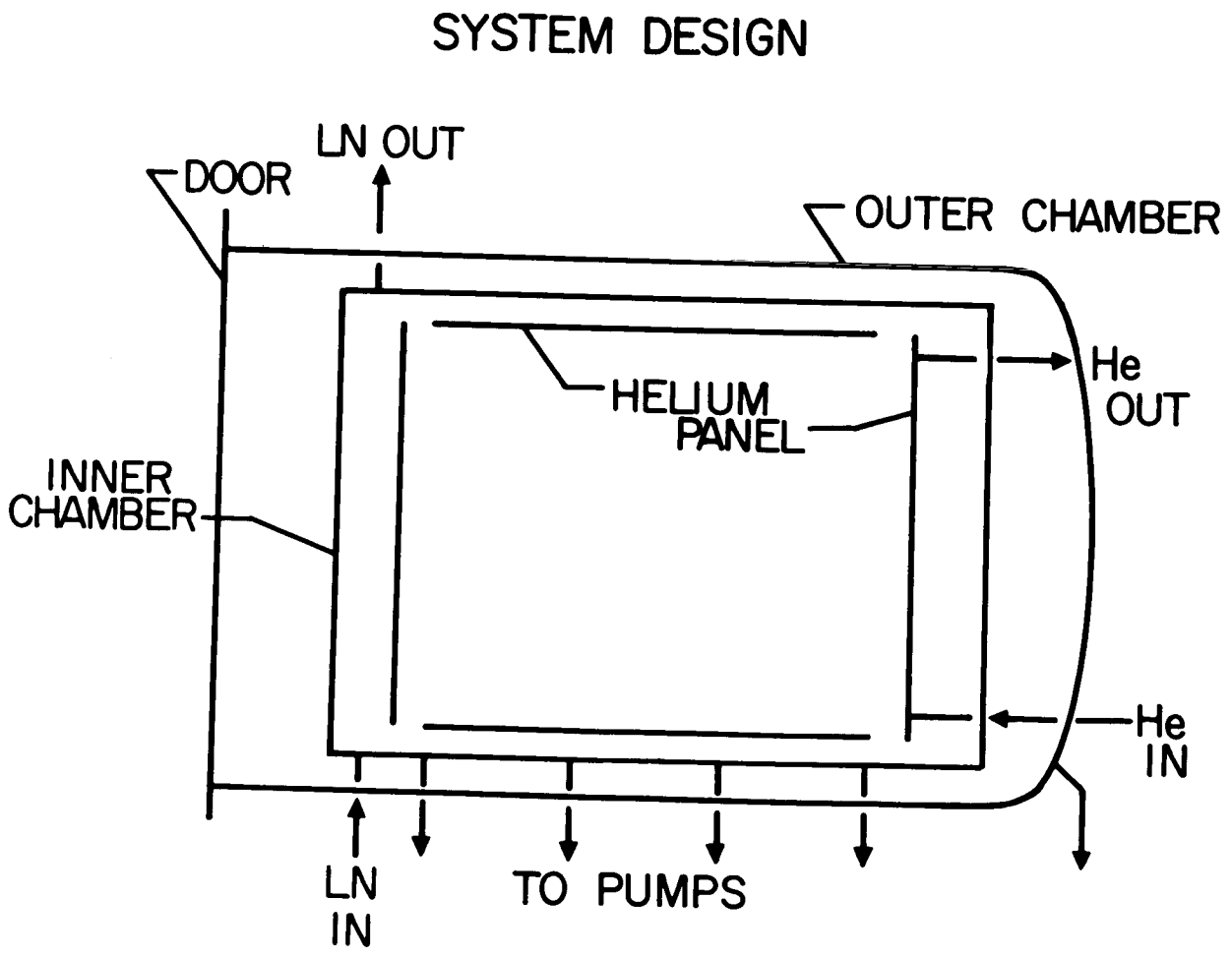

Figure 1.

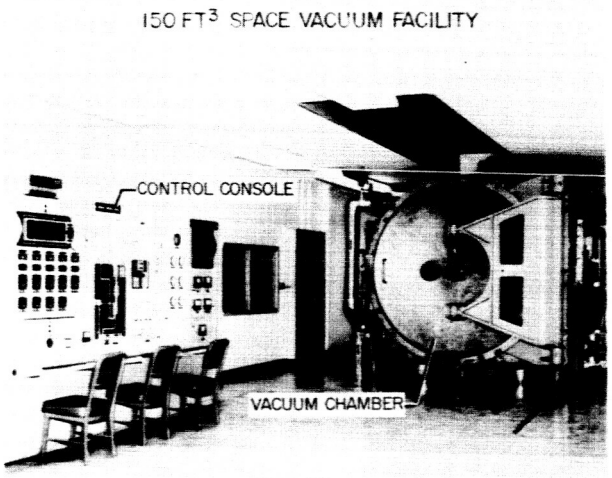

Figure 2

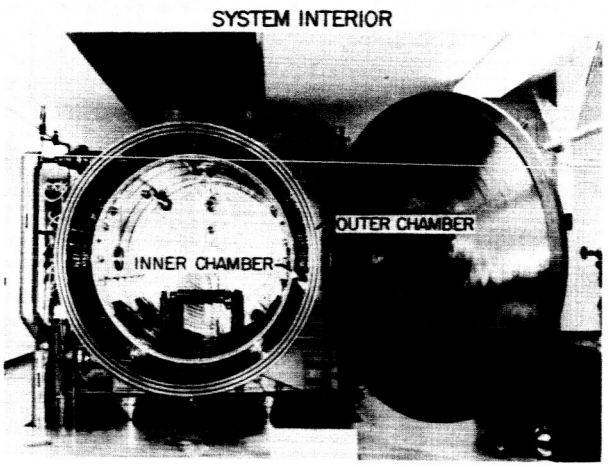

Figure 3

SYSTEM CAPABILITIES

CHAMBER CONFIG.	TEST VOLUME	PRESSURE	THERMAL LOAD
NORMAL	150 FT^3	$< 8 \times 10^{-11}$ TORR	1.4 KW
He PANEL REMOVED	300 FT^3	5×10^{-10} TORR	10 KW
INNER CHAMBER REMOVED	400 FT^3	2×10^{-8} TORR	

Figure 4

EXPERIMENTAL RESULTS OF A 1500-CUBIC-FEET UNBAKED ULTRAHIGH VACUUM SYSTEM

by T. A. Keller and G. A. Wise

Lewis Research Center

INTRODUCTION

A program was started at Lewis Research Center to convert one of its large vacuum chambers to a 10^{-10} torr vacuum system without using helium cryopumping or a bake-out system.

Ion thrustors have been operated with 20-kilovolt inputs in the existing facilities at pressures of 10^{-6} to 10^{-7} torr with no appreciable voltage breakdown problems. At present there is a program that requires the operation of a colloidial thrustor at 450 kilovolts and possibly as high as 600 kilovolts depending on the radiation shielding requirements (ref. 1). To operate this thrustor a 1500-cubic-foot facility was constructed in a test cell that was isolated with heavy concrete walls to avoid X-ray hazards. The chamber was designed to have a vacuum capability of 10^{-8} torr. Installation with the exception of the cold liner was completed in October 1964. The pressure performance specifications were met, and a mass spectrometer scan showed no evidence of diffusion pump oil in the residual gases.

Recently, a program was proposed to operate a cesium-fueled thrustor in a pressure range of 10^{-10} torr and a relatively hydrocarbon free environment to eliminate any poisoning of the tungsten emitter. The first step in achieving the desired environment was to install a low vapor pressure silicon diffusion pump oil. The initial performance tests using a mass spectrometer showed only minor peaks at 77 and 78 atomic mass units, indicating that back streaming of the oil was very low. The next step was to decrease the contribution of outgassing to the total pump load. The methods tried included decreasing the differential pressure across the 0-rings, cooling the 0-rings, and using electron bombardment of the chamber walls to clean the surfaces. Results of these modifications are presented herein.

DESCRIPTION OF FACILITY

Figure 1 is a photograph of the 1500-cubic-foot chamber showing the ports and carriage for the movable head. The chamber is 19 feet in length and 10 feet in diameter. It is made of type 304 stainless steel with 5/8-inch-thick walls. The interior wall finish ranges from 32 to 64 root mean square. There are two 36-inch ports, twelve 24-inch ports, and three 20-inch ports for access, instrumentation, or viewing. The ports are all flanged and sealed with double Buna N 0-rings with a groove between the rings for evacuating or cooling. There are 236 lineal feet of 0-ring material exposed to vacuum.

One end of the chamber is flanged and mounted on a movable carriage. This arrangement allows mounting of large thrustors or component parts in the chamber. Figure 2 is the pumping system schematic. The pumping equipment for the facility consists of four 50,000-liter-per-second oil diffusion pumps using DC 705 as the pump fluid. The diffusion pumps are backed by a 5000-cubic-foot-per-minute lobe-type blower, and this in turn is backed by a pair of 600 cubic-foot-per-minute mechanical pumps. Between the diffusion pumps and the chamber are liquid nitrogen cooled optically dense chevron type traps.

Ionization gages used were the hot-cathode Bayard-Alpert type for pressures from 10^{-3} to 10^{-8} torr and the cold cathode Redhead and the cold cathode triggered gage for 10^{-6} to 10^{-12} torr. Figure 3 shows the location of the various instruments used. Pressure measurements are made at the wall and in the center of the chamber. The mass spectrometers were located on the opposite wall of the chamber. The time-of-flight mass spectrometer was at the end port of the chamber and the magnetic deflection instrument on the middle port.

The residual gas analysis was performed with a magnetic deflection instrument for a 2 to 80 mass range and a time-of-flight instrument with a mass range of 1 to 250. Most of the data were taken with the magnetic deflection instrument. Connections to the chamber were made with large diameter, short pieces of tubing, and in the case of the time-of-flight instrument, a 4-inch vacuum valve was placed between the instrument and the chamber to allow the instrument to be maintained at a vacuum when the chamber was being vented. All data were taken after a minimum of 2 hours of operation to insure that the instruments were in equilibrium with the chamber. The time to reach equilibrium was established from previous runs. Care was taken to maintain the values of all the instrument parameters in order that the data could be comparable from run to run.

The electron bombardment cleaning probe was a 0.020-inch-diameter thoriated tungsten wire 17 feet long mounted on the horizontal centerline of the chamber. The filament wire was heated to emission temperature and then a negative bias of 2.5 kilovolts with respect to the chamber wall was applied. An average emission current of 1 ampere was maintained for a 24-hour period.

The cooling system used for the 0-rings was a simple available system to see if a more elaborate freon system would be warranted. The coolant used was a 50-50 mixture of glycol and water. This fluid was circulated with a pump through a heat exchanger that was cooled with a dry ice glycol solution, and then through the 0-ring cooling grooves. A temperature of 20^{o} to 25^{o} F was maintained on the flanges.

PERFORMANCE

Figure 4 is a typical pumpdown curve of the facility showing the time variation in pressure readings for the hot and cold cathode gages at the wall and in the center of the chamber. After a steady-state condition had been reached, 0-ring cooling was started. The pressure readings decreased appreciably with the cold cathode triggered gage in the center of the chamber reaching a value of 8×10^{-10} torr. The pressure for the triggered gage is based on a current to pressure conversion value of one ampere per torr as reported in reference 2. Figure 5 shows the minimum pumpdown time to reach the low 10^{-9} torr range. This pumpdown was performed after venting the vacuum system with gaseous nitrogen and without exposing the system to air. Other data showed no significant change in pumping characteristics when this system was vented with air. This pumpdown included 0-ring cooling after 15 hours of pumping. Total time to reach low 10^{-9} torr was 30 hours. Figure 6 is a typical mass spectrometer scan of the residual gases prior to any testing in the chamber. The peak heights were normalized at mass 18 to facilitate comparison of the two instruments. It can be seen that there is no significant difference in the distributions except for the indication of a very small leak in the time-of-flight instrument. Scans taken recently show no deviation from the scans presented herein. Particularly there are no new peaks to indicate hydrocarbon or silicon oils. Analysis of the spectrometer scans showed that cooling of the 0-rings had a negligible effect on the distribution of the mass species in the chamber. Others, as reported in reference 3, have used this technique to eliminate certain species of hydrocarbons and permeation of the 0-rings. This technique may be effective only at lower temperature (0^{o} F was used in ref. 3) than we obtained. It appears that the cooling to 20^{o} F only retarded the local outgassing of the walls in the area of the 0-rings; this consisted of 10 percent of the metal exposed to vacuum.

Evacuation between the 0-rings to lower the differential pressure gave no indication of a pressure drop in the chamber and no change in the mass spectrometer scans. Figure 7 shows the results of the attempts to clean the walls by electron bombardments. The results on the ultimate pressure and the overall characteristics were negligible.

Bombardment itself shows some very interesting behavior. Initially there is a large rise in pressure which is followed by a decrease in abundance of all species but at dif-

ferent rates. This is shown on figure 7 in the period of 3 to 4 hours after start of bombardment. The next data point 24 hours after start of bombardment shows the decrease has continued with the exception of hydrogen, which has increased by a large amount. Explanation of the large amount of hydrogen is not straightforward, since it can be derived from several sources. One source, as indicated by the increase in the methane abundance, could be the liberation and cracking of hydrocarbon products from the wall of the chamber. Another source according to reference 4 is the back diffusion of gases through the diffusion pumps.

The effectiveness of the cold traps was examined by allowing the traps to warm up. Figure 8 shows that no effects were noted until the outlet temperature of the traps was between -180° and -140° F. After this point all species showed a rapid increase in partial pressure together with the appearance of several new principal peaks at 36, 60 to 61, and 94 to 96. These new peaks are not readily identified but are assumed to be cracked products of hydrocarbons originally pumped by the traps. After recooling the traps the peaks disappeared and the mass spectra appeared as they did prior to warm up.

During the original cooling process of the 0-ring flanges an implosion occurred in the chamber. As the flanges were cooled on the two 24-inch viewing ports, stresses were set up in the glass and both windows imploded. The vacuum pumping system was shut down immediately and quick cooling of the oil diffusion pumps was started. Examination of the glass showed it had shattered to a fine sand-like material all of which was contained in the vacuum system. The diffusion pump oil, a low-viscosity silicon oil, that had been exposed to atmosphere at elevated temperatures was removed and compared with new oil by refractrometer examination. No change was apparent and the oil was filtered and replaced in the pumps, after the system was cleaned up. Subsequent pumping has shown no deterioration. Although there are no directly comparable scans before and after the implosion, it is possible to conclude that the net effect of the implosion was negligible with regard to both the species and their relative abundance in the chamber. Although the time-of-flight instrument was not available after the implosion to indicate any new mass species over 80 there were no new low mass peaks or significant increases in cracking product peaks to indicate that the chamber retained any persistant hydrocarbons or silicon oil residue. In particular, the peaks 77 and 78, which would indicate the presence of diffusion pump oils, were negligible.

FUTURE IMPROVEMENTS

The steps to be taken before any further ultimate vacuum tests are conducted will be the installation of the liquid nitrogen cooled liner and two additional oil diffusion pumps and their traps. Also a liquid nitrogen cooled propellant trap will be installed in the

foreline to keep any thrustor propellant from going into the mechanical pumps. Another possible step to reach even lower pressures is to include an oil diffusion pump in the foreline.

CONCLUSION

The tests discussed herein have shown that ultrahigh vacuums in the low 10^{-9} torr range can be obtained in large vacuum chambers (1500 cu ft) with conventional practices and without bakeout of the chamber or gages. Cooling of the 0-rings and the cleaning attempts with electron bombardment were not effective in achieving further pressure reduction. It is felt, however, that refinement of the techniques could yield an improvement of chamber ultimate pressure. With a few additional simple modifications, however, it appears that the pressures of 10^{-10} torr should be possible in the facility described.

REFERENCES

1. Norgren, C. T.: Onboard Colloidal Particle Generator for Electrostatic Engines. Progress in Astronautics and Aeronautics. Vol. 9 - Electric Propulsion Development. Academic Press, Inc., 1963, pp. 407-434.

2. Moore, R. W.: Experiments with a Liquid Helium Cryopumped Extreme High Vacuum System. Paper presented at Sixth Annual Symposium on Space Environmental Simulation, McDonnel Aircraft Corp., St. Louis (Mo.), May 17-18, 1965.

3. Farkass, Imre; and Barry, E. J.: The Origins and Composition of the Limiting Gas Load in Ultrahigh Vacuum Systems. Trans. Eighth Nat. Vacuum Symposium and Second Int. Cong. on Vacuum Sci. and Technology, vol. 1, Pergamon Press, 1961, pp. 66-72.

4. Hengevoss, J.; and Huber, W. K.: The Influence of Fore-Vacuum Conditions on Ultra-High Vacuum Pumping Systems with Oil Diffusion Pumps. Vacuum, vol. 13, no. 1, Jan. 1963, pp. 1-9.

1500 CUBIC FEET VACUUM FACILITY

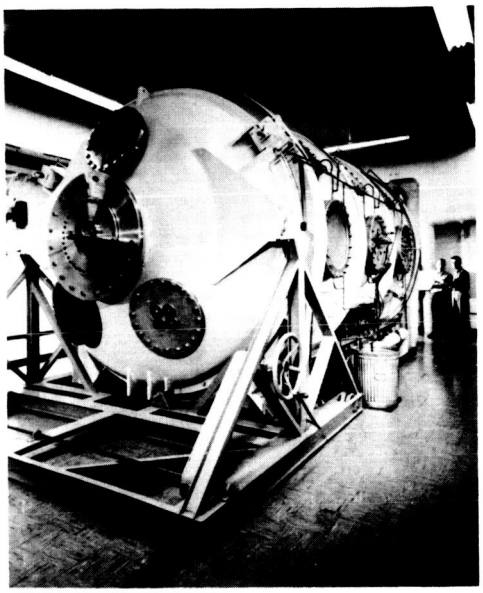

Figure 1

PUMPING SYSTEM SCHEMATIC

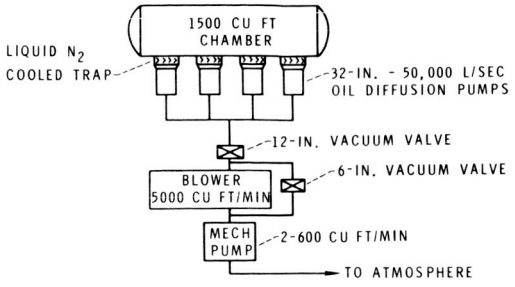

Figure 2

SCHEMATIC OF CHAMBER SHOWING INSTRUMENT LOCATION

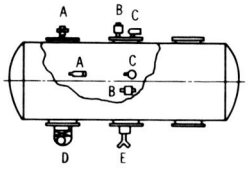

A - COLD CATHODE
B - COLD CATHODE TRIGGERED
C - BAYARD-ALPERT HOT CATHODE
D - TIME-OF-FLIGHT MASS SPECTROMETER (1-250)
E - MAGNETIC DEFLECTION MASS SPECTROMETER (2-80)

Figure 3

TYPICAL PUMPDOWN CURVE

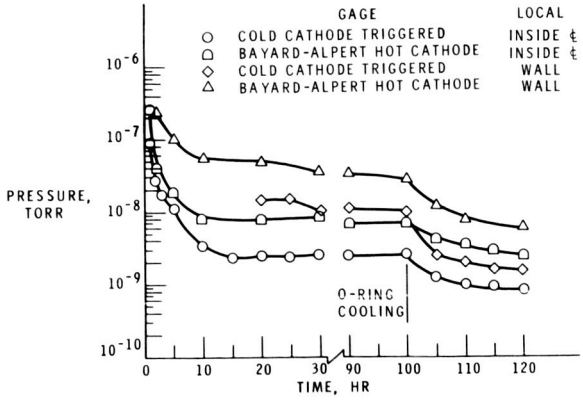

Figure 4

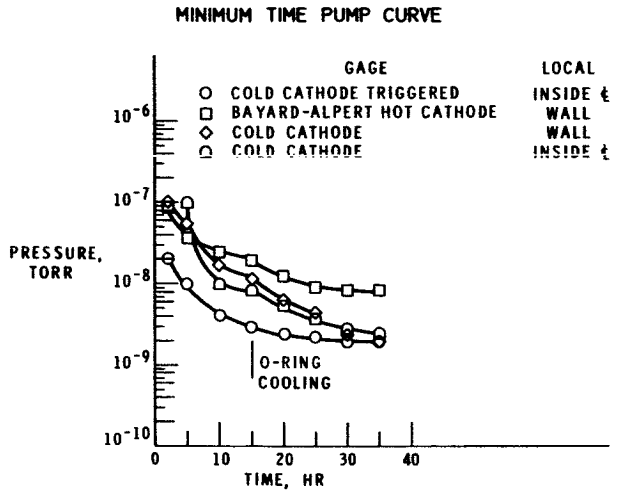

Figure 5

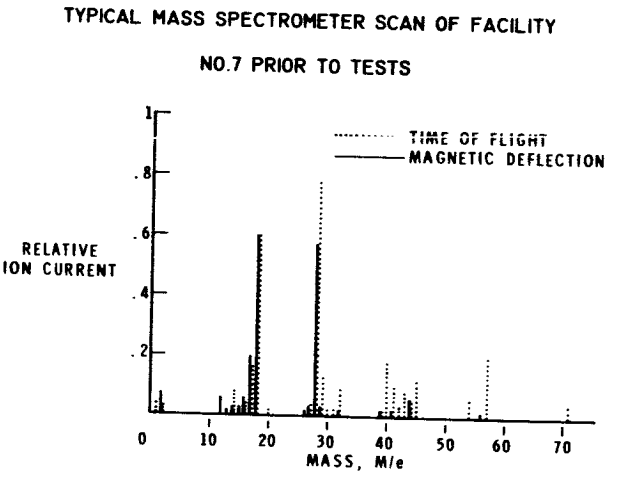

Figure 6

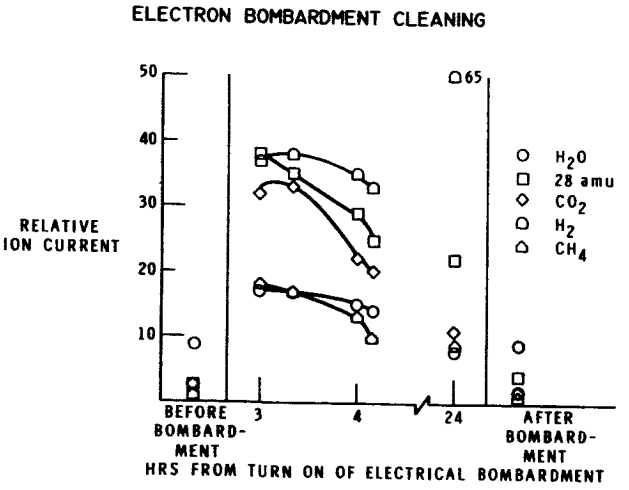

Figure 7

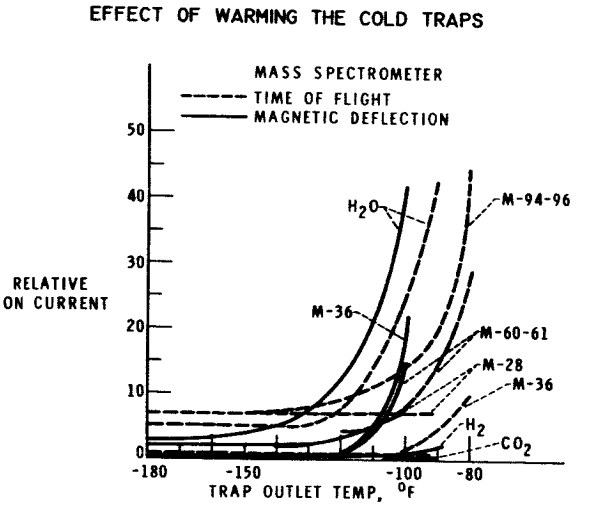

Figure 8

PRESSURE-TIME LAUNCH SIMULATOR

by Arthur D. Holmes and Charles R. Nichols

Lewis Research Center

INTRODUCTION

On July 20, 1964, an ion thrustor first operated successfully in space. The thrustor was a component of the Space Electric Rocket Test (SERT) payload. High voltage was programed to the contact ion thrustor 5 minutes after lift-off. This short time for outgassing was recognized early in the test program as a critical problem with respect to electrical breakdowns. It was apparent that there was a need for a pressure-time launch simulator tank to determine the magnitude of the electrical breakdown problem and for evaluation of design changes. The simulator, the shakedown program, and some tests that have been conducted in it are described herein.

DESCRIPTION OF LAUNCH SIMULATOR AND SHAKEDOWN TESTS

The basic simulator criteria required a sufficiently low pressure to operate an ion thrustor 5 minutes after starting a pumpdown with the complete SERT payload installed in the tank. Several configurations were considered; the design finally selected consisted of a small appendage-like tank attached to a 15-foot-diameter by 60-foot-long vacuum tank located in the Electric Propulsion Laboratory at the Lewis Research Center.

The launch simulator is shown in figure 1. Access is gained through the removable top. Three 12-inch ports are utilized as windows or for feedthroughs. The launch simulator is attached to the 15-foot-diameter tank with a 3-foot valve. Roughing pumps are tied to the launch simulator by an 8-inch line. The pumping schematic is shown in figure 2. Normally, first the 15-foot-diameter tank is pumped down to between 5×10^{-7} and 1×10^{-8} torr. The pumps on this tank remain in operation during the entire simulation. The roughing pumps are started, and simulation is initiated when the 8-inch isolation valve is opened. Speed of the first phase of the pumpdown can be varied with the number of roughing pumps utilized. Each pump has a capacity of 530 cubic feet per minute. In 1 minute, with four pumps in operation, the pressure drops to approximately 1 torr. At this pressure the roughing line isolation valve is closed and the 36-inch valve

to the 15-foot vacuum tank is opened to complete the launch simulation.

A comparison of the pressure-time variation of a spacecraft during launch with the pressure-time variation of the empty launch simulator is shown in figure 3. A pressure of 1×10^{-5} torr was observed in the center of the tank 90 seconds after the pumpdown was started. The pressure-time profiles for the spacecraft and the simulator crossed at just under 2 minutes. At the end of 7 minutes the pressure in the simulator was 1.6×10^{-6} torr. During this run the liner of the simulator was at -310° F.

Liquid nitrogen is introduced to this liner under pressure at the beginning of the pumpdown; -310° F was attained in 45 seconds. The liner configuration is shown on the drawing of the simulator (fig. 4). It covers the major portion of the bottom and side walls of the tank and is fabricated from thin copper sheets soldered to 3/4-inch copper tubing. The interior of the tank is 54 (inside diameter) by 72 inches. The inside diameter of the liner is 48 inches.

Bayard-Alpert gages were utilized to determine pressures below 1×10^{-4} torr. To determine the effect of location and possible transient effects due to the fast pumpdown, three gages were installed in the simulator: one on the wall, a second in the center of the tank, and a third in a preevacuated chamber. Prior to taking a launch simulator pressure reading, the chamber is evacuated by opening the small valve to the 15-foot tank, which was previously pumped down. The gage is activated and warmed up. A launch simulator pressure is then obtained by closing the insulation valve to the 15-foot tank and by opening the 12-inch valve to the simulator. A comparison of the three pressures observed during a pumpdown with a SERT payload installed is shown in figure 5. Outgassing of the tank accounts for the typically high wall pressure compound with that at the center. In most cases, the preevacuated chamber pressure is between the wall and center pressures. From these measurements it was concluded that the transient effects of fast evacuation were not significant. A model is normally located close to the tank center, therefore, that location was selected as the reference for this discussion.

The crossover point between the flight profile and empty tank occurred in the mid 10^{-5} torr range during the first runs. The cryogenic liner previously described was installed to improve the performance by removing condensables during the pumpdown. The effect of the liner in the empty tank is shown in figure 6. With the liner at -310° F improvements of 0.2 decade between the first points of the curves and 0.4 decade between the last points of the curves were realized.

To further improve the performance, a purge of dry nitrogen gas for varying durations prior to a pumpdown was considered. Figure 7 shows the effect of a 10-hour purge on an empty tank with the liner warm. The 10-hour purge indicated an improvement compared with no purge of 0.4 decade between the first points of the curves and 0.5 decade between the final points of the curves.

In figure 8 the effect of a nitrogen purge and liquid nitrogen cooled liner with a SERT

payload installed is compared with a no purge, warm liner pumpdown. An improvement of between 0.7 decade and 0.4 decade were realized with a cold liner and nitrogen purge. It was determined that a 1-hour nitrogen purge combined with the cold liner was more effective than the 10-hour purge.

The preceding tests determined the capabilities of the facility, and the appropriate operating procedures. They also indicated that the facility design criteria for providing operating pressures for an ion thrustor 5 minutes after start of pumpdown had been met.

TESTS CONDUCTED IN THE LAUNCH SIMULATOR TANK

Development tests on SERT flight hardware were initiated. During the end of 1963 and the first of 1964, tests were conducted to evaluate batteries, various outgassing ports on components, and the complete payload. The final test on the complete payload, shown in figure 9, was made in May 1964. The payload, which was approximately 4 feet in diameter and 3 feet in height, consisted of two ion thrustors, power supplies, telemetry and control equipment, harnesses and other related hardware. This test duplicated as precisely as possible the entire prelaunch and flight sequence. Twenty minutes prior to pumpdown warmup of payload equipment was started. The final test profile is shown in figure 10. The crossover point between flight profile and pumpdown rate was in the low 10^{-4} torr range. The programer was activated at 6 minutes and the thrustor at 7 minutes from start of pumpdown. This pumpdown was not the best simulation. It imposed a more severe environment than would be encountered in flight, but since performance of the payload was excellent the test program was concluded.

Four months after the SERT flight a nose cone failure occurred on a Mariner flight. Data indicated that the inner skin of the honeycomb shroud had failed, thus interfering with normal mission functions. The Centaur shroud was fabricated from a similar fiberglass honeycomb material. Since a Centaur flight had been scheduled for a date shortly after the Mariner failure, a test program was immediately initiated to evaluate the effects of aerodynamic heating during the first 4 minutes of flight. The Atlas-Centaur flight profile and simulator profile are shown in figure 11. The flight profile of the Atlas-Centaur was much slower than for the SERT spacecraft. Only the roughing pumping system was required for the simulation. Since this test was conducted techniques have been developed to decrease the pressure difference between the simulator and flight profile during the first minute.

The test apparatus and test specimen are shown in figure 12. A 2-foot square of fiberglass honeycomb shroud material is located approximately 5 inches in front of a quartz lamp heat bank, which is composed of thirty 500-watt lamps.

Skin temperatures during the pumpdown are shown in figure 13. The drawing on the

corner of the plot shows a section of the honeycomb material; the coating, outer skin, bond line, honeycomb core, and inner skin. The solid graph indicates the outer skin flight temperature was a maximum of 670° F. In the launch simulator the test specimen went to 690° F. The test specimen bond line temperature went to 640° F. The maximum allowable bond line temperature is 300° F. This test emphasized the marginal condition that could occur in flight. A subliming compound coating was applied to a similar specimen and the test result indicated a maximum bond line temperature of 230° F. The effect of overheating is shown in figure 14. The skin separated explosively from an uncoated honeycomb sample. The failure was caused by the difference between ambient and honeycomb cell pressure with a simultaneous weakening of the bonding agent. On the next Centaur flight,which was a success, the nose shroud was coated with a subliming compound. The ablation of the subliming compound during pumpdown is shown in figure 15. A flow of material is generated when the subliming compound acts as a heat barrier. This flow of particles could be a critical factor for some missions.

The shroud protecting the OAO payload was fabricated from a similar honeycomb material. The photograph of the craft (fig. 16) shows that several optical components are exposed to the ambient environment. A coating of foreign materials could adversely affect the mission of the flight. The subliming coating solved the thermal structural problem, but the cloud of particles generated could coat the optics. Tests are currently underway to evaluate the contamination effects of several shroud coatings. The thermal effectiveness of a subliming compound, cork, and a thin aluminum and stainless steel "shingle" are shown in figure 17. The subliming compound and cork are under the 300° F limitation, but the shingle is marginal. A comparison of flow particles from the three different specimens is shown in figure 18. An evaluation of these coatings and others is currently being conducted.

CONCLUSION

During the last 2 years over 50 research and development tests have been conducted in the launch simulator. A pressure of 2.6×10^{-5} torr has been achieved 2 minutes after start of pumpdown with a large model installed. Effectiveness of SERT payload design modifications were verified. Structural weakness of the fiberglass honeycomb nose shroud material was proved, and the utility of a subliming compound as a thermal shield was demonstrated. An evaluation of nose shroud thermal barriers with respect to contamination of optical devices is currently underway.

LAUNCH SIMULATOR

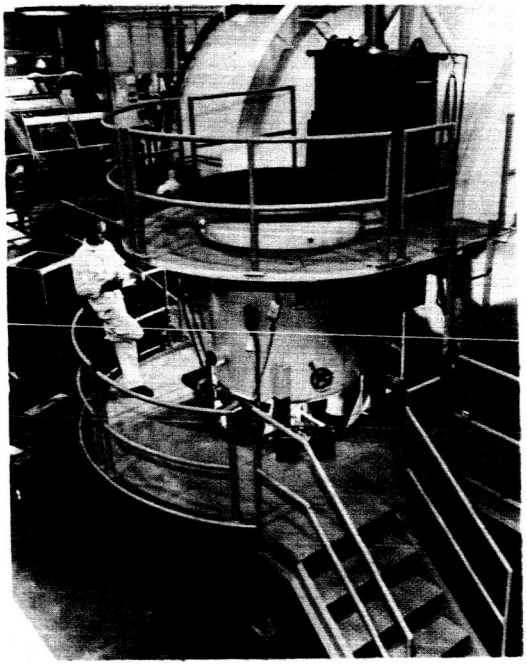

Figure 1

PUMPING SYSTEM SCHEMATIC

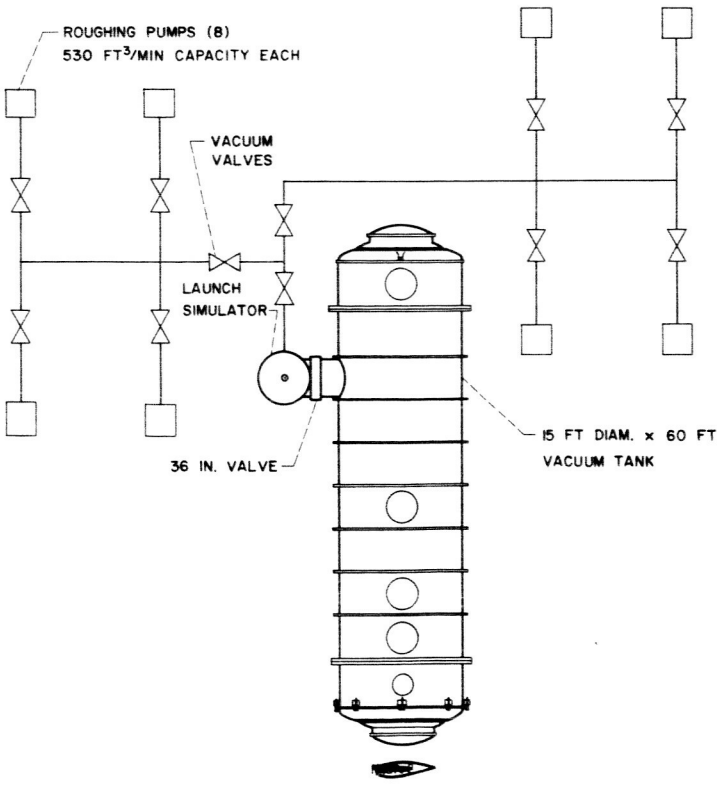

Figure 2

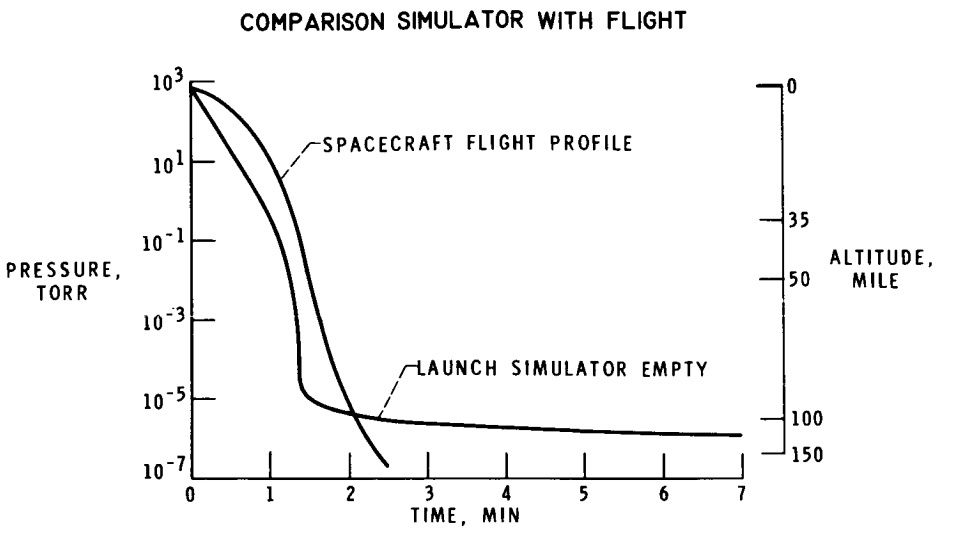

Figure 3

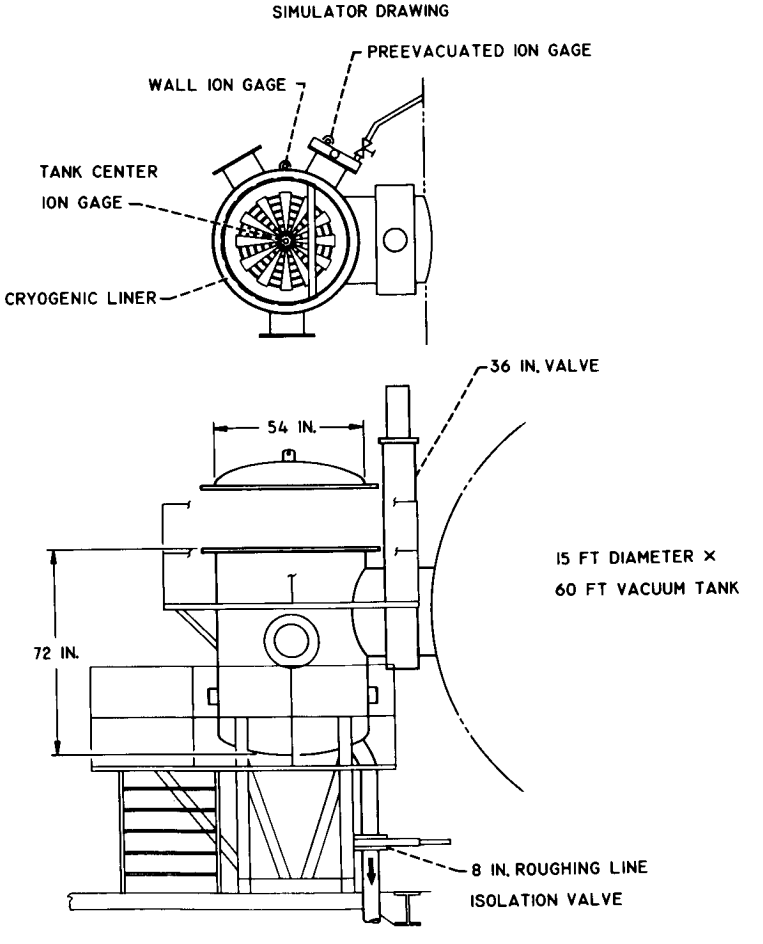

Figure 4

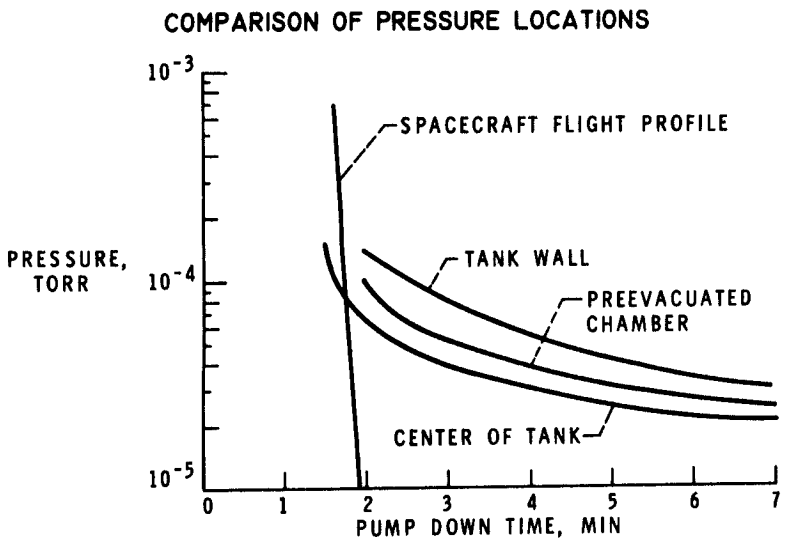

Figure 5

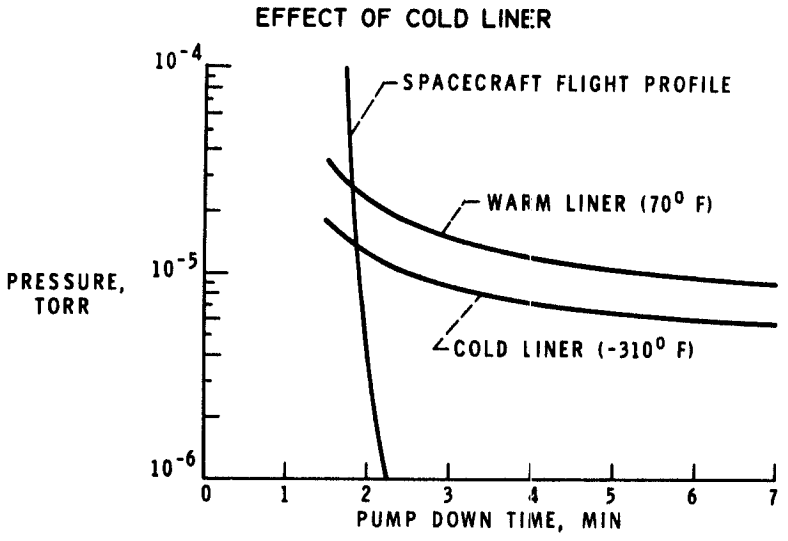

Figure 6

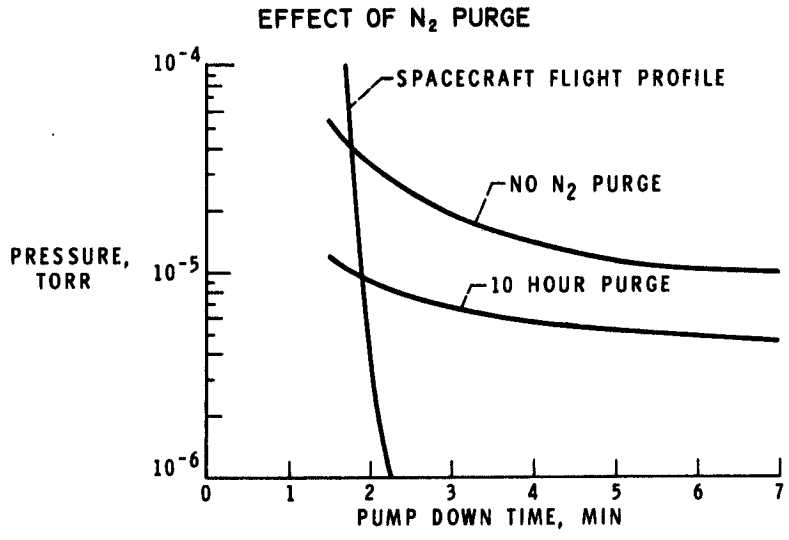

Figure 7

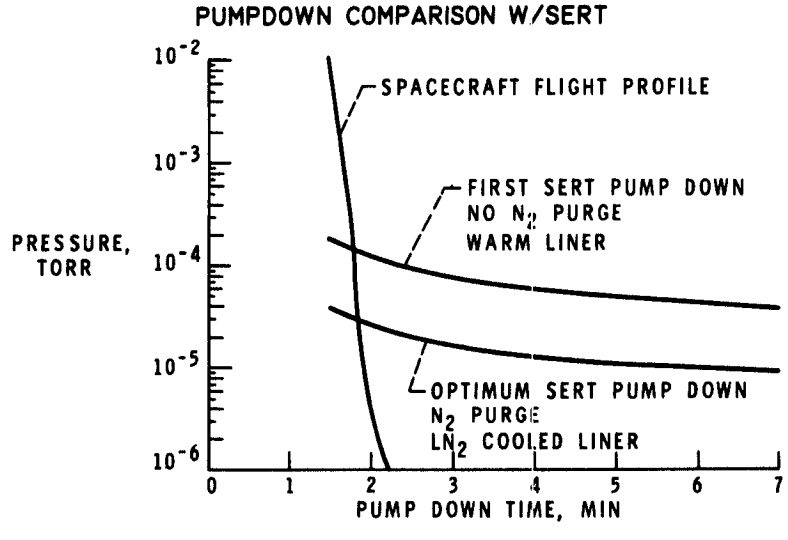

Figure 8

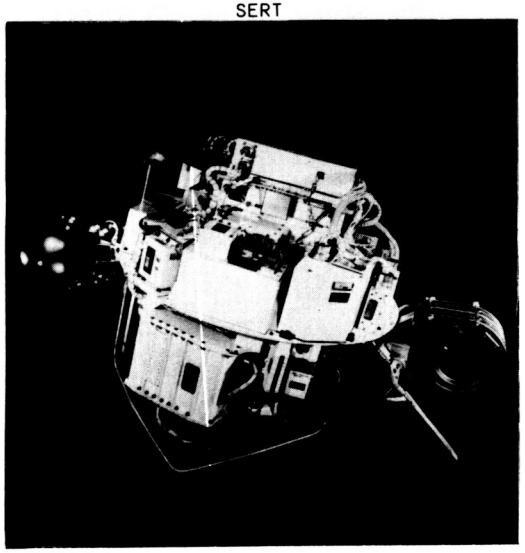

Figure 9

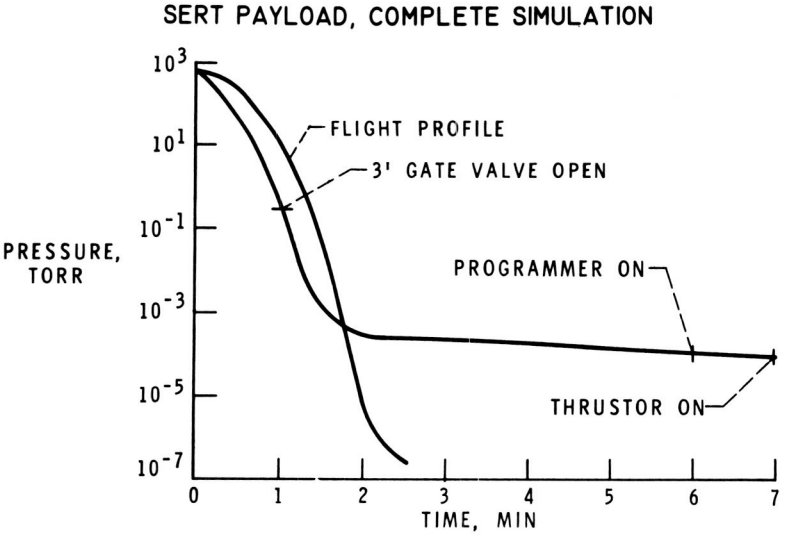

Figure 10

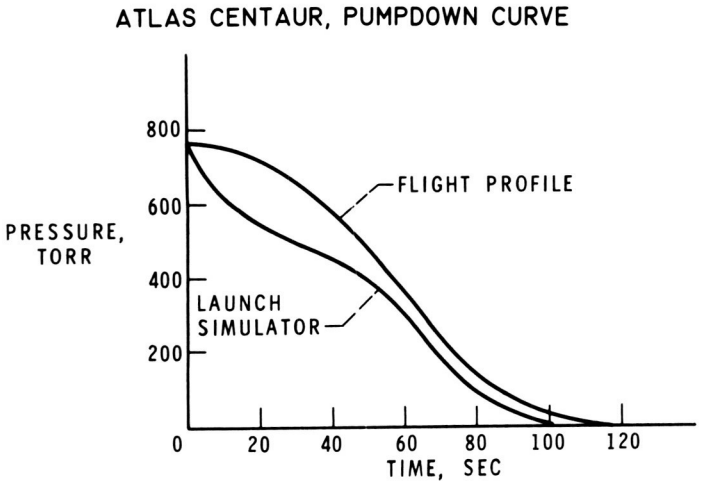

Figure 11

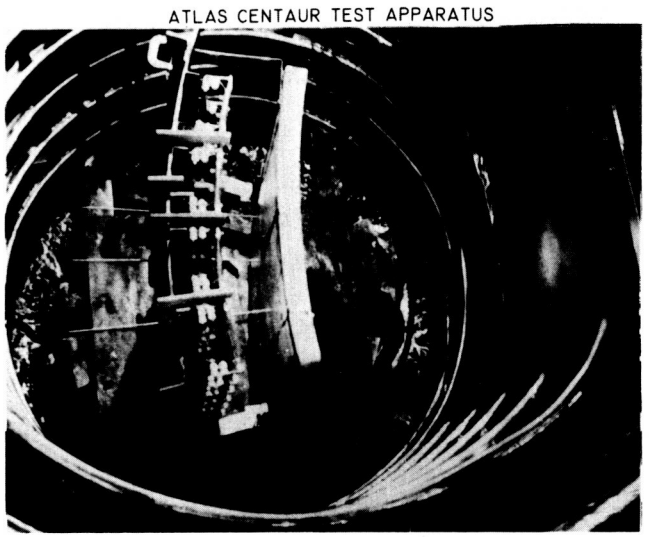

Figure 12

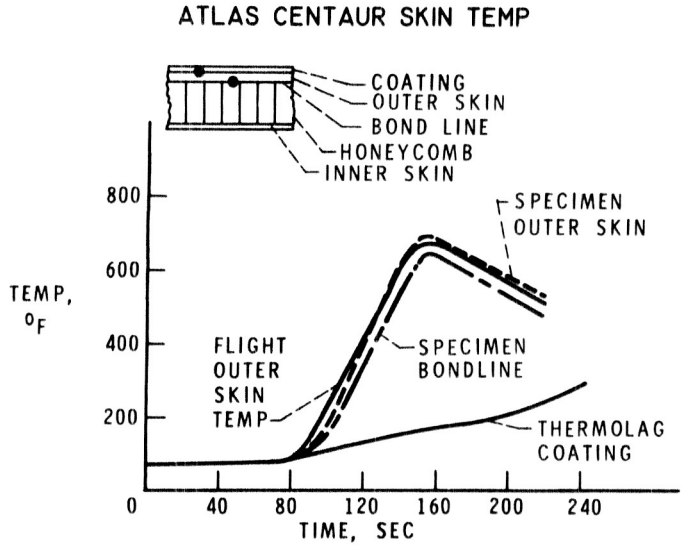

Figure 13

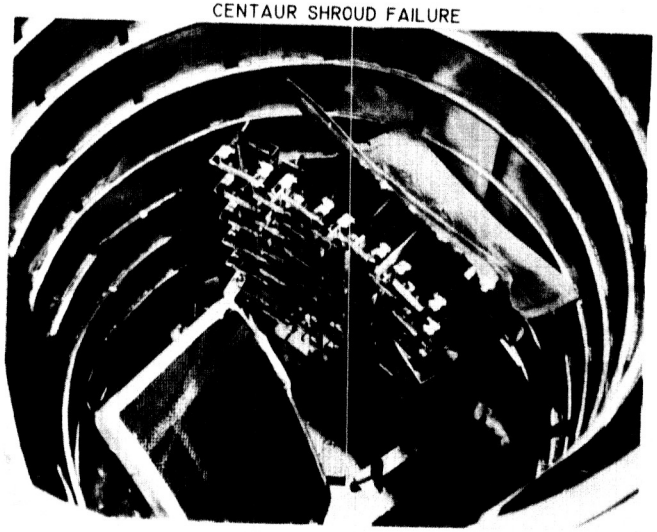

Figure 14

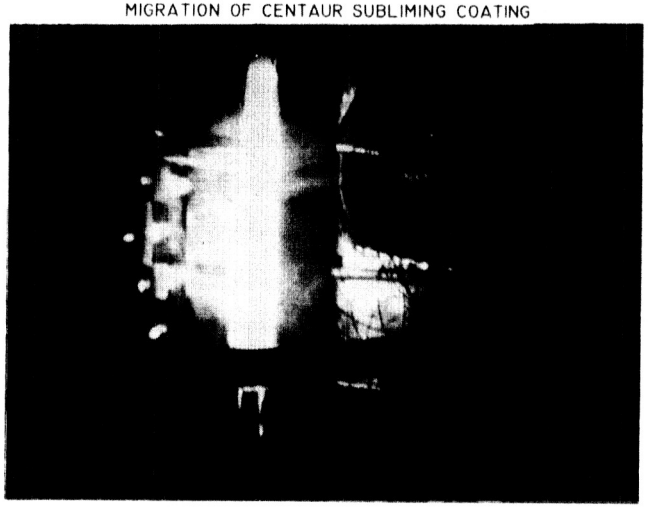

Figure 15

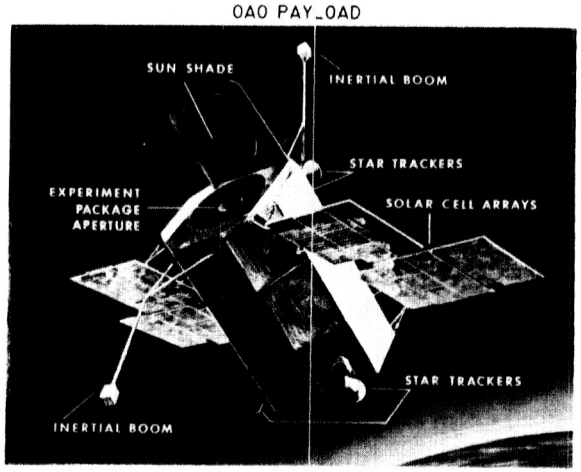

Figure 16

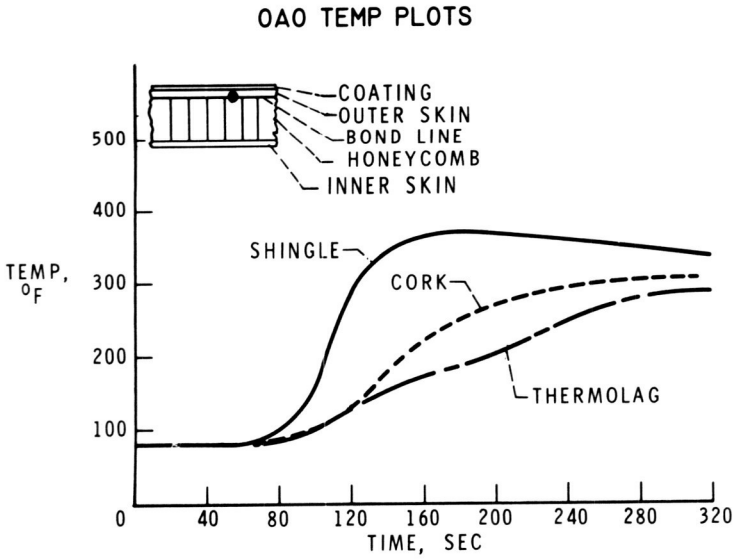

Figure 17.

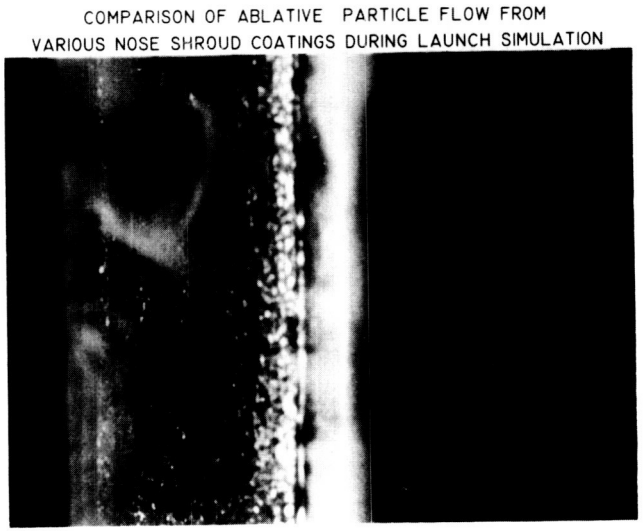

Figure 18. (a) Subliming compound.

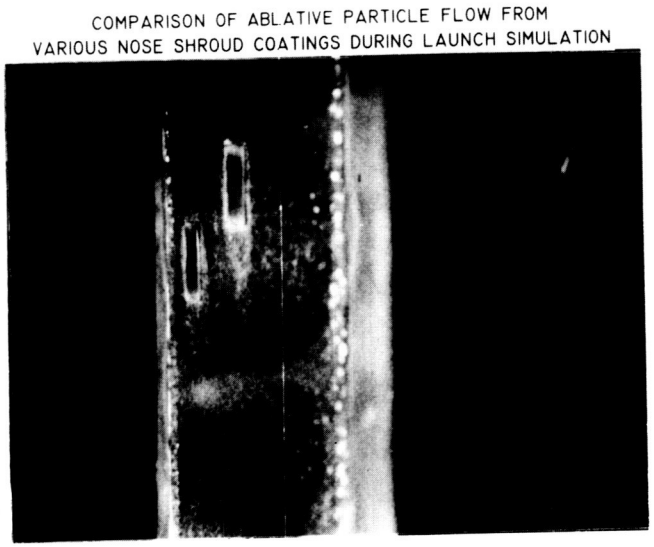

Figure 18. (b) Cork.

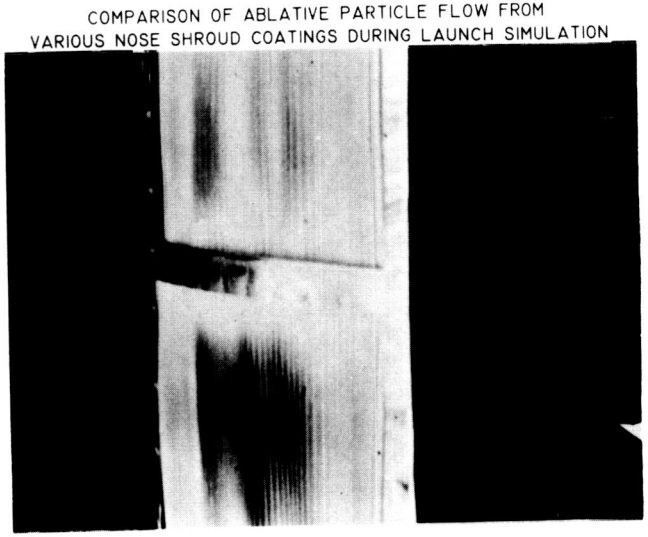

Figure 18. (c) Stainless "shingle."

VACUUM SYSTEM FOR THE BOILING LIQUID-METAL HEAT TRANSFER FACILITY

by Donald E. Groesbeck

Lewis Research Center

The vacuum system used for providing a clean, almost oxygen-free environment for the columbium-1 zirconium high-temperature portion of the Lewis Boiling Liquid-Metal Heat-Transfer Facility is described herein.

The facility was built for the basic study of high-temperature liquid-metal heat transfer. It is composed of two practically identical loops; one loop transfers heat to the other within a counterflow, tube-within-a-tube heat exchanger. The main heater in the heat supply loop is resistance heated by supplying up to 600 kilowatts to 250 feet of 1-inch diameter by 50-mil wall columbium tubing.

The heat rejection loop heater is heated by supplying up to 125 kilowatts to 100 feet of tubing. The two heaters are integral parts of their respective flow loops and give up the heat generated within them to the liquid metal flowing inside the tubing. The portions of the two loops to be operated between 1500° and 2200° F are constructed of the columbium alloy for the required strength at these elevated temperatures. The balance of the two loops is constructed of 316 stainless steel.

Columbium, like tungsten, tantalum, and other refractory metals at elevated temperatures, reacts with oxygen to result in serious deterioration, embrittlement, and loss of ductility. (This is discussed in more detail in the paper by Barrett and Rosenblum.) Because of this oxygen reaction, columbium must be protected from oxygen and oxygen-bearing compounds when it is heated above roughly 400° F.

The columbium test section with all the interconnecting piping attached is shown in figure 1. The eight adaptors on the right side are furnaced-brazed bimetallic joints (columbium - 316 stainless steel) for welding the test section to the stainless steel piping. Most of the columbium welds were made in a clean room by either electron beam under vacuum or tungsten-inert-gas in a dry box. Field welds were made under high-purity argon. Figure 2 shows a typical field welding operation. A polyethylene bag with glove ports was fabricated for each field weld. This type of weld was necessary for a few final welds because of the size of the finished components. Figure 3 is the dry box welding setup in the clean room. The clean room is in another building where the complete columbium package was welded. In the clean room all material was handled with white gloves after the final pickling and cleaning operation. Clean room coats and boots were also worn.

The completed columbium research package is shown in figure 4. Most of the radiation shielding is off at this time since the package had to be moved from the clean room to the test cell. Subsequently, all connecting piping was welded to the package, research thermocouples were attached, and radiation foil wrapping was installed on all the unwrapped piping.

The surface areas on the complete columbium package are as follows:

(1) Radiation shields consisting of 25 dimpled sheets of 10-mil thickness, (8 inner ones of molybdenum and 17 outer ones of stainless steel), amounted to 7800 square feet when both sides of the shields were included.

(2) High-purity alumina insulating blocks between the coils of the two heaters plus the high-purity alumina thermocouple wire insulation accounted for 120 square feet. (About one-fifth of the surface of the insulating blocks created trapped volumes by the way they had to be stacked on top of each other.)

(3) Radiation wrapping of 1-mil tantalum foil on all pipe and component surfaces, stainless steel and molybdenum support structures, and the pipe and component surfaces amounted to 1000 square feet.

(4) Including the inner surface of the vacuum vessel adds another 400 square feet for a total exposed surface inside the vacuum vessel of over 9300 square feet.

The containment, or vacuum, vessel used (fig. 5) is $17\frac{1}{2}$ feet long and a little over 7 feet in diameter, with an internal volume of roughly 700 cubic feet. Hinged doors on each end are sealed with double Viton-A O-rings. Between the two O-rings is a copper tube for cooling water and a groove for a guard vacuum in the event the outer ring leaks. The double tubes shown are for cooling water. In the spaces between them were placed strip heaters and Cal-Rod type heaters for bake-out purposes. The vacuum system was connected at the 24-inch flange near the top. Stainless steel reflective foil was placed 2 inches above the heaters and was covered with 1 inch of insulation.

Figure 6 is a view of the columbium package installed inside the vessel. The photograph was taken from inside an inflatible, portable clean room attached to one end of the vessel. The tent idea was used to provide a means of recirculating a filtered and cooled supply of air whenever it was necessary to open the vessel to do any work on the package. Cambridge absolute air filters are used and the clean room is all plastic with a vinyl floor. Here again clean room garments are used - hats, coats, gloves, and boots.

Schematically shown in figure 7 is the complete vacuum system.

A photograph of the Boiling Liquid Metal Facility is shown in figure 8. In the foreground is the vacuum system for the facility. Behind the roughing pump - Roots blower combination are two mercury diffusion pumps. On top is the vac-ion pump. Just visible is the end of the containment vessel and at the other end of the room is the air lock entry into the inflatible clean room.

The only solution to locating leaks in the vacuum system is patience, a reliable

helium leak detector, and possibly some luck in locating them rapidly. Usually twice every 8-hour shift the vessel and the vacuum system were leak checked. This is a laborious and time-consuming job but well worth the trouble since a small leak could develop into a serious one.

The first 4 weeks of operation were spent trying to increase the bake-out temperature and to stop leaks as fast as they could be located. Most of the minor leak troubles were around the eight electrical feed-throughs on top of the vessel. These were sealed with two pure 0.030-inch-diameter gold wire O-rings. As the vessel wall temperature was increased the flange mounting bolts would relax and a small leak could develop. Retightening the mounting bolts stopped the leaks. One of the worst leaks involved the 24-inch liquid-nitrogen cold trap. The liquid inlet line developed a crack on the inside of the mounting flange and for nearly 2 days everything was tried to seal off the leak, but to no avail. Then rather suddenly the residual gas analyzer showed an increased level of nitrogen in the vacuum system. A proportional increase in the oxygen level was not evident, which meant that the leak was not to the atmosphere. The inevitable had to take place - removal of the cold-trap baffle assembly, which was coated with mercury. After the mercury was cleaned off the baffles and tubes, the cold trap was cold shocked, and leak checked; a crack was found in a brazed joint in the flow tube. The system was not back in operation until a week had passed.

Figure 9 shows the last 4 weeks of operation as time history of the vacuum pressure in torr after all the leaks had been stopped. Finally, a vessel wall temperature of 400° F was achieved and a respectable vacuum could be held. Then the vessel wall was allowed to cool in preparation for charging the piping system with liquid sodium. The lowest pressure during bakeout at 400° F was 3×10^{-6} torr and at 80° F was 3×10^{-7} torr. The interesting feature to note on this plot is the steady improvement in the vacuum at roughly the same system temperature level. The temperatures noted here are the hottest in the columbium package, the outlet of the 600-kilowatt heater. These are by no means the environmental temperatures within the vessel itself, in fact the vessel wall temperature barely reached 200° F. The lowest pressure achieved was 8×10^{-8} torr.

The first half of the research section of figure 9 is shown in figure 10, to bring out the relation of the vacuum pressure to the system temperature level. Every increase in temperature was accompanied by a vacuum pressure increase and vice versa.

Figure 11 is a reproduction of a typical ultrahigh vacuum residual gas analyzer trace. The ordinate is a three-decade scale, which can be confusing in a cursory comparison of relative peak magnitudes. This trace was made fairly late in the vacuum run, and as a result it is relatively clean in the sense that the residual gases are rather few and well defined. A residual gas analyzer is in essence a mass spectrometer. Ions are formed by electron bombardment, a varying accelerating voltage is applied, and the ions are separated by their respective mass to electron charge ratio M/e. The greater the

ion concentration, the larger the resulting peak. The peaks represent partial pressures. Computing the partial pressure of each constituent and adding them can approximate the total pressure in the vacuum system. The only trouble is that a partial pressure calibration has to be made of each constituent present prior to the actual facility operation, and then it is not necessarily constant over extended periods of time. However, in this operation the interest was not in partial pressures as such, but rather in the relative magnitudes of the residual gases - principally, M/e of 32 (oxygen).

In any vacuum system, cleanliness is mandatory, and in this system the modest precautions taken were very rewarding. Roughly 4 to 5 days were required to evacuate the vessel and its contents to a pressure in the low 10^{-6} torr range. This is rapid in view of the nearly 10 000 square feet of surface area that were outgassed. At the end of the research run, the tank was opened and a piece of tantalum foil radiation wrap was removed. It was still very ductile.

In the immediate future a section of the columbium tubing will be removed for the addition of another liquid-metal pump. This columbium will be used for a complete chemical, mechanical, and metallurgical analysis. These analyses are not expected to show any serious effects of the high-temperature operation in the vacuum. We feel we were well below the minimum requirement for oxygen contamination, enough possibly, so that the life of the system may approach 10 000 hours at 2000° F rather than the 5000 hours of the original design.

COLUMBIUM TEST SECTION

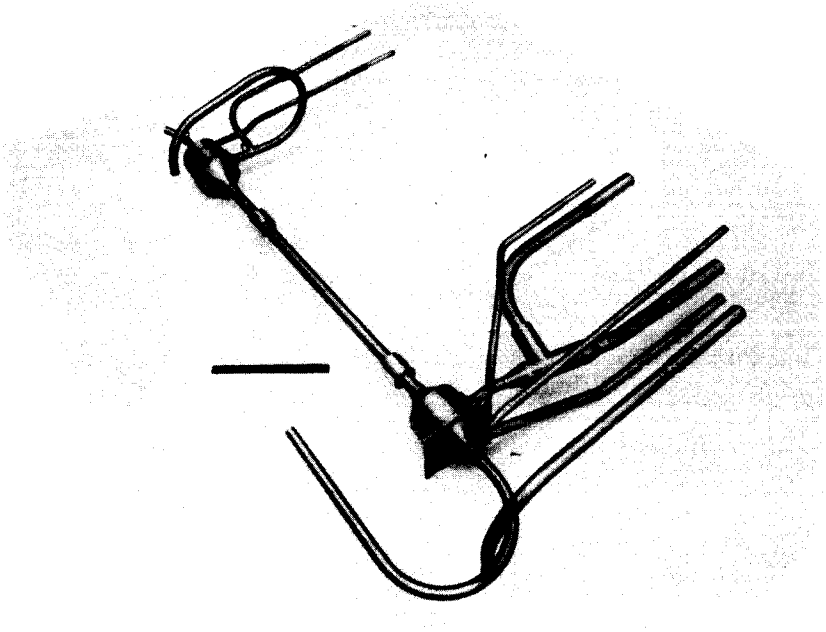

Figure 1.

FIELD WELDING OPERATION IN CLEAN ROOM

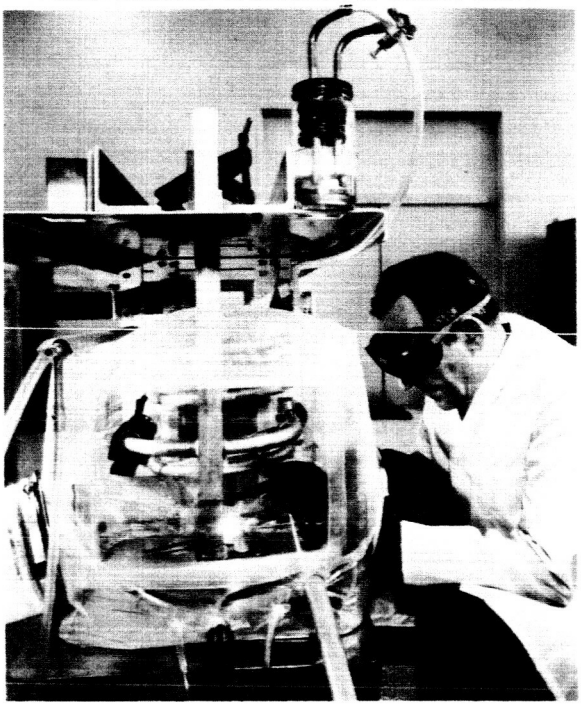

Figure 2

DRY BOX WELDING OPERATION IN CLEAN ROOM

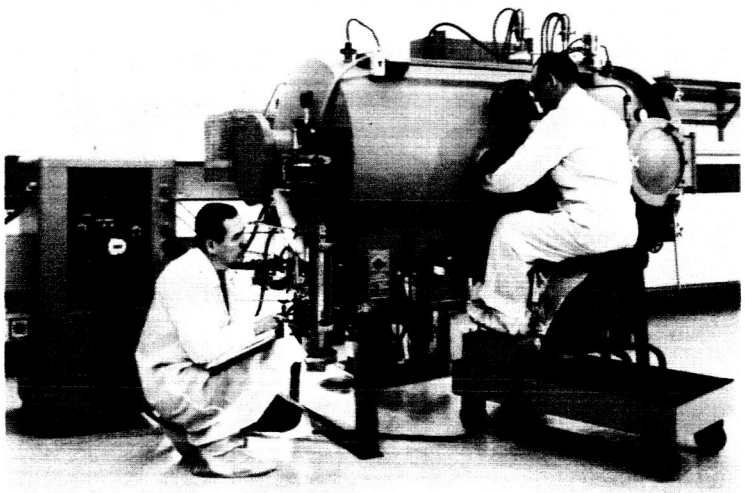

Figure 3

COLUMBIUM RESEARCH PACKAGE

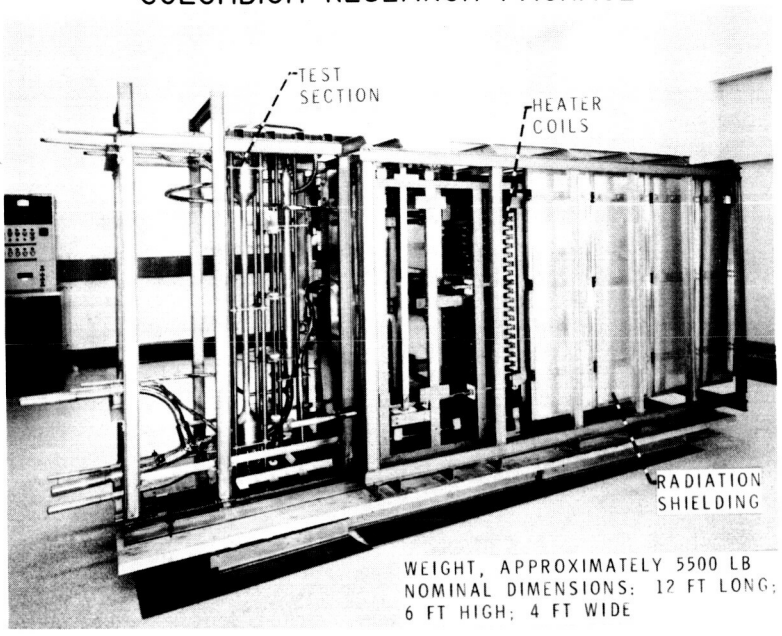

Figure 4

UNINSULATED VACUUM VESSEL

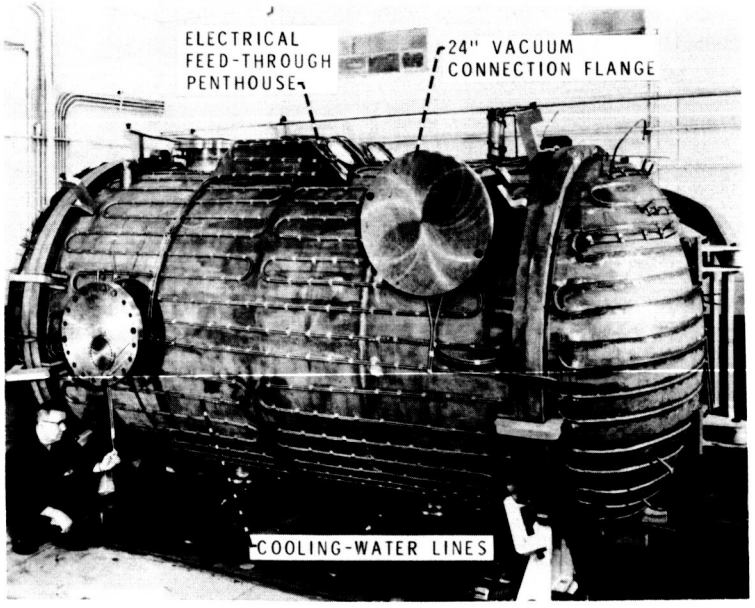

Figure 5

INSTALLATION OF HIGH TEMPERATURE PACKAGE
IN PORTABLE CLEAN ROOM

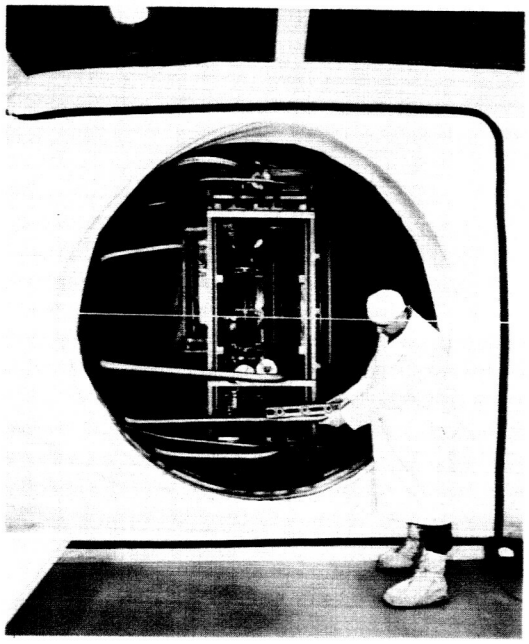

Figure 6

VACUUM SYSTEM FOR LIQUID METAL HEAT TRANSFER FACILITY

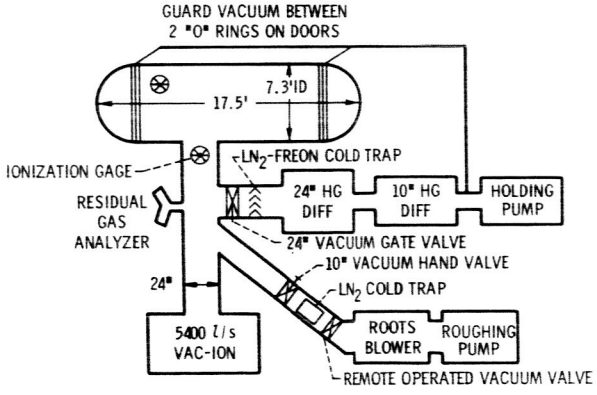

24" HG DIFF
2500 l/s 4 STAGE ULTIMATE $1X10^{-8}$ TORR
10" HG DIFF
3 STAGE ULTIMATE $<1X10^{-6}$ TORR
HOLDING PUMP
(MECHANICAL) 2 STAGE ULTIMATE 0.2 MICRON
5400 l/s VAC-ION
ULTIMATE $1X10^{-8}$ TORR
ROOTS BLOWER
1300 CFM ULTIMATE $1X10^{-5}$ TORR
ROUGHING PUMP
130 CFM ULTIMATE 10 MICRONS

Figure 7

BOILING LIQUID METAL FACILITY

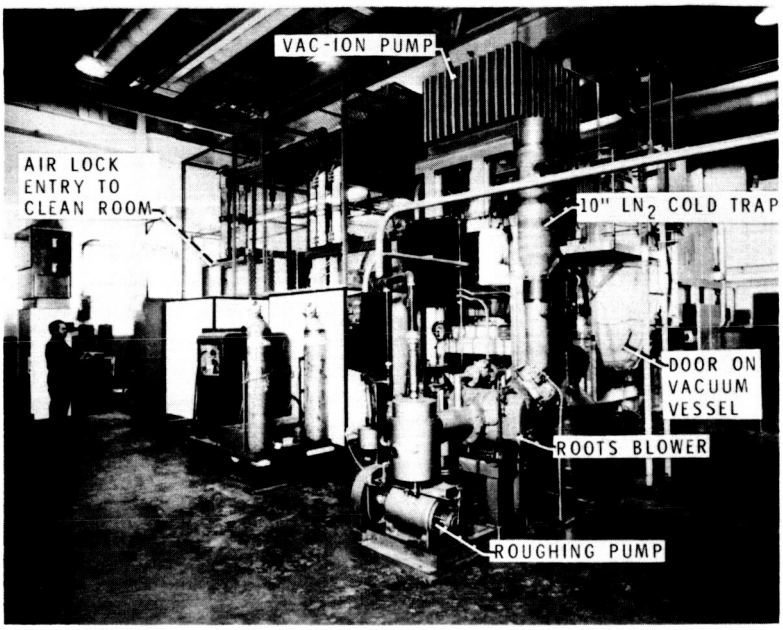

Figure 8

VACUUM-TIME HISTORY OF LIQUID METAL FACILITY

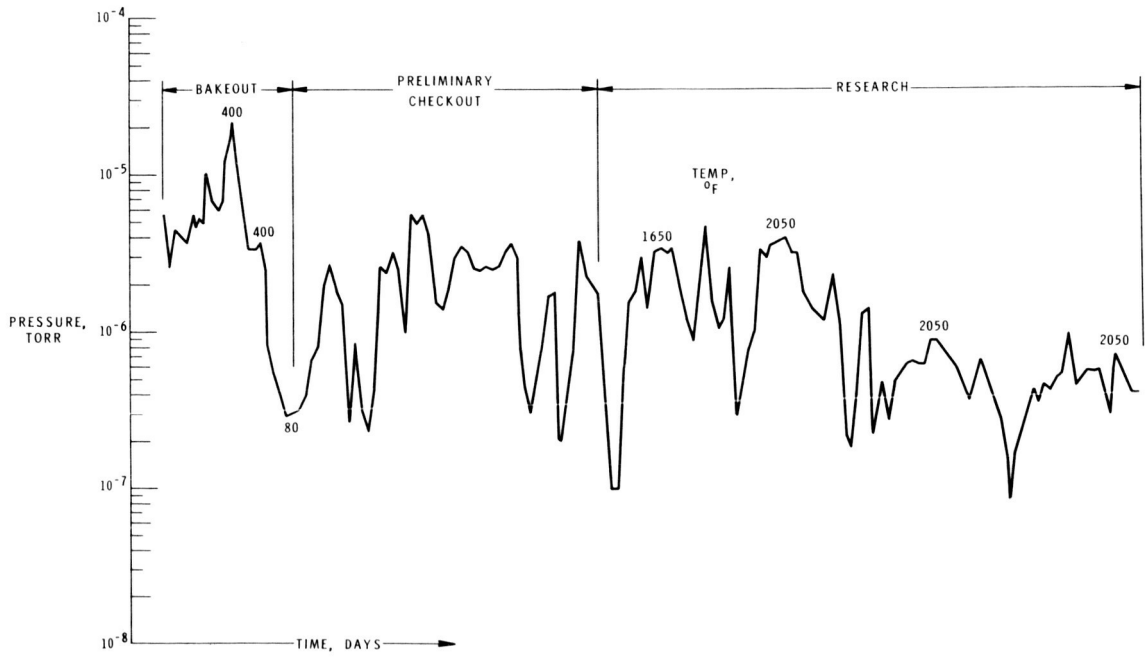

Figure 9

DETAIL OF VACUUM–TIME HISTORY OF LIQUID METAL FACILITY

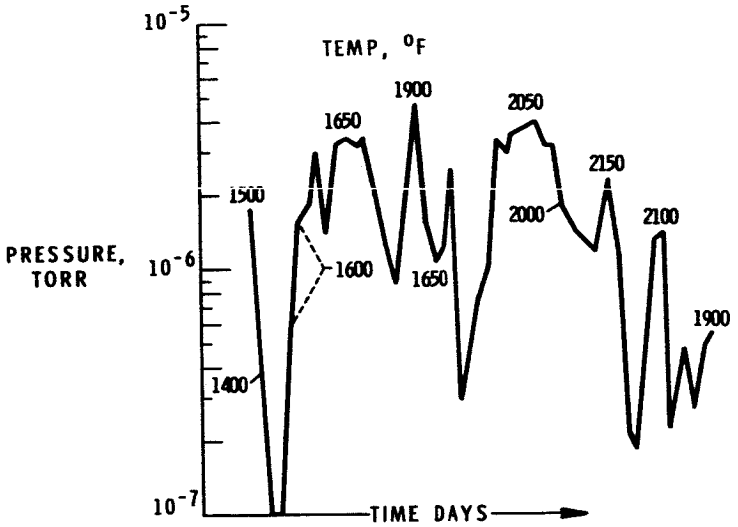

Figure 10

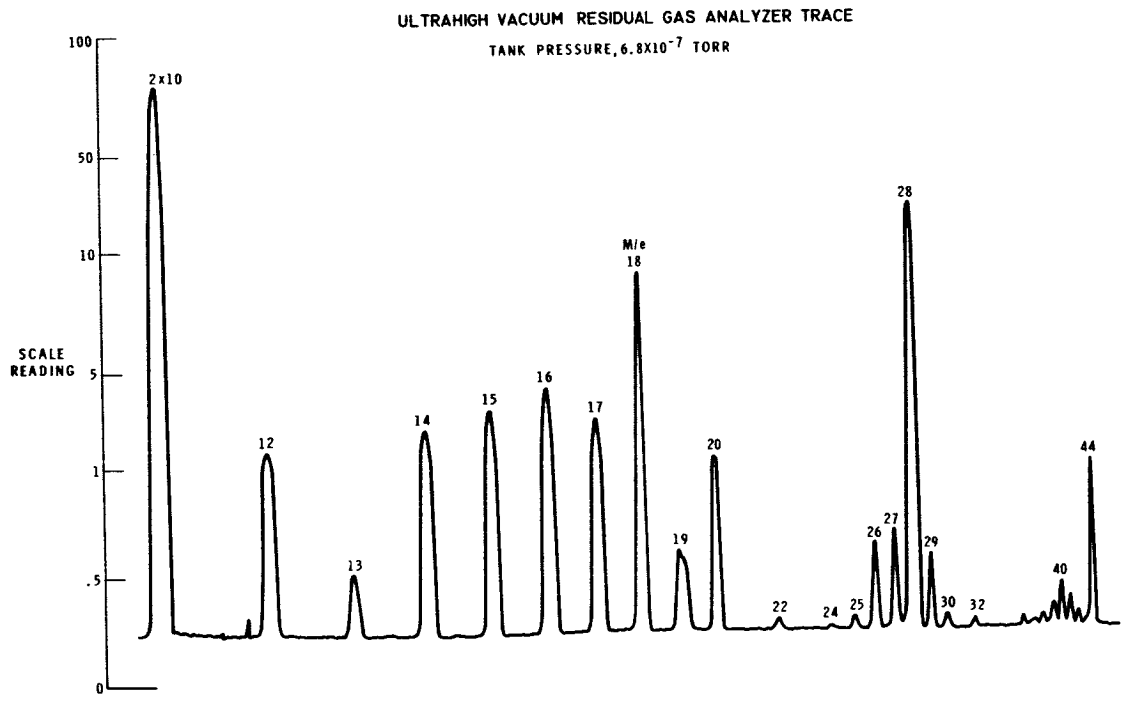

Figure 11

SPACE SIMULATION AND FULL-SCALE TESTING IN A CONVERTED FACILITY

By John H. Povolny

Lewis Research Center

FACILITY

The Space Simulation Chamber described in this paper was converted from a former wind tunnel complex (fig. 1). Conversion consisted of removal of the turning vanes, cooling coils, and circulation fan and the addition of three bulkheads. The large chamber is approximately 60 feet in diameter with a volume of 250 000 cubic feet and is utilized for tests to altitudes of 100 000 feet. The second, smaller chamber, and the one of interest, is approximately 30 feet in diameter and 100 feet long and has a volume of 70 000 cubic feet. A $22\frac{1}{2}$-foot extension was added to provide a total height of 45 feet in order to accommodate the Centaur test vehicle. Present vacuum pumping capability is 2×10^{-6} millimeter of mercury, and with the Centaur test vehicle installed an ultimate of 2×10^{-5} millimeter of mercury is attained. Figures 2 to 5 show various views of the Space Simulation Chamber (SSC) and the installation of the Centaur vehicle.

The vacuum system consists of ten 32-inch, 50 000-liter-per-second oil diffusion pumps, one 30 000-cubic-feet-per-minute blower and two 7500 cubic-feet-per-minute roughing pumps. Pumpdown time to reach ultimate vacuum is 24 to 30 hours. The vacuum in the chamber is broken by using dry air (-20° F dewpoint). Breaking the vacuum normally takes 2 hours. A continuous purge with dry air is used when the chamber is open for repairs.

Figure 6 is a pictorial view of the modified chamber used for space simulation with the Centaur test vehicle installed. A liquid-nitrogen cold baffle, tailored to the Centaur test vehicle and consisting of an assembly of copper finned tubes has been installed. It is approximately 20 feet in diameter and 42 feet high. The thermal syphon system is utilized to maintain a full baffle, with three 7000-gallon Dewars supplying liquid nitrogen to the system.

A solar simulator system tailored to the Centaur test vehicle consists of six separately controlled zones of quartz-iodine (500 W) lamps. There are four zones in the forward array and two in the aft. These arrays provide approximately 60 percent open area between the vehicle and the cold baffle and are designed to approximate a collimated light source.

In order to ensure good vacuum capability, the 15-foot access door was provided with a dual O-ring seal. The dome which seals off the extension was provided with a 1/4-inch-plate lip seal, which when welded shut makes the chamber vacuum tight. During modification it was found that the original welds, made some 20 years ago, were structurally sound but contained many porous areas. As a result, all old welds were removed and replaced with high-quality welds. The interior surfaces were sandblasted and given two coats of aluminum paint for sealing.

All chamber penetrations and joints within the chamber were leak checked with helium using a helium leak detector to determine leak rate. All penetrations and joints were required to have less than 1×10^{-8}-atmospheric-cubic-centimeter-per-second leakage.

CENTAUR INVESTIGATION

The Centaur vehicle under test consists primarily of a 10-foot-diameter-pressure-stabilized tank made of 0.010-inch-thick type 301 stainless steel. Most of the electronic and control systems and components are mounted on the forward end, and most of the mechanical and propulsion systems are mounted on the back end. The RL 10 engines, which will not be fired for these tests, are of early vintage. All remaining components have been updated to match current flight configurations.

The purpose of the investigation on the Centaur vehicle is to evaluate the performance of the various vehicle subsystems under simulated thermal conditions encountered during the coast phase of flight. All systems will be operated to determine if there are system interferences as well as to provide operating histories of each component. Parameters being monitored are

(a) Package (component) temperature

(b) Package (component) pressure

(c) Operating time

(d) Power consumption

(e) Package or system output

In addition to the normally supplied facility systems that are required to accommodate the Centaur test vehicle, it was necessary to add several others. One such addition was a pneumatic system with automatic controls for maintaining a nearly constant pressure differential across the vehicle tank structure during, before, and after a pumpdown. This was necessitated by the fact that the structure was not designed to withstand repeated pressure (and resulting stress) cycles inasmuch as such cycling would cause fatigue of the tank structure. The system as now operated maintains the fuel tank pressure between 4 and 6 pounds per square inch above the chamber pressure, and the oxidant

pressure 8 to 10 pounds per square inch above fuel tank pressure. In addition to these pressure systems, a pneumatic stretch system was added. This system, which will support the vehicle in the event of an inadvertent loss of internal pressure, makes use of three pneumatic cylinders and mechanical linkage for applying a tensile load to the tank structure.

Inasmuch as the main (RL 10) engines, which provide the power to drive the main hydraulic pumps, are not to be fired during these tests, it was necessary to provide an external hydraulic power supply to the engine gimbal system so that it could be actuated during a simulated flight. In a normal preflight ground checkout, the vehicle pneumatic and fluid systems are connected to ground services through quick-disconnect devices. These devices have a stringent leak rate specification, which is dictated by the flight requirement, but even leakage within the specification will degrade the vacuum in the chamber. Thus, the quick disconnects had to be replaced with AN fittings. Further modifications to the vehicle systems consisted of ducting all vents and relief valves to a point outside the space chamber.

Auxiliary heat was added to some of the components in order to maintain normal flight temperatures during pumpdown. This additional heat was necessary because some of the airborne components on Centaur are normally exposed to an abnormally low temperature environment for only a short period during flight, whereas in this test setup, a long period under extreme cold is required to reach simulated space conditions. Four separate areas are conditioned in this manner: two with radiant heat lamps (aft instrument box and destruct), and two with wraparound heaters (hydraulic and hydrogen peroxide supply lines). A possible consequence of the long pumpdown time to reach space simulated pressure environment is some gas leakage of the pressurized airborne electrical packages so that they would not be at normal internal pressures. Therefore, a separate system was installed to provide the capability of monitoring and adjusting pressures where required. This system functions for 16 of the packages and can supply either of two pressurant gases.

In order to maintain a reasonable heat balance on the overall vehicle during pumpdown and activation of the liquid nitrogen baffles, the solar simulator is operated in an automatic mode that utilizes slug-type calorimeters with a "feedback" thermocouple connected to the controller unit. In addition, water-cooled calorimeters are used to measure the amount of heat in each of the six heat zones on a nominal target plane to check the operation of the automatic system.

At the start of each test the airborne packs must be conditioned to the temperatures that they would have at that point in flight time. In general, raising the temperature is accomplished either by increasing the heat produced by the solar simulator panels or by operating the individual packs and generating internal heat. Where packages require cooling, the solar simulator in the appropriate zone is operated at reduced or zero

power, or cold-gas cooling coils installed on some of the larger packages are utilized. (These coils are installed so as not to impair normal solar or space radiation.)

For redundancy during a test, the vehicle electric power supply is arranged so as to provide two parallel systems, airborne and ground, for both 400-cycle and direct-current power. Normal testing is done using the airborne static inverter and batteries, but if troubles develop either or both systems can be switched to the ground power supplies.

The wiring to interconnect the vehicle and control room for both vehicle functions and instrumentation (excluding facility) requires

(a) Controls and airborne instrumentation - 1000 conductors

(b) Hardline instrumentation (including thermocouple) - 900 conductors

Instrumentation for parameter monitoring consists of

(a) 350 channels for temperature

(b) 36 channels for power

(c) 120 channels of events recording

(d) 40 channels of elapsed-time recording

(e) 350 channels of telemetry data

Some of the data are radiated via telemetry and recorded on FM tape at a ground receiving station. Similar data are also recorded via landlines as a check. The data transmitted via telemetry can be used to aid in interpretation of flight data.

Currently the testing program on the Centaur vehicle is just getting underway. Some preliminary runs have been made during which the various facility and vehicle systems have been operated and checked out. One of the most troublesome problems is cross talk or noise pickup in the extensive temperature instrumentation that is installed on the flight packages. This problem has been solved by using an extensive filtering system. Another problem is that of obtaining a reasonable solar heat simulation on the systems and packages within the limitations of the existing solar simulator. It is being overcome by extensive calibrations and some mechanical equipment which will help to approximate a collimated solar source.

Generally, the program requires the investigation of the performance of the systems and components of a parking-orbit Centaur vehicle during that period of time starting with separation from the Atlas booster. Of particular interest are the extremes in environment that could be encountered. Figure 8 shows some extreme (temperaturewise) trajectories that could be encountered during the next flight of a Centaur two-burn vehicle depending on which launch window is met. If the vehicle is launched during the window for November 16, 1965, the trajectory would be as shown and the forward equipment would receive practically no solar heating. If it is launched during the November 4, 1965, window, the forward equipment would receive maximum solar heating. Similar trajectories exist with respect to the propulsion and mechanical systems mounted at the rear of the vehicle.

The trajectory that was actually attempted on the Atlas-Centaur 4 vehicle is shown in figure 9. Unfortunately the vehicle started tumbling about 10 minutes after it was separated from the Atlas and therefore the thermal data after that point in time are not too meaningful. A comparison of the flight and vacuum (SSC) rate-gyro-cover temperatures for the first 10 minutes of Centaur flight is shown in figure 10. Although the starting temperatures were different, the similarity in trends indicates that a reasonable simulation was obtained. Although only preliminary tests have been made to date, a variety of functional difficulties have been uncovered. These are listed in table I. Thus full-scale environmental test chambers appear to be a valuable tool in the development of flight hardware.

CENTAUR NOSE FAIRING SEPARATION TESTS

In addition to space thermal environment testing of full-scale vehicles, the Lewis Space Simulation Chamber was also extremely useful in investigating dynamic problems such as the jettisoning of the Centaur nose fairing. This investigation occurred primarily as a result of the Atlas-Centaur 3 flight, wherein a shock and an interruption of the guidance computer were experienced during nose fairing jettison. Although extensive sea-level jettison tests had previously been conducted without any indication of nose fairing malfunction, it was felt that the jettison events and computer malfunction were related in some manner. A decision was made to investigate the jettisoning of the nose fairing under space simulated pressure conditions (in the chamber) to learn what had actually happened to Atlas-Centaur 3. The prime objective of this investigation was to determine which, if any, of the structural components of the nose fairing were underdesigned and to flight qualify the redesigned nose fairing if necessary. Additional objectives were to determine the nose fairing trajectory, possible interferences, system function and redundancy hinge dynamic loads, and pressure impingement effects on the payload.

A standard flight type fiberglass-honeycomb nose fairing was used for all tests. A photograph of it installed in the facility is shown in figure 11. The salient features of the nose fairing are that it consists of two halves held together by explosive bolts, which are fired just prior to separation, and that the separation force is provided by two high-pressure-gas thrustor bottles installed in the upper end. It was felt that the pressure forces resulting from discharge of the bottles and the resulting nose fairing dynamics could have contributed to the anomaly detected during the Atlas-Centaur 3 flight.

The installation of the full-scale Centaur nose fairing for the Atlas-Centaur 4 flight qualification tests conducted in SSC is illustrated in figure 12, which presents a diagrammatic sketch showing the relation between the nose fairing and the stopper on the left side and the catcher net on the right. Briefly, the stopper on the left in conjunction with a

facility-type hinge permitted about 20^{o} rotation of the left fairing, whereas the net on the right permitted about 50^{o} rotation and allowed the fairing to jettison freely in a manner similar to that which occurs in flight (fig. 13). Space limitations (the proximity of the Centaur vehicle) prevented the net from being installed and thus permitting a greater degree of freedom.

The test procedure employed in the nose fairing jettison tests was relatively simple and straightforward. It consisted primarily of pumping down the chamber to the desired pressure and then actuating the nose fairing jettison system in a manner similar to that used in flight. Instrumentation was installed on the fairing to measure pressures, strains, accelerations, and fairing trajectory and motion-picture cameras were installed inside and outside of the fairing to record all events to check the trajectory. Special techniques included the installation of the cameras in hermetically sealed enclosures and the selection of transducers (or the manner of their installation) that would not overheat or malfunction during their long exposure to the vacuum of the chamber.

The chief uncertainty concerning the validity of the test was the change in chamber pressure that occurs during the test. Although thrustor bottle firing is initiated at the correct pressure altitude (100 miles) by the time they are finished discharging the chamber pressure is up to an equivalent altitude of about 100 000 feet.

The answer to this problem was eventually obtained by comparing the chamber data with flight data; however, prior to flight the best that could be done was to compare the sea-level test with the vacuum-chamber test and observe that a considerable difference existed. This difference is illustrated in figure 14, which shows the hardware after the first firing in a vacuum; this compares with no damage for the sea-level firings. A comparison of the nose fairing trajectories obtained at sea level and in a vacuum (Atlas-Centaur 3) is shown in figure 15. The trajectory in a vacuum is much faster than at sea level and accounts for the damage experienced.

Inasmuch as no serious damage occurred when the fairing followed the trajectory labeled "AC-3 Sea Level," it was decided to adjust the bottle pressure and throat size in order to obtain a similar trajectory for flight. When this was done, the trajectory labeled "AC-4 vacuum" was obtained in the chamber. A comparison of this trajectory with Atlas-Centaur 4 flight data indicates good agreement.

A further comparison of flight and vacuum chamber dynamic measurements is presented in figure 16, which shows nose fairing hinge loads during jettison as measured in the vacuum chamber and as measured during Atlas-Centaur 4 flight. Again, relatively good agreement was obtained. Comparison of pressures measured in the fairing thrustor bottle compartment during the Atlas-Centaur 4 flight and in the vacuum chamber also agreed well with a peak pressure of 9.2 pounds per square inch absolute measured in flight and 8 pounds per square inch absolute in the vacuum chamber.

In addition to obtaining good agreement between flight and vacuum chamber data, the

chamber proved to be a most valuable tool in developing the nose fairing flight hardware for Atlas-Centaur 4. All of the changes and modifications made between the flights of Atlas-Centaur 3 and 4 were first checked out in the vacuum chamber, and as a result the first completely successful Centaur nose fairing jettison was accomplished on Atlas-Centaur 4.

TABLE I. - CENTAUR VEHICLE EQUIPMENT FAILURES

Unit	Failure mode
1. Main power changeover switch	While in a simulated flight environment, switch failed to respond to command signals to go to airborne position
2. Telemetry system	During an environmental test, subsystems 1, 2, and 4 failed to radiate properly after a primary power source transient
3. Airborne inverter	Unit failed to turn on after long exposure to simulated environmental conditions, even though it was well above the lower red line temperature limit
4. Range safety system	Electrical arming device, after long exposure to liquid nitrogen temperatures, failed to respond to commands

LEWIS ALTITUDE WIND TUNNEL

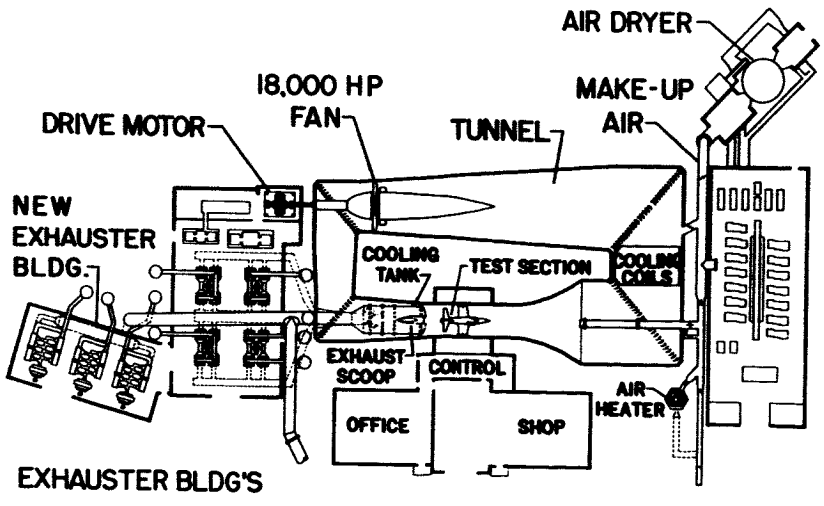

Figure 1.

OVERALL VIEW OF SSC

Figure 2

SSC EQUIPMENT ENTRY HATCH

Figure 3

LOWERING OF CENTAUR INTO SSC

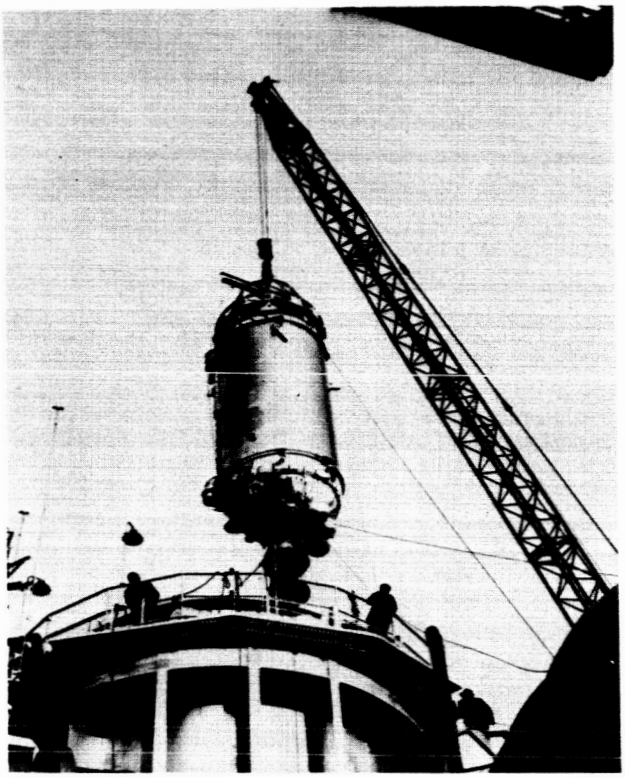

Figure 4

VIEW FROM BOTTOM AS CENTAUR IS LOWERED INTO SSC

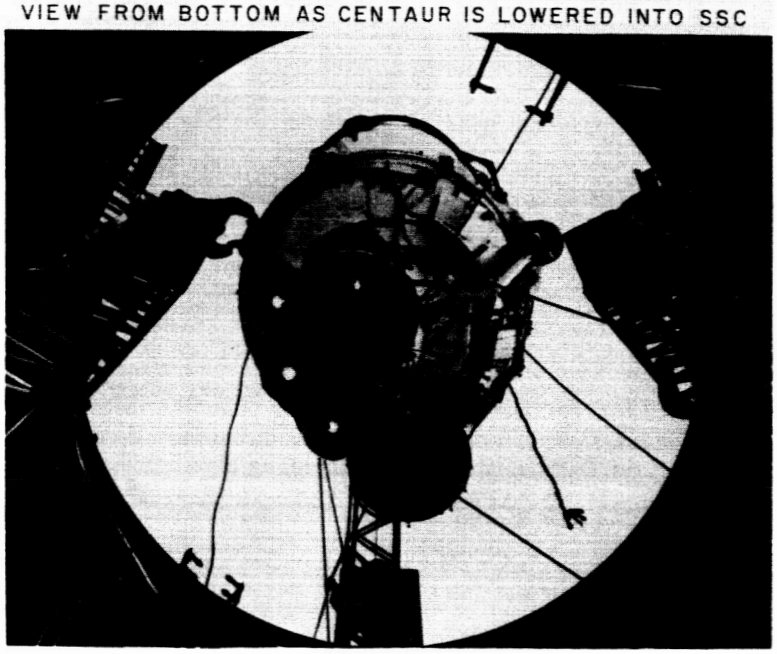

Figure 5

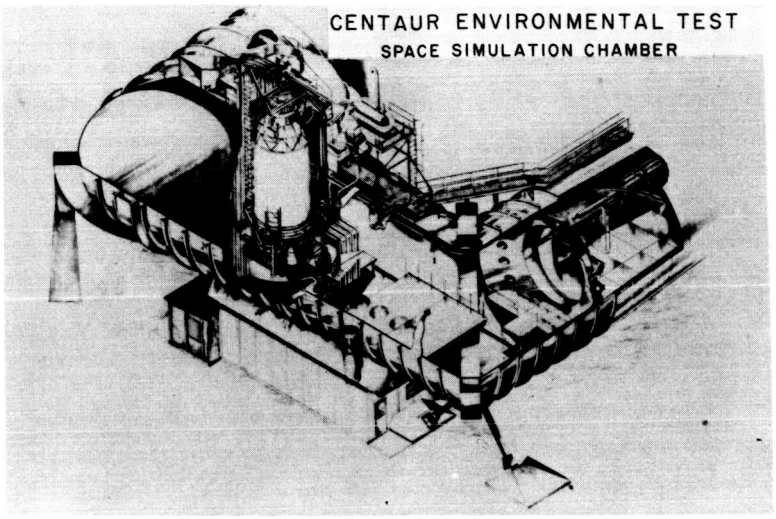

Figure 6

CENTAUR VEHICLE

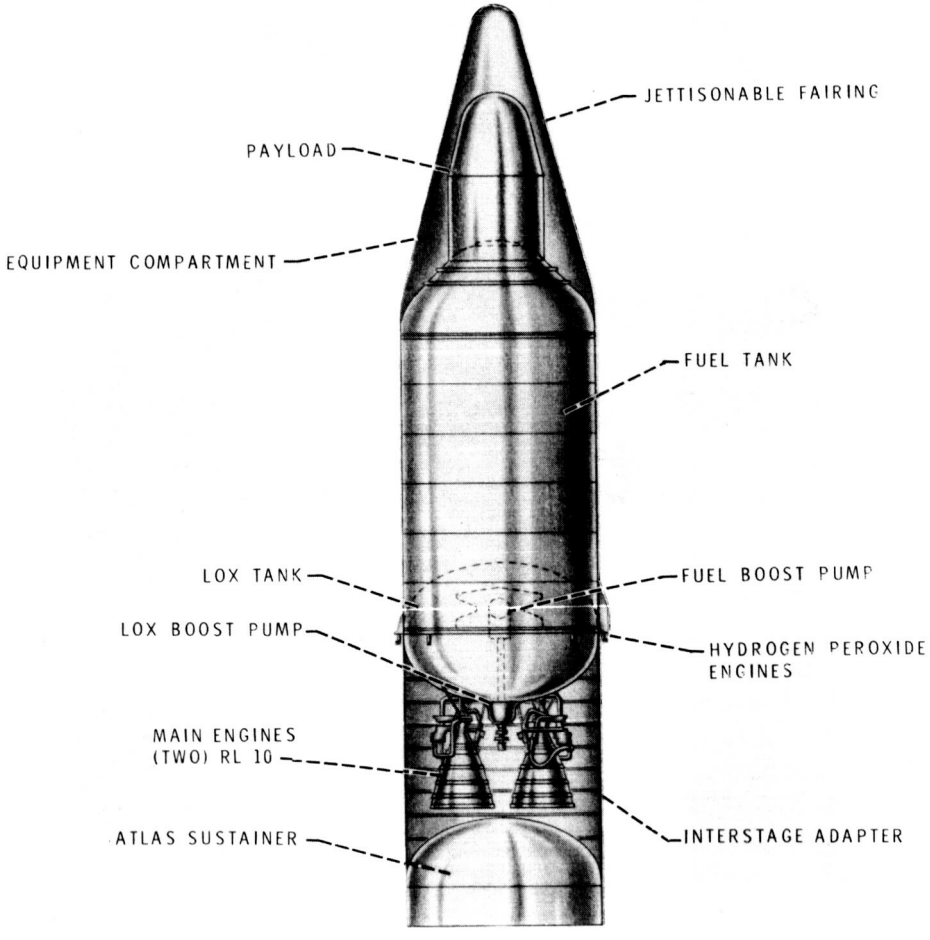

Figure 7

POSSIBLE CENTAUR COAST PHASE PROFILES

25 MINUTE COAST PERIOD

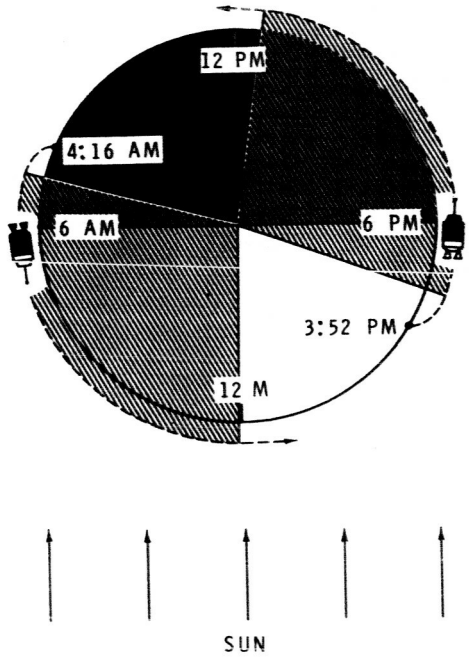

Figure 8

AC-4 FLIGHT PROFILE

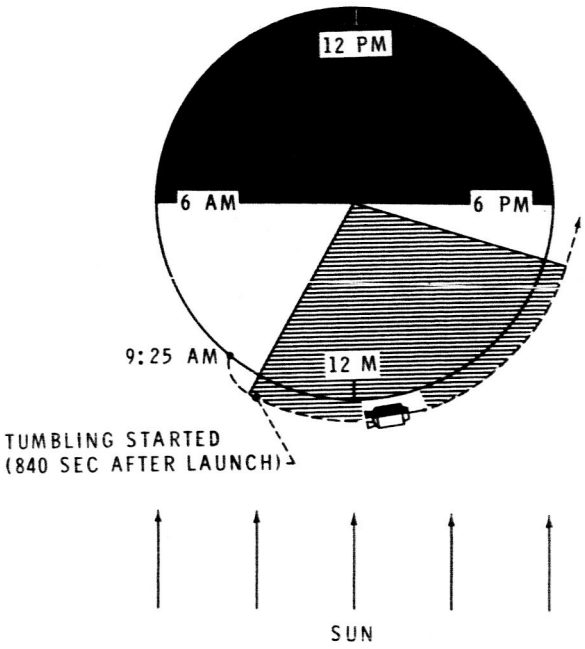

Figure 9

TEMPERATURE COMPARISON, RATE-GYRO-UNIT COVER TEMPERATURE

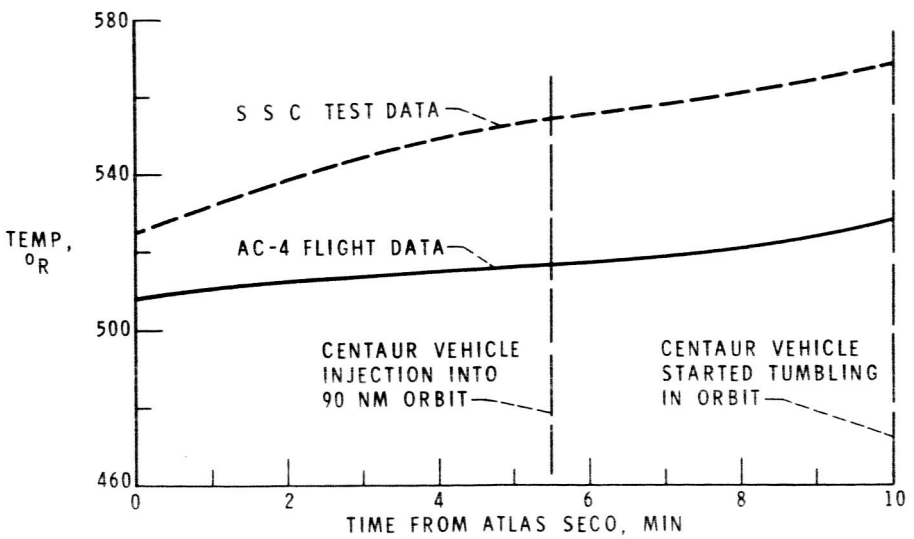

Figure 10

NOSE FAIRING INSTALLED IN SSC

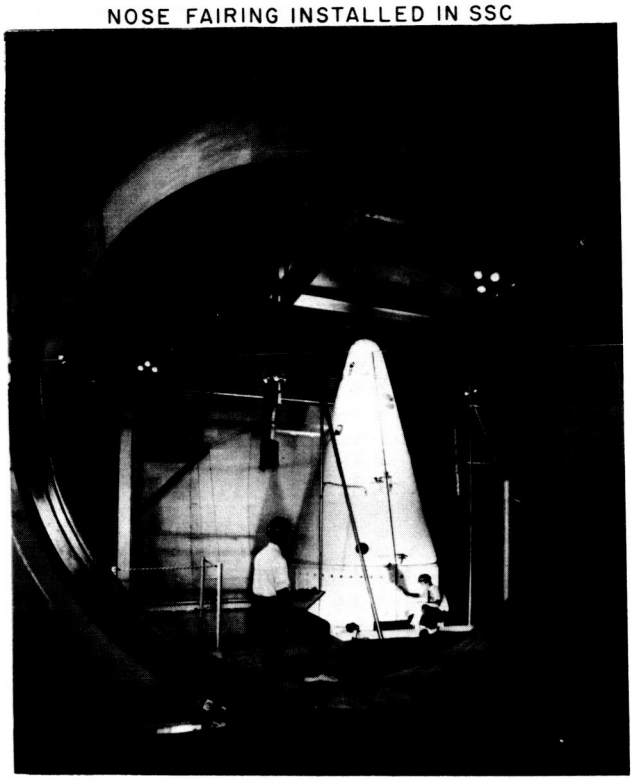

Figure 11

NOSE FAIRING JETTISON SETUP IN S S C

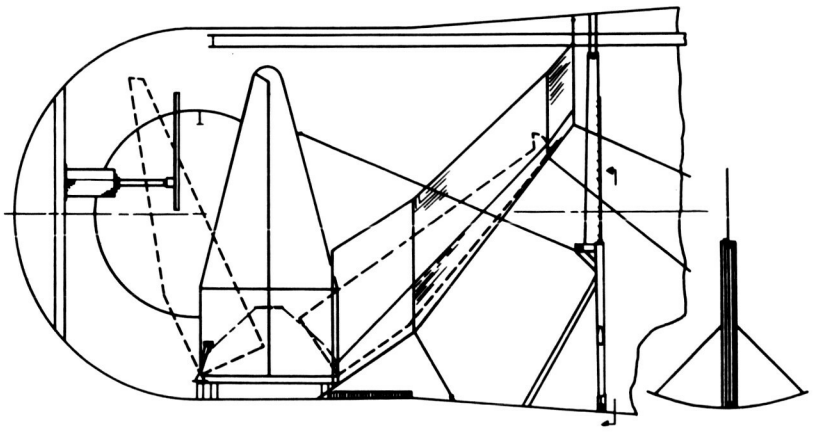

Figure 12

NOSE FAIRING AFTER JETTISON IN S S C

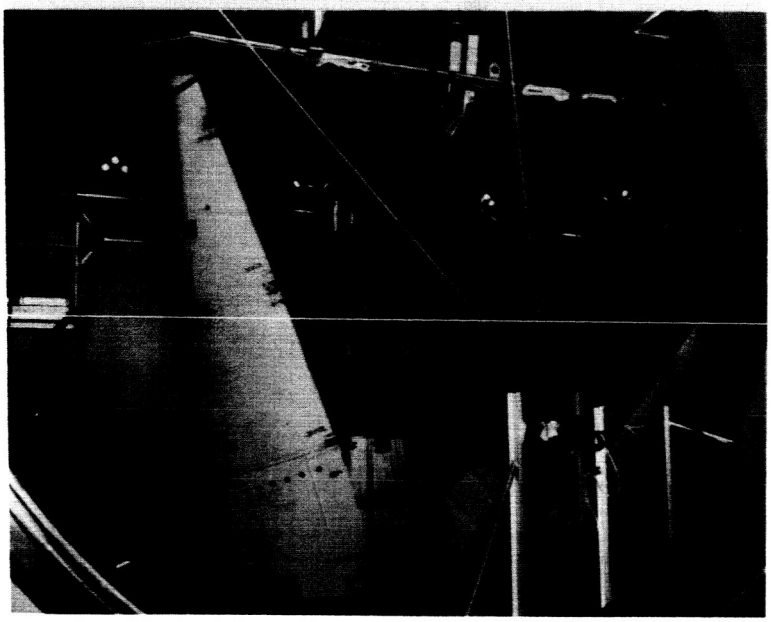

Figure 13

DAMAGED NOSE FAIRING AFTER FIRING IN VACUUM

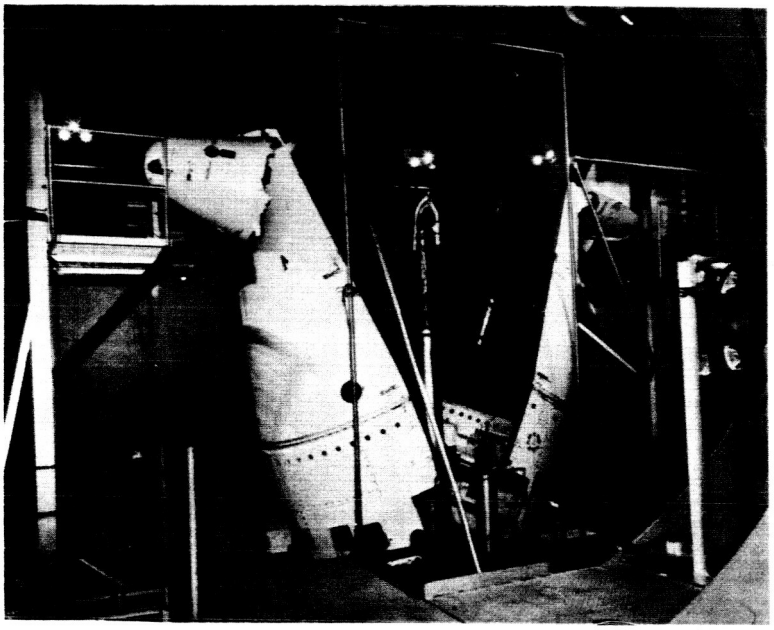

Figure 14

COMPARISON OF CENTAUR–SURVEYOR NOSE FAIRING TRAJECTORIES

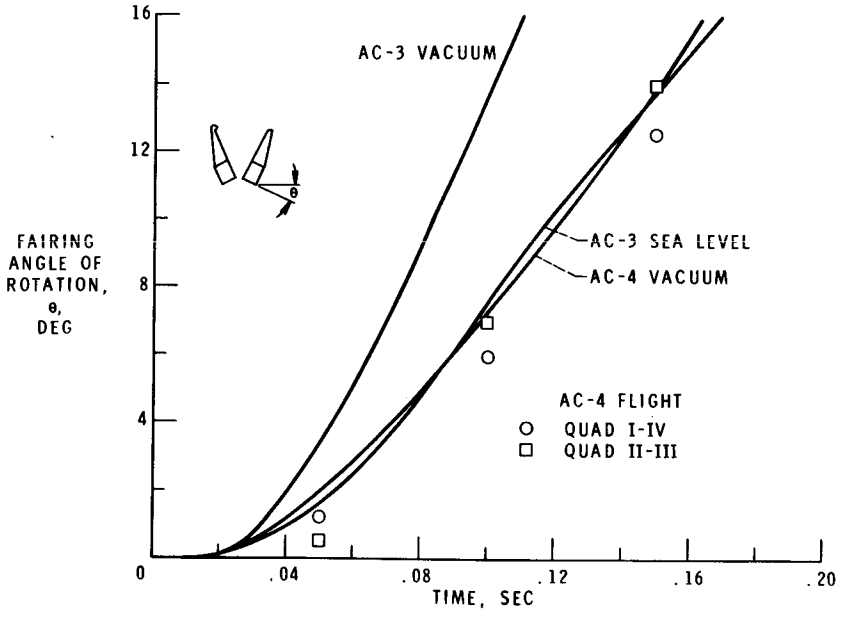

Figure 15

AC-4 NOSE-FAIRING SEPARATION, VERTICLE HINGE LOADS

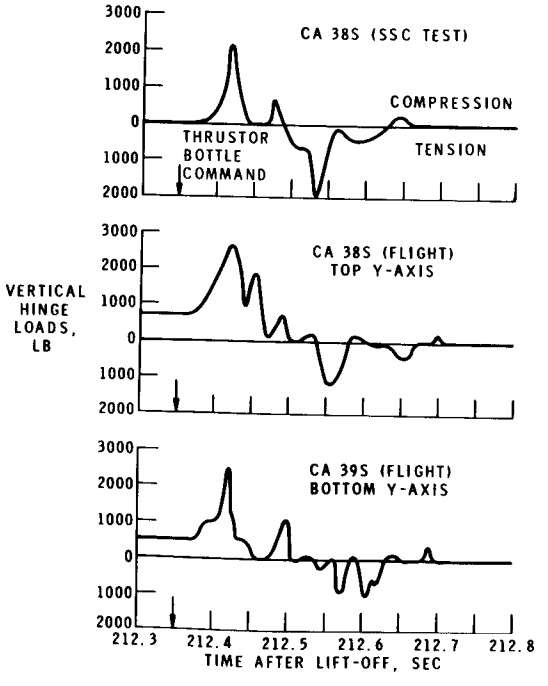

Figure 16

Small Glass Systems-A Comparison with Metal Systems

Ilmars Dalins

George C. Marshall Space Flight Center
Huntsville, Alabama

INTRODUCTION

The discussion presented herein is a result of experiences gained using glass, metal and ceramic vacuum components in connection with surface physics research. For the most part this involves the design and fabrication of vacuum glass tubes used in field emission, field ion microscopy and low energy electron diffraction. In the majority of cases such research requires the control of surface conditions on atomic scale, which implies the necessity for ultra-high vacuum in 10^{-10} to 10^{-12} Torr range. Such small vacuum chambers usually require several electrical feedthroughs, some means to deposit (by evaporation) controlled and reproducible amounts of some substances, (e.g., the adsorbate in adsorption studies). In some instances, there is an additional requirement for means to transmit mechanical motion into the chamber to manipulate some of the components which have been placed in the vacuum environment.

Purification of such substances as alkali metals by repeated distillation in ultra-high vacuum can be accomplished in a relatively straightforward manner. The system requires a number of seals that can be opened in vacuum by breaking them off with a magnetic hammer, and glass constrictions that can be sealed from outside without breaking vacuum. Frequently, in conjunction with surface physics research, there arises a need to perform vacuum brazing in connection with some metal ultra-high vacuum component fabrication. The brazing requires pressures only in 10^{-5} to 10^{-6} Torr range. A "hybrid system" consisting of a glass bell jar, a metal oil-diffusion pump, metal valves, chevron baffles, o-rings, etc., of rather conventional design is suitable for this purpose. This system involves considerable gas-handling capability because of degassing; therefore a pumping system of large pumping capacity is required. Since this type of system, although indirectly useful to surface physics research, does not represent anything unique experience-wise, it will not be discussed further.

In general, the use of vacuum in surface physics research involves techniques which are considerably different from those associated with testing of spacecraft or its components in large space simulators. In surface physics the investigation is usually directed toward

clarifying details of some atomic interactions such as adsorption, desorption or atomic surface migration, etc., while an engineering design detail is usually tested in a large space chamber. In small glass systems the dimensions of the vacuum chamber and the associated components, not the test object, determine the size and volume. Thus, in a small demountable vacuum system, the flanges and seals generally determine the size of the system. The size can be reduced considerably by using an all glass, one-piece construction. This, however, results in an assembly that cannot be conventiently disassembled for modification or repair, and subsequently reassembled without taking into consideration the limitations imposed by the glass-blowing operation.

In the following discussion the advantages and disadvantages of glass systems are compared with metal ones. This is not an attempt to justify the exclusive use of the glass vacuum system in testing spacecraft, but to point out that in the development of some components the glass ultra-high vacuum system might be a solution to certain problems. The lower cost of such a system is a major factor in its favor. For instance, in connection with spacecraft component testing, there might arise the need to study some atomic interactions with the surfaces. Some considerations follow which might be helpful in the selection of a vacuum system for the task.

ADVANTAGES AND DISADVANTAGES OF GLASS ULTRA-HIGH VACUUM COMPONENTS

The discussion of the unique features of glass is arranged in the order that they arise in surface physics research. It appears that this order will remain substantially unaltered in some other applications.

The Transparency of Glass

This feature of glass as a material for ultra-high vacuum applications is of basic importance. Certain complicated operations and manipulations can be readily accomplished without resorting to a complex instrumentation, which might even require its own development. A typical example is again the vacuum distillation of alkali metals mentioned earlier. A suitable, yet inexpensive glass apparatus can be readily constructed so that the distillation process and the location at which the alkali vapors condense may be observed. This distillation has become a rather routine process. There are other processes in surface physics research which involve some sort of

manipulation of certain components inside the ultra-high vacuum chamber. The transparency of glass can simplify these manipulations considerably. Ultra-high vacuum components of unique design may be readily fabricated in glass shop.

Excellent Electrical Insulation Properties of Glass

Electrical feedthroughs are quite a common requirement in a vacuum chamber. There are ample variations in design available commercially since glass-to-metal sealing is a rather well-developed process. It is customary however, to use ceramic insulators in a metal system. Consequently, it appears desirable to discuss their shortcomings in comparison with glass. Since these insulators are not transparent, they cannot be utilized even as crude viewing ports. In addition, only limited forms of ceramic insulators are available commercially. Unique requirements for insulators occur quite often, but ceramic-to-metal sealing processes are quite critical, and, consequently, very much exclude the possibility of fabrication in the research laboratory requiring the special design. The ceramic-to-metal seal development is a major effort itself. The two processes known as: (a) active alloy process and (b) sintered metal powder sealing are described quite satisfactorily by Kohl [1] and Rosebury. [2] Recently, both types of ceramic seals became available commercially. The active alloy version was available first. The chemical reaction essential to accomplish the sealing between the ceramic and metal is quite often incomplete and continuous if raised to sufficiently high temperatures. This limits the bakeout temperatures of the order to 300°C to 350°C.

The sintered powder sealing technique requires hydrogen firing above 1200°C. This process has become quite popular in the electron tube field. The electrical feedthrough made by this latter method can be baked at 450°C for many hours. In order to arrive at suitable seals in a laboratory following of instructions in the literature alone is usually not quite enough. [1, 2] Some time and effort must be devoted to master the technique which results in leakproof seals. After this is achieved it is advisable follow the procedure carefully. Otherwise, in the event of difficulties, it becomes very time consuming to pinpoint the difficulty and eliminate it. It is possible for problems to arise in connection with the constituents of the sealing compound, as well as the procedures used in firing (e.g., the purity of the hydrogen gas and the geometry of the seal).

In general, it is necessary to recognize that the ceramic-to-metal sealing procedures are quite complicated, and the basic

mechanisms involved in the sealing process are not satisfactorily understood. In view of their great importance and bearing to the field of vacuum technology, more detailed study is in order. Elegant tools such as the "electron probe microanalyzer" are available to many laboratories, and can yield very good insight into sealing processes. The electrical feedthrough problem is practically nonexistent with glass insulators. Glass can be readily shaped so that various geometrical forms from various manufacturers of insulators can be adapted to the chamber. In the case of ceramic insulators, the dimensions must be carefully selected to suit the mating parts.

Leak Detection

Leak detection in a vacuum technology has been described by many authors as a very unpleasant task, [4, 5] usually requiring special and relatively expensive detection equipment. In glass systems, the unpleasant task of leak hunting can be alleviated by using an inexpensive Tesla coil (approximately $13) which is capable of detecting most of them. The task is further simplified since the examination for leaks is performed at pressures in the micron range, i.e., operating the forepump only. Repairs of a leak can readily be performed in all glass systems by fusing the glass shut with a glass blower's torch.

This leak detection method also has its limitations. Leaks around glass-to-metal seals cannot be detected with this equipment. Alternative methods, such as use of a mass spectrometer type of leak detector, have not been very popular with glass system operators, primarily because of the substantial cost of such an instrument. Acetone, freon, or various gas probes are commonly used together with the ion gauge as the leak indicator.

A word of caution with regard to the use of the Tesla coils when field ion microscope or field emission microscope tubes have been sealed to the vacuum test chamber. The field emitter point is often lost as a result of the high voltage sputtering. This inconvenience can be readily eliminated by testing the system before the field emission tube is sealed on the vacuum system.

Ease of Fabrication

This convenience is quite useful in certain preliminary exploration when the experimental parameters and procedures to be followed are not well defined and modifications of the geometry of the vacuum test chamber will be necessary during the course of the test. For instance, the fastening of side arms at odd angles and the adding of an extra set of electrical feedthrough, etc., can readily

be made. Thus the advantages of glass are quite apparent in this respect, and often result in substantial savings of time, funds, and effort.

Chemical Resistance of Glass

Ultra-high vacuum achievement in small chambers is associated with bakeout at as high temperatures as are compatible with the structural materials used. In a Pyrex (Corning 7740) glass system the bakeout temperature is limited to 450°C, because graded seals involve glasses that soften and collapse above that temperature. Oxidation is also a problem insofar as the metal parts of various seals and feedthroughs are concerned. Use of oxidation-resistant metals or alloys for the leads has been quite satisfactory. Previously, it has been necessary to resort to such expensive procedures as employing a protective atmosphere during bakeout. If alumino-silicate glasses like the Corning 1720 (EE glass) are used, 600°C bakeout is readily possible. Even 680°C has been reported. [6] Molybdenum is used as leads in the electrical feedthrough construction. Inert atmosphere normally is required to protect such leads from oxidation during the elevated temperature heating. Such measures appears to be avoidable by chromalizing [7] these metal parts. Chromalizing implies a vapor phase deposition of a dense layer of chromium on molybdenum or other substrates. High temperatures are used in the process so that diffusion occurs and the resulting coating adheres well to the molybdenum and is oxidation resistant. The chromium content at the coating surface is the highest, therefore, most resistant to oxidation. Such leads are oxidized in a wet hydrogen at 1100°C before beading them with glass. The subsequent glass working is rather standard.[8]

The Fragility of Glass

The fragility of glass is one of the major disadvantages to its use. It is also a major reason why glass vacuum systems are not very popular in various laboratories. Usually, lack of scientific glass-blowing capability in, or associated with, a particular laboratory is the principal reason not sufficiently investigating glass system capabilities. Nevertheless, even after a suitably skilled glass blower is integrated into the laboratory personnel, certain accidents with glass systems occur from time to time. Some are as a result of negligence and can be readily prevented. Others occur even in spite of careful consideration and substantial efforts to eliminating troublesome design details.

As a rule, accidents occur more often with glass systems in which one or more large magnets are present (e.g., ion pumps, magnetic type of mass spectrometer, etc.). These magnets are

especially dangerous if placed in close proximity to each other. Accidental placement of magnetic materials, such as steel screw drivers, wrenches, etc., can provide a low reluctance pass for the magnetic field which subsequently results into generation of large forces and breakage.

Difficulties in Holding Tolerances

This is by far the most serious drawback in the use of glass in ultra-high vacuum technology, especially where accurate geometrical relationships of parts must be maintained. Except when certain fixtures are used, the control of dimensions in glass-blowing operations is very limited, usually to the glass blower's visual judgment and approximate measurements. This results in the dimensions of a glass vacuum chamber being much less accurate (about 1/32 of an inch) than the corresponding metal parts prepared in machine shops. Since glass blowing is associated with temperatures in the range of 1000°C, there is always the danger of deformation of prealigned components such as various electrodes of an ion or an electron gun. High temperatures are not only necessary for sealing but for annealing of glass after the glass sealing or joining operation is completed. Although a somewhat cooler flame is used, it is larger and, combined with a relatively long time required for annealing, is more likely to produce deformation and misalignment than the glass-blowing operation proper.

A lack of special holders and jigs used to improve the control of dimensions is very common in a research laboratory in which the items to be fabricated have a unique design. The design and fabrication of auxiliary fixtures and tools is quite often as time consuming as the fabrication of a prototype tube or chamber itself. The variety of tools available commercially for glass shops is inadequate. Most of them have been developed in connection with research in chemistry. The electron tube industry, on the other hand, can very well justify a development of certain special tools, because it is usually involved in the subsequent manufacture of a considerable number of tubes developed earlier. The effort and cost associated with this type of operation consequently becomes well justified. This is not so with efforts expended in a research laboratory. Even in numerous instances where the use of glass ultra-high vacuum chambers indicates distinct advantages, they are reluctantly accepted primarily because of lack of the necessary tool development that must be made to perform certain alignments. Improvements in this area are urgently needed.

Helium Permeation Through Glass

It has been known for some time that the very popular Pyrex brand (Corning 7740) glass is permeable to atmospheric helium to the extent that pressures of 10^{-9} Torr accumulate in an evacuated glass envelope in a matter of hours. [9] Surface physics, especially field emission microscopy, quite often requires lower pressures.

Several techniques used to improve this have met with quite satisfactory results. It is possible to store small sealed tubes in an evacuated container (i. e., in an evacuated glass dessicator). If the experimentation lasts less than an hour the helium accumulation will be relatively small. Keeping glass at liquid nitrogen temperatures is also very helpful and can be accomplished in some instances. There are other techniques like cesiation of Pyrex glass (decomposition of cesium nitrate in a heating process at about 420°C). A coating forms on the inside wall [10] of the vacuum chamber lessening the helium permeation.

Helium migration through the wall can be reduced by as much as 10^4 [11] by using alumina silicate glass such as Corning 1720. As mentioned earlier, this glass permits high bakeout temperatures (600 to 680°C) and can be joined with molybdenum. With such an extensive degassing it is possible, with some precautions, to seal off a field emission tube with temporary pressure increase to 10^{-9} Torr. By use of gettering, pressures in 10^{-12}or even 10^{-13} Torr range can be maintained. The use of Corning 1720 at the present time is limited to laboratories with quite well-equipped glass shops that can afford to make their own feedthroughs, glass-tp-metal seals, etc. Very little, if any, are available commercially. Commercial availability of such items as three-stage mercury diffusion pumps made of Corning 1720 would be an asset to the ultra-high vacuum technology involving all glass systems.

SUMMARY AND CONCLUSIONS

In some instances, glass ultra-high vacuum systems offer special features which should not be overlooked, especially in various preliminary tests when the exact geometry and number of electrical feedthroughs are subject to change or there is a definite requirement for visual observation. An ultra-high vacuum pumping station, using a commercially available three stage glass (Pyrex) mercury diffusion pump, is by for the least expensive (about $2000 in components), and pressures in 10^{-10} Torr range can be readily achieved.

The limited acceptance of glass ultra-high vacuum systems can be easily traced for the most part to fragility of glass and difficulties in holding tolerances in fabrication processes. Another major shortcoming of small glass systems at present is the lack of a partial pressure analyzer which is compact enough, light enough, and does not depend upon a magnetic field for operation. Improvement in this area is recommended.

REFERENCES

1. Kohl, W. H., "Materials and Techniques for Electron Tubes," Reinhold Publishing Corporation, New York, New York, 470-518, (1960).
2. Rosebury, F., "Handbook of Electron Tube and Vacuum Tube Techniques," Addision-Wesley Publishing Co., Reading, Mass., 67-75, (1965).
3. Birks, L. S., "X-Ray Spectrochemical Analysis," Interscience Publishers, Inc., New York, 98-123, (1959).
4. Roberts, R. W., Vanderslice, T. A., "Ultra-high Vacuum and Its Applications," Prentice-Hall, Inc., Englewood Cliffs, N. J., 130, (1963).
5. Tasman, H. A., Boerboom, A. J. A., and Kistemaker, J., (chapter on Vacuum Techniques), "Mass Spectrometry" edited by McDowell, McGraw-Hill, New York, 327, (1963).
6. Private communication from staff of Field Emission Corporation, McMinville, Oregon.
7. Hees, G. W. and Earley, D. K., "Advances in Electron Tube Techniques," edited by D. Slater, Proc. 5th National Conf., 45-46, (Sept., 1960).
8. Wheeler, E. L., "Scientific Glassblowing," Interscience Publishers, Inc. New York, 157-182, (1958).
9. Rogers, W. A., Buritz, K. S. and Alpert, D., J. Appl. Phys., Vol. 25, 868 (1954).
10. Bryant, P. J., Private communication. South West Research Institute, Kansas City, Missouri.
11. Norton, F. J., J. Am. Ceram. Cos., Vol. 36, 90, (1953).

LARGE SPACE CHAMBER REQUIREMENTS

Norman A. Crone
Office of Manned Space Flight
NASA Headquarters
Washington D. C.

We are more than a little concerned about the relatively new and complex technique of ground testing. The extensive investment required for such test facilities, particularly those of large size, dictates the need for a very careful evaluation of any new requirements. It also requires the assurance of proper utilization of existing facilities. Congress has proved to be most critical of such costly facilities, particularly when direct program support is not easily identified. Efforts to obtain congressional approval are further complicated by the long lead time necessary to design and construct a large vacuum chamber.

Advance studies now underway for NASA's future programs indicate that space systems, and even subsystems, will exceed the size limitations of existing vacuum chamber facilities. This projected gap in facilities is largely due to the present ground testing philosophy which requires full scale operational systems testing, with astronauts, in the simulated space or lunar surface environment. If developments in model testing yield significant and useful data under simulated space environment conditions, the need for much larger vacuum chambers would be considerably reduced. Perhaps, with time, our knowledge of the effects of space conditions on materials and equipment will give us enough confidence so that we may drop the requirement for combined systems testing altogether. This, however, is not foreseen at the present time.

The United States Air Force Systems Command is also concerned about their future space program requirements. Through the Arnold Engineering Development Center, Tullahoma, Tennessee, they have expended considerable effort in developing a "state-of-the-art" concept for a suitable space simulation chamber known to most of us as the 220' diameter Mark II chamber. The requirements for such a chamber are based on future program projections as yet unapproved and, consequently, the project has not received DOD approval so far.

General Ritland of the Air Force Systems Command discussed the matter more than a year ago with Dr. Mueller, the NASA Associate Administrator for Manned Space Flight, and suggested that our requirements be combined to strengthen the justification. He further suggested that a single national facility concept be considered. As a result, a joint NASA/DOD Working Group has been established to review and evaluate large space chamber requirements. This group, consisting of four Air Force officers and four NASA representatives, first met in May 1964. Since that time, the developments in advanced studies for future programs have been closely monitored, and projections have been made for future program schedules.

As a result, our future projections indicate that we still have some breathing time before having to make a decision whether any larger chamber would be required.

For, unlike large wind tunnels and propulsion facilities, the projected requirements for large vacuum chambers tend to fall in the category of complete systems proof testing - or even astronaut training, and not the early developmental testing of components and configurations so familiar in wind tunnel work. It, therefore, appears that the requirement for large vacuum chambers shows up somewhat downstream in a development program, rather than at the start.

The most effective use of this breathing time, then, is our current objective. In addition to keeping track of changes in future programs and their schedules, the NASA/DOD Working Group is attempting to study trends in the development of current chambers and their utilization. In so doing, the group will monitor technological progress in Space Environment Simulation and keep abreast of developments in ground testing philosophy. Special studies will be initiated as necessary to clarify vague requirements and to identify alternate possibilities. It is intended that a sound basis be developed for evaluation of future program requirements which will enable complete and proper justification of the needed facilities before the Congress.

Studies already undertaken by this working group include a detailed evaluation of existing facilities and potential modifications to those facilities that would satisfy the test philosophy specified for the "Apollo Logistics Support System" (ALSS). This study was conducted by the Army Corps of Engineers under a special task to NASA. Other programs have been studied within NASA to identify future systems configuration, dimensions, and functions. The majority of these studies have resolved most testing requirements into two basic environments. One is the suspension of vehicles in space exposed to the direct rays of the sun, vacuum, and the cold blackness of space in all directions. The other environment is operation on the lunar surface. Movable vehicles and lunar construction problems present many complex simulation requirements. Some of these requirements appear to be prohibitive either for cost reasons or for technical complexity. Many of the environment simulation techniques now in use require improvement to assure confidence in the validity of test results.

Some of the areas in which the Joint Working Group is particularly interested and in which both government and industry will be encouraged to greater activity are:

1. The establishment of an acceptable standard for "Man Rating" vacuum chambers.

2. The development of a practical ground test philosophy compatible with mission reliability requirements.

3. The continued improvement of environment simulation techniques and the development of a suitable standard of reference for each one.

4. The development of instrumentation techniques and a standard for comparison of various chambers throughout the Government and Industry.

The Joint Working Group will insure a close coordination of requirements for large space simulation chambers by both NASA and the DOD. It will aid in the exchange of information on technological progress and improved techniques. It will encourage more efficient utilization of existing large chamber resources through cooperative planning efforts. When the time comes to build a larger chamber, this group will study the matter of a joint national effort and determine such parameters as siting and appropriate ownership.

It has been my intent to acquaint you with the purpose of the Joint NASA/DOD Working Group, its plans and objectives. I would like, also, to solicit your continued support and cooperation on this subject. You can do this through reports of significant developments and progress in your particular areas of effort. You can provide invaluable assistance in the evaluation of study efforts undertaken by this group. You will also be asked at times to provide information on operational experience, planning efforts, or even facility availability in support of our activities. Your cooperation in this effort will be greatly appreciated.

A SURVEY OF VACUUM TECHNOLOGY RELATED PROGRAMS OF AERO-ASTRODYNAMICS LABORATORY

by

JAMES O. BALLANCE
FLUID MECHANICS RESEARCH OFFICE
AERODYNAMICS DIVISION
AERO-ASTRODYNAMICS LABORATORY
MARSHALL SPACE FLIGHT CENTER

PRESENTED AT THE NASA HIGH-VACUUM TECHNOLOGY, TESTING, AND MEASUREMENT MEETING, JUNE 8-9, 1965, NASA, LEWIS RESEARCH CENTER, CLEVELAND, OHIO

A SURVEY OF THE VACUUM TECHNOLOGY RELATED PROGRAMS OF AERO-ASTRODYNAMICS LABORATORY

A. INTRODUCTION

There are several programs within the Aero-Astrodynamics Laboratory at MSFC which are based on the same foundations as vacuum technology. It is very interesting to note that, when vacuum techniques are mentioned, normally one thinks of stainless steel chambers, cold traps, diffusion pumps, etc., and all the problems associated with this equipment. There are problems, however, which are of the same character as those in a typical vacuum system but are in no way bounded by the same conditions. For example, consider the measurement of densities at high altitudes. For densities low enough, ionization gauges not unlike those used on a convential vacuum chamber are plagued with the same uncertainties such as composition of the gas, ionization efficiencies, tabulation conductances, outgassing rates of components, as well as more unique disturbances due to their use, such as the high relative speed of the probes (on an orbiting vehicle) to the random, thermal speed of the molecules, charged particles, orientation, etc. Other examples are free molecular flow drag coefficients which are based on the same fundamental concepts as molecular flow through tubes, and when concave surfaces are considered, the calculations are quite similar to molecular flow in tubes.

Thus, many of the studies conducted by the Aero-Astrodynamics Laboratory and classified mainly as rarefied gas dynamic studies have application in the general area of vacuum technology, and in fact, the solutions from vacuum studies form a boundary condition for most of our application.

This paper presents a brief survey of the program areas and tasks pertinent to this meeting. These areas can conveniently be categorized into three topics: (1) Rarefied Gas Dynamic Studies; (2) Environmental Measurements at Ultra High Altitude; and (3) Aerodynamic Testing Facility Improvement Studies. A brief description of problems within these areas, the effort being expended (both in-house and on contract), and some results are discussed.

B. RAREFIED GAS DYNAMIC STUDIES

These efforts include (1) the theoretical studies of free molecular flow and transition flow with a close look at the parameters which define the flow, (2) probe response in free molecular flow, (3) molecule-surface interaction studies, (4) theoretical and experimental studies of drag coefficients, and (5) jet-spreading studies at orbiting altitudes.

1. Free Molecular Flow and Transition Flow

Since the work of Clausing in the determination of transmission probabilities for molecular flow through configurations of various geometries, perhaps the most significant, but little used, effort is that of Oatley, who showed the method of coupling transmission probabilities of simple components into a total transmission probability for a complex system. Oatley's [1] method has some obvious faults and has yet to be applied to several important configurations in use by vacuum technologists today. Santeler [2] pointed out several of these needs. Some of the limitations of Oatley's method have been pointed out by Ballance [3] where Monte Carlo computer programs examined the configurations. Some of the analytical models being used are shown in Figures 1 and 2; Figure 3 and 4 show the comparison of Monte Carlo and probability methods.

2. Probe Response

Two solutions of pressure probe response have been reported, one by deLeeuw and Rothe [4] and the other by Ponds [5]. After some manipulation of the data by deLeeuw and Rothe, it is seen that these solutions are identical. Since these solutions are based on parameters calculated by Clausing for straight bore tubes, the addition of orifices, blocking plates, etc., to the probe configuration changes the problem so greatly that these same methods cannot be used. To examine the complicated configurations, a Monte Carlo computer program quite similar to that used by Davis [6] has been developed, including the speed ratio; i.e., the ratio of the relative mass motion of the gas and the probe to the thermal motion of the gas. This is described fully in Reference 13. Since this program is written very simply in Fortran, anyone interested in these configurations can easily adapt it to their computer. Figure 5 shows a typical set of solutions. From the basic program, the information which may be obtained in addition to the transmission probability includes entrance flux distribution, exit flux distribution, the flux exiting the tube through the entrance plane, the number of collisions for each molecule, the distribution of molecules along the wall at the first collision, and the angular distribution of molecular trajectories exiting the tube. Other parameters which can be included, but not shown in the basic program, are reflection coefficients and accommodation coefficients.

3. Molecular-Surface Interaction Studies

These studies are being conducted by Dr. Walter J. Schaetzle at the University of Alabama, NASA Contract NAS8-5326. The objective of the program is the determination of normal, tangential, and thermal accommodation coefficients at high molecular velocities as a function of

speed ratio. The technique being used to produce the molecular beam is straightforward. Ions are to be produced in modified Kaufman ion engine, accelerated to the desired velocity, focused by electromagnetic focusing, de-ionized, and the neutral particles impinged on the surface of interest. The experimental system is in various stages of progress. Although the vacuum system is completed, improvements are being made to allow 10^{-8} Torr pressures in the target chamber during tests. The accelerator is being assembled and preliminary calibration of the force probes are being made. It is expected that valid data will be taken within six months. The design criteria for the acceleration is shown in Figure 6.

4. Drag Coefficients

Free molecular flow drag coefficients are easily calculated for simple surface as shown by Patterson [7] . When complicated geometries are considered, especially concave surfaces, little work has been done. Chahine [8] and Sparrow [9] have examined concave cylindrical surfaces and a concave hemispheres and Wimberly [10] has extended concave hemispheres at angle of attack. These calculations, though, are for hypervelocity regions where the thermal velocities of the molecules can be ignored. The Monte Carlo approach can be applied to this problem and can be used to look at all speed ratios.

5. Jet Spreading

The program being considered is classified as jet spreading, since it is the free molecular flow analogy to the more usual jet spreading calculations made for rocket engines, etc. The flow distribution exiting from tubes under free molecular flow conditions, both within the tube and outside the tube, was examined in detail by Clausing [11] and re-examined more fully by Dayton [12]. The total probability of passage,

the angular distribution can easily be calculated with this approach. The change in the angular distribution with a change in Knudsen number for the flow in the tube will be examined in detail both analytically and experimentally.

C. ENVIRONMENTAL MEASUREMENT PROGRAMS

Among the areas of responsibility of the Aero-Aerodynamics Laboratory is that of defining the natural environment for the Saturn class launch vehicles. One of the critical areas for orbital lifetime studies is the density of the atmosphere at orbital altitudes. Conventional and modified laboratory-type vacuum instruments are now being used by many space systems, and the problems encountered in using and interpreting the data in laboratory conditions are magnified by their use on the vehicle. Two systems with great promise are being considered by our Aerospace Environment Office. One of these is a modification to the thermosphere which was developed by the University of Michigan for Goddard Space Flight Center. This probe will be launched in a ballistic trajectory by a Nike-Tomahawk launcher and should make measurements from 120 km to about 350 km. Basically this probe is a cylinder with an orifice at one end behind which is an omegatron-type spectrometer. This spectrometer will alternately scan for oxygen (both O and O_2) and nitrogen. The earlier thermospheres had a Bayard-Alpert-type, nude ionization gauge at the other end of the cylinder. For this program, this gauge will be replaced by an earth aspect sensor so that, with radar tracking and with the sun aspect sensor on the thermosphere, analysis of the tumbling body may yield angle-of-attack data from which any "winds" which might exist at these altitudes might be calculated. The first measurements with these probes are scheduled for December 1965.

The second system being considered is a cryogenically-cooled collection device which is used as a type of McLeod gauge. This device was proposed by the Celestial Research Corporation. A preliminary design of the probe is shown in Figure 7. The molecules would enter the cold (4^{o} K) honeycomb areas and would condense on the plates. At orbital velocities and for reasonable accommodation coefficients, the capture probability for the system should be quite high. After collecting for a known length of time, the cold collector is rotated, cammed into a sealing plate, and warmed to a preselected temperature. The condensate evaporates, and the pressure is high enough ($\approx$ .1 to 1 Torr) where simple measuring devices can be used. A complete engineering study of this system is being made.

D. AERODYNAMIC FACILITY IMPROVEMENT STUDIES

To determine the base heating ratio on Saturn type launch vehicles, an impulse base heating technique has been developed. This is a shock tube type system where combustion is initiated in the mixing of the gases from two shock tubes, and the high temperature gas flows through a model engine assembly into a vacuum system. Measurement times during this process range up to about 10 to 15 milliseconds. One of the limiting parameters in the system is the interference of the reflection of the initial shock wave into the vacuum tank with the continuing flow through the nozzles. If this interference could be removed, useful measurement times could be extended by 50 to 100 milliseconds.

The volume flow from a typical hydrogen-oxygen combustion is approximately 50 per cent water vapor and 50 per cent hydrogen. It would be quite easy to cryopump the water vapor with a liquid nitrogen cooled

shroud around the nozzle exit. The hydrogen, of course, would not condense. It is possible, however, to cryotrap the hydrogen within the condensate of the water vapor. Some success in this method has been reported. However, even without cryotrapping as the main mechanism, it may be possible with appropriately designed cryopanels to lessen or even destroy the shock wave. An even more important mechanism would be entrainment of hydrogen in the space of a honeycomb material by incoming water vapor, acting as a type of diffusion pump during the flow. Although the hydrogen would escape, when the flow stopped, this would be of no consequence.

E. CONCLUDING REMARKS

This brief survey of programs within the Aero-Astrodynamics Laboratory at MSFC indicates the relationship of other disciplines to vacuum technology. None of the programs have been described in depth, but if anyone would like further information personnel of our Laboratory would be more than happy to meet with him.

F. REFERENCES

1. Oatley, C. W., "The Flow of Gas Through Composite Systems at Very Low Pressures," British Journal of Applied Physics, Vol. 8, pp 15, January 1957.
2. Santeler, D. J., "Probability and Molecular Flow in Vacuum Systems," Proceeding of the Fifth Annual Symposium on Space Environmental Simulation, D. W. Male, Chairman, May 1964.
3. Ballance, J. O., "Transmission Probability Determination with Directed Mass Motion and with Mean Free Path Considerations," To be presented at the Third International Vacuum Congress, June 1965.

4. deLeeuw, J. H., and Rothe, D. E., "A Numerical Solution for the Free-Molecular Impact-Pressure Probe Relations for Tube of Arbitrary Length," UTIA Report No. 88, December 1962.

5. Pond, H. L., "The Effect of Entrance Velocity on the Flow of Rarefied Gas Through a Tube," Journal of the Aerospace Sciences, Vol. 29, No. 8, August 1962.

6. Davis, D. H., "Monte Carlo Calculation of Molecular Flow Rates Through a Cylindrical Elbow and Pipes of Other Shapes," Journal of Applied Physics, Vol. 31, pp 1169, July 1960.

7. Patterson, G. W., "Molecular Flow of Gases," John Wiley & Sons, Inc. New York, 1956.

8. Chahine, M. T., "Free Molecular Flow Over Non-convex Surfaces," Proceeding of the Second International Symposium on Rarefied Gas Dynamics, L. Talbot, Editor, Academic Press, 1961.

9. Sparrow, E. M., Manson, V. K., Lundgren, T. S., and Chen, T. S., "Heat Transfer and Forces for Free-Molecular Flow on a Convane Cylindrical Surface," Journal of Heat Transfer, February 1964.

10. Wimberly, C. R., "Determination of Aerodynamic Force and Heat Transfer Properties for a Concave Hemispherical Surface in Free Molecular Flow," R-AERO-IN-11-65, April 1965.

11. Clausing, P., "On Jet Formation in a Molecular Flow," Zeitschrift Fur Physik, Vol. 66, pp 471, 1930.

12. Dayton, B. B., "Gas Flow Patterns at Entrance and Exit of Cylindrical Tubes," 1956 Vacuum Symposium Transactions, pp 5, 1956.

13. Ballance, J. O., "A Monte Carlo Program for Transmission Probability Calculations Including Mass Motion," To be published.

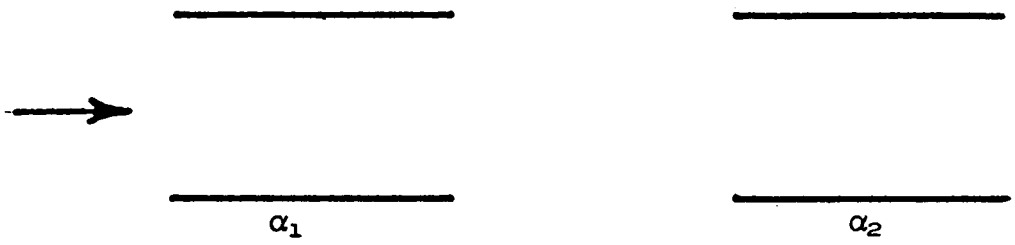

$$\frac{1}{\alpha_T} = \frac{1}{\alpha_1} + \frac{1}{\alpha_2} - 1$$

$$\frac{1}{\alpha_T} = \frac{1}{\alpha_1} + \sum_{i=2}^{N} X_{(i-1)} \left[\frac{1}{\alpha_i} - 1\right] \qquad X_i = \frac{\alpha_i'}{\alpha_j}$$

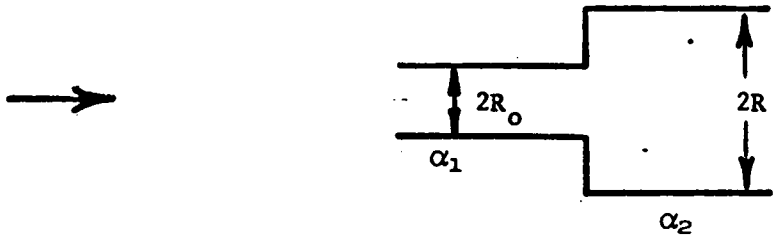

$$F = \left(\frac{R}{R_o}\right)^2$$

$$\frac{1}{\alpha_T} = \frac{1}{\alpha_1} + \frac{1}{F}\left(\frac{1}{\alpha_2} - 1\right)$$

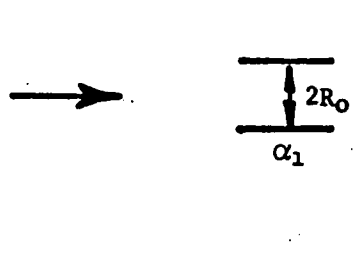

$\alpha_2 = 1$

$X_1 = 1$

$X_2 = (R_o/R)^2$

$$\frac{1}{\alpha_T} = \frac{1}{\alpha_1} + \sum_{i=2}^{N} X_{(i-1)} \left[\frac{1}{\alpha_i} - 1\right]$$

FIGURE 1. ANALYTICAL MODELS

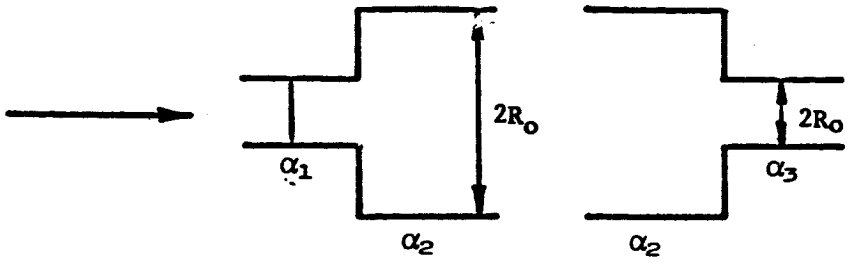

$$\frac{1}{\alpha_T} = \frac{1}{\alpha_1} + \frac{1}{\alpha_2} + \frac{1}{F}\left(\frac{2}{\alpha_3} - 3\right)$$

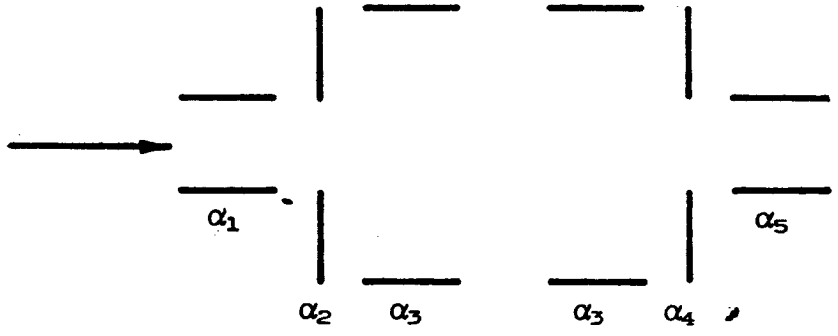

$$\frac{1}{\alpha_T} = \frac{1}{\alpha_1} + X_1\left(\frac{1}{\alpha_2} - 1\right) + X_2\left(\frac{1}{\alpha_2} - 1\right) + X_3\left(\frac{1}{\alpha_3} - 1\right) + X_3\left(\frac{1}{\alpha_4} - 1\right) + X_4\left(\frac{1}{\alpha_5} - 1\right)$$

Equation 6

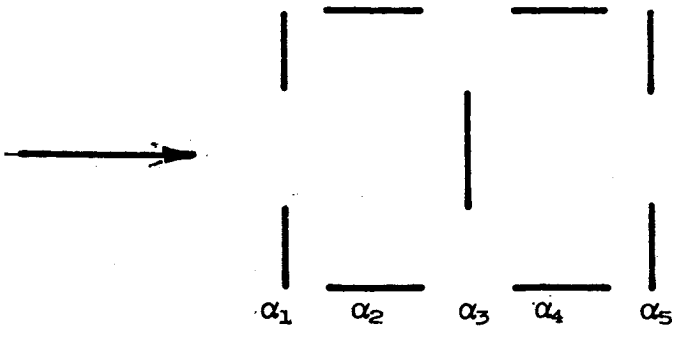

$\alpha_2 \cong \alpha_4$

Equation 7

$$\frac{1}{\alpha_T} = 2 - 3\left(\frac{R_o}{R}\right)^2 + \frac{1}{\alpha_2}\left(\frac{R_o}{R}\right)^2 + \frac{1}{\left(\frac{R}{R_o}\right)^2 - 1}\,\frac{1}{\alpha_2}$$

FIGURE 2. ANALYTICAL MODELS

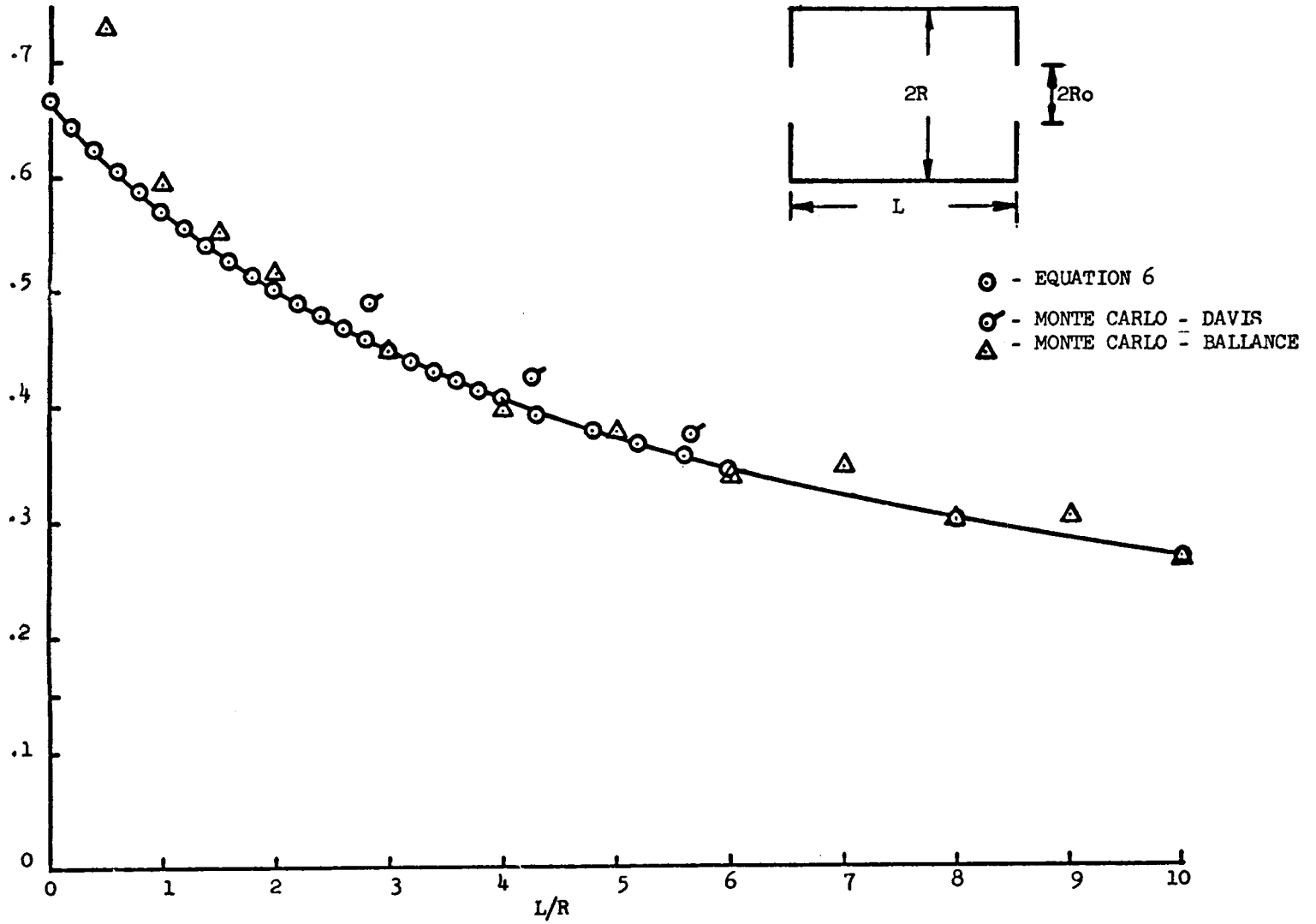

FIGURE 3 - TRANSMISSION PROBABILITIES FOR ORIFICE RESTRICTED TUBES $(R/Ro)^2 = 2$

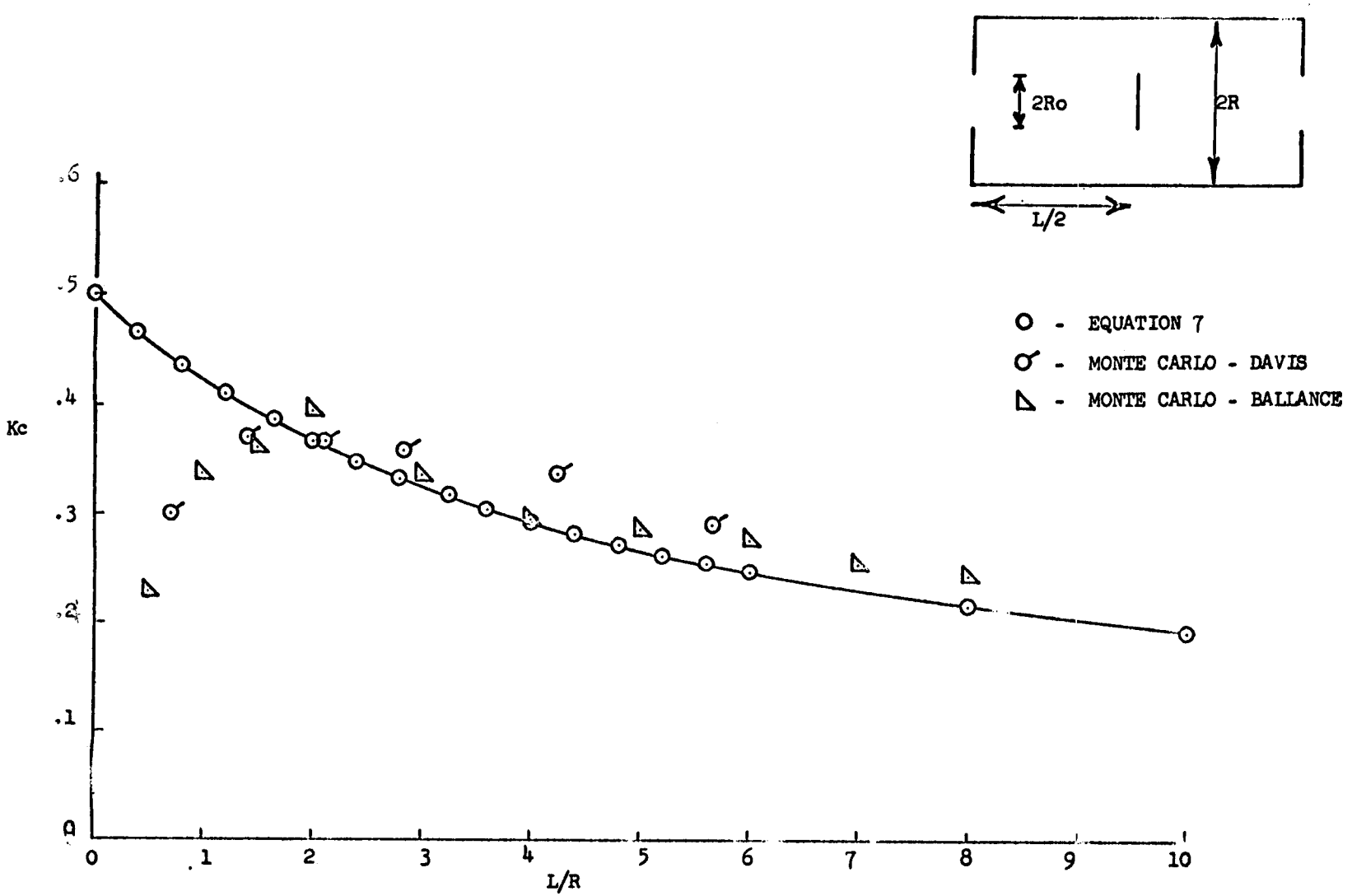

FIGURE 4 - TRANSMISSION PROBABILITIES FOR TUBES WITH CENTRAL BLOCKING PLATE $(R/Ro)^2 = 2$

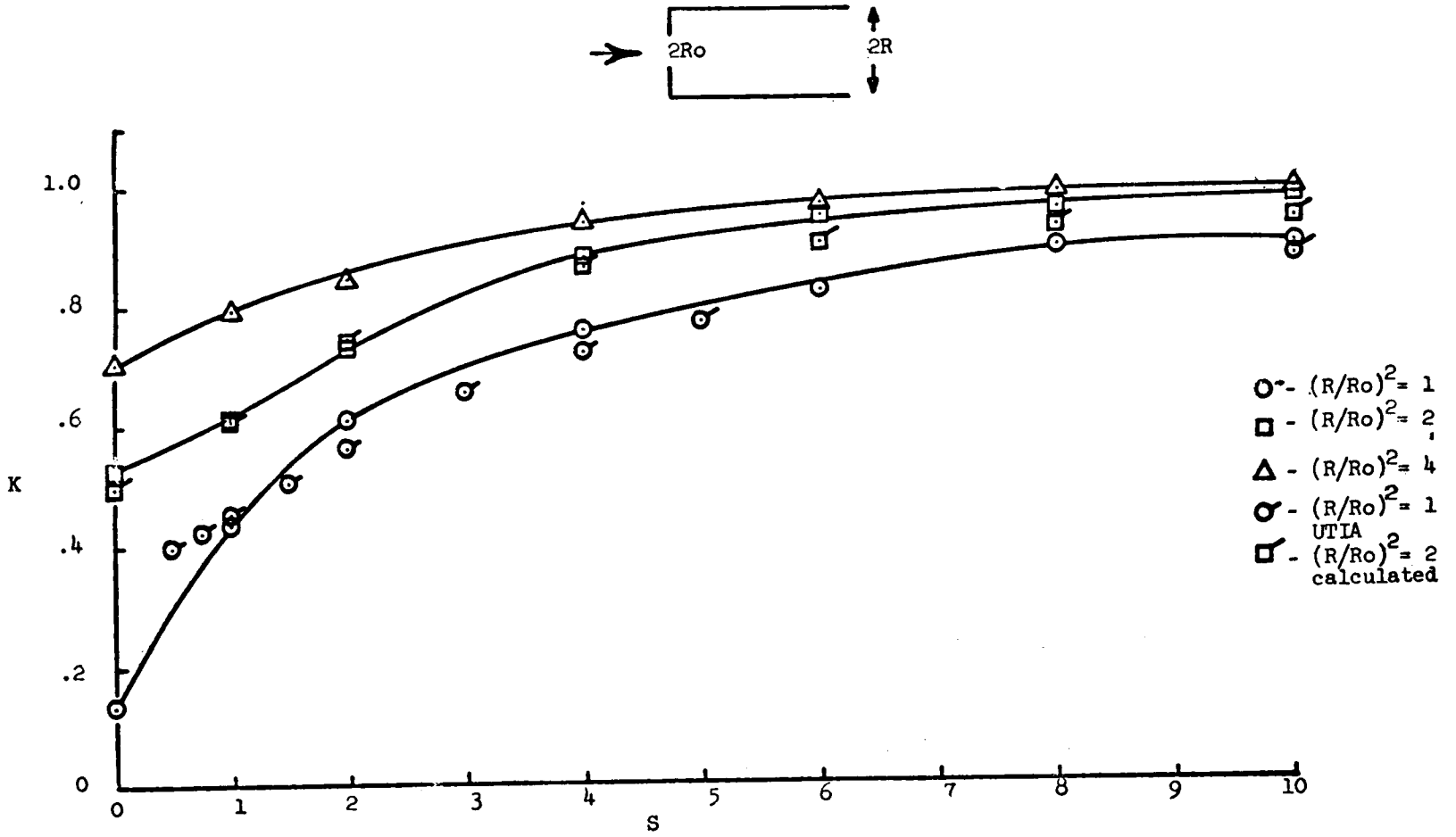

FIGURE 5 - TRANSMISSION PROBABILITIES FOR TUBES AT ZERO ANGLE OF ATTACK FOR VARIOUS SPEED RATIOS L/R = 4

DESIGN CRITERIA FOR ACCELERATOR TO BE USED ON
NASA CONTRACT NAS8-5326 "AN EXPERIMENTAL STUDY
OF MOLECULAR SURFACE INTERACTIONS AT VELOCITIES
UP TO AND EXCEEDING SPACE PROBE ESCAPE VELOCITIES"

PARTICLE VELOCITIES	FROM 4 km/sec
PARTICLE ENERGIES	4 to 1000 EV/molecule
BEAM INTENSITY	10^{10} to 10^{16} molecules/sec
BEAM DENSITY	10^{12} to 10^{18} molecules/cm^3
BEAM DIAMETER	0.2 to 1.0 mm
BEAM CURRENT	10^{-11} to 10^{-4} amperes

FIGURE 6

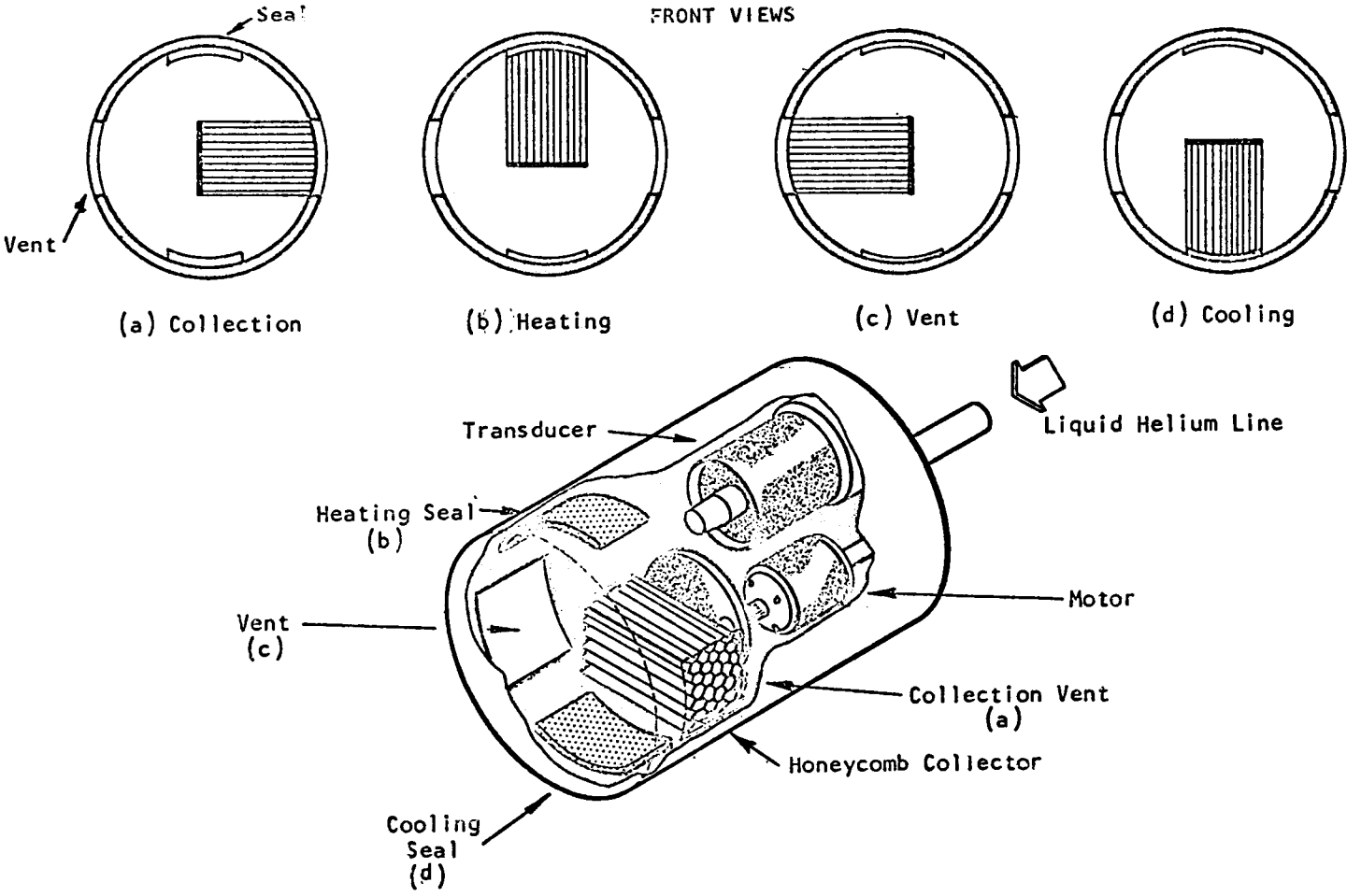

ORBITAL DENSITY METER

FIGURE 7

SOME SPECIAL DESIGNS FOR UHV APPLICATIONS

I. Dalins
Marshall Space Flight Center†
Huntsville, Alabama

The design and development of certain vacuum components was undertaken in connection with research in surface physics utilizing a field emission microscope to which a modulated molecular beam apparatus is attached.[1,2] Several versions of a chopper for molecular beam apparatus were developed, the design of which has certain unique features that could be useful in other work involving vacuum. One of the molecular beam choppers is essentially a small electric motor that operates in ultrahigh vacuum and, as such, could be useful in other applications. Magnetic field has been used in many vacuum component designs to produce certain kinds of mechanical motions within the vacuum chamber. Transmitting mechanical motion through the walls by a magnetic field is possible without running into the risk of weakening the walls of the chamber to the extent that it becomes very difficult to seal. In the design of a molecular beam chopper, this rather old idea was again used. The difference in this case was that the parts were machined to a considerable degree of precision, and that a magnetic material such as nickel was used to produce a low reluctance circuit, while nonmagnetic #304 stainless steel was used to isolate one magnetic circuit from another. The whole chopper assembly was small enough to fit inside a 35-mm O.D. glass tube (chopper, 1.2 inches O.D.). The chopper armature assembly operation, i.e., oscillatory motion, is produced as a result

† This development was performed in cooperation with the University of Alabama Research Institute, Contract NAS8-2585.

of variable reluctance path created by the armature as it moves in and out of the magnetic field. The details of the design are described in Reference 1.

While passing the magnet through glass is certainly the easiest method of avoiding leaks, the nonmagnetic glass wall attenuates (i.e., reduces the intensity of) the magnetic field to a considerable extent. Marked improvement is readily possible by sealing nickel sections into the walls of the vacuum chamber opposite the corresponding magnetic circuit elements of the chopper. The design of the oscillating chopper involves the use of a spring that determines the resonant frequency of the armature (i.e., the maximum chopping rate). The increased magnetic field intensity allows the use of a spring with greater stiffness, and therefore higher chopping rates are possible. Leak-proof seals can be conveniently produced by vacuum brazing techniques using a low vapor pressure brazing alloy[1] (e.g., Nioro, nickel-gold alloy, from Western Gold Platinum Company, melting point, 925 °C). For extensive bakeout, electron beam welding seems to produce a more durable joint. Inert gas welding is also possible, but requires that the parts be designed in such a way to enable access to all joints with the welding torch. A special welding torch is very useful. In selecting the shape of magnetic material that is placed into the walls of the chamber, it appears that circular sections can be brazed into the walls more easily than any other, especially those involving corners. Cornered inserts appear to be very susceptible to leaks; it is harder to machine parts to close tolerances (0.001 inch) which involve corners. Round nickel sections (plugs) were used in the design of the rotating chopper. This enables high copping rates because several holes can be placed on the armature, and the beam can be chopped many times during one armature

revolution. The armature rotation is in phase with the magnetic field and, consequently, the chopping rate can be controlled.

The rotating chopper design has an inherent disadvantage in that the axis of rotation must be displaced somewhat less than the diameter of the rotor with respect to the beam. This increases glass blowing difficulties, especially sealing-in the beam oven.[1] The use of flanges makes possible separate assembly of the molecular beam and the field emission microscope and permits the critical alignments of this apparatus. Another disadvantage of the rotating chopper is that it is difficult to stop the chopper armature, but not so with a rotating one. For reasonable shaft clearances, the friction forces will permit the armature to rotate when the field is cut off. Energizing all coils with constant field is helpful, but as a rule it is still not possible to stop the armature in a short time required to execute several chops. The distance between holes on the armature becomes shorter as the number of holes increase, and thus more chopping is done in one revolution.

The use of the magnetic (nickel) and nonmagnetic material (304 stainless steel) and the low vapor pressure brazing material enables construction of vacuum components that are compatible witn ultrahigh vacuum operation. Bakeout of 450 °C is readily possible. Afterward, the apparatus can be immersed into liquid nitrogen. Immersion into liquid helium also appears feasible, except that it is necessary to adjust the tolerances so that the chopper operates as a result of extensive shrinkage at liquid helium temperatures. This is most critical in regard to tne armature shaft bearings. In the present surface pnysics studies, which involve liquid nitrogen immersion only, simple cone-in-cup bearings[1,3] appear to be quite adequate. Both the cone and the cup are made

of stainless steel for this limited time operation. Tungsten-sapphire combination in certain shapes might be required for long-time operation.

The use of magnetic and nonmagnetic material produces a reliable and compact chopper design that can be used to modulate a molecular beam, even in a compact all-glass or metal vacuum chamber. The use of such materials is feasible in several other designs of vacuum components that are compatible with high-temperature bakeout and subsequent immersion into a cryogenic fluid such as liquid nitrogen and helium.

REFERENCES

1. Dalins, I., "Modulated Molecular Beam Apparatus for Studies of Atomic Interactions with Surfaces," a paper presented at the Third International Vacuum Congress, Stuttgart, June 28 - July 2, 1965.

2. Dalins, I., " A Study of Surface Ionization Conditions in Field Emission Microscope," a paper presented at the APS Summer Meeting, Nonolulu, September 2-4, 1965.

3. Hudson, J.B., T. L. Donnelly, and W. W. Sears, Tenth National Symposium, AVS, 1963.

A LOW-TORQUE SUPPORT FOR LOW THRUST MEASUREMENT AND ATTITUDE CONTROL TESTING

by Edward W. Otto

Lewis Research Center

INTRODUCTION

The Lewis Research Center is employing a three-axis gas bearing as a low-torque support system to study spacecraft attitude-control systems in a simulated space environment. The bearing is mounted in the Lewis 15 by 60-foot high-vacuum facility, where the necessary vacuum environment is provided for proper testing of thrustors, which include ion-engine systems. In order to avoid degradation of the chamber vacuum because of discharge of gas from the bearing into the chamber, the bearing is equipped with a separate vacuum scavenge system. The performance and the effect on environmental test chamber vacuum of this gas bearing facility are described herein.

Author

ATTITUDE-CONTROL-SYSTEM EXPERIMENTAL PACKAGES

A typical attitude-control-system experimental test package is shown in figure 1. The thrustors for this test package use a subliming solid as a propellant and can be seen about halfway out on two of the arms. The four arms carry adjustable weights to obtain the desired moment of inertia of the system. The angular position sensor, control electronics, electric power supply, instrumentation, and telemetry are mounted on the top plate as shown. The propellant tank is mounted underneath (fig. 1(b)). The position sensor system consists of a light-sensitive device, which senses the angular position of a light source mounted external to the test package on the wall of the environmental test chamber.

BEARING CONFIGURATION AND OPERATION

The bearing is mounted on a pedestal in the center of the vacuum chamber as shown

schematically in figure 2. Figure 3 is a photograph of the bearing system mounted in the test chamber with the weights used for calibration. The design details of the bearing are shown in figure 4. The gas inlet consists of a series of 12 holes 0.031 inch in diameter uniformly spaced in a plane parallel to the diametral plane. The scavenging port is an annulus lying in a plane parallel to that of the inlet holes as shown. The bearing has 360 degrees of freedom about the vertical axis and about 5 degrees of freedom about the other two axes. The maximum rated load of the bearing is 500 pounds. The gas used in the bearing is carbon dioxide, which is supplied from high-pressure bottles. The gas supply and scavenge system is shown schematically in figure 5. The pressure required to obtain various bearing gap heights is shown as a function of load on the bearing in figure 6. Satisfactory bearing operation is uncertain below a gap height of 8×10^{-4} inch, while gas losses are high with the larger gap heights. A gap height of 10×10^{-4} inch provided a suitable compromise between consistent bearing operation and low gas losses.

EFFECT ON CHAMBER VACUUM

Because of the small allowable size and constricted nature of the scavenge annulus and passages in the bearing, the pressure in the scavenge annulus is not as low as the pressure in the environmental chamber. Some gas therefore escapes into the environmental chamber and tends to degrade the vacuum. The relation among tank pressure, gap height, and bearing load is shown in figure 7 for conditions of warm tank walls and cold tank walls (liquid nitrogen circulating through baffles). These data are for the bearing alone without a thrustor. The operation of a thrustor causes a further loss of vacuum. The pressure conveniently obtainable in the vacuum facility without bearing operation is approximately 4×10^{-6} torr for warm wall conditions and somewhat less than 1×10^{-7} torr for cold wall conditions. Thus, the vacuum loss is approximately a decade for both warm and cold wall conditions at the bearing operating gap height of 10×10^{-4} inch. For the thrustor systems under test, this loss was not serious.

TORQUE GENERATED BY BEARING

Figure 8 shows the magnitude of the torque generated by the bearing as a function of angular position at a given set of operating and loading conditions. The positions beyond $+100^{\circ}$ and -100° were not obtainable with this particular bearing because an accidental scratch on the sphere caused the bearing to lock in this region. The maximum torque under the conditions shown is approximately 600 dyne-centimeters, which is from 2 to 20 percent of the torque of the thrustor systems being studied. A torque of 600 dyne-

centimeters is representative of the torques encountered by small spacecraft in medium to low earth orbits. Two regions where the torque is low can be used to simulate spacecraft with high orbits where disturbance torques are low. At these points an adjustment of the supply pressure shifts the torque pattern sufficiently to provide torque variation from one direction through zero to the other. The torque sensitivity at these points is approximately 50 dyne-centimeters per pound per square inch.

ATTITUDE CONTROL SYSTEM EXPERIMENTAL PACKAGES

(a) Top view.

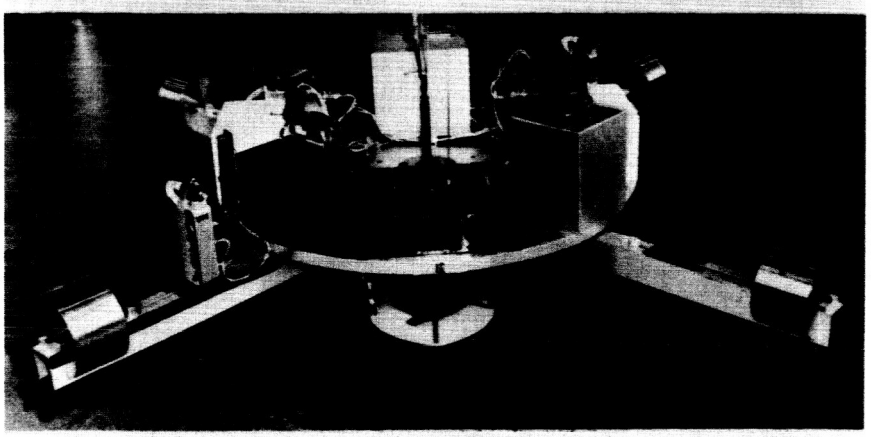

(b) Side view.

Figure 1.

BEARING LOCATION IN LEWIS 15 BY 60 FOOT VACUUM FACILITY

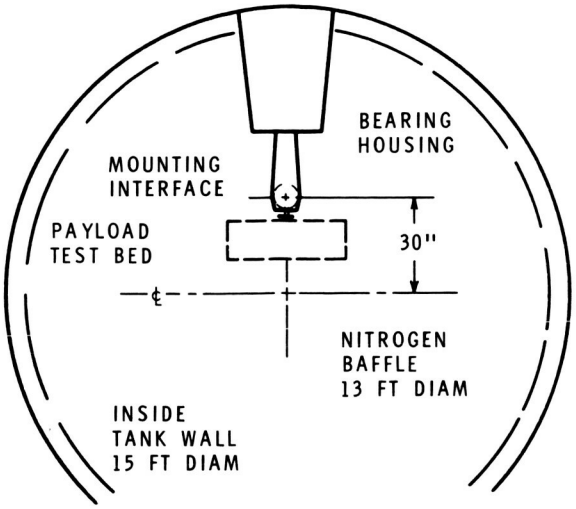

Figure 2

BEARING MOUNTED IN TEST CHAMBER WITH LOAD CALIBRATION WEIGHTS

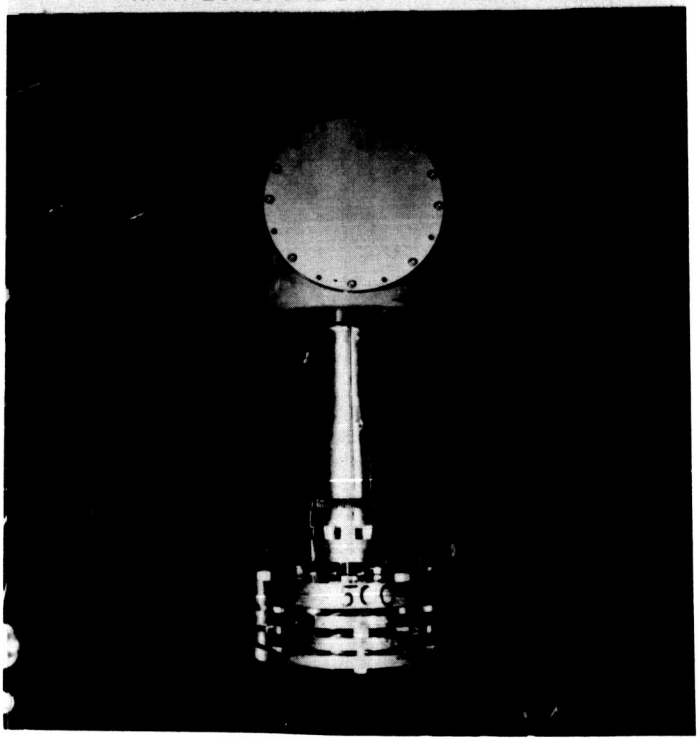

Figure 3

DESIGN DETAILS OF GAS BEARING

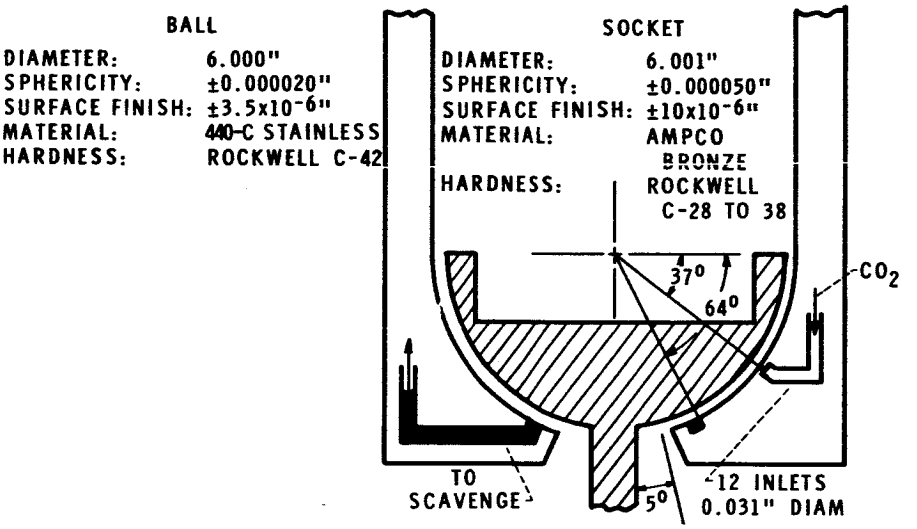

Figure 4

SCHEMATIC OF GAS SUPPLY AND SCAVENGE SYSTEM

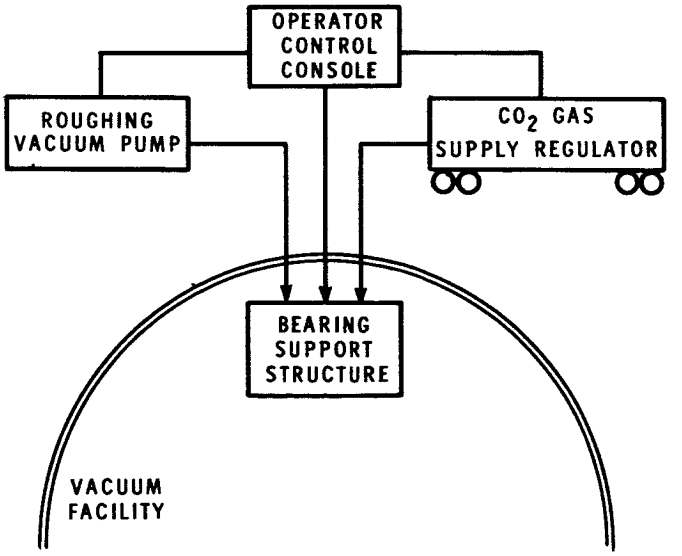

Figure 5

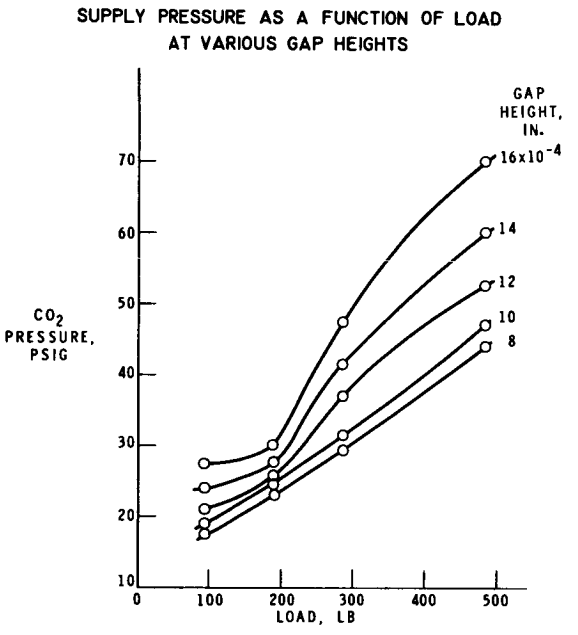

Figure 6

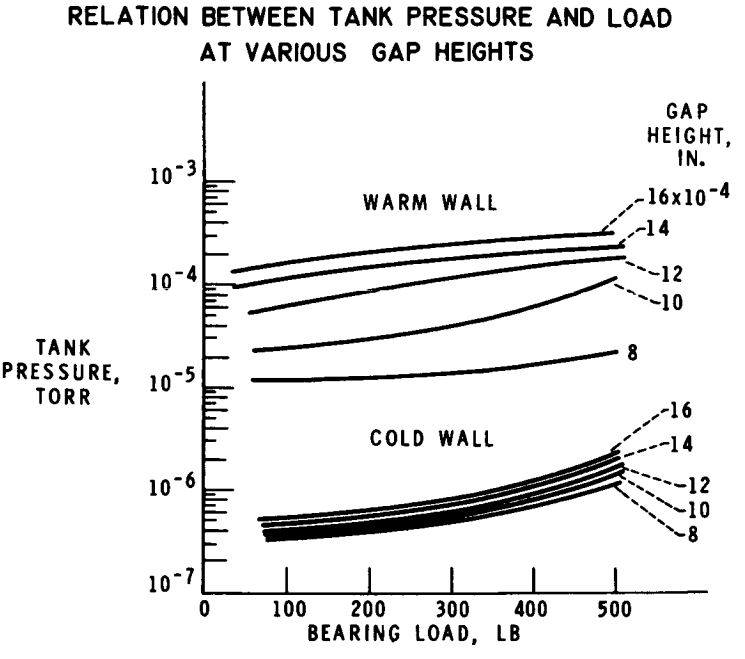

Figure 7

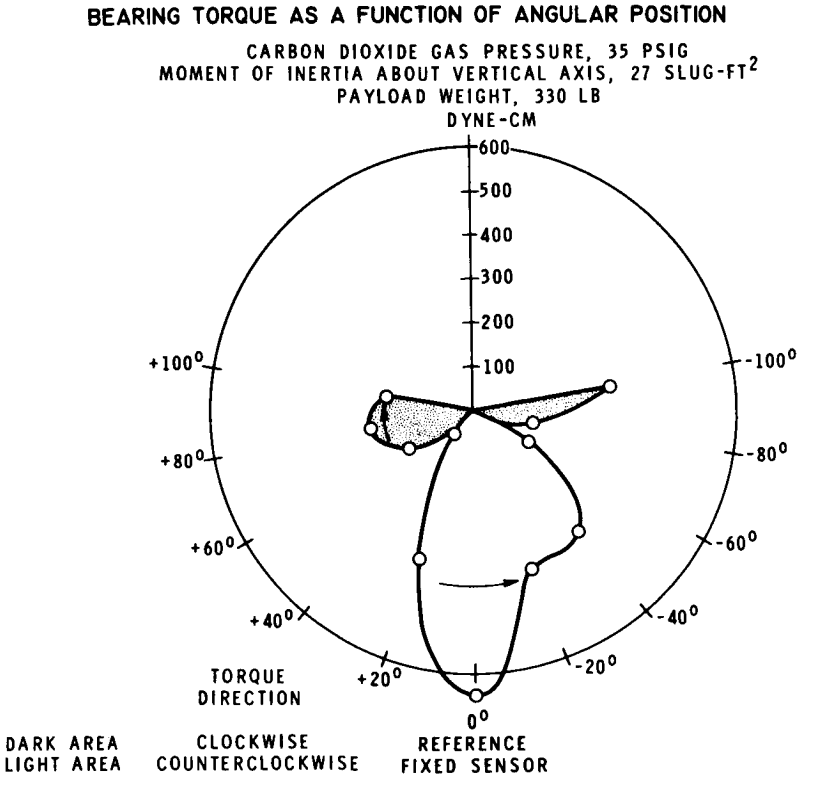

Figure 8

SAFETY PROBLEMS ASSOCIATED WITH CRYOGENIC SYSTEMS FOR SPACE ENVIRONMENT FACILITIES

by Daniel J. Peters

Lewis Research Center

Space simulators generally use large amounts of cryogenic fluids. Numerous safety problems are connected with the use of these cryogenic fluids that should be considered when planning the installation and operation of such a facility. An accident that occurred at one of the Lewis space environment facilities and some of the safety hazards that caused the accident are discussed. Other safety hazards and some recommendations concerning the use of cryogenic fluids are also presented.

The Lewis Research Center has in operation a space simulation chamber capable of reproducing most of the conditions of the space environment for the determination of the performance characteristics of space vehicles and their components. A cross section of the facility is shown in figure 1. The chamber is a 6-foot-diameter by 10-foot-long ultrahigh vacuum tank with liquid helium cooled walls and simulated solar radiation. The chamber is pumped by two 32-inch oil diffusion pumps through liquid nitrogen cooled elbows. The carbon arc light source is shown with the appropriate optical components that provide a simulated solar radiation beam.

The overall facility is 44 feet high, 21 feet of which are below the floor in two sublevels. The first sublevel, or pit, contains the vacuum pumps, liquid nitrogen and helium lines, and other miscellaneous apparatus and facility piping. The extreme lower portion of the tank extends into the second sublevel, which is not normally entered by operating personnel. There is an open stairwell for access to the pit, and the pit covering at the floor level is an open steel grating.

An accident occurred in the first sublevel which resulted in the near asphyxiation of three men, one of whom was the author. During the preliminary operations prior to a test, a leak developed in a liquid nitrogen supply line in the first sublevel. The leak was at a separated soft soldered joint in a copper line and was the result of an improper soldering technique and the use of a makeshift tube fitting during a previous modification to the liquid nitrogen piping. This modification had taken place 1 year previous to the accident and the system had been operating satisfactorily since. A very lengthy pre-operational procedure is involved for a test, which includes installation of the test model,

instrumentation, evacuation, and precooling of the chamber. A permanent repair of the leak would have meant aborting the scheduled test; therefore, it was decided to make a temporary fix. The leak was severe, and dense nitrogen vapor sank to the bottom of the second sublevel gradually displacing the air in both sublevels. Two technicians were instructed to enter the pit to make the temporary repair. A third technician entered the pit to open a compressed air supply line for breathable air. Meanwhile the first two technicians returned to the floor level after having experienced a mild sensation of dizziness, apparently due to the diminishing oxygen content of the pit environment. At this point the vapor cloud caused by the cold nitrogen gas was extremely dense. The third technician was not visible, nor did he respond when being called. Suspecting he had been rendered unconscious, three men rushed into the pit to retrieve him. In the ensuing struggle much physical effort was expended and a great deal of nitrogen rich air was inhaled, which resulted in the loss of consciousness to two more men. Other personnel in the area observed what was happening and took the necessary steps to perform a rescue. The liquid nitrogen system was completely cut off, fans were obtained to ventilate the area, and the victims were removed and revived by mouth-to-mouth resuscitation. The victims were hospitalized for a brief period but fortunately did not suffer any permanent after effects. Minor bruises and a slight back injury were sustained by one man; however, it is believed these were inflicted during the rescue process while he was being brought up the steps.

This accident exemplifies the existence of safety hazards when operating cryogenic systems and emphasizes the need for strict adherence to regulations to ensure the safety of operating personnel. The following is a discussion of some of these hazards and some of their preventive measures.

Venting cryogenic gases from cold baffles, storage dewars, leaks, etc. could gradually diminish the oxygen content of the air in a confined area to a value below the minimal requirements for normal respiration. Large space environment chambers are sometimes released to atmospheric pressure with a dry inert gas, that is, nitrogen, to prevent water vapor from being absorbed by the chamber walls. This results in the attainment of the ultimate pressure in a shorter length of time. Large storage tanks are usually charged with an inert gas when not in operation and they often require interval maintenance. Personnel entering these areas are susceptible to anoxia, and precautions should be taken to insure their safety.

Anoxia is a general term meaning a deficiency of oxygen in the body tissues and can be a result of many factors, one of which is a low oxygen partial pressure of the air inspired into the lungs. Some of the symptoms of anoxia, some of the effects of anoxia on the physiological functions, and the tolerable limits of oxygen concentration in the air are presented in table I. The column at the left shows the range of oxygen concentration in the atmosphere at sea level, while the column on the right shows some of

the effects of the reduction in oxygen concentration. Cyanosis is a blue, purple, or black tinge in the color of the skin frequently seen on the lips, ears, nose, cheeks, fingers, or toes. It becomes prevalent when the oxygen concentration falls below 12.3 percent where the period of useful consciousness is only a few minutes. Below 5 percent oxygen it is impossible to sustain life. These effects can vary with oxygen concentration depending on the rapidity with which the oxygen concentration is decreasing, the amount of physical exertion the person is subjected to, and the general physical condition of the person. This table is only to be used for a guide and will not hold true for all cases. In my particular case, I had absolutely no forewarning before passing out. I did not experience any of the aforementioned symptoms. Although some of these symptoms may have been present, they were overshadowed by my state of excitement and preoccupation with the problem at hand.

Two safety practices to guard against the exclusion of oxygen in confined areas are to provide a continuous supply of fresh air by the use of ventilating fans and to incorporate an oxygen content monitoring system. Also, emergency breathing apparatus such as air packs fresh air or oxygen masks should be readily available and convenient to use when the situation arises. Detailed instructions on emergency rescue procedures should be given to all personnel involved. This should include information on the proper use of emergency breathing apparatus and administration of mouth-to-mouth resuscitation to asphyxiated victims.

Another hazard is the inadvertent buildup of high pressure in lines or containers. The confinement of cryogenic fluids at low temperatures followed by the loss of insulating capacity can result in extremely high pressure buildup. Loss of vacuum in vacuum-jacketed lines or vessels, formation of ice in the neck of small dewars, or cryogenic fluid trapped between valves can cause the temperature to rise above the critical temperature. These are potentially hazardous conditions as the working pressure of the lines or containers may be exceeded. It is therefore necessary to adhere to proper piping fabrication and assembly techniques. This includes adequately sized and properly located relief valves, rupture discs, and vents, along with appropriate alarms and safety devices to guard against rapid vaporization of large quantities of cryogenic fluids. Correct soldering and welding practices are essential to prevent the development of leaks under the extreme low temperature conditions. Metals may be satisfactorily joined by soft soldering, silver-brazing, or welding. Soft solder is limited to joints where stresses are low and not cyclic due to low ductility at low temperatures.

Most materials exhibit substantial changes in physical properties when subjected to the extremely cold temperatures of cryogenic fluids. These properties should be taken into consideration when specifying materials for cryogenic applications. Some properties of type 304 stainless steel are shown in figure 2. Note that these changes are quite drastic, in one case varying more than an order of magnitude from room temperature to

liquid hydrogen temperature. Figure 3 shows the variation in yield strength of some common materials of construction. Observe that the yield strength of titanium more than doubles from room temperature to liquid hydrogen temperature.

It is important not to be misled by the fact that materials exhibit an increase in strength at cryogenic temperatures. This is strictly an indication of the strength of materials in tension and does not reflect any of their weaknesses. For instance, the impact strength decreases as the temperature drops, and in the case of the 400 series stainless steels, impact strength decreases almost to zero at about -300° F. The addition of nickel improves the impact strength although there is still a decrease with decreasing temperature. In the case of the 300 series stainless steels, which contain a minimum of 8 percent nickel, the impact strength is maintained at a respectable value.

One of the more significant shortcomings is the low temperature brittleness of body-centered-cubic metals such as carbon steel. In general most structural metals with a face-centered-cubic crystal lattice retain their ductility throughout the low temperature range. They also undergo an increase in tensile and yield strength.

Some metals acceptable for cryogenic services are 18-8 stainless steel, aluminum, copper, nickel, and their alloys. In general, most plastics such as Teflon, Kel-F, polyethylene, PVC, nylon, and mylar are quite strong at low temperatures and may be used if thermal shock and flexing are avoided. Fluorinated hydrocarbons are the only plastics reported to be somewhat ductile at cryogenic temperatures. The U.S. Department of Commerce publication Cryogenic Materials Data Handbook provides specific guidance in the selection of materials. It lists mechanical and physical properties of most metals and nonmetals.

It is essential that cryogenic fluids be prevented from accidentally coming in contact with body surfaces. Serious burns or frostbite can occur which results in damaging of the tissues. Direct contact can be avoided by the use of protective clothing including gloves and face shields. If a part of the body comes in contact with a cryogenic fluid for a period long enough to cause a serious burn, the affected area should immediately be immersed in tepid water. This will prevent further damage in adjacent areas to the cellular structure of the tissues.

This has been a brief discussion of some of the safety problems present when operating space simulators. It is by no means complete. Its purpose is to illustrate some of the safety hazards to those planning new space simulators, and also to remind those operating existing facilities to take a second look for existing safety violations. Safety is something that cannot be overemphasized, and because people tend to become too familiar and adopt a nonchalant attitude toward cryogenic fluids, a periodic reminder is essential.

TABLE I. - EFFECTS OF REDUCTION OF OXYGEN CONCENTRATION

ON PHYSIOLOGICAL FUNCTIONS

Percent of oxygen in air at sea level	Symptoms of anoxia
20.9 to 16.8	No effect
16.8 to 14.4	Respiration is stimulated, heart accelerates, not noticeable to subject
14.4 to 12.3	Sense of happiness and security, development of slight headache, lack of energy, drowsiness, nausea, evidence of cyanosis
12.3 to 6.2	Lack of coordination, inability to move arms, legs, etc., dulled sensations, unconsciousness after a few minutes, cyanosis is prevalent
5	Minimum concentration for sustainment of life

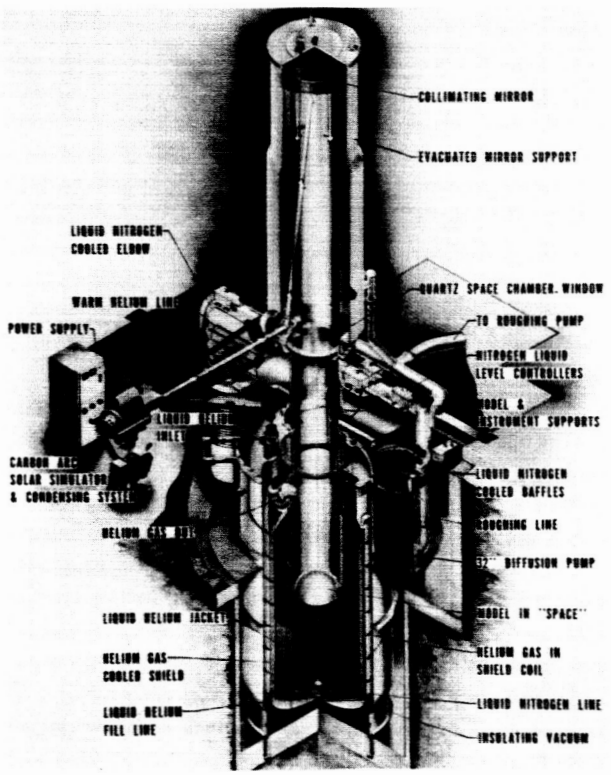

Figure 1. 10-By 6-Foot Solar Space Simulator

EFFECT OF CRYOGENIC TEMPERATURE ON SOME PROPERTIES OF 304 STAINLESS STEEL

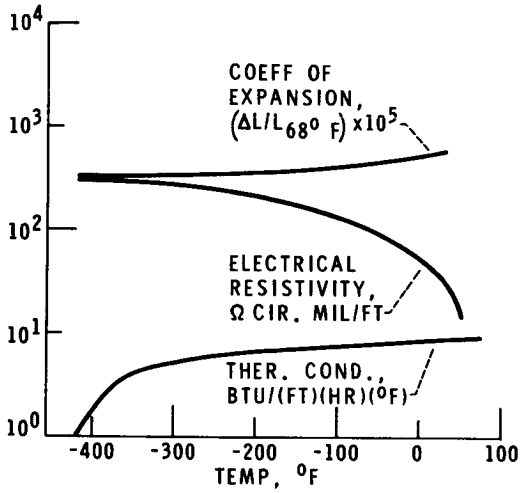

Figure 2

EFFECT OF CRYOGENIC TEMPERATURE ON YIELD STRENGTH OF SOME MATERIALS

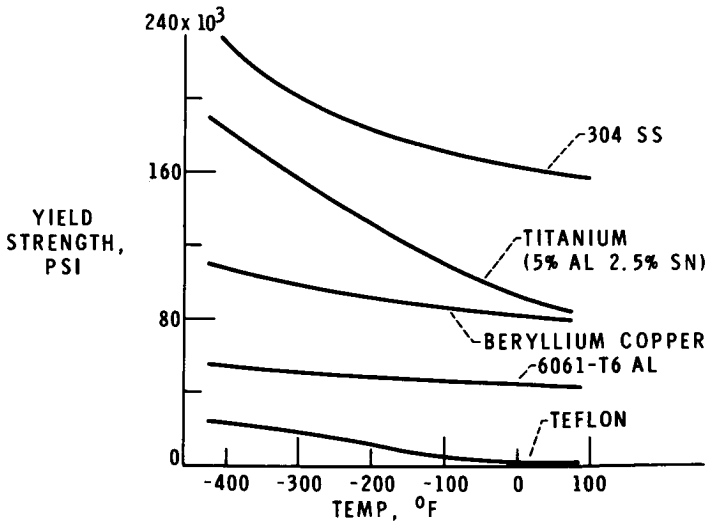

Figure 3

REPORT ON A DIFFUSION PUMP EXPLOSION AT GSFC

BY: R. T. Hollingsworth

Introduction

The following is a report on an explosion which occurred within one of two diffusion pumps on one of our large (7 ft. diameter by 21 ft. high) vacuum facilities. The cause or causes have not been determined but investigations are being continued at the Goddard Space Flight Center.

Summary of Events on the Day of the Incident

On Friday, March 19, 1965, after several days of testing on an experiment package within the VOB vacuum facility, it was determined that the ultra-violet light source lamp used to excite the experiment package required adjustment. Accordingly, the high vacuum valves were secured (see Figure #1) at approximately 1200 hrs. The closing of the valves isolated the vacuum system from the chamber. At 1300 hrs. the chamber was vented to atmospheric pressure, the port in the chamber to the UV source lamp opened, while the vacuum pumping system remained in an operating mode awaiting the continuation of the test. Adjustments and corrections continued throughout the day till early evening. At 1850 hrs., an explosion was heard within diffusion pump #1 of the vacuum system. At the same time, the engineer working on the UV lamp source through the open 15½" diameter port in the chamber felt a "pushing" sensation and saw a "blue fog" fill the chamber. The noise of the explosion was of a sufficient level to cause personnel in the adjacent room at the Low Temperature Optical Facility (see Figure #2) to come in and inquire about the noise. A short time after the first explosion (described by one of the technicians as "about four minutes") a second and much louder explosion occurred in the same diffusion pump. The technician responsible for the operation of the vacuum system realized that the vacuum blower (Figure #1) had ceased operating. He then started the pump through manual reset and noted that the fore line vacuum pressure gauge readings were near atmospheric pressure. Since the holding pump had been running but isolated from the system by valves "B" and "C" (Figure #1), the technician opened these valves to achieve the proper fore line pressure to the diffusion pumps. This did not

accomplish the desired results quickly enough. The power to the diffusion pump was then turned off and the "quick cool" water to the diffusion pumps turned on. The entire vacuum pumping system was then turned off. The engineer in charge of operating the thermal-vacuum facilities was called at home and reported to the facility within an hour. The engineer entered the chamber and saw that two 2"x2"x½" mirrors and an approximately six pound experiment package had been displaced from the horizontal portion of the high vacuum elbow of diffusion pump #1 to the bottom of the vacuum vessel. In addition, pieces of aluminum foil used as an antimigration barrier on the liquid nitrogen baffle for diffusion pump #1 were found in the chamber and under the high vacuum valve seat. The engineer, while in the chamber, asked for the high vacuum valve to be opened but had it closed quickly because of a very irritating vapor being issued from the diffusion pump.

The engineer instructed the operating personnel to clean up portions of the vacuum system including the diffusion pump #1, the main mechanical pump, the blower, the holding pump, and baffles and traps. Upon removal of the #1 diffusion pump, its interior was found to contain a light-weight carbon material adhering to the entire surface area except the outside area of the diffusion pump jet assembly (Figure 3).

Highlights of the Investigation

The UV light source uses a free flow hydrogen gas which is ionized and then pumped through the vacuum pumping system. It was thought at first that this may have been the cause but subsequent determinations minimize this.

The vacuum system (Figure 1) had been operating against the high vacuum valves during the period of approximately six hours that the chamber was at atmospheric pressure. Valves "D" and "E" were open and valves "B" and "C" were closed. The diffusion pumps were energized as were all other pumps. Diffusion pump #1 had a calculated leak of 3.6×10^{-6} std cc/sec based on an earlier probing with a CEC helium leak detector.

The liquid nitrogen traps and the water baffles had been functioning during this time. Although the ioization vacuum gauges were not connected to read the vacuum level within the elbows, the foreline thermocouple vacuum gauges (TC #1 and TC#2, Figure 1) indicated a proper foreline pressure of less than 10 microns throughout the day. These gauges were real every hour on the hour. TC gauge #1 was energized at all times except when TC gauges #2 and #4

were energized hourly to take readings. The last reading was taken fifty minutes prior to the explosion. There was no indication of power deviation or water failure on the vacuum system which would have caused abnormal operating conditions in these last fifty minutes.

Other characteristics of the diffusion pump which were later measured, but are considered to be similar to the conditions at the time of the explosion are the temperature sampling of 14.5 KW to the pump. Figure 4 shows the three temperature samples taken in the oil reservoir, the top of one fin on the heaters, and the interior "ambient" temperature of the jet assembly. All three of these temperatures are above the flash point of 210°C of the diffusion pump fluid, Dow Corning DC 704, at atmospheric pressure. It is noteworthy that the greater majority of the heating elements are above the pump fluid level with only the bottom portion of the heater fins in contact with the fluid. With this configuration, the surface fluid is vaporized and super-heated, rises upward and then deflected downward through the jet assembly, is condensed on the water cooled pump wall, and returns to the reservoir to repeat the cycle. Any contaminants with a density greater than the fluid could accumulate at the bottom of the reservoir. The 14.5 KW heater input is greater than the optimum heat of 11KW recommended by the manufacturer. (Variable autotransformers have subsequently been ordered and installed to determine the performance of the diffusion pumps at varied power inputs.)

The Pumping Fluid

Although the foreline conductance of diffusion pumps #1 and #2 are essentially the same to the point where they are manifolded from a common line, the explosion occurred only in the #1 pump. The fluid taken from pump #1 was ordered impounded as was the fluid taken from pump #2. It was reasoned that the fluids from both pumps contained the same contaminants prior to the explosion, and that there should be some correlation between the two which would indicate the possible cause. To pursue this, Trident Engineering Associates were given samples of the fluids to see if they could determine if there were any indications of combustible or explosive mixtures in the fluids. Their report showed that carbon and silicon dioxides were present in fluid from pump #1, but that the only contaminant identifiable in pump #1 was some mechanical pump oil, Sunvis #931.

The IIT Research Institute of Chicago had made a study for NASA - Houston, entitled "Hazard Potential of Diffusion Pump Fluid" (Contract NAS 9-1178), in which they had tried to cause various clean pump fluids, including DC 704, to explode. Their results were essentially negative. They had later submitted a proposal to the GSFC to study the effects of contamination upon the fluid DC 704. When the explosion occurred in the VOB, IITRI was contacted to elaborate on their report of fifteen other known diffusion pump explosions, as well as to study a sample of fluid taken from diffusion pump #2, and a sample of new oil taken from a supply container. The chemical analysis performed by them indicated trace quantities of aluminum and magnesium in both the new and used oil as well as Freon "TF" in the used oil. Dow Corning verified that there is trace quantities of aluminum and magnesium in DC 704. Freon "TF" is used in very profuse quantities to clean the VOB chamber and the spacecraft optics. IITRI could not find any other contaminants but suggested that further study of perfluoro compounds reacting with magnesium and/or aluminum be made since so very little is known about their behavior of reacting spontaneously.

Personnel of GSFC also ran an analysis of the various fluids and could find very little difference between new fluid and that from pump #2. He could not verify the silicon dioxide in fluid from pump #1 and a question was raised on the technique Trident employed in the identification of silicon dioxide.

In reviewing the possible causes of the explosion, it was realized that if the total pressure of ten microns or less existed at the time immediately preceding the explosion, a vapor phase explosion could not have occurred due to the lack of an oxidant to support propagation. Accepting the facility log book and the operator's statements that the vacuum system was in an apparent equilibrium mode for 5-6 hours, it was necessary to look further for the possible causes. Therefore, the possibility of a liquid phase reaction was investigated.

The first effort was spent in reviewing with IITRI the fifteen know previous explosions. The source of their information was revealed to be the F. J. Stokes Division of the Penn-Salt Chemical Company. Arrangements were made to talk directly with those at Stokes who were familar with the incidents. On April 5, 1965, GSFC personnel met with an engineering group at Stokes to discuss these explosions. The common denominator in the incidents reported

by Stokes is that the systems (vacuum coaters) were undergoing a dynamic change prior to the explosions. Efforts to repeat these changes with subsequent explosions have been successful by Stokes. The diffusion pump fluid in the vacuum coaters reported was a hydrocarbon rather than the silicon fluid used in our facilities. The only apparent similarity to our incident is the large (32") diffusion pump on a small volume vacuum system.

The Naval Ordnance Laboratory was contacted for assistance in our problem. They disqualified themselves as experts in the area of explosive chemistry in which we were interested but suggested that we contact Dr. Guenther von Elbe of the Atlantic Research Corporation who is recognized internationally as an expert in explosive chemistry. On April 13, 1965, we met with Dr. von Elbe to review the known information concerning the explosion. Again, based on the facility log book information, Dr. von Elbe stated that we must look for a liquid phase explosion and further, we should look for trace contaminants such as peroxides. He cited several examples of unusual explosions that he has investigated for the Department of Defense and Industry in which trace contaminants were responsible. Dr. von Elbe has subsequently submitted a program of effort he would pursue if so authorized by the NASA.

Prior to offering our conclusions and recommendations, it is important to note that an investigation of utility failures at about the time of the incident was made. No utility (air, water, electricity) was reported malfunctioning which could have altered the normal operating conditions. In addition, efforts were made to "accidentally" cause changes in the operating mode of the facility by sitting on the operating console, leaning against control switches and in general perform such acts which could later be described as an "accident". It was concluded that a very deliberate act is required to change the settings of the switches and that an accident is highly improbable.

Conclusions and Recommendations

Early in the investigation, a decision was made to pursue the liquid phase rather than the vapor phase explosion more rigorously. This decision was not to be construed as final but more the logical first course of action since if the vacuum systems were functioning properly, the total pressure within the evacuated system would be less than that required to support an explosion. Since our preliminary investigation supported this theory, we decided to follow the course of a liquid phase explosion. Should the chemistry of this route ultimately prove that there was not a sufficient quantity of material or contaminants present to support this hypothesis, then a re-examination must be made of the

possibilities supporting a vapor phase explosion.

Our effort has been directed toward identifying contaminants in either gross or trace quantities, however, since early studies and experiments with the DC 704 fluid made c. 1960 by our research people demonstrated that the pure fluid can be suddenly exposed to atmospheric pressure repeatedly without any adverse effect upon the fluid. It was because of this investigation that we adopted DC 704 fluid.

Our recommendations are threefold and perhaps related. First, continue the investigation looking for any trace contaminants. This is based on the discussion with Dr. von Elbe and the information presented above. Second, investigate the possibility of obtaining an exothermic DC 704 fluid reaction at low pressure and elevated temperatures in a large volume system. Third, investigate the little known area of reactions involving perflurocompounds, magnesium and/or aluminum. This is discussed in paragraph III of the IITRI report (Attachment #10).

This report has been issued to summarize events as they happened on the day of the explosion as well as to highlight the investigation efforts. Details surrounding efforts, decisions, and facility repairs have not been included. We recognize that it may be several months before the causes of the explosion can be reasonably defined if definition is at all possible.

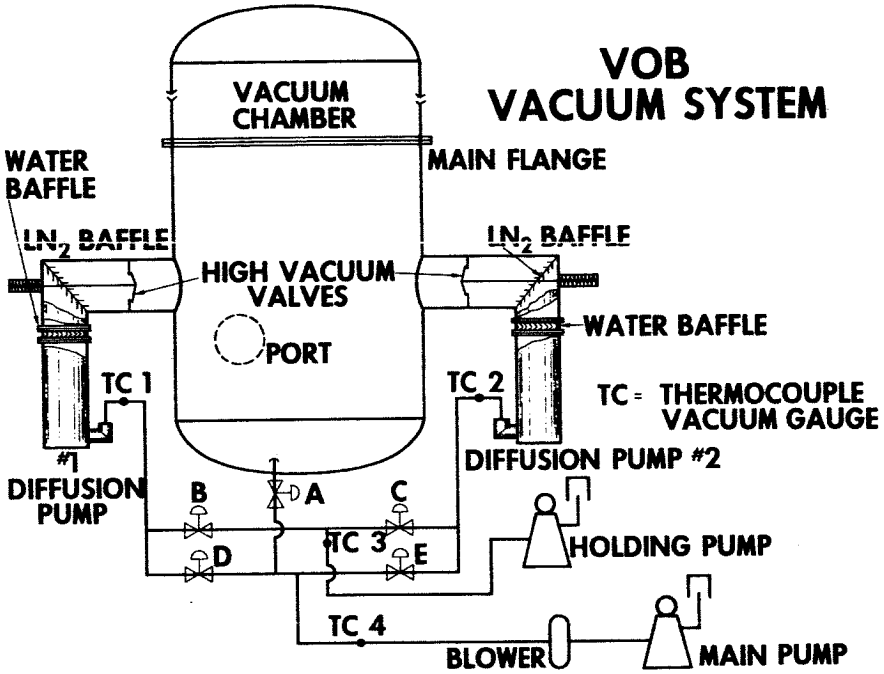

Figure 1

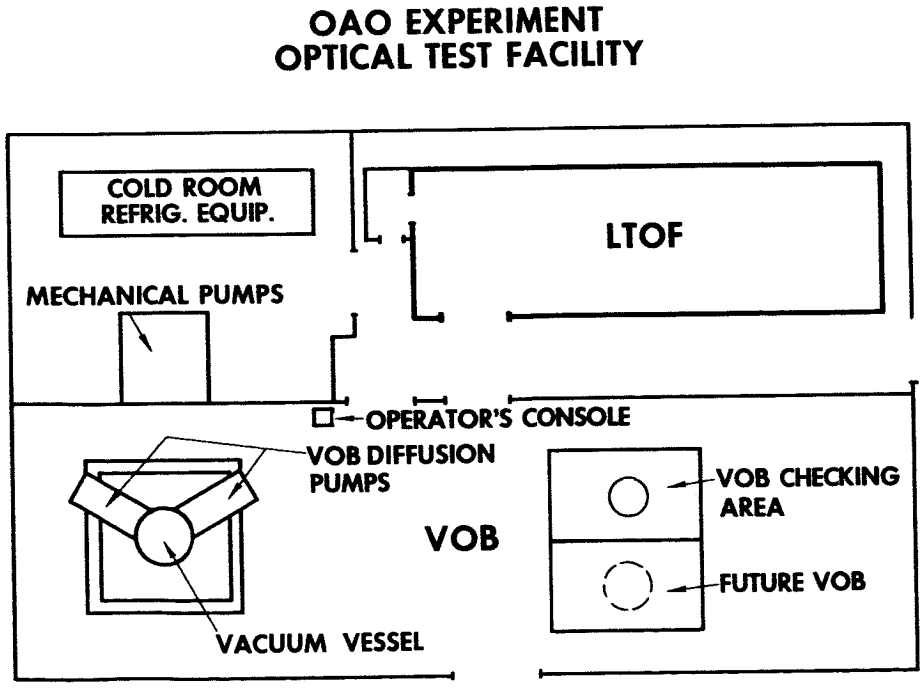

Figure 2

VOB DIFFUSION PUMP NO.1
PHYSICAL APPEARANCE AFTER EXPLOSION

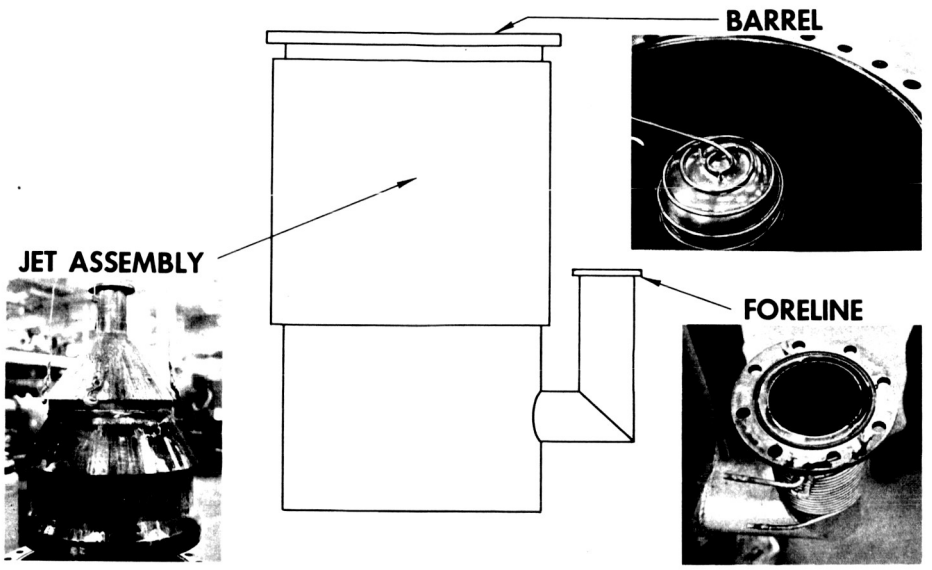

Figure 3

VOB DIFFUSION PUMP #1
APPROXIMATE OPERATING CONDITIONS AT TIME OF EXPLOSION

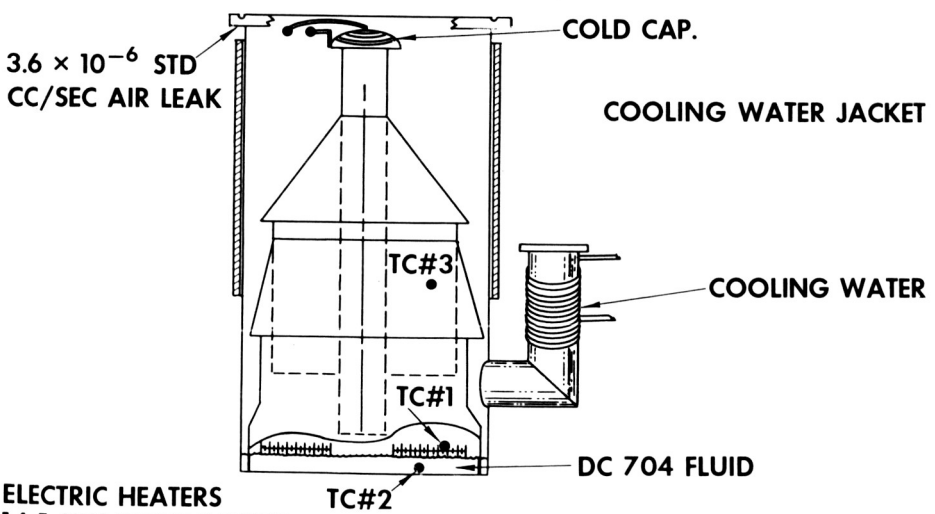

TC#1 =268°C
TC#2 =218°C
TC#3 =230°C

Figure 4

ATTACHMENT I
Excerpt From IITRI Report

The results of the analyses, although not at first apparent, may have supplied considerable knowledge and information as to the possible cause of the diffusion pump explosion. For instance, it was not known until now that Freon 113 was a contaminant in the diffusion pump fluid. Actually, its presence would not be considered too likely in view of its relatively low boiling point of about 47.6°C. Nevertheless, it was present in the oil phase and consequently may have been at much greater levels in the vapor phase. This will be discussed later.

The significance of identifying a Freon contaminant is enhanced by the identification of both aluminum and magnesium in the used silicone fluid. These two components, perfluoro-compounds and magnesium or aluminum, have the little known property of reacting spontaneously and unpredictably under conditions not yet understood. The reaction sequence can be shown as follows:

$$Mg + CnX_{2N+2} \quad MgX + C + heat$$

The above reaction is extremely exothermic and produces the metal halide and carbon as the reaction products. Should a condition exist where magnesium or aluminum could be collected or concentrated, such as the underside of the chimney, the exposure of the metal to Freon 113 vapor could indeed initiate an instantaneous flash or ignition. This reaction is not considered violent in the sense of high-pressure increases, but produces a flash discharge.

This initiating step could then be followed by the ignition of hydrocarbon vapor which gas-chromatography has also confirmed to be present. Some contribution from the DC 704 vapor may also take place. Also, if particulate material, (dust) such as inorganics or carbon particles, is entrained into the gas phase of the diffusion pump system, they could serve as nuclei for the condensation of hydrocarbon vapor. This phenomena greatly increases the potential fuel available for the event.

Consequently, it may not be too unreasonable to consider the metal-Freon interaction as an initiating or ignition step and the hydrocarbon and possibly air (assuming a leak in the

system) as the propagation reaction. If both events were to occur in a millisecond interval, a violent explosion could well result. The relative degree or severity of ignition or explosion would be expected to be a function of the relative amounts of the four "factors" (Freon, metal, hydrocarbon and air) available.

The nonoccurrence of explosions in the combustion apparatus does not necessarily rule out the Freon-metal reaction. Since the mechanism of this reaction is poorly understood, it is possible that conditions favoring it exist within a diffusion pump but were not investigated in this experimentation. The reactants may have volatilized and been drawn off before the fluid was extracted, or, they may not have accumulated insufficient quantities in the fluid tested to initiate combustion.

It is possible, of course, that the particular reaction which caused the explosion has not yet been discovered and that the experimental techniques employed have excluded its detection.

PROGRESS OF THE LANGLEY RESEARCH CENTER VACUUM MEASUREMENT PROGRAM

By Paul R. Yeager

NASA Langley Research Center

INTRODUCTION

In 1963 at the Vacuum Technology Review held in Washington the capabilities, programs, and plans of the Langley Research Center for vacuum measurements were described. Since then considerable increase has been made in capabilities, and programs have advanced in accordance with plans laid down at that time. Some program changes have been necessary to keep pace with the rapidly advancing vacuum technology, but the fundamental concepts of the measurements program have remained intact. In order to demonstrate the progress of the program, this paper gives a comparison of the capabilities in 1963 and now, outlines the major programs currently underway and gives some results of in-house programs.

CAPABILITIES

The vacuum measurement development capability of LRC for 1963 and 1965 are compared in figure 1. In 1963 capability was severely limited as to number of available systems and range. Only one system of the three then available had an ultimate below 1×10^{-10} torr ($\approx 1 \times 10^{-8}$ newton-meter^{-2}) and usage was limited to pressures at least one decade above that. Two of the three 1963 systems are still in operation, and for certain tests have all the capability needed. However, to fully meet LRC measurement needs it has been necessary to add systems with much improved capability. Early systems were bell jar or manifold types pumped by oil diffusion pumps with cold baffles. None of the five major systems since added are this simple. While the manifold-bell jar approach is still widely used, pumping methods are considerably changed with combination systems quite popular (i.e., Hg pumps in series, turbo molecular-sublimation combinations, oil D.P. - cryogenic assemblies). Some of these new systems, with working spaces up to 3 cubic feet, are capable of going below measurable limits. The solid lines on figure 1 show systems in use; the broad dashed line, systems under evaluation; and the short dashed line, systems under construction.

The next two figures represent two of these systems, with figure 2 showing a gage manifold mounted atop an ion pump cart, on the asbestos bakeout oven plate, the bleed valve at the top and the LHe finger at the left. Shown mounted on the system are three Redhead gages and one modulated B-A gage. Figure 3 is a Hg D.P. system featuring two LN_2 traps and a water baffle above the pump. Heater coils are shown on the chamber, pumps, and traps. Fore pressure and guard vacuum are obtained by mounting the entire system in a standard 18- by 30-inch bell jar pumped by a 4-inch oil D.P. Three gage ports are supplied

which open into the variable-temperature dome. The ports are designed so as to accept either nude or tubulated gages.

While these systems have been under development a parallel effort has gone on to improve calibration capabilities.

The improvements in vacuum gage calibration facilities at LRC have extended capabilities at least two orders of magnitude since 1963. Figure 4 shows a comparison of "then" and "now" capabilities. In 1963 calibrations were made to 10^{-7} torr with about 5-percent error by using a McLeod gage from 10^{-3} to 10^{-5} and extrapolating to 10^{-7} with a Residual Gas Analyzer on the system to guarantee gas composition constancy. Ultimate then was 10^{-8} torr. This type system is still utilized over the 10^{-3} to 10^{-6} range when calibrations are limited to that range. Now two systems have been obtained which can make calibrations to 1×10^{-9} torr ($\approx 1 \times 10^{-7}$ newton-meter^{-2}) with 8-percent and 17-percent accuracy, respectively. These systems are shown in the next two figures. Figure 5 shows system 1. This is an orifice-type system using ion and sublimation pumping. Pressure is controlled by a positive displacement flow meter bleeding gas through staged orifices. Accuracy of the system is limited by the extent to which flow rate can be measured. Ultimate of the system is in the 10^{-1} torr range. This system has been thoroughly evaluated and is now in operation. System 2, figure 6, which is now undergoing evaluation, is an oil diffusion pumped system of the orifice type. Principal differences from system 1 is that pressure is controlled by flow rate through a porous plug from a constant pressure source rather than a positive displacement flow meter. The porous plugs have been calibrated for flow rate, and system pressure is controlled and measured by accurate measurement of the upstream pressure with an absolute pressure-measuring device.

The systems just described are typical and representative of the types used for gage development and calibration at LRC. It is with systems such as these that LRC's in-house programs are carried out.

RESEARCH PROGRAMS

Research programs at LRC are aimed to meet anticipated needs as well as immediate problems. The basic approaches used are to divide measurement requirements into two categories, total pressure and partial pressure. Partial-pressure measurements are considered the ultimate and most desirable approach, with total pressure obtained by a summation of the partial pressures. However, where requirements are not too strict, pressure measurements may be made directly by the simpler total-pressure techniques. Also, total-pressure measurements are made in lieu of partial-pressure measurements in many instances because of the relative simplicity of the total-pressure approach, and because of the generally lower limit that can be obtained with total-pressure devices.

In order to improve our position with respect to both total- and partial-pressure measurements both contract and in-house programs are carried on. The more significant of the contract efforts currently underway or recently

completed are shown in figure 7. Item 1 is aimed at providing a low-temperature ion source suitable for use in both total- and partial-pressure devices. The low-temperature source will reduce many problems inherent with the high temperatures of hot tungsten sources and greatly reduce the contribution of the gage to the system gas load. Item 2 is designed to complete the evaluation of performance characteristics of the cold cathode UHV gages by carefully examining the "Trigger Gage" as has been done earlier for the other cold cathode gages.

Item 3 is a study of thermal transpiration, primarily aimed at the slip flow region, to establish the characteristics between viscous and molecular flow. While the effort is aimed primarily at small-diameter tubing for wind-tunnel application, enough range will be covered to establish characteristics of tubing up to the sizes commonly used in ion gages.

Item 4 is a development project aimed at producing an improved flowmeter of very low flow range to be used with orifice-type calibration systems.

Item 5 is a program of study, design, and testing of a magnetron-type ion source for mass spectrometers. Designed primarily for the quadrupole, the ion source provides considerable improvement in sensitivity over existing methods of ion production.

Item 6 is a study of cold cathode gages and modulated and suppressor gages in the XHV region. Emphasis is placed on calibration techniques and beaming effects on the gages. This is a Headquarters funded project, but is included here since it was monitored at LRC.

Item 7 is an actual calibration of several magnetron gages at pressures into the 10^{-11} torr range. This work is followed by preparation for installation in an UHV chamber at LRC in order to survey the chamber to determine pressure gradients and sources of beaming in the facility.

These are a representative sampling of the vacuum measurements efforts being carried out at LRC under contract. However, the list is by no means complete, nor does it represent the in-house efforts which are basically shown in figure 8.

The in-house measurement effort is divided into two distinct phases: (1) total pressure and (2) partial pressure.

In the total-pressure effort several programs are being carried on to give improved measurement capability across a broad front. Work is being carried on to extend gage range, improve response time, and increase accuracy. At the same time, related studies in general gage performance, characteristic behavior, and individual anomalies are being studied.

The effort in partial-pressure measurements is broken into the same groupings as the parts of the mass spectrometer, the principal instrument used for these measurements, that is: (a) ion sources, (b) ion collectors, and (c) ion separators. We have taken the approach that the weakest part of the mass spectrometer is the ion source, followed by ion collection, with the ion separator fairly well developed. Therefore our principal effort up to now has

been in the improvement of ion sources and adapting specialized sources for individual needs. We are now beginning efforts on the ion collector, or ion collection techniques. Efforts have been started on pulse counting techniques, coincidence counters, and general electron multiplier improvement. For the time being the mass separator portions of mass spectrometers are considered sufficient, and their development is not being considered.

RESULTS OF PROGRAMS

The results of some current in-house research are shown in the next series of figures. Figure 9 shows two types of ion gages currently under development. On the left is a gage (designed to have a lower X-ray limit than B-A gages) which is basically an ion gage with the collector shielded in such a way as to protect it from the impingement of soft X-rays. The gage consists of a filament, collector, fine wire grid, and, in addition, a shield plate for the collector and an electron focusing ring to increase sensitivity by controlling the electron trajectory. Experiments to date have only been to the 10^{-8} torr range, but excellent characteristics have been obtained to that pressure. The gage on the right is a modified Schumann suppressor gage with the addition of a shield grid and a split collector to obtain modulation. Experiments with this design have been successful into the 10^{-10} torr range.

In addition to work with in-house designs, considerable effort has been put into the full exploration of characteristics of commercial gages. The next two figures are calibrations of commercial gages made on the number 1 orifice calibration system previously described. Figure 10 is a tubulated gage which shows excellent characteristics down to 1×10^{-9} torr, being linear over the entire range. The figure 11 is a nude gage which also shows good performance, behaving extremely well in the lower ranges.

The next group of figures are results of some gage behavior experiments. Figure 12 shows nude gages calibrated against a tubulated gage in a warm wall chamber. This is a strong difference from the excellent agreement obtained when the gages were calibrated with the chamber walls cold. The differences in calibration cannot be accounted for by temperature induced thermal transpiration effects. Several experiments were conducted after the calibration runs to determine the cause of the nude gage nonlinearity and all point to contamination as the cause. Although not proven as yet, indications are that the gage contamination is a direct result of outgassing from the walls of the chamber, primarily water vapor. These data agree closely with those published by Normand in the 1961 AVS Transactions, who at that time offered no explanation for the nude gage behavior.

Figure 13 is a series of tests made on a tubulated gage. Run one is the response of the gage without being outgassed, but after 12 hours at 1×10^{-9} torr or lower. The run two curve shows the response of the gage after outgassing using the manufacturer's control unit. The gage now follows true pressure more closely, but still not exactly at the low end. The run three curve is the response of the gage after 1/2 hour of electron bombardment outgassing

at 100 ma and 800 volts. This shows the cleanliness of the gage improving considerably, and actually indicates that the standard gage was dirty in the lower 10^{-9} torr region.

The data on the four previous slides have not been published, but will be in the near future as part of comprehensive studies of gage performance. However, several papers have been published recently by LRC or on contract to LRC on the subject of measurements and gage techniques. These are listed in figure 14. The first paper is the contractor report on the gage studies made on NASw-625. It is an excellent report on gage behavior in the lower pressure ranges. The second paper is a TN on calibration of thermal conductivity gages over the range of .1 to 20 torr in several condensable gases and describes the method used for these experiments. Numbers three through six are LRC working papers. Number three gives suggested standards for LRC vacuum chamber measurements, the suggested gages to use, and methods of operation. Number four is a detailed discussion of the McLeod gage and its problems. Number five describes the error in tubulated ionization gages due to differences between calibration and use temperatures for both the gage and chamber. The last paper describes a method for accurately determining the capillary and volume dimensions of McLeod gages.

SUMMARY

In summary, LRC is pushing forward in a broad program designed to improve both total- and partial-pressure measurement capability. The effort is carried on both in-house and on contract to (1) advance the general state of the art, with present and near future efforts concentrated on the weaker points of the program to give an evenly balanced measurement capability, and (2) to solve special problems peculiar to LRC as they arise.

Even though considerable advancements have been made during the past 2 years, measurement capability still lags facility requirements by several orders of magnitudes. In order to reasonably meet space simulator requirements, calibration capabilities must be extended another four decades (i.e., to the present limit of measurement capability) and measurement capability must be increased a minimum of two decades. Not only must ranges be extended but general accuracies and techniques must be upgraded to give better certainty to the measurements as they are made. To do this will require the continued effort and support level of the past 2 years. However, the effectiveness of the present program has decreed that furture planning be based strongly on the present efforts. Therefore, the next 2 years should see no major changes in LRC measurement programs or implementation, but rather a continued strong program based on the present successful efforts.

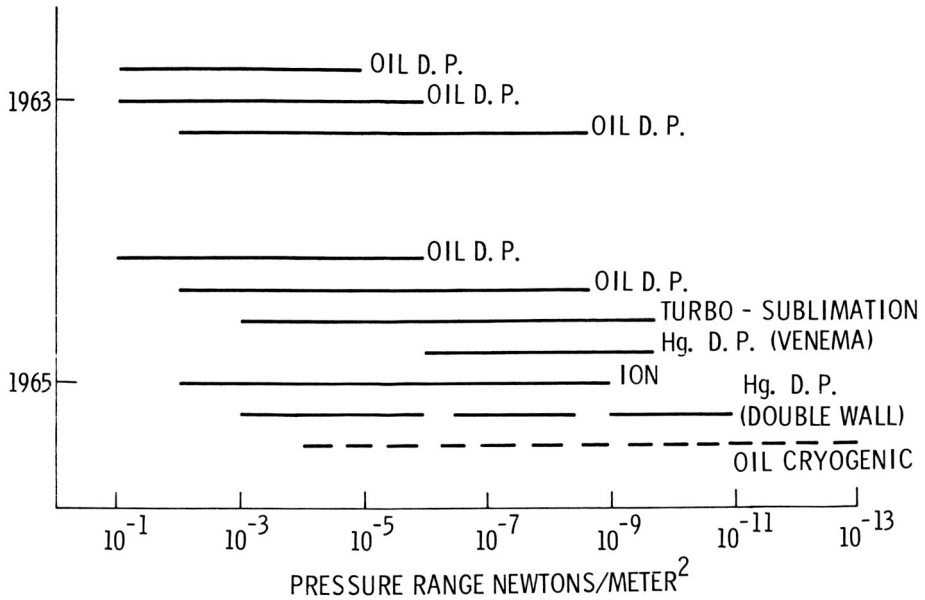

Figure 1.- Vacuum gage development systems.

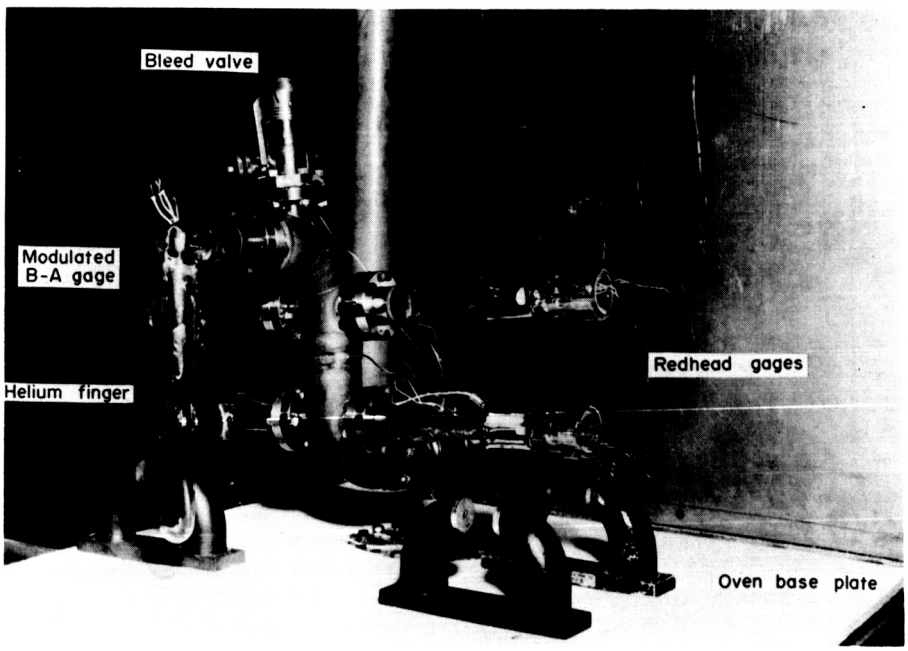

Figure 2.- UHV gage experiment system.

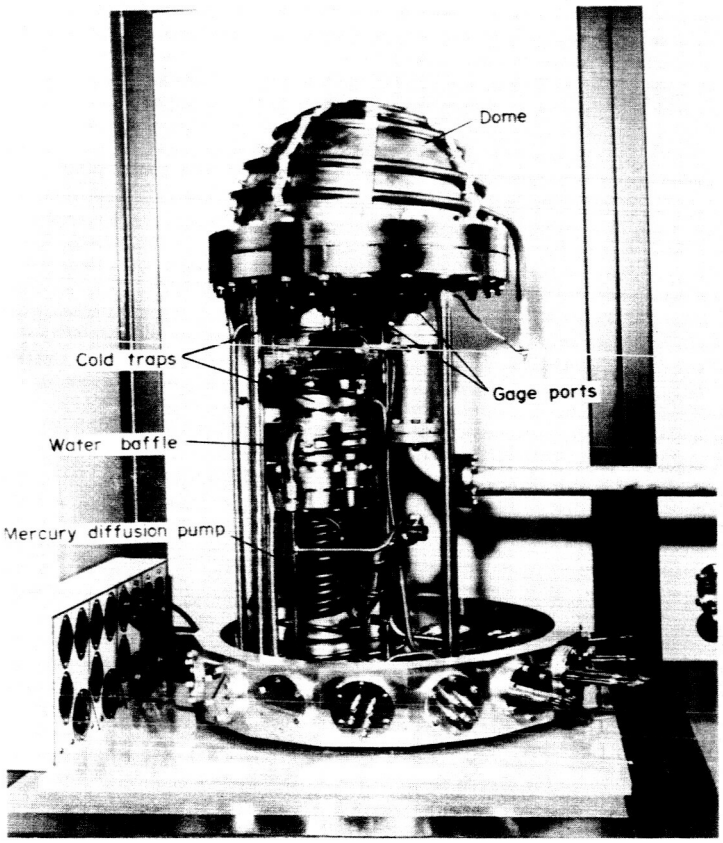

Figure 3.- Experimental gage development system.

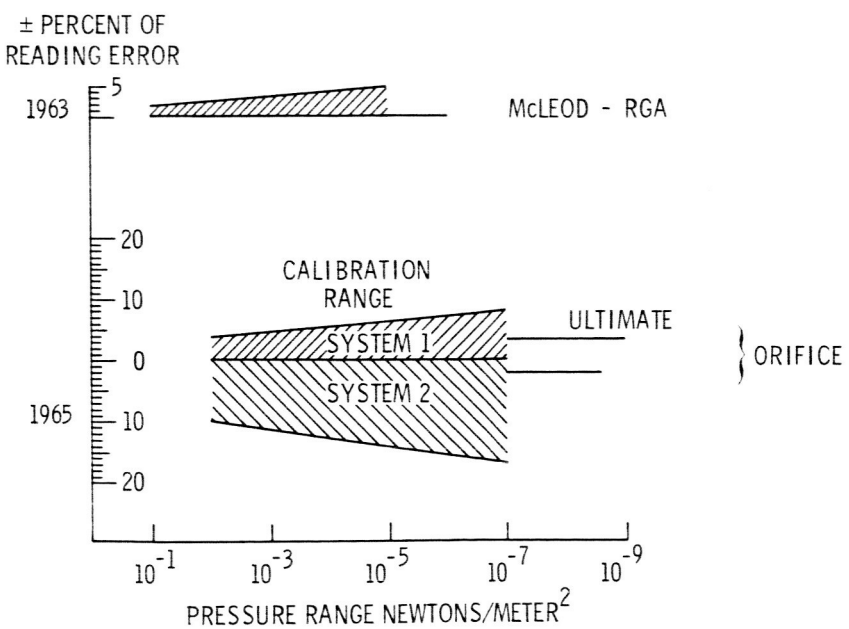

Figure 4.- Range and accuracy of calibration systems.

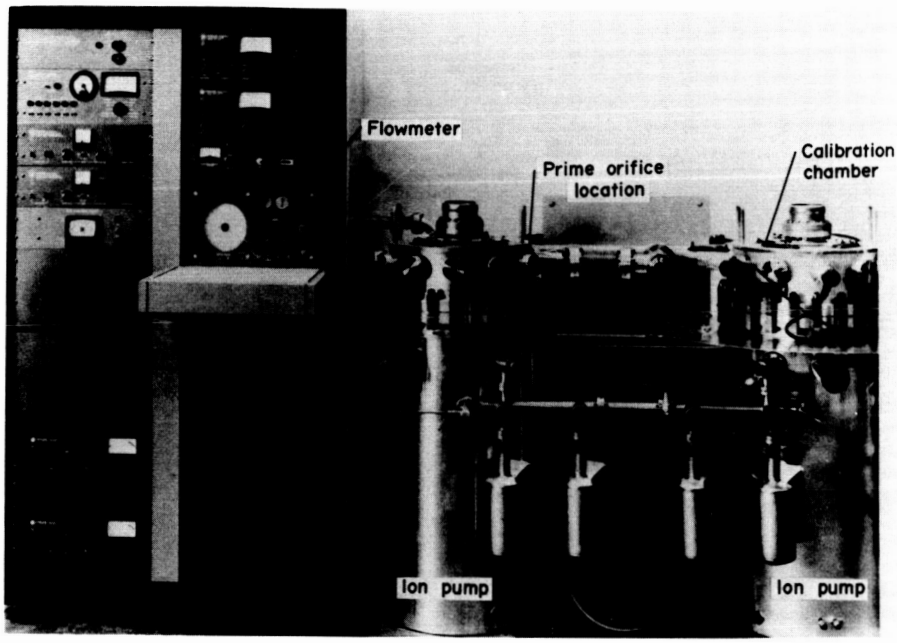

Figure 5.- Calibration system 1.

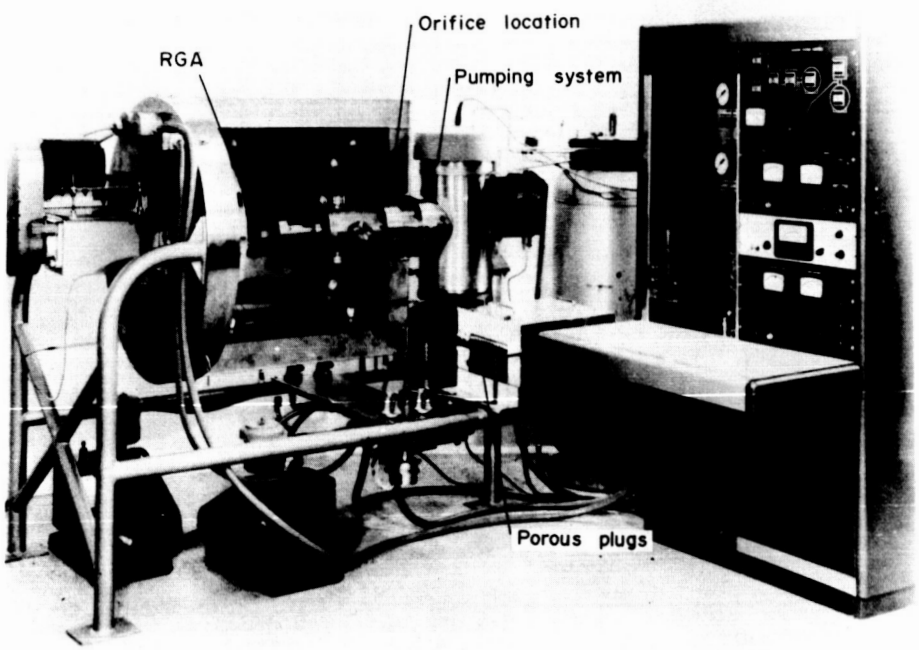

Figure 6.- Calibration system 2.

1. DEVELOPMENT OF TUNNEL EMITTER CATHODE (NAS1-4776) 125-24-03-03
2. EVALUATION OF YOUNG TRIGGER DISCHARGE GAGE (NAS1-3865) 129-01-08-21
3. STUDY OF THERMAL TRANSPIRATION (NGR-34-002-024) 129-01-08-21
4. DEVELOPMENT OF GAS FLOWMETER (NGR-34-002-020) 125-24-03-03
5. DEVELOPMENT OF COLD CATHODE ION SOURCE (NAS1-2691) 125-24-03-03 AND 124-09-04-05
6. GAGE CALIBRATION STUDY IN EXTREME HIGH VACUUM (NASw-625) 124-09-04-
7. ULTRA HIGH VACUUM GAGE PREPARATION AND INSTALLATION (NAS1-2691) 124-09-04-01

Figure 7.- Vacuum gage development - contract effort.

1. TOTAL PRESSURE
   a. EXTEND GAGE RANGE - IMPROVED TECHNIQUES
      NEW GEOMETRIES
   b. IMPROVE RESPONSE TIME
   c. IMPROVE ACCURACY - IMPROVE CONTROL UNITS
      IMPROVE CALIBRATION
      REDUCE GAGE ANOMALIES
2. PARTIAL PRESSURE
   a. IMPROVE ION SOURCES - NONFRACTIONATING SOURCES
      SPECIALIZED SYSTEMS
   b. IMPROVE ION COLLECTORS - PULSE COUNTING TECHNIQUES

Figure 8.- Vacuum gage development - in-house effort.

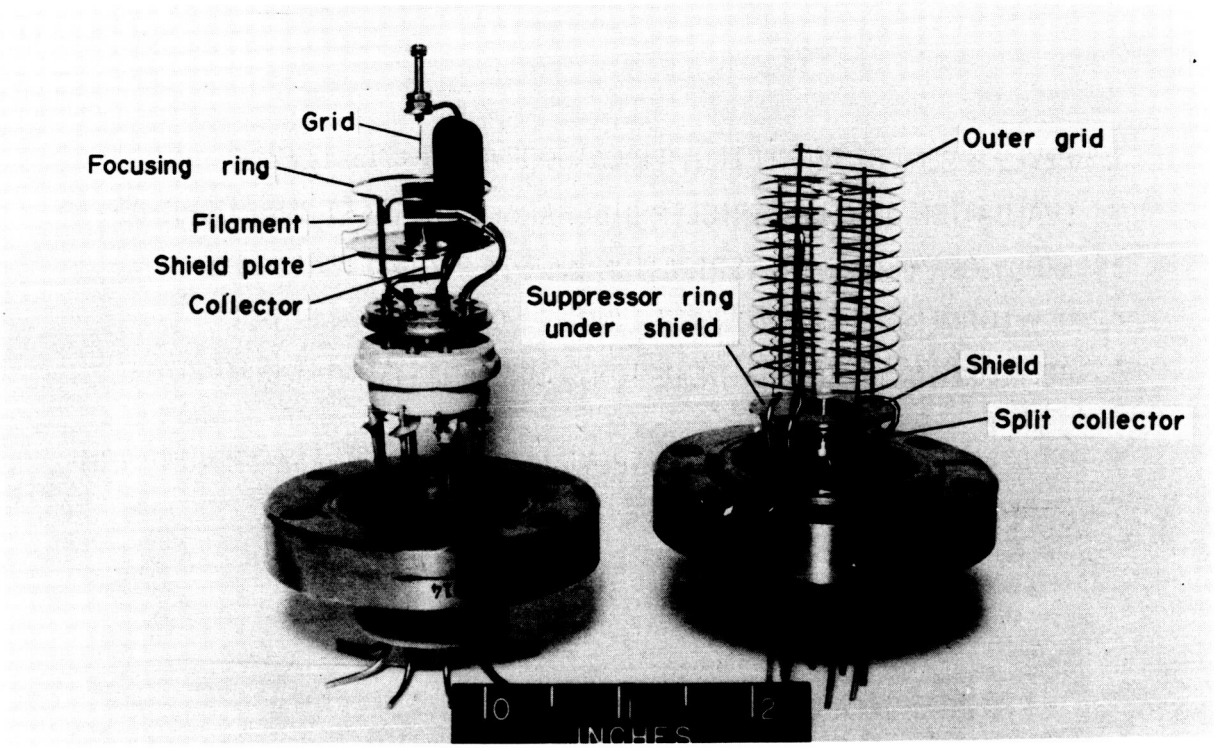

(a) Low X-ray limit gage. (b) Modulated-suppressor gage.

Figure 9.- Experimental vacuum gages.

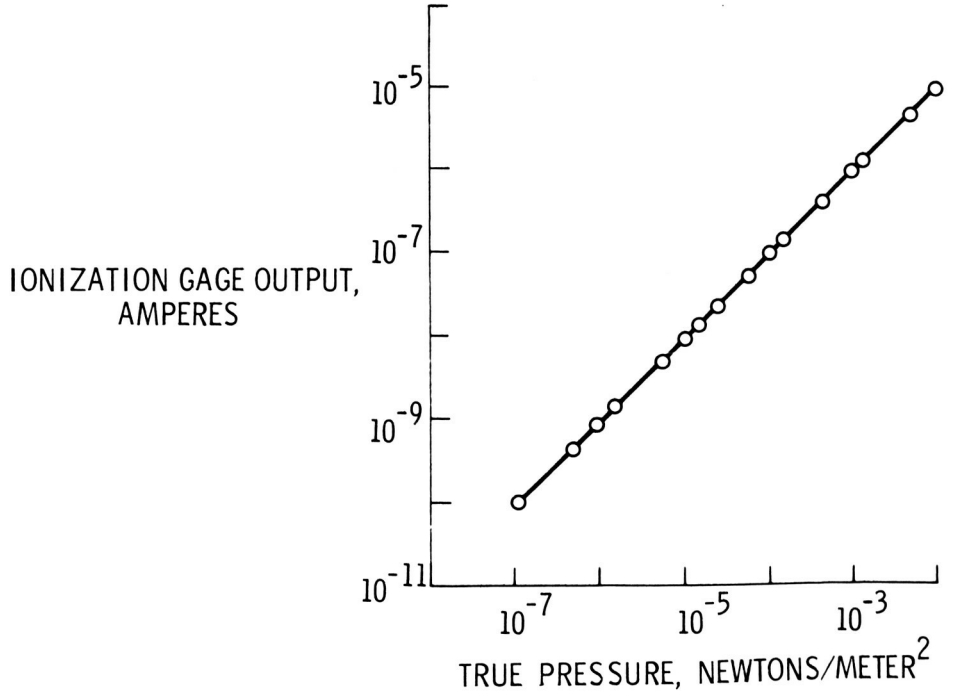

Figure 10.- Tubulated ionization gage nitrogen gas.

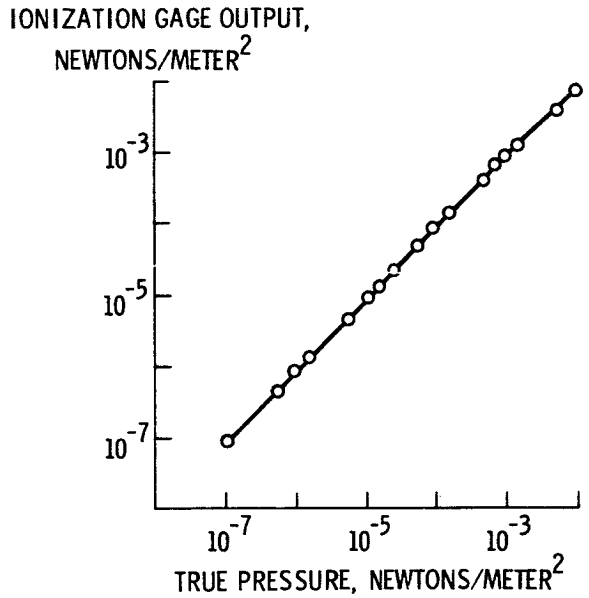

Figure 11.- Nude ionization gage nitrogen gas.

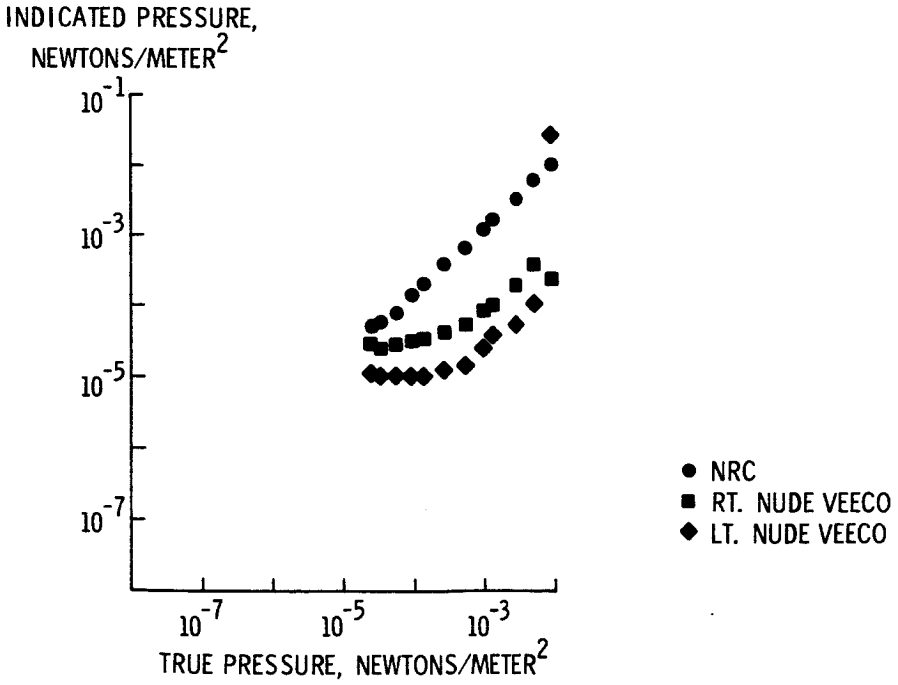

Figure 12.- Gage anomalies.

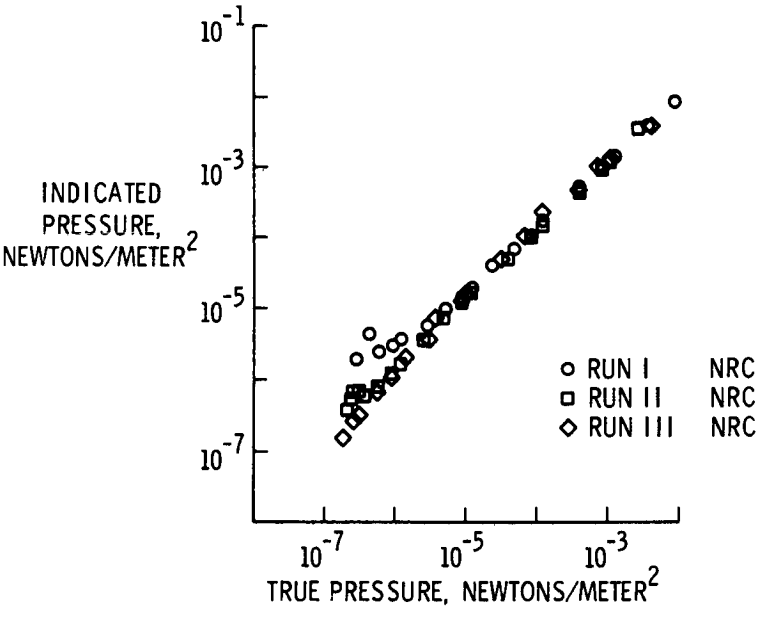

Figure 13.- Gage comparison curves.

1. GAGE CALIBRATION STUDY IN EXTREME HIGH VACUUM (NASA CR-167)
2. A METHOD FOR CALIBRATION OF GAS COMPOSITION - SENSITIVE PRESSURE GAGES IN CONDENSIBLE VAPORS (TN D-2567)
3. STANDARDIZATION OF VACUUM MEASUREMENTS IN THE LANGLEY RESEARCH CENTER GROUND FACILITIES (LRC WP 34)
4. LABORATORY AND FIELD USE OF THE McLEOD GAGE AS A WIDE RANGE PRESSURE STANDARD (LRC WP 36)
5. IONIZATION GAGE ERRORS DUE TO TEMPERATURE VARIATION (LRC WP 66)
6. A METHOD FOR DETERMINING THE VOLUME RATIOS OF A McLEOD GAGE (LRC WP 89)

Figure 14.- Current LRC vacuum measurement publications.

COMPARISON OF PARTIAL-PRESSURE ANALYZERS

By James M. Bradford

NASA Langley Research Center

We have investigated three different gas analyzers in the course of our work at Langley - the omegatron, the 90° magnetic sector with electron multiplier, and the time of flight. I would like to discuss briefly some of the advantages and disadvantages of each.

The omegatron in the past has been used primarily in the pressure range around 10^{-6} to 10^{-7} torr. There seemed to be no reason that the instrument could not be used in the ultrahigh vacuum range and so we investigated the operating characteristics of the omegatron in the ultrahigh vacuum range and the results of the investigation are being published in NASA TN 4242. Briefly, the omegatron is usable down to about 2×10^{-11} torr but has a limited mass range. Since it has no electron multiplier, the output of the omegatron is very reproducible and the instrument is an excellent quantitative analyzer. The analyzer tube of the omegatron is simply constructed so the instrument can be cleaned well enough to eliminate its self-spectrum.

The 90° magnetic sector type partial-pressure analyzer will measure very low partial pressures, 10^{-12} or 10^{-13} torr, and with an electromagnet has an acceptable mass range. In our use, however, we encountered two main problems. The first problem was that we were not able to clean the instrument sufficiently even after weeks of baking and electron bombarding. The second problem was that the sensitivity of the instrument shifted after baking. Because of this change in the sensitivity it is difficult to use the instrument as a quantitative analyzer. The analyzer tube that we used was not nude, by the way, and a nude analyzer may help with the first problem.

The time of flight mass spectrometer will measure partial pressures to 10^{-13} torr and has separation of adjacent peaks at mass 200. The main advantage of this instrument is its flexibility. Its various capabilities are too numerous to go into here but it can be used in many useful modes of operation. We have used the instrument primarily as a partial-pressure analyzer utilizing a nude flight tube that we have installed in a 20-cubic-foot ultrahigh vacuum chamber. Figure 1 shows the nude flight tube installed in the chamber along with a sample of solid-rocket-propellant fuel that we were investigating. You can see that the analyzer section of the mass spectrometer protrudes through the port in the far door and is in close proximity with the sample under investigation. We feel that it is very advantageous to have a nude analyzer tube when trying to measure partial pressures in the ultrahigh vacuum range. The main disadvantage of the time of flight is probably the fact that there are so many "black boxes" that can develop electronic troubles.

We have found that the time flight mass spectrometer gives us the best all-around capabilities for partial-pressure analysis.

EXPERIMENTAL SET-UP

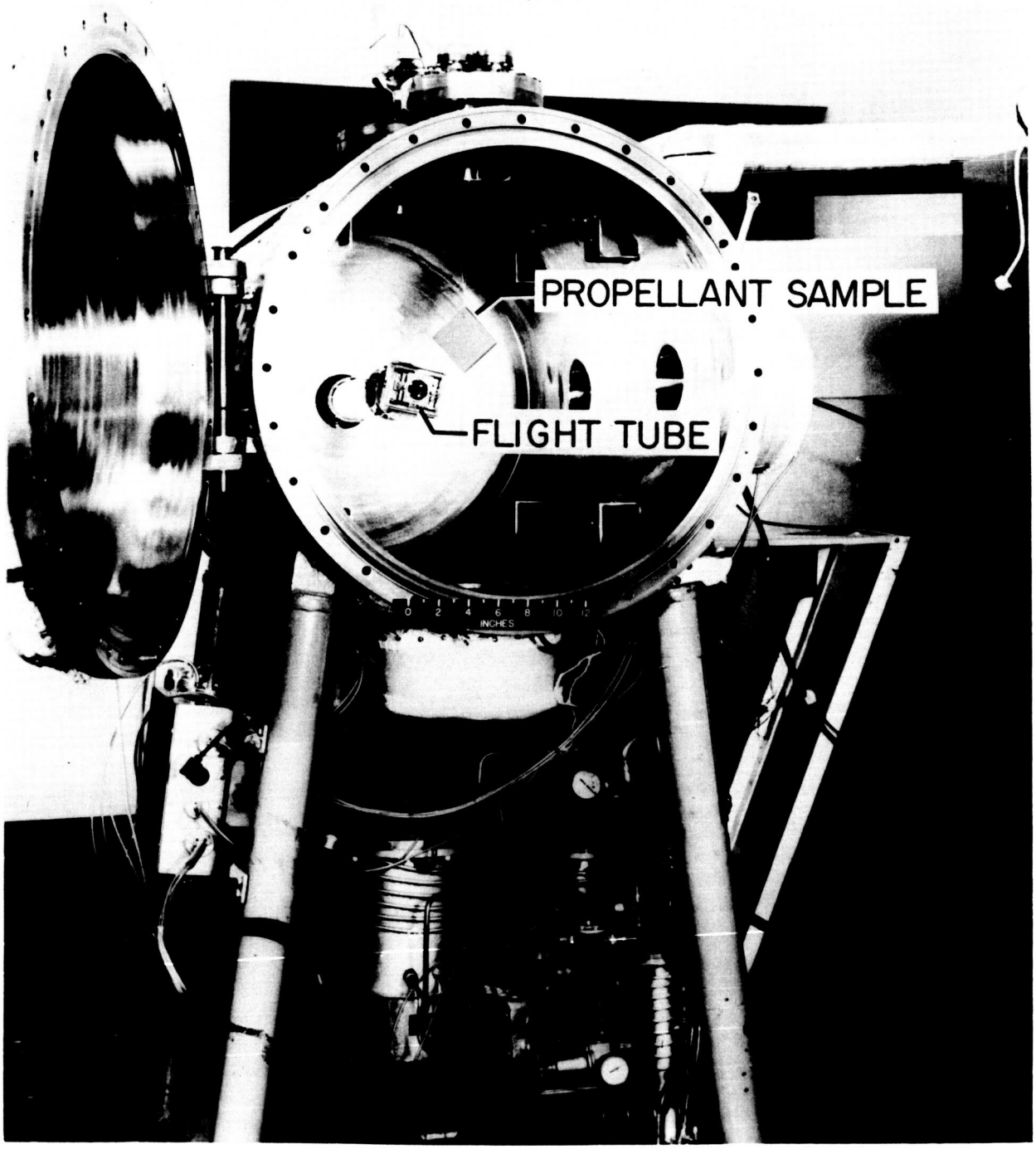

Figure 1

SELECTION AND USE OF A RESIDUAL GAS ANALYZER

by William W. Hultzman

Lewis Research Center

INTRODUCTION

Many types of residual gas analyzers utilizing the mass spectrometer principle are now commercially available. Although principles of operation vary somewhat, all those discussed ionize gas molecules by electron impact and separate the ionized molecules according to their mass-to-charge ratio. All are attached directly to vacuum systems and provide instantaneous readout, as distinguished from batch analysis.

Table I lists some of the research projects at the Lewis Research Center which currently utilize mass spectrometers. Although most of these are magnetic-sector types, the nonmagnetic quadrupole and monopole instruments now becoming available are likely to become more popular.

The requirements of a vacuum system determine the choice among the many instruments now available. Some of the more important instrument characteristics to be considered in such a selection are

(1) Performance factors
  (a) Sensitivity
  (b) Minimum detectable partial pressure
  (c) Maximum operating total pressure
  (d) Mass range
  (e) Resolution
(2) Operating features
  (a) Reliability
  (b) Flexibility
  (c) Convenience
  (d) Construction

PERFORMANCE FACTORS

Table II lists some of the performance factors of some of the commercial instru-

ments now available. Those which have been evaluated at Lewis by the author are indicated. Many of the instruments offer interchangeable Faraday-cup and electron-multiplier ion detectors.

Sensitivity

Sensitivity is proportional to the slope of the curve of ion current against partial pressure and is generally different for different gases. It is usually measured as amperes per torr at the stated normal operating emission current of the instrument. The sensitivity of instruments using Faraday-cup ion collectors is generally of the order of 1×10^{-4} ampere per torr. The sensitivity for nitrogen when electron multipliers are used has been measured at Lewis as 0.5, 1, and 10 amperes per torr for the Bendix, G.E., and Veeco spectrometers, respectively. The manufacturer's stated sensitivity for quadrupole-type spectrometers using electron multipliers ranges from 10 to 100 amperes per torr.

Minimum Detectable Partial Pressure

The lowest detectable partial pressure is herein defined as the nitrogen pressure represented by a signal twice the peak amplitude of the noise of the system. The ratio of minimum detectable pressure to total pressure, although not often specified, varies from one part per hundred for a space-charge-limited instrument like the Farvitron to better than one part per million (under favorable conditions) for some other types of gas analyzers equipped with electron multipliers.

Minimum detectable pressure is usually decreased one thousand to ten thousand times when a Faraday cup is replaced with an electron multiplier. An accompanying increase in noise level prevents obtaining the millionfold gain of which the average electron multiplier is potentially capable.

Maximum Operating Total Pressure

Maximum operating total pressure is usually about 10^{-4} torr. However, instruments with electron-multiplier ion detectors are preferably limited to pressures below 10^{-5} torr because of multiplier current saturation and because of the danger of contamination from hydrocarbons, water, and other impurities.

Mass Range

The mass range of the instruments discussed herein varies from 2 to 50 atomic mass units for some, to 1 to 500 atomic mass units for others. Although atomic mass unit has become a conventional designation, the physical quantity actually represented is the ratio of mass to charge.

Resolution

The resolution of a mass spectrometer is a figure of merit that defines the ability to separate mass peaks adequately. Various means of describing resolution (measures of resolution) are illustrated in figure 1. Although there is great variety in the measures that are used, they are not all just different ways of measuring the same performance parameter. Each of the measures actually describes a different feature of performance, although some are so slightly different that the conversion from one measure to another involves little approximation.

The principal types of measures are obtained as follows:

(1) By measurement on a single peak at mass number M. The resolution is given as $M/\Delta M$, where ΔM is the width (in mass units) at a stated fraction x of peak height usually 50 percent (fig. 1(a)).

(2) By measurement on two peaks separated by one mass number. The mass number for stated cross-contribution is the highest mass number at which one peak contributes a given percentage (generally 1 percent) to the height of the adjacent peak (fig. 1(b)). When not actually specified, it is tacitly assumed that both peaks are of the same height.

(3) By measurement on two peaks separated by one mass number. The mass number for unit resolution is that mass number at which the height of the valley between peaks is a stated fraction x of the average of the two peak heights (fig. 1(c)). Sometimes the average is not mentioned in the description and, instead, both peaks are stated to be of the same height (fig. 1(d)). The definition of figure 1(c) is more general than that of figure 1(d), and also more realistic, since the user rarely can arrange to have both peaks of equal height.

The measures used by different manufacturers are indicated in figure 1, to the extent that they are known or understood by the author. Some manufacturers give more than one measure for the same instrument, in order to clarify performance. Others provide an incomplete description, so that the author has had to guess at the remainder of the description.

In order to provide some common basis for comparison, the data listed in the column headed Resolution in table II were based on measure (1). The numbers represent

actual measurements for those instruments which have been evaluated at Lewis. For the other instruments, the numbers are based on the manufacturer's published literature. Where the manufacturer uses a measure other than (1), the author has estimated the equivalent value in terms of measure (1) from his experience with evaluated instruments by establishing a crude empirical relation between measures (1), (2), and (3).

Quadrupole-type instruments have approximately constant ΔM (fig. 1(a)); typical values range from 0.5 to 5 atomic mass units. Resolution can be traded for sensitivity; a front-panel control usually is available for this purpose. The resolution of omegatron-type instruments varies inversely with the mass number. The resolution ($M/\Delta M$, fig. 1(a)) of the other magnetic-deflection instruments is approximately independent of mass number.

The electrostatic and radiofrequency types, which do not require magnets, have not been widely used in this country up to this time, presumably because of their comparatively low sensitivity, low resolution, and glass construction. However, they may become more popular as the residual gas analyzer is adopted for routine engineering use as a process monitor.

It should be noted that maximum resolution and maximum accuracy of peak-height indication can be obtained only when the rate of mass scan, expressed as atomic mass units per unit time, is small compared to the reciprocal of the overall time constant of the amplifying and recording system.

OPERATING FEATURES

Table III lists some of the operating features considered important in selecting a mass spectrometer. The following text clarifies the entries in the table.

Reliability

Reliability of operation has varied widely among instruments used at Lewis. Some instruments of certain manufacturers have a record of frequent mechanical and electrical breakdown; others have a record of continuous trouble-free service. Flexibility and sensitivity are not correlated with reliability. Poor mechanical reliability is generally associated with inadequate attention to details of design and construction. Poor electrical reliability may be associated with poor choice of components, with inadequate voltage or frequency regulation of power supplies, or with highly complex circuitry in which the mere number of components is sufficient to increase the probability of a failure. Some types of spectrometers inherently require closer voltage or frequency regulation than

other types; the time-of-flight, quadrupole, monopole, and radiofrequency types require very high voltage regulation, and the last three of these also require very high frequency regulation.

Some of the measures that may be applied to calibration stability are

(1) Ability to monitor a single mass continuously, without frequent manual readjustment of controls

(2) Constancy of proportionality between ion current and partial pressure over several decades of pressure. (The Farvitron analyzer generally operates in a space-charge-limited condition, in which it produces a spectrum whose total area is constant. If a new gas is then injected into the chamber or removed from it, the heights of all other peaks will also change; however, the relative heights usually will correctly represent the relative partial pressures.)

(3) Ability to maintain constant magnet orientation relative to the electrodes, and, in the case of electromagnets, to maintain constant magnetizing current

(4) Freedom from susceptibility to contamination which may contribute excessive background noise or excessive electrical leakage between closely spaced electrodes

Flexibility

As shown in table II, many instruments have electron multipliers to increase sensitivity over the Faraday-cup - electrometer combination. The gain of these multipliers is affected by contamination of the electrodes, becomes nonlinear at higher pressures, and is a function of mass number. Contamination becomes more serious because bakeout temperature is limited. Thus, the increased sensitivity is obtained at the cost of requiring frequent recalibration and cleaning.

Since stray magnetic fields affect multiplier gain, it is impractical to provide electron-multiplier detectors for the cycloidal and omegatron spectrometers, whose ion collector is immersed in the magnetic field. The Veeco instrument provides magnetic shielding for its electron multiplier and thereby increases gain by a factor (30 to 70) which varies with mass number.

Faraday-cage detectors are thus preferable, in most applications, when pressures exceed 10^{-9} torr.

All instruments, other than the Farvitron, provide for panel-meter readout and for strip-chart recording of collector current as a function of time. The Farvitron and all instruments that have electron multipliers provide for cathode-ray-oscilloscope display. The Veeco analyzer uses the sawtooth signal from the oscilloscope to produce the mass sweep and thereby provides high flexibility in scan time and mass range selection.

Veeco's three-segment linear scale, which resembles a logarithmic one, permits a signal of 0.05 percent of full scale to be detected at any one amplifier gain setting. The General Electric instrument has a five-decade logarithmic scale. Bendix circuitry permits monitoring five channels continuously while the spectrum is being scanned; alternately, as many as six peaks can be monitored continuously if scan is not monitored.

Output voltages that can be applied to an X-Y recorder, to produce a direct time-independent plot of equivalent partial pressure as a function of mass, are provided by a few manufacturers.

In addition to total-pressure indication by the instruments identified in table II, the Aerovac, Bendix, and Varian instruments provide overpressure protection circuits.

Limited or fixed voltage and current adjustments are desirable in an instrument intended for routine field operation. Operational reliability is often higher when there is a minimum number of controls. On the other hand, flexibility is desirable in instruments intended for research. The G. E. instrument provides for magnetic scanning as well as for scanning by voltage variation. Magnetic scanning provides (1) a more open mass scale and (2) lesser reduction in sensitivity at higher masses.

Convenience

Mass spectrometers require a full bakeout (at least 400° C) in order to make their spectrum representative of vacuum-chamber conditions. Electron multipliers ordinarily must be baked to restore sensitivity after there has been any contamination. The best procedure for accomplishing this has yet to be learned, both by manufacturers and users, because it is presumably affected by the nature of the contamination. To date, the author has found, in his limited experience, that a manufacturer's instructions, when followed literally, do not always produce a full restoration of gain.

Magnet position is very critical in magnetic-deflection instruments; in those instruments where fixed stops are not provided, the user must devote considerable effort to provide reliable means for restoring the magnet to its original position after an operation such as removal for bakeout. The omegatron, with its very powerful magnet and glass tube, provides an operational hazard because a steel object attracted to the magnet may break the glass tube.

The Aerovac spectrometer requires a manual change of magnets to change mass range. The G. E. instrument can cover almost the entire mass range with one magnet, at the expense of resolution. Full resolution can be achieved if two magnets are used or if a single electromagnet is used; the latter, of course, is controllable remotely. The Veeco instrument offers both manually changed and pneumatically changed shunts; the manually changed shunted magnet, although providing a mass range up to 50, does so

with reduced sensitivity. The ranges obtainable for the spectrometers just discussed are listed in table IV.

Construction

Envelope size affects handling and mounting; it also affects outgassing ability if the ion source is not nude. The Bendix spectrometer requires a separate high-vacuum pumping system to maintain a low vacuum in the flight tube.

As additional metal analyzer tubes become available, the engineering application of residual gas analyzers becomes more feasible than it was when only glass tubes were obtainable.

As in the case of the tubulated ion gage, the limited conductance of any tubulation and, even more importantly, any limitation on the bakeout capability of the tubulation and of the envelope, may seriously affect the accuracy of gas analysis. On the other hand, the dangers of mechanical damage and of gage-element contamination are increased when a nude gage is used. In many cases, such as that of the quadrupole instruments, the distinction between nude and tubulated is not sharp, since the spectrometer may be inserted to various depths into the vacuum system. The omegatron and the C. E. C. spectrometers, which have ion sources immersed in the magnetic field, are not adaptable to a nude construction; nevertheless, in the Nuclide instrument the entire spe spectrometer, including the magnet, is immersed in the vacuum chamber.

CONCLUDING REMARKS

The preceding comments reflect experience to date at Lewis. The comments have been most detailed on those spectrometers which have been systematically evaluated by the author. They have been less detailed on other spectrometers which are in use but have not been evaluated because they have depended on comments and findings of users whose primary interest was not in instrument evaluation; nevertheless, the users have been most cooperative and their comments have been very valuable. The techniques of application of partial-pressure analyzers are just being learned, and this learning is accelerated as the diversity of applications increases.

Since instrument development is proceeding very actively, prospective purchasers of spectrometers are advised to check with manufacturers to determine which improvements have been made since the writing of this paper.

TABLE I. - RESIDUAL GAS ANALYZERS IN USE

AT LEWIS RESEARCH CENTER

Research area	Partial-pressure range, torr	Number of instruments
Solar simulation	10^{-14} to 10^{-6}	2
Lubrication	10^{-12} to 10^{-5}	5
Surface physics	10^{-11} to 10^{-5}	4
Materials	10^{-10} to 10^{-8}	2
Instrumentation	10^{-10} to 10^{-4}	6
Electric propulsion	10^{-8} to 10^{-5}	2
Energy conversion	10^{-9} to 10^{-6}	5
Liquid metals	10^{-9} to 10^{-6}	2
SNAP testing	10^{-7} to 10^{-5}	1
Centaur testing	10^{-6} to 10^{-4}	1

TABLE II. - PERFORMANCE FACTORS OF SOME COMMERCIAL RESIDUAL GAS ANALYZERS

Type of analyzer	Minimum detectable nitrogen pressure, torr		Mass range, amu	Resolution at 50 percent of peak height, $(M/\Delta M)_{0.5}$
	Electrometer	Electron multiplier		
Magnetic deflection:				
[a]Aerovac AVA-1 (60°)	10^{-9}	-----	2-70	45
[a]C. E. C. 21-612 (180°)	10^{-9}	-----	2-80	40
C. E. C. 21-614-1 (cycloidal)	$<10^{-10}$	-----	2-200	200
C. E. C. 21-614-2 (cycloidal)	$<10^{-11}$	-----	2-200	80
[a]G. E. 22 PC-110 (90°)	$<10^{-10}$	$<10^{-13}$	1-300	130
Nuclide 21-90-MB (90°)	-----	10^{-14}	1-100	100
[a]Veeco GA-4 (60°)	$<10^{-10}$	$<10^{-13}$	2-300	150
Omegatron:				
Edwards	10^{-10}	-----	2-200	------
[a]Leybold	10^{-9}	-----	1-250	1000/M
Sloan OMS-2	10^{-10}	-----	2-50	------
Vacunetics	10^{-10}	-----	2-86	1000/M
Electrostatic and radiofrequency:				
Abcor WB-7 (Bennett)	10^{-9}	-----	1-250	40
[a]Leybold Farvitron	10^{-8}	-----	1-250	20
Leybold Topatron (Bennett)	10^{-8}	-----	2-100	30
Time of flight:				
[a]Bendix 17-210 (modified)	-----	$<10^{-12}$	1-400	50
Quadrupole or monopole:				
Atlas AMP-3 (quadrupole)	10^{-10}	$<10^{-12}$	1-100	[b]100
G. E. 22 PC-150 (monopole)	-----	10^{-14}	1-300	[b]250
Ultek 200 (quadrupole)	-----	$<10^{-14}$	1-500	[b]500
Varian 980 (quadrupole)	10^{-10}	$<10^{-12}$	1-250	[b]50

[a]Evaluated by the author. Data on other instruments are based on manufacturer's published literature.

[b]At high end of range.

TABLE III. - SOME OPERATING FEATURES OF SOME COMMERCIAL MASS SPECTROMETERS

[Data obtained from manufacturer's published literature; x indicates feature is present.]

Operating feature		Spectrometer										
		Aero-vac	C. E. C 180°	G. E. 90°	Veeco	Omega-trons	Farvi-tron	Bendix	C. E. C. cycloidal	Nuclide	RF (Bennett)	Quadrupole and monopole
Reliability												
Mechanical workmanship[a]												
Electronic design[a]												
Calibration stability[a]												
Circuit complexity				x			x	x			x	x
Flexibility												
Presentation	Cathode ray oscilloscope			x	x		x	x				x
	X-Y	x		x								x
Total-pressure indication		x									x	x
Adjustability of operating parameters	Full			x		x		x		x		x
	Limited	x	x		x		x		x		x	
Convenience												
Bakeout capability	Full	x	x	x	[b]x	x	x			x	x	[b]x
	Limited							(c)	(d)			
Magnet positioning	Fixed	x			x		(e)	(e)		x	(e)	(e)
	Not fixed		x	x		x			x			
Range change	Remote			x	x	x			x	x	x	x
	Local	x		x	x							
	None						x	x				
Construction												
Envelope size	Small		x			x	x				x	
	Medium	x		x					x			x
	Large				x					x		
	Very large							x				
Envelope material	Metal	x	x	x	x			x	x	x		x
	Glass			x		x	x				x	
Ion source	Nude	x		x	x			x		x	x	x
	Tubulated		x	x	x	x	x		x		x	x

[a]See text for discussion of reliability.

[b]Bakeout limited to 300° C with electron multiplier.

[c]Bakeout limited to 200° C.

[d]Bakeout limited to 250° C.

[e]No magnet required.

TABLE IV. - MASS RANGES FOR SOME

COMMERCIAL SPECTROMETERS

Spectrometer	Mass range, amu
Aerovac	
Small magnet	2-11
Large magnet	12-70
G. E.	
Small magnet	2-200
Large magnet	12-300
Electromagnet	1-300
Veeco	
Manually changed shunt, shunt in	2-50
Manually changed shunt, shunt out	12-300
Pneumatically shunted magnet, shunt in	2-12
Pneumatically shunted magnet, shunt out	10-250

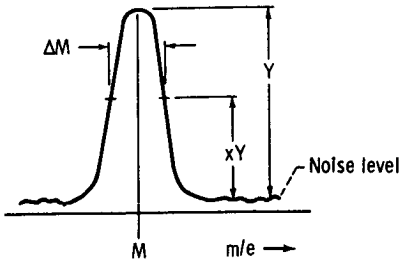

Spectrometer	x
G.E. 60°	0.01
Leybold Farvitron	0.5
Leybold omegatron	0.01, 0.5
Leybold Topatron	0.1, 0.5
Varian quadrupole	0.5

(a) Resolution expressed as $M/\Delta M$, by measurement on single peak.

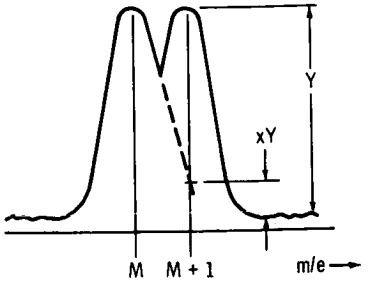

Spectrometer	x
C.E.C. cycloidal	0.01
Bendix time of flight	0.01, 0.015, 1.0
G.E. 60°	0.01

(b) Slated cross contribution of one peak to another, when the two peaks are separated by one mass number.

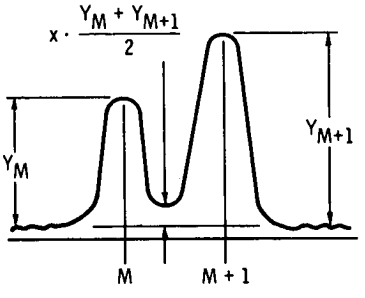

Spectrometer	x
Atlas quadrupole	0.1
G.E. monopole	0.2
Nuclide 90°	0.001
Sloan omegatron	0.2
Veeco 60°	0.02

(c) Mass number for unit resolution, by measurement of valley between two unequal peaks separated by one mass number.

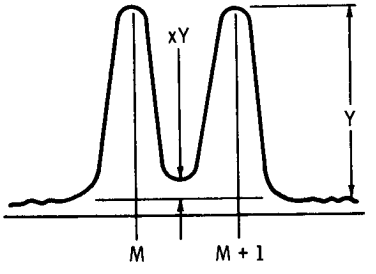

Spectrometer	x
Abcor RF	0.35
Bendix time of flight	0, 1.0
C.E.C. 180°	0.02
Ultek quadrupole	0.1

(d) Mass number for unit resolution by measurement of valley between two equal peaks separated by one mass number.

Figure 1.- Some methods of describing resolution, as used by various manufacturers.

RESIDUAL GAS ANALYSIS IN THE TEST AND EVALUATION DIVISION AT GSFC

BY: Harold Shapiro

Testing spacecraft and spacecraft components has more than enough variables to keep the evaluators busy. So, the isolation of any significant variable is worthwhile from both the technical and economic point of view. Residual gas analysis via mass spectrometry is a multifaceted tool which informs the evaluator about the environment in which he tests his craft. More than that, it is a dynamic probe which he uses to ascertain the health of the test object. It provides him with information concerning the materials that go into the manufacture of his spacecraft or about the fixtures, wiring, plastics, adhesives, sealants and elastomers which he uses to construct his chamber, manipulate his test object, heat it, cool it or read its output. The mass spectrometer tells him which pump he may use to create his vacuum if he knows the level of cleanliness he needs, and the degree of vacuum he has achieved, far more readily than any total pressure gauge in current use, to any degree of ultra-high vacuum.

However, instead of extolling the virtues of the instrument let us examine some of the uses to which it is put in the Test and Evaluation Division at GSFC.

Chambers in which spacecraft or major components are tested are equipped with a mass spectrometer with a mass range of at least 150. The spectrum is scanned as indicated by the first pattern. The first pattern itself is taken when the pressure is reduced to the working level of the spectrometer, 10^{-4} - 10^{-5} torr. Figure 1 shows a scan taken from a chamber which has been cleaned with "Freon TF". The characteristic peaks for this trichlorotrifluoroethane disappear soon after startup. When equilibrium has been achieved, spectral scans are collected about once every 8 hours. If no irregularity in the pattern is found then a final scan is made just before return to ambient. If an irregularity is observed it will generally be a sign of trouble. A leak in a pressurized part of the craft, an

unusual sublimation or outgassing or the breakdown of a component is not usually suspect. A typical example of the value derived from running each test with a mass spectrometer attached is illustrated by the test run on an international spacecraft designed for top side sounding of the ionosphere (S-27A). This satellite is powered by five batteries which, for test purposes, were cycled through on-off modes. Figure 2 shows a portion of the mass spectrum scanned and illustrates a large increase in the mass 16 peak with the batteries operating. Contrasting this peak with the same mass number when the batteries are quiescent before and after discharge indicates some unusual phenomenon is taking place. Such an increase in any mass number is to be viewed with suspicion. An atmospheric leak into the chamber would be seen as a large increase in masses 32 and 14 as well as an increase in 16. These were not present and since the phenomenon appeared only during activation of the batteries our efforts were concentrated on them. Power performance via electronics did not indicate battery degradation. Investigation of the batteries revealed breakdown of the nylon separators in one battery. Nylon, a polyamide, was decomposing and releasing NH_2 with a molecular mass of 16. Thus, the time it took to find a fault, pinpoint the source, and apply a remedy, was shortened from weeks to hours.

In the area of materials screening Test and Evaluation's program is progressing at a moderate rate. As an original goal, new materials intended for use in vacuum would be sampled and subjected to mass spectrometer analysis. The "fingerprint" or spectral pattern of the material would then be fed to a computer memory. During a routine run on spacecraft or components, the mass spectrometer output would be taken and recorded on tape and the tape compared to the stored patterns. In this manner analysis would be performed automatically by the computer resulting in an accurate and rapid feedback. In addition to providing a fingerprint of commercial preparations and devices the data which has been gathered is providing some guidance to designers, particularly where vacuum stability of the material is a required property. To mention but two such cases, one was the use of RTV-102 as an adhesive near a high voltage terminal. We found a huge increase in the water peak due to this RTV so that we were able to warn the experimenter of possible coronal effects.

Another case involved the use of G. E. low vapor pressure greases to lubricate a gimbal in a high vacuum chamber. Of three greases submitted for test all proved acceptable and we were able to recommend one. When the mass spectrometer is used as a sifting screen for the best material where a large number of choices is available, the technique is time consuming. The results of such a procedure can be classified as good, bad, and indifferent and a table shows the experimenter at a glance which material he can safely use. The table continues to have a permanent value after the individual use has been satisfied. For example, a Goddard experimenter recently needed an epoxy potting compound to embed an ion spectrometer. He submitted ten variations of epoxy compounds for vacuum use. The resulting table showed two Armstrong resins to be "good", seven contributed small amounts to the gas load and were labeled "indifferent", one, Epon 815, was graded "poor". Shortly after these tests were completed a sample of non-sensitive propellent material was submitted for test. As a binder the manufacturer used the same Epon 815 resin. We were able to recommend a more certain epoxy be used in its place. Along these lines of search for patterns to be stored in the computer, it very shortly became apparent that DC 704 diffusion pump oil played a prominent role. Despite manufacturers' claims for their pumps, baffles, traps, etc. using such words as "negligible backstreaming","virtually eliminates", "reduces to practically nothing", we always observed the characteristic peaks for DC 704 oil. Figure 3 illustrates the major peaks together with the molecular fragments which produce them. Without exception, regardless of cold shrouds, cold baffles or any technique of startup procedure, at least at the beginning and at the end of a run the oil peaks were observed. Figure 4 is a composite of scans taken at the beginning, middle and end of a test performed in a 12' x 15' chamber. Reading from the bottom up, the scan was taken shortly after diffusion pumps were turned on, then after 8 hours of pumping,and finally just prior to return to ambient. The masses at 150, 135 and 119 are prominent to begin with, disappear during the entire working period and then finally re-appear as the pumps begin their cool-off. This possibility of oil contaminating an experiment led us to examine other methods of preventing backstreaming. Here again mass spectrometry is being used to evaluate the

effectiveness of a new development. Without describing our efforts to find a suitable filter, I will just say that we could not find a suitable filter material that would remove the oil during a prolonged run and permit suitable pumping speeds. Examination of the problem from the point of view that it would be sufficient to remove the objectionable properties of the oil led to the invention under evaluation as a thermal barrier (Figure 5). It consists of two separate rings fabricated from any high temperature, non-outgassing non-conductive material. Alumina, Steatite, Zirconia are but three suitable materials. The rings are made with holes or slots to accept a nichrome wire and hold them in place. The rings can be fitted across any part of the path between the chamber proper and the pump throat. When current is passed through the nichrome heaters, a thermal barrier to backstreaming oil is interposed which disrupts the oil molecule reducing it to its simpler components. Carbon, hydrogen, methane and some higher molecular weight hydrocarbons are expected among the fragments. The advantages to be gained by this usage are twofold. First, the oil pumped chamber can be cleaned after the experiment is finished, since most of the fragments are gaseous and the remainder readily attacked by the common solvents. Secondly, none of the fragments have the tendency to plate out on optical or painted surfaces as has diffusion pump oil. The first trials of this invention consisted of two rings with a combined total area of 96 square inches. The wire used gave a hot section equal to only 10 square inches. Mass 150 was used to monitor oil contamination within the experimental chamber. Without a cold trap in the line, and the pumps operating at their normal temperatures the 150 peak rises to about 30 chart divisions. When the thermal barrier is turned on the peak drops at once to about 23 divisions and rises back to 30 divisions when the current is turned off. Unfortunately, the thin gauge wire used in this first attempt showed a great deal of expansion during heating with resulting movement, touching of adjacent wires and shorting out of the central section, which is the reason why our hot section only contained 10 square inches. Currently, redesign of the wiring scheme is underway and, hopefully, more complete results will be obtained soon. An interesting variant of this scheme requires a positive potential on the upper ring while the lower ring provides the thermal barrier. In this way the fragments of the oil

molecule, which are not as obnoxious as the oil molecule itself, may be prevented from reaching the working area.

I would like to conclude with a suggestion for an ART program; the data gathered by users of mass spectrometers for the screening of materials should not be lost. This information is of great value to NASA as a whole, and to the many individuals who build experiments and have these experiments tested in earth bound vacuum chambers. There is a problem of getting these results into the hands of the users in such a manner that they are aware that such information exists and would be helpful to them. I would suggest a NASA-wide pool properly advertised, readily available, perhaps in handbook form, or if the information be put on tape, in the form of a telephone number. Into such a pool each unique material tested, vapor pressure information, weight loss, mass spectral data and such other pertinent information of importance, could be fed by those of us who do the original work. In this way duplication of effort could largely be avoided, a real savings in both time and money instituted and the information not be lost once the single objective has been accomplished.

We have reviewed the application of residual gas analysis via mass spectrometry in the Test and Evaluation Division at GSFC. There are many more uses and situations which lend themselves to this powerful technique which were not mentioned in passing, and which are in use today. The use of the mass spectrometer in the future will, I am sure, be even more prominent as the demands for control of the environment become more clearly defined.

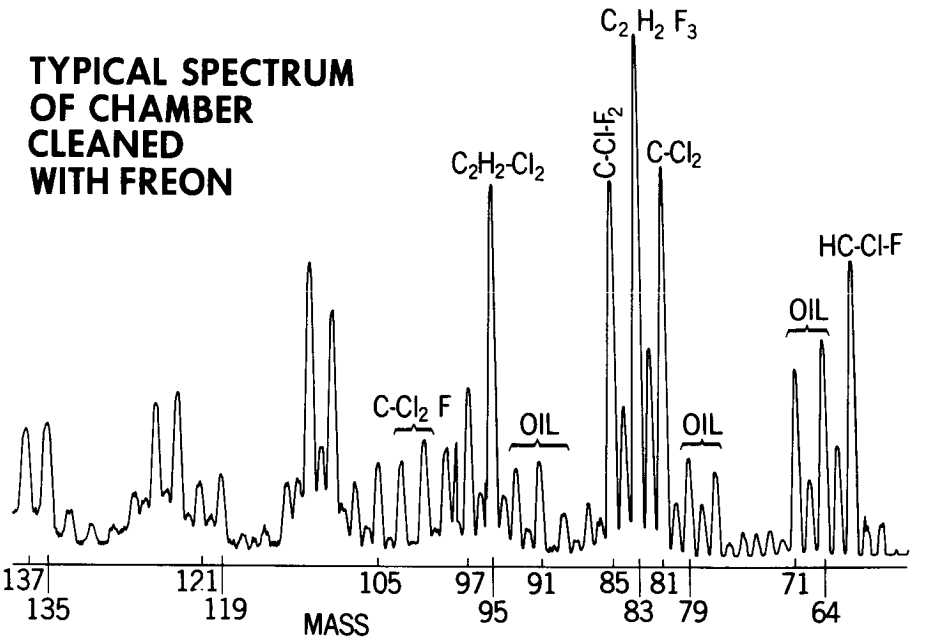

Figure 1

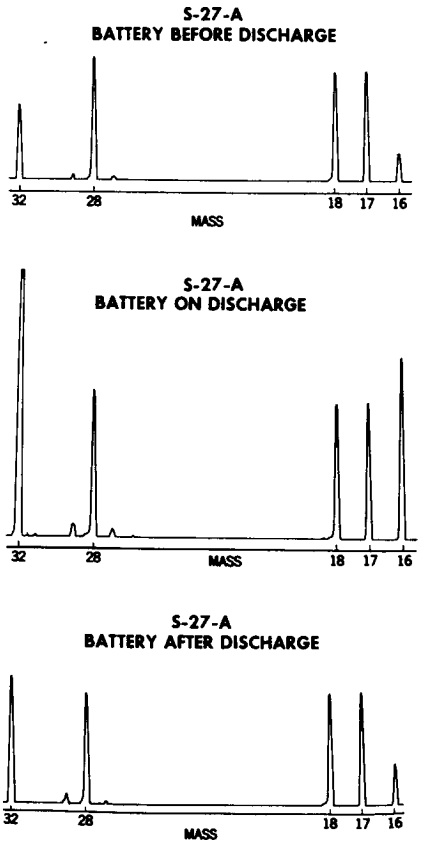

Figure 2

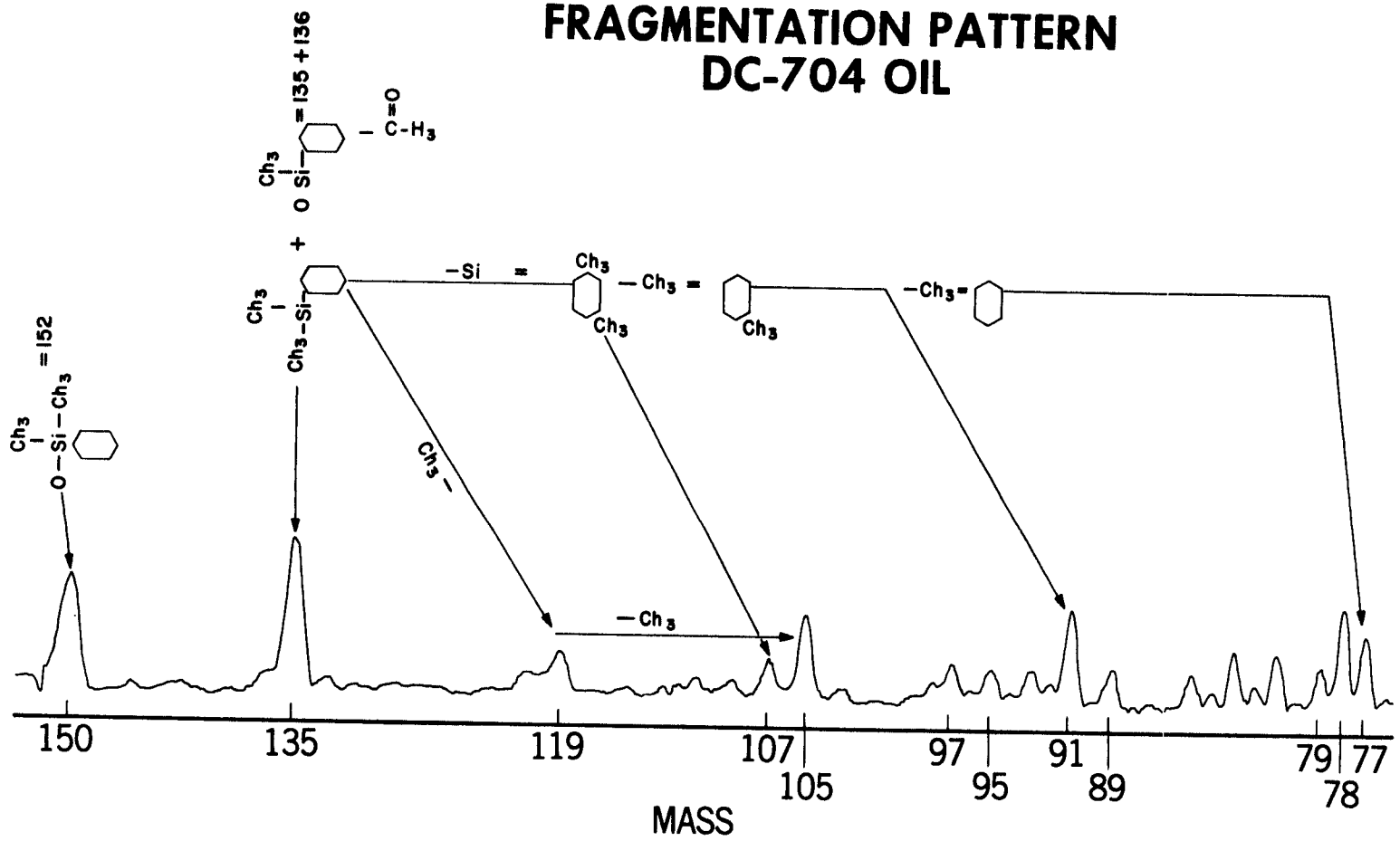
FRAGMENTATION PATTERN
DC-704 OIL
=152
=135 +136
-Si =
-Ch3 =
-Ch3-
-Ch3
150
135
119
107
105
97
95
91
89
79
77
78
MASS

Figure 3

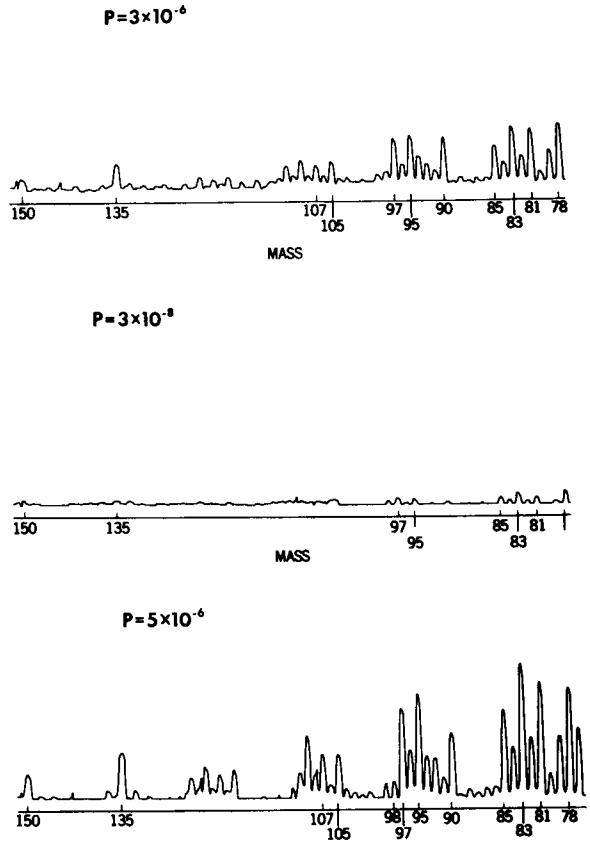

Figure 4

BACKSTREAMING THERMAL BARRIER

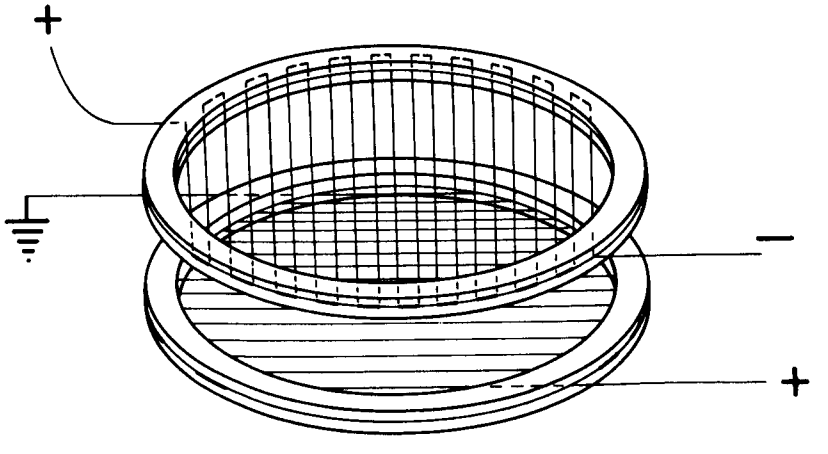

Figure 5

STATUS REPORT: MANNED SPACECRAFT CENTER CHAMBERS "A" AND "B"

BY: Bill Roberts

INTRODUCTION

In order to support the mission of the NASA, Manned Spacecraft Center (MSC), Space Environment Simulation Facilities (figure 1) are being constructed at the Clear Lake, Texas, site to provide the following:

a. To provide for simulated space environment testing of spacecraft configurations for the Apollo Spacecraft Program in modular and multimodular assemblies.

b. To provide for developing and testing the capability of man to perform various operations and maneuvers, both inside and outside the spacecraft, in a simulated space environment and on a simulated lunar plane.

c. To provide for reliability testing of manned spacecraft designed for space travel and lunar surface landing by tests covering an extended period of time.

CHAMBER "A" (Space and Lunar Surface Environment Simulation Chamber)

This chamber (figure 2) is a stainless steel vessel 65 feet in diameter by 120 feet high with a side loading door 40 feet in diameter. A vehicle of maximum dimensions 25 feet in diameter and 65 feet in height can be tested in this chamber.

The test item is supported inside the chamber by the "lunar plane". This test item support platform is a rotable table that can be rotated through 360° at velocities variable from 0.167 rpm to 1.67 pm. This "lunar plane" can support concentric test items up to 150,000 pounds and nonconcentric loads up to 30,000 pounds. The temperature of the "plane" can be varied from 100°K to 400°K during vacuum tests. Four 25-ton cable hoists can be lowered through penetration ports in the top of the chamber for use in handling test items on the "lunar plane".

The chamber pumping system consists of a mechanical roughing system with a standard diffusion pump system, backed by a mechanical pumping train and supplemented by liquid nitrogen and 20°K helium cooled panels completing the pumping system. This system is sized to give a pumping speed of approximately 2,760,000 liters/second at 1×10^{-5} torr.

Chamber "A", when completely operational, will have solar simulation. This consists of a modular "top sun and side sun" system (figure 2)

simulating the thermal flux of the sun (Johnson Curve). These "suns" have a flux variable from 60 to 140 watts/ft^2 and use a carbon arc source. The present "top sun" is 13 feet in diameter while the "side sun" is 13 feet wide and 33 feet high.

Attached to the chamber at ground level is a double manlock and at the 32 foot level is a single lock. These manlocks are constructed of carbon steel and have their own mechanical pumping system which can pump the "locks" down to approximately 10^{-3} torr.

Table I describes the chamber dimensions and operational characteristics.

Chamber "A" is now undergoing acceptance tests and has been pumped down clean, dry and empty, using three diffusion pumps, to approximately 2×10^{-6} torr for the purpose of proving the vessel vacuum integrity.

For these tests the maximum allowable leak to the chamber was 0.03 torr-liters/second. Because the chamber has such a large surface area and cannot be baked to drive off the CO_2 and water vapor (a gas load contributed by the chamber) a small LN_2 cooled panel was installed to pump these gases. Figure 4 is a pressure-time curve of one of several pumpdowns of the chamber.

These tests have indicated that the Chamber "A" leak rate is approximately 0.04 torr-liters/second; however, several large structures had been added to the inside of the chamber and it was decided that this accounted for at least 0.01 torr-liters/second. For this reason, 0.04 torr-liters/second was judged acceptable.

An additional test that has been made is the chamber structural integrity test. A structural failure occurred during the first chamber pumpdown around the nozzle on the 40 foot loading door. Additional bracing has been added to the chamber and the chamber tested during pumpdown by instrumenting with approximately 140 deflection and strain gauges. Data obtained from these sensors indicate the additional bracing has limited the wall movement to acceptable values, and based on this data, the chamber structural integrity has been proven.

CHAMBER "B" (Space Chamber for Life Systems and Astronaut Training Studies)

This chamber (figure 3), the smaller of the two, is constructed of stainless steel and is approximately 35 feet in diameter by 43 feet high. A vehicle of maximum dimensions 16 feet in diameter and 27 feet high can be tested in the chamber.

The top head of the chamber can be removed for loading and unloading the chamber.

The test item is supported inside the chamber as in Chamber "A" by the "lunar plane". This is a fixed platform that will support a concentric load of 70,000 pounds. As with the Chamber "A" "lunar plane" the temperature can be varied from 100°K to 400°K.

The chamber is equipped with the same type roughing, holding and diffusion pumping system as "A". Chamber "B" has an LN_2 heat sink but no helium cooled surfaces. This combination of systems gives a pumping speed of approximately 2,560,000 liters/second at 1×10^{-5} torr.

Chamber "B" has an identical solar simulation system producing a thermal flux covering the same spectral range and intensity as the Chamber "A" "suns" with the exception that Chamber "B" has only a "top sun" approximately 7 feet in diameter.

The chamber has one double manlock located at ground level. These locks are the same as those on Chamber "A" and are used for chamber ingress and egress during tests.

Table II describes the chamber dimensions and operational characteristics.

Chamber "B" has undergone acceptance tests on several systems. These are chamber vacuum integrity, manlock vacuum integrity and emergency repressurization.

a. Chamber Vacuum Integrity - The chamber has been pumped down using all 12 diffusion pumps to approximately 2×10^{-5} torr (no heat sink used), clean, dry and empty. The total allowable leak to the chamber during these tests was 0.03 torr-liters/second.

The chamber has passed all vacuum integrity tests. Figure 5 is a typical pumpdown curve of Chamber "B".

b. Manlock Vacuum Integrity - These tests are still being performed. A number of leaks have been discovered in the welds on the chamber manlocks.

Numerous leaks have been found in the carbon steel - carbon steel and carbon steel - stainless steel welds. Several attempts were made to use carbon steel or stainless steel as fillers, but the leaks still existed. Only after the welds were covered with heli-arc welds, were the leaks stopped.

Another problem area has been caused by outgassing of the painted inner manlock walls. Tests on the manlocks indicate that the outgassing of the paint causes a gas load on the pumping system equal to approximately 80% of the load the pump system was designed to handle. Figure 6 is a typical manlock pumpdown curve.

c. Emergency Repressurization - Since the chamber is manrated, a system is required to bring the chamber pressure from 10^{-5} torr operating pressure to about 250 torr in 30 seconds in case an accident occurs in the chamber. To do this, an emergency repressurization system is installed. This system injects high pressure oxygen and nitrogen into the chamber through the emergency repressurization nozzles which act as sound generators.

Two tests have been made on the emergency repressurization system. The acoustical data recorded during these tests are shown in figure 7. The 30 percent and 70 percent figures indicate that the gas bottles to be used during the test were filled to 30 percent and 70 percent, respectively, of their normal capacity. The first peak at about 1 second is caused by the chamber admission valve opening and admitting air to the chamber from piping connecting the chamber and the high pressure tanks. The second and very wide peak is caused by the valve at the high pressure tanks opening and admitting the high pressure oxygen and nitrogen. The rather narrow peak on the negative slope of the curve is unexplained at this time. The cause of the shift in time base for the two curves is due to different programmed times between various valve operations during the 30 percent and 70 percent tests. Figure 8 shows the mounting fixture with microphone.

CHAMBER "D"

The chamber is being constructed as a bottom loading, stainless steel, single-wall facility that will operate at 5×10^{-12} torr. It is approximately 15 feet high and 10 feet in diameter. The chamber internal test volume is 6 feet by 6 feet. An off-axis solar simulator will irradiate a right cylinder 3 1/2 feet in diameter and 6 feet long.

The pumping system is comprised of ion pumps, located around the lower part of the chamber wall (figure 9), titanium sublimation pumps, liquid nitrogen and helium surfaces located inside the chamber (figure 10). A mechanical and diffusion pump comprise the roughing system. The specifications require that the following minimum pumping speeds be provided:

a. H_2O - 2,000,000 liter/second
b. N_2 - 500,000 liter/second
c. H_2 - 18,000 liter/second

The source for the solar simulator is a commercially available 25 kw plasma located as shown in figure 9. A 2.5 kw xenon lamp is used to fill the energy band between 0.5 and 0.7 microns. A mosaic lens is used to project the non-uniform radiation from the plasma arc onto the collimating parabola inside the vacuum chamber. Located between the

mosaic lens and the parabolic mirror is the vacuum window. This is a double window; the outer window provides a vacuum seal, the inner window provides a molecular seal. The volume between these windows is differentially pumped to maintain vacuum integrity.

The surface temperature of the parabola is controlled by a refrigeration system and cooling coils on the rear of the mirror.

Table III gives a description of the chamber and its operational characteristics.

TABLE I

CHAMBER "A"

CAPABILITY AND DESCRIPTION

Outside Dimensions	65 ft. dia. x 120 ft. high
Inside Dimensions	55 ft. dia. x 90 ft. high
Maximum Vehicle Size	45 ft. dia. x 75 ft. high
Maximum Vehicle Weight	150,000 lbs.
Loading	Side opening - 40 ft. door
Support Platform (Lunar Plane)	45 ft. dia.
Pressure Level	
Empty	1×10^{-8} torr
27.6 torr l/s leak (Twice expected Apollo leak rate)	1×10^{-5} torr
Pumpdown	19 hrs.
Temperature	
LN_2 heat sinks	100°K
Lunar Plane	100°K to 400°K
Solar Simulation	
Target Area	13 ft. dia. "top sun"
	13 ft. x 33 ft. "side sun"
Radiant Thermal Flux	Variable from 60 to 137 watts/ft.^{2}
Uniformity	$\pm$5% (1.0 ft.^{2} detector)
Source	Carbon Arc
Decollimation	$\pm$30' (1/2 Angle)
Manrated	Yes

TABLE II

CHAMBER "B"

CAPABILITY AND DESCRIPTION

Outside Dimensions	35 ft. dia. x 43 ft. high
Inside Dimensions	25 ft. dia. x 30 ft. high
Maximum Vehicle Size	16 ft. dia. x 27 ft. high
Maximum Vehicle Weight	75,000 lbs.
Loading	Top Loading - 25 ft. dia.
Pressure Level	
Empty	1×10^{-7} torr
25 torr l/s leak	
(Twice expected Apollo leak rate)	9×10^{-5} torr
Pumpdown	90 minutes
Temperature	
LN_2 Heat Sink	100°K
Lunar Plane	100°K to 400°K
Solar Simulation	
Target Area	7 ft. dia. "top sun"
Radiant Thermal Flux	Variable from 60 to 137 watts/ft.^{2}
Uniformity	5% (1.0 ft.^{2} detector)
Decollimation	$\pm$30' (1/2 angle)
Manrated	Yes

TABLE III

CHAMBER "D"

CAPABILITY AND DESCRIPTION

Outside Dimensions	11 ft. dia. x 14 ft. high
Inside work volume	6 ft. dia. x 6 ft. high
Loading	Bottom loading
Pressure Level	5×10^{-12} torr
Solar Simulation	
(0.2μ to 2.0μ)	Variable from 60 to 140 watts/ft.^{2}
Temperature	
LN_2 Heat Sinks	100°K
Bakeout	750°K
Scheduled Operational Date	Spring, 1965

SPACE ENVIRONMENT SIMULATION LABORATORY

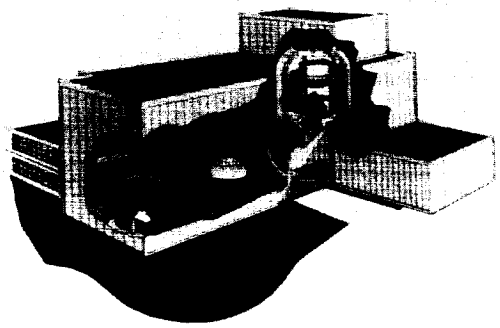

Figure 1

SPACE ENVIRONMENT SIMULATION LABORATORY
CHAMBER A

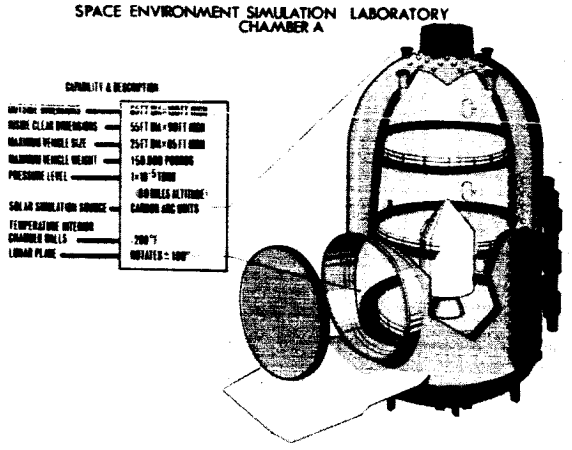

Figure 2

SPACE ENVIRONMENT SIMULATION LABORATORY
CHAMBER B

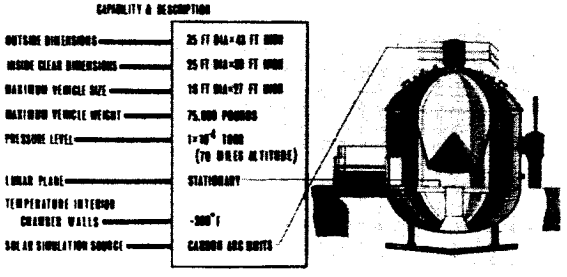

Figure 3

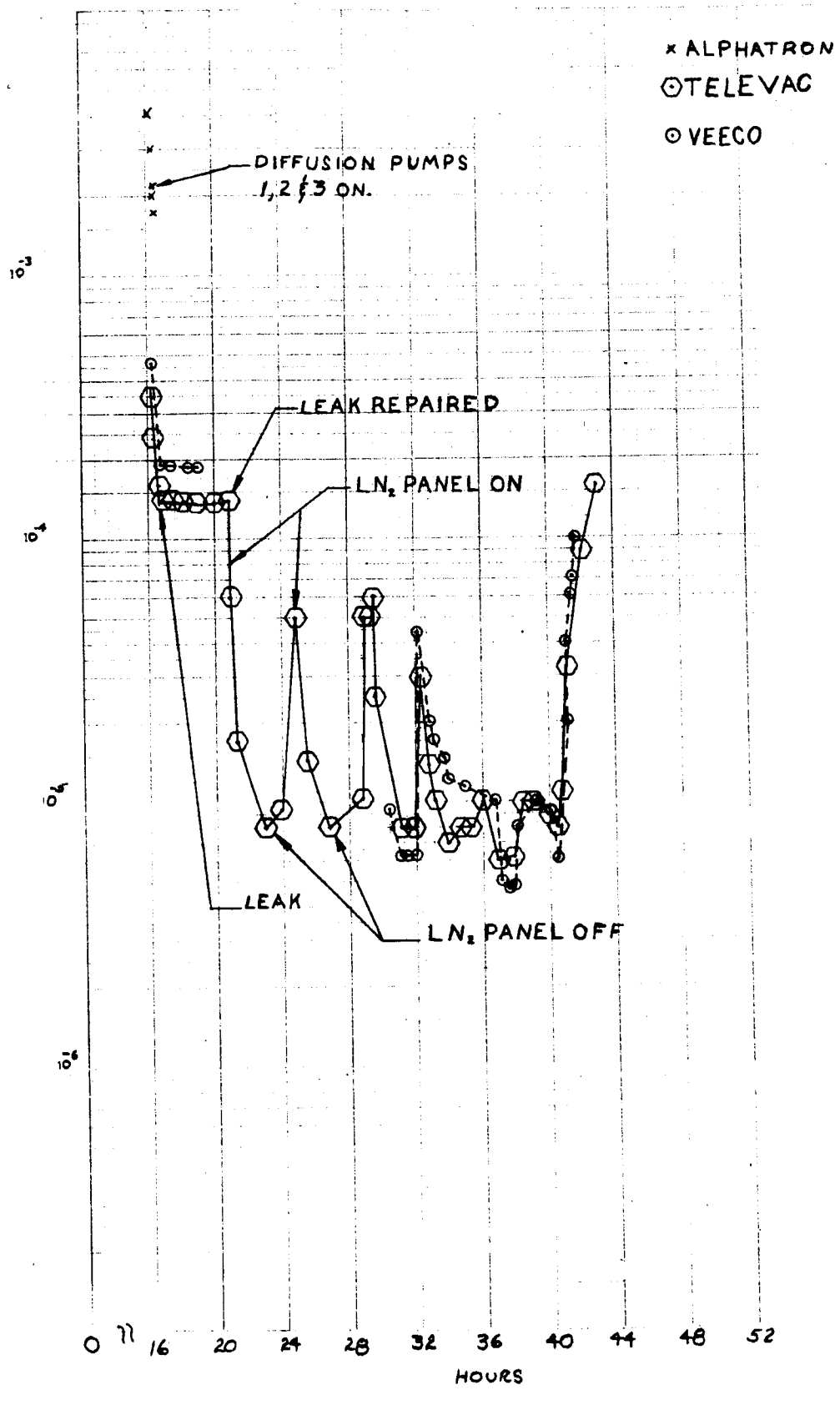

Chamber "A" Pumpdown

Figure 4

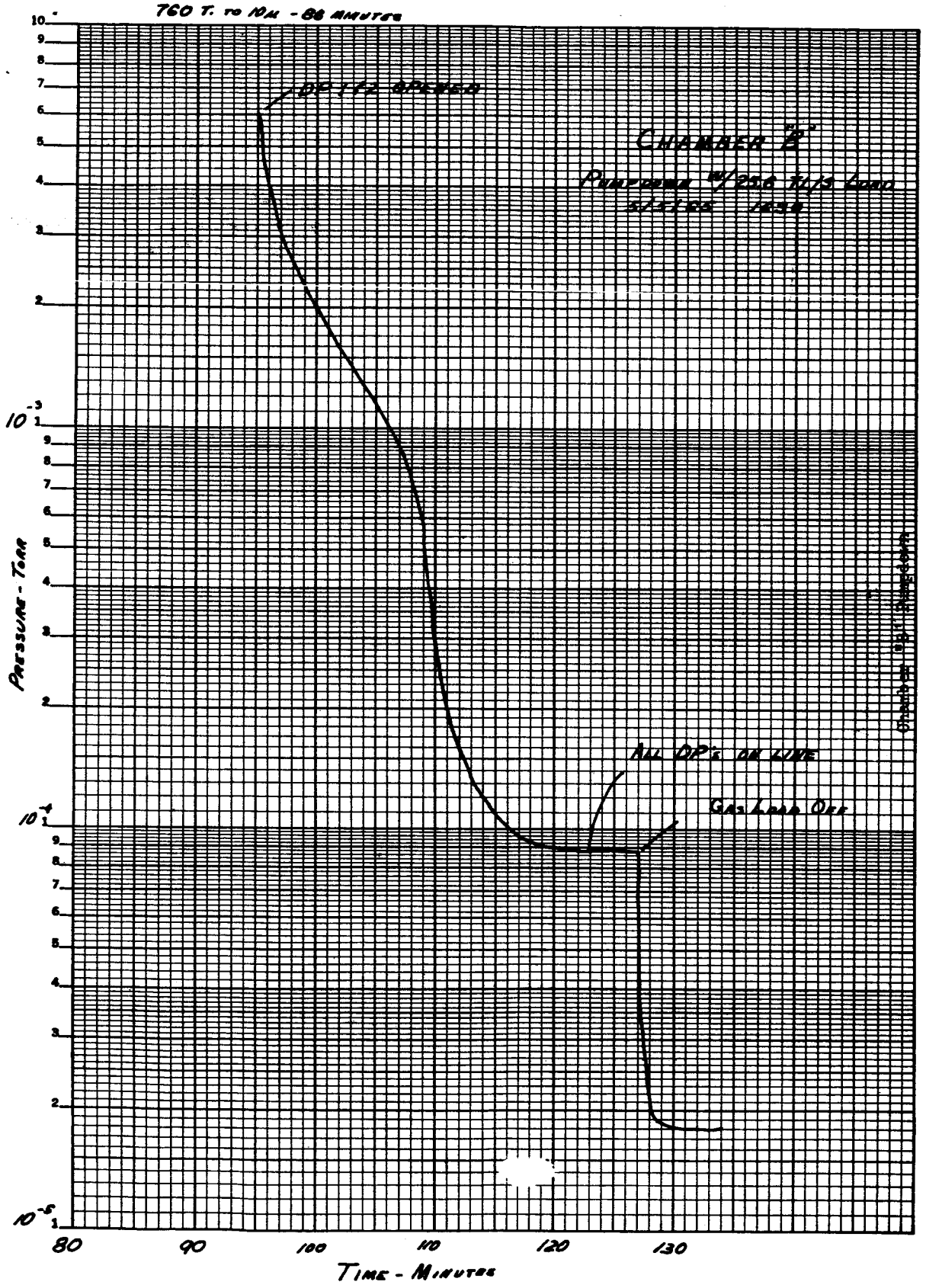
760 T. TO 10μ - 88 MINUTES
DIFFUSION PUMPED
CHAMBER "B"
PUMPED W/250 L/S ION SORB SYSTEM
ALL OP'S ON LINE
GAS LOAD OFF
PRESSURE - TORR
TIME - MINUTES
80
90
100
110
120
130

Figure 5

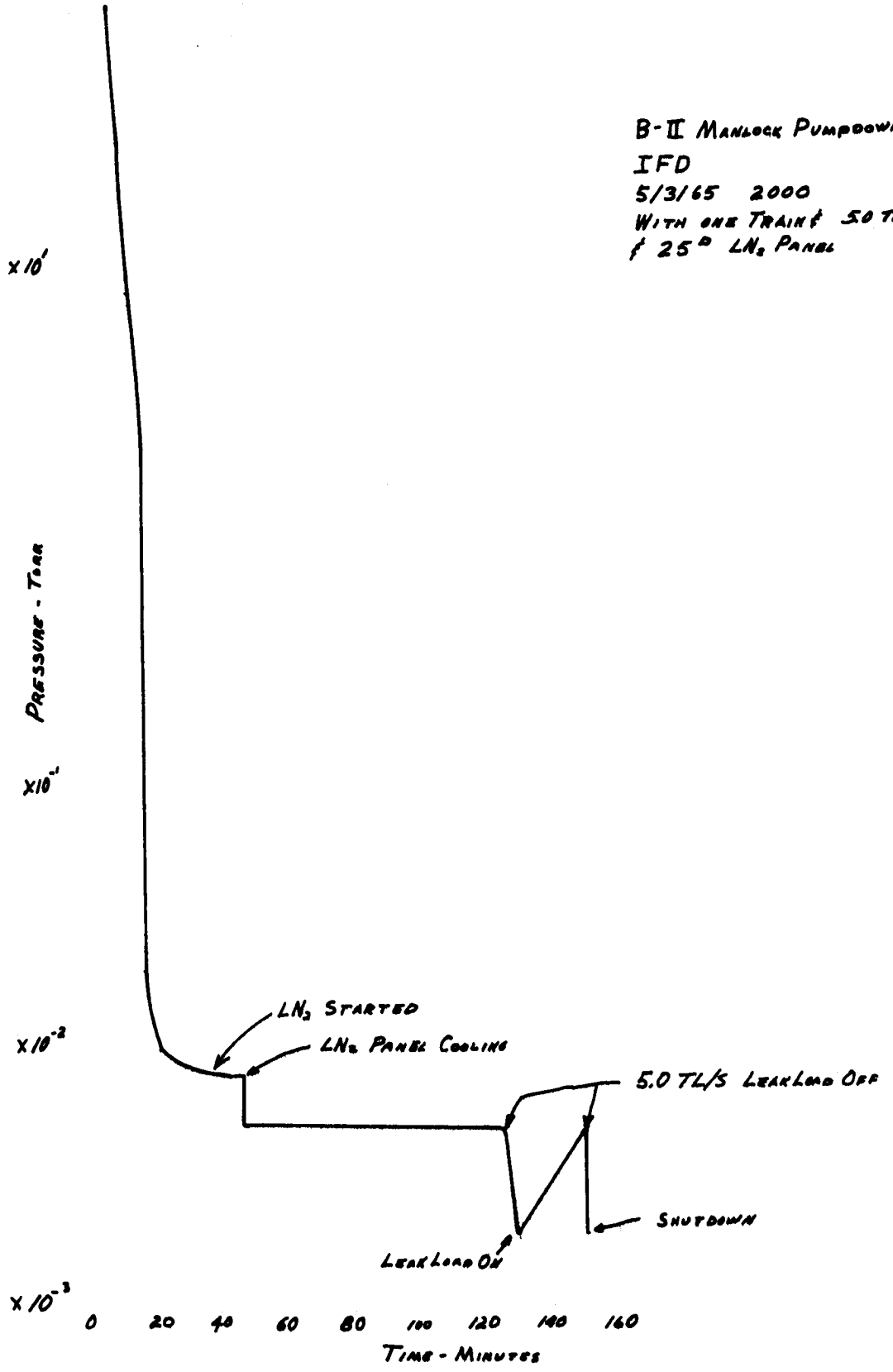

Chamber "B" Manlock Pumpdown

Figure 6

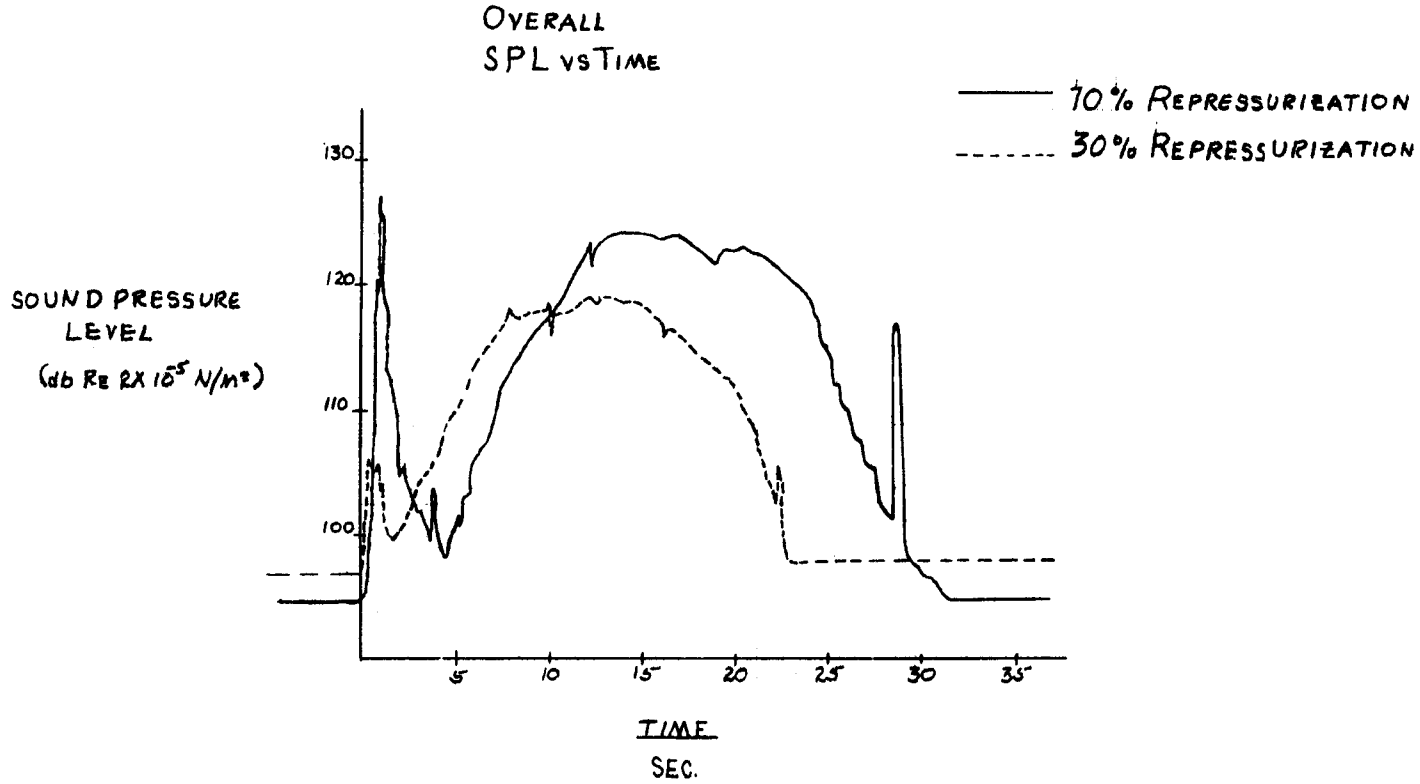

Chamber "B" Acoustic Measurements

Figure 7

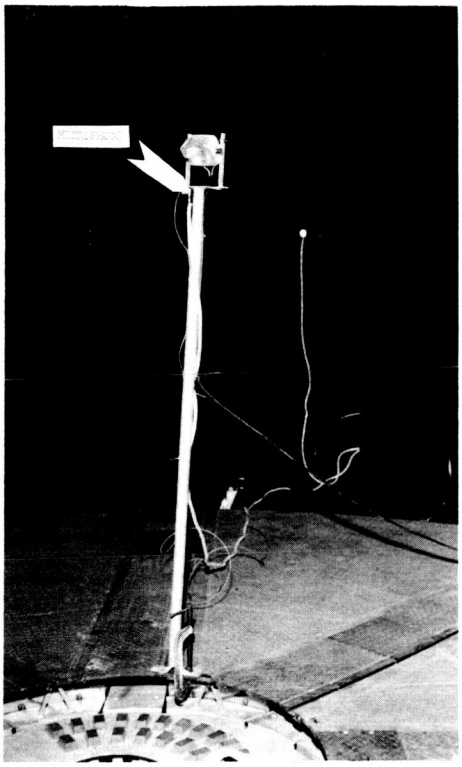

Figure 8

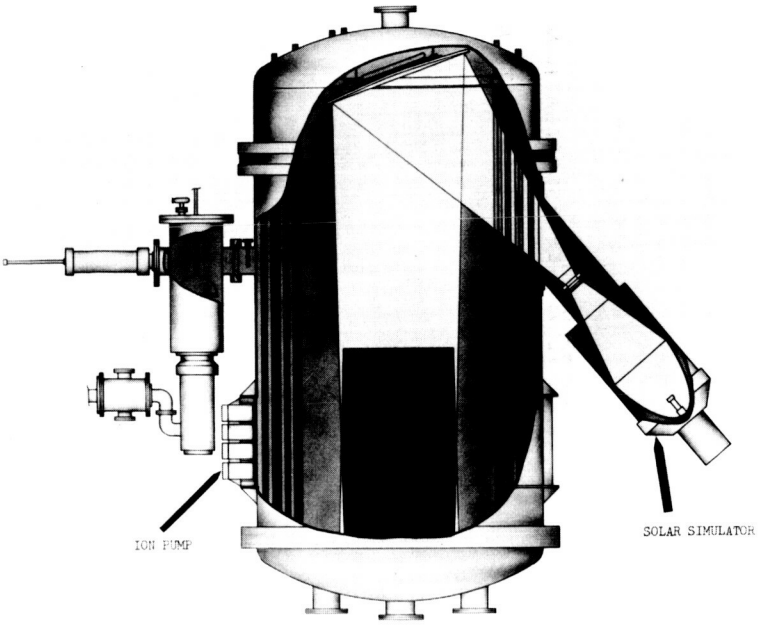

Figure 9

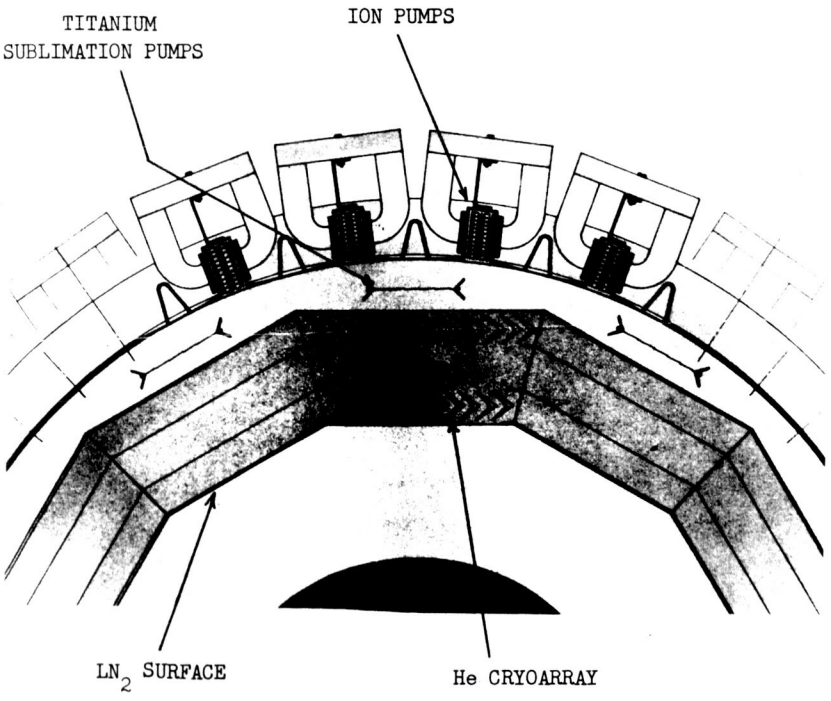

Figure 10

BY: James B. Stephens
JPL

2. Space Molecular Sink Simulator

During flight through space, a considerable molecular flux emanates from various parts of a spacecraft. Some of this flux impinges upon surfaces of the spacecraft and deposits upon them as contaminants; the remainder leaves the vehicle and does not return. Various parts of the spacecraft may be affected by this contamination. Optical and temperature control surfaces can be adversely affected while bearing surfaces may be prevented from cold welding.

In addition, many of the active environments of space (particle and radiation fluxes) produce marked effects upon the surfaces of spacecraft components. The action of these fluxes is dependent upon the gases produced being removed by the permissive molecular sink once they are dislodged from the surface. The effect of the active environments is also modified by the aforementioned contaminants.

Because of the many cold welding, surface degradation and contaminant migration problems encountered in today's more sophisticated spacecraft, a need has arisen for a space molecular sink simulator (MOLSINK) in which spacecraft self-contamination and surface-effect problems can be investigated.

The MOLSINK system, illustrated in Fig. 1, is an extreme-high-vacuum chamber with walls which cryogenically and chemically pump gases produced by the test item. The cryopumping is accomplished by a 96-inch spherical wedge-fin array (MOLTRAP) constructed of a .020-thick aluminum sheets spot welded to aluminum tubes through which 21°K hydrogen is pumped by a 1000-watt refrigerator (2000-PSI staged J-T type). These fins are tangent to a 10-inch sphere at the center of the MOLTRAP. This arrangement provides an order of magnitude capture improvement over a smooth wall when the test item is within the 10-inch sphere. Only about 34 out of every 100,000 300°K molecules emitted from a 10-inch spherical test item would restrike the test item provided the gases were oxygen, nitrogen, argon, carbon monoxide, or carbon dioxide.

The chemical pumping is accomplished by an electron beam titanium sublimator mounted on the inner door of the chamber, about 7 million liters per second of hydrogen can be pumped by the 2000 square feet of 21°K surface which is continuously coated by the sublimator. In addition, the cryo-deposit is chemically fixed by the titanium and the effective capture coefficient of the cryopumping surface is also increased.

The chamber is constructed so that it can be periodically disassembled and bead-blasted to remove accumulated contaminants. The lower part of the outer chamber and the vacuum tight inner liner can be lowered by the hydraulic lift and the MOLTRAP array can then be removed by the overhead winch.

After cleaning, the chamber is reassembled and pumped down by a 1300 CFM blower and a turbo molecular impact pump to 4×10^{-3} torr during a bake-out at 250°C for up to 100 hours. A 10-hour bake without disassembly is used when the chamber has not been exposed to atmospheric contaminants or contaminated test items.

The test item is prepared and mounted on the double door in a gaseous nitrogen purged skirt under the chamber. The chamber is backfilled with high purity argon, the vacuum bake-out door removed and the test item is inserted by raising the double door on the hydraulic lift.

With the inner door open, the chamber is rough pumped by the 1300 CFM blower and maintained at 100 microns by an argon sweeping purge while the inner liner and MOLTRAP array are cooled to 77°K. The inner door is closed and loaded to 20,000 lb. by the hydraulic lift while the turbo-molecular impact pump, in conjunction with cryopumping from the hydrogen manifolds, pumps the guard vacuum to below 1×10^{-6} torr. The MOLTRAP is cooled to 21°K and the sublimator is started.

The outgassing rate of the test item is monitored with a $4^{o}K$ cryogenic quartz crystal microbalance and the titanium sublimator, which is monitored and controlled by a $300^{o}K$ quartz crystal microbalance, is made to match this gas load with an appropriate titanium sublimation rate. The titanium to gas-load ratio is dependent upon the gas species evolved and this is qualitatively measured with a cryogenic quadrapole mass spectrometer. These instruments are also useful in analyzing the test item outgassing characteristics which determine their performance in space. Test item instrumentation leads are fed through the ports provided in the inner and outer doors and are used to suspend the test item in the center of the MOLTRAP array.

A shuttered, 12-inch diameter, double sapphire window is provided in the top of the chamber through which a high-intensity solar simulator can impinge its beam upon the test item.

The test item is unloaded from the chamber into the nitrogen-purged skirt area under the chamber by relaxing the hydraulic lift and back-filling the chamber with high-purity argon while the MOLTRAP and inner liner are still cold. When the test item clears the door port, the vacuum bake-out door is held in place and the chamber is rough pumped to 100 microns for start of bake-out cycle.

At this time, the chamber support structure, the vacuum chamber and the molecular trap are under construction and the sublimation pump and the refrigerator are being purchased. The 1300-CFM blower is installed and the tubo-molecular impact pump is being checked for backstreaming characteristics.

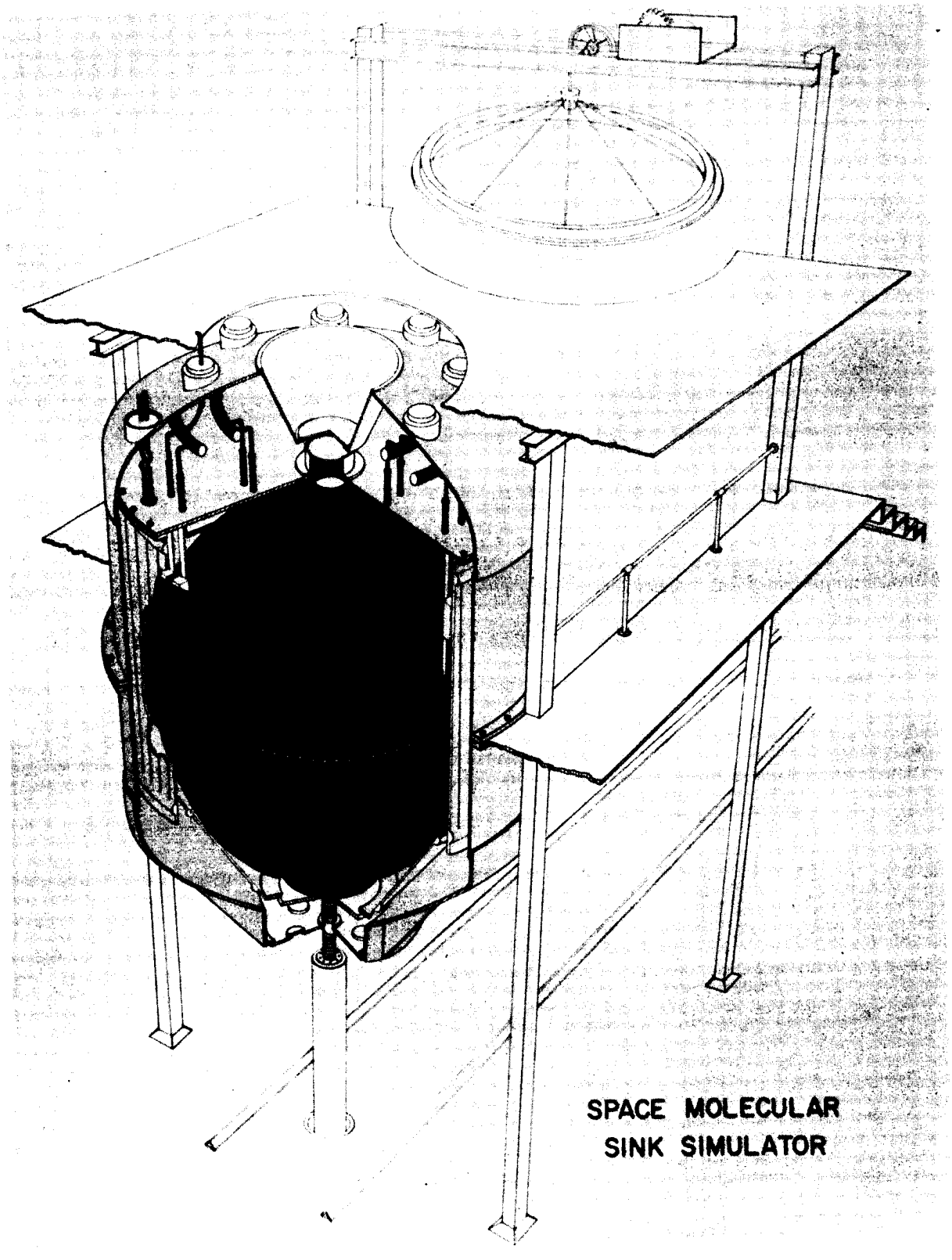

Figure 1

AMES VIBRATING-ELEMENT PRESSURE GAGES

by R. J. Debs

Ames Research Center
National Aeronautics and Space Administration
Moffett Field, California

At the High-Vacuum Technology Review and Planning Meeting held in 1963, the Ames representative described a vibrating-diaphragm pressure transducer that had accuracies of 1 to 3 percent of reading over the range of 10^{-2} torr to 4×10^{2} torr. At that time preliminary work on a vibrating-ribbon gage was described; this work was expected to extend the lower range to 10^{-8} torr.

This paper describes the extended work on the vibrating-ribbon gage and notes the extension of the vibrating-diaphragm gage to lower pressure ranges. This work was done by J. Dimeff, J. W. Lane, J. W. Albers, G. Coon, and R. Jordan.

The useful range of the vibrating-diaphragm pressure transducer was extended to pressures below 10^{-5} torr with a 30-microinch-thick diaphragm. During preliminary experiments on the high-pressure end of the range, it was demonstrated that the transducer with the usual 0.0005-inch-thick diaphragm operated to an upper limit of about 10^{3} torr.

The remainder of the paper deals with the vibrating-ribbon gage. The vibrating-ribbon gage should yield useful measurements in the range of 1 torr to below 10^{-7} torr. The principal advantage of such a gage is that it bridges the gap in vacuum measurements between the liquid-column gages and the ion gage and that it should be less sensitive to gas composition than the ion gage.

The principle of operation of the vibrating-ribbon gage is the same as that of the vibrating-diaphragm gage; therefore, a description of the vibrating-diaphragm gage will serve to illustrate the operating principles of both.

Consider a thin metallic diaphragm (0.0005 inch thick, $R_o = 0.362$ in.) under uniform radial tension (resonant frequency in vacuo 5,000 cps), spaced 0.003 inch from an electrostatic forcing plate on one side and a capacitance amplitude-sensing plate on the other. An A.C. voltage at the resonant frequency of the diaphragm and a D.C. voltage are applied between the forcing plate and the diaphragm. The diaphragm then vibrates at some given amplitude that is dependent on a balance between the viscous damping forces determined by the gas, and the driving force which is determined by the magnitude of the drive voltages. If the pressure in the cavities was originally P_o and changes to P_1, where $P_1 > P_o$, both the damping force and the restoring force will increase, causing the amplitude to decrease and the frequency to increase. The drive frequency must then be increased to

match the new resonant frequency, after which the drive voltage must be increased to bring the amplitude to its original value. For a fixed D.C. voltage one could therefore obtain a calibration curve of A.C. drive voltage vs. gas pressure. (In practice, a closed-loop electronics system (fig. 1) makes these adjustments automatically.)

The vibrating-ribbon gage (fig. 2) is similar in operating principle to the vibrating-diaphragm gage: it is driven electrostatically by a voltage applied between the ribbon and a forcing plate on one side; the motion of the ribbon is sensed by measuring the capacitance between the ribbon and a sensing plate on the other side.

There are, however, some important differences between the two gages:

(a) The vibrating-ribbon gage has, on each side of the ribbon, a relatively wide cavity; these cavities are each sinusoidal in longitudinal cross section to allow large-amplitude ribbon excursions with relatively uniform, close approaches of the ribbon to the cavity walls. Such a configuration facilitates maximum interaction with the gas but minimizes longitudinal gas flow along the vibrating ribbon.

(b) The ribbon vibration amplitude actually used is a very large fraction of the ribbon-to-wall spacing, whereas the vibrating-diaphragm amplitude is of the order of 1 percent of its diaphragm-to-plate spacing.

(c) A narrow gap (0.002 in.) is provided between the ribbon edges and the side walls of the cavity allowing cyclic gas flow from one side of the ribbon to the other, thereby increasing viscous losses.

(d) The mounting surface for the ribbon is relatively much smaller than it is for the diaphragm; therefore, smaller mounting losses, or coupling of energies, to the mounting structure are obtained and, hence, higher Q's are obtained. In the final analysis, the mounting or coupling losses determine the ultimate resolution of the instrument. Whereas diaphragm instruments generally have Q's of about 20,000, a Q measurement of 225,000 was obtained with the prototype vibrating-ribbon instrument. (Here $Q = 2\pi(W_S/\Delta W_L)$ where W_S is the stored energy and ΔW_L is energy lost per cycle.) Note that the top and bottom halves of the vibrating-ribbon instrument are separated and insulated from each other by sapphire spheres so that, if desired, the entire sinusoidal surfaces could be used for drive and readout.

Preliminary pressure measurements with the vibrating-ribbon gage were made from 5×10^{-8} torr to 10^{-1} torr. These results are shown in figure 3.

Physical data on the vibrating-ribbon gage are as follows:

Ribbon length = 12 in.
Ribbon width = 0.10 in.
Ribbon thickness = 0.0005 in.
Ribbon material = Ni steel
Ribbon - Pickoff plate spacing = 0.060 in.

Ribbon - drive plate spacing = 0.080 in.
Gap (top-bottom) = 0.003 in.
Gap (ribbon-side) = 0.002 in.
Body material = nonmagnetic stainless steel
Resonant frequency = 360 cps
Stress = 60,000 psi
Q = 225,000 (typ.)
All seals are silver soldered

The equation describing the force acting on an electrostatically driven element moving sinusoidally is given below:

$$F = \frac{V^2}{2X_p^2} = \frac{V_{DC}^2 + 2V_{AC}V_{DC} \sin \omega t + V_{AC}^2 \sin^2 \omega t}{2(X_o + a_o \cos \omega t)^2} \tag{1}$$

(See list of symbols at end of paper.)

Note that the effect on the diaphragm of the $\sin^2 \omega t$ (or, second harmonic) term in the force equation can be minimized under the following conditions:

(a) if V_{AC}^2 can be adjusted so that it is much smaller than $2V_{AC}V_{DC}$; and/or

(b) if the frequencies of the higher modes of vibration are not harmonically related to the fundamental resonance frequency. Under these conditions, the force is given by

$$F = \frac{V_{AC}V_{DC}}{X_o^2} \sin \omega t \tag{2}$$

Both (a) and (b) conditions are satisfied by the vibrating-diaphragm transducer as designed and operated: it is operated so that $V_{AC}^2 \ll 2V_{AC}V_{DC}$, and the higher diaphragm modes are related to the fundamental resonance frequency by Bessel functions; that is, nonharmonically. The exact relationship between V_{AC}, V_{DC}, and P_o for the vibrating-diaphragm transducer is given by equation (3). (For the Ames design at low pressures, the bracketed factor reduces to unity.)

$$V_{AC}V_{DC} = \frac{32a_o}{\epsilon} \frac{B\bar{c}}{\omega} \frac{X_o^2}{R_o^2} \left[1 - \frac{16(\mathrm{ber}\alpha R_o \mathrm{ber}'\alpha R_o + \mathrm{bei}\alpha R_o \mathrm{bei}'\alpha R_o)}{\alpha^3 R_o^3 (\mathrm{ber}^2\alpha R_o + \mathrm{bei}^2\alpha R_o)}\right] P_o \tag{3}$$

where

$$\alpha = \left(\frac{\omega K}{P_o}\right)^{1/2}, \qquad K = \frac{\mu}{[3B\lambda X_o + (X_o^2/9)]}$$

The situation for the vibrating-ribbon transducer is not so simple: here, the higher mode frequencies are (for small-amplitude vibrations) harmonically related to the fundamental resonance frequency, and the vibration amplitude closely approaches the total spacing. Partial suppression of the second-harmonic mode is achieved by driving at the antinode point of the fundamental mode, and by operating so that $V_{AC}^2 \ll 2V_{AC}V_{DC}$. Additional suppression of the second-harmonic and higher order modes arises almost fortuitously from the necessity that the ribbon have a large vibration amplitude, explained as follows:

In order to obtain maximum compressive damping from the gas under measurement, the ribbon must closely approach the boundaries of its containing cavity; that is, the amplitude, a_o, closely approaches the spacing, x_o. Such large vibration amplitudes result in nonlinear equations, whose higher order mode frequencies are not harmonically related to the fundamental resonance frequency. Thus, the effect of the $\sin^2 \omega t$ drive term is further minimized. Efforts toward the solution of these nonlinear equations are continuing.

An operational complication is also caused by the large excursion of the ribbon. For a driving plate set flush with the wall surface, as in the prototype transducer, the driving force increases very rapidly (for constant drive-voltage amplitude) as the ribbon closely approaches the plate. Control of ribbon drive by means of voltage control under these conditions is very difficult. In later models, therefore, this situation was avoided by recessing the driving plate 0.020 inch behind the wall surface.

The preliminary data on the prototype vibrating-ribbon gage (fig. 3) were taken with a system in which the phase was not the optimum 90° but was about 60°. Much better results are expected when the new closed-loop electronic drive servo is completed and installed. At this time little can be said about repeatability of measurements of the vibrating-ribbon gage, since the phase relationships were not repeatable from calibration to calibration.

In order to vibrate in a simple fundamental mode with no torsional excursions, ribbons must be straight, flat, uniformly stressed, and fabricated to the necessary tolerances. The original ribbons (machined by the manufacturer) were not straight and flat and proved to be completely unusable, twisting in torsional modes at various times during operation. When a 0.0005-inch-thick ribbon was made by etching a sheet mounted on glass, a ribbon giving good performance was obtained. Satisfactory 0.0001-inch-thick ribbons have not yet been obtained.

There still remains a considerable amount of work to be done on this project. It will be necessary to investigate the gas dependence of the ribbon experimentally with a gas analyzer. Theoretical work needs much more development. Extensive testing of the ribbon (repeatability, temperature effects, etc.) is necessary and requires a very reliable set of closed-loop electronics, currently in the process of development. To date, however, preliminary test results indicate that this instrument shows promise.

SYMBOLS

a_o	vibrating diaphragm amplitude
B	momentum transfer accommodation coefficient
$\bar{c}$	velocity of sound
F	electrostatic driving force per unit area
K	empirically determined damping constant
P_o	pressure
R_o	diaphragm radius
V_{AC}	alternating-current drive voltage
V_{DC}	direct-current drive voltage
X_o	diaphragm to plate spacing (diaphragm at rest)
X_p	diaphragm to plate spacing
ϵ	dielectric constant
λ	mean free path
μ	coefficient of viscosity
ω	driving frequency of diaphragm

VIBRATING RIBBON PRESSURE MEASURING SYSTEM

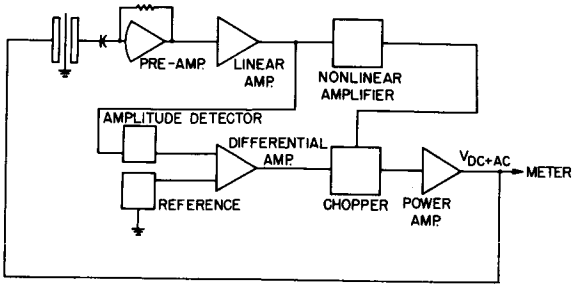

Figure 1

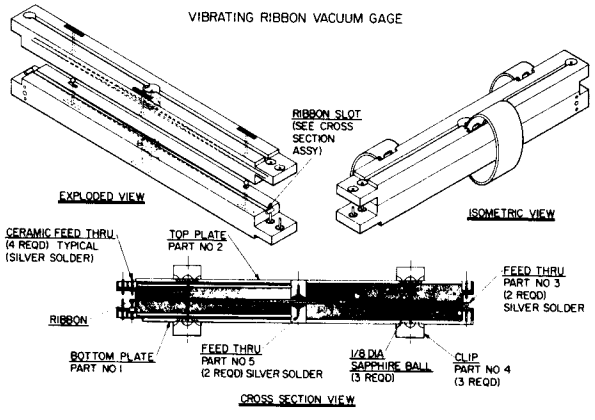

Figure 2

A.C. DRIVE VOLTS$_{pp}$ VS PRESSURE

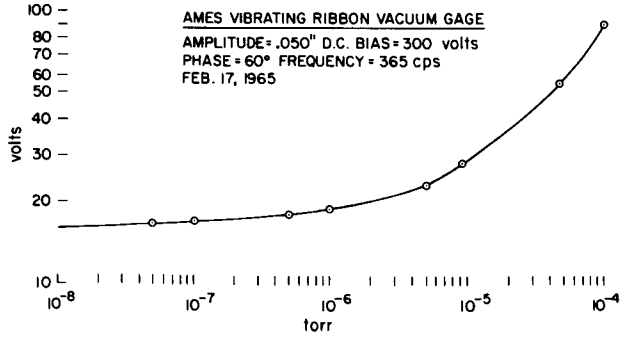

Figure 3

Areas of Investigation in Ultra High Vacuum Measurement

D. T. Pelz and G. P. Newton
Goddard Space Flight Center

INTRODUCTION

One of the interests of the Center's Aeronomy Branch, Laboratory for Atmospheric and Biological Sciences, is the study of the physics and chemistry of planetary atmospheres. The branch has an extensive program to conduct direct in-situ measurements in the earth's upper atmosphere, references 1&2. As part of this program we have made density and temperature measurements at altitudes from 250 to 900 kilometers using vacuum ionization gauges, reference 3, and are thus involved in obtaining an understanding of the response characteristics of these devices to atmospheric gases.

This is a review of our supporting vacuum measurements program and may be of interest to other NASA workers involved with vacuum gauging.

The three areas which command the majority of our vacuum effort are:

(1) Development of improved absolute calibration techniques.

(2) Understanding physical and chemical phenomena occurring within our flight sensors when exposed to atmospheric gases.

(3) Measurement of pressures below 10^{-11} torr.

ABSOLUTE CALIBRATION

Absolute calibration is important because we want to measure absolute atmospheric densities. The major uncertainty in the density values obtained from Explorer 17 was due to the calibration accuracy of the gauges. The Explorer 17 calibration uncertainty was $\pm$ 25% in the range 10^{-6} to 10^{-9} torr, $\pm$ 35% at 10^{-10} torr, and $\pm$ 100% at 10^{-11} torr. (All pressures are equivalent N_2 pressures)

In our laboratory we have a comparison volume and a pressure-attenuation system, with a capability of attaching McLeod gauges to both. The comparison volume is pumped by a mercury diffusion pump, and the attenuation system, by four oil diffusion pumps. We believe these systems will allow the achievement of 8 to 10% accuracy. However, McLeod gauges demand considerable time and effort and these requirements are not always compatible with flight oriented programs. Also, since we routinely compare gauge responses with a precision of a few percent, we think that better calibrations are desirable and attainable.

We are supporting contracts in two categories of absolute calibration: the use of pressure-attenuation techniques with an absolute standard operating at an accurately measured high pressure; and direct comparison against a standard operating at the pressure at which calibration is desired.

In the first category, the National Bureau of Standards is investigating the precision of the laws of molecular flow. An objective of this contract is to verify experimentally, within 1%, the values obtained from

the usual conductance calculations. Another objective is a determination of the linearity and time behavior of Bayard-Alpert gauges following small pressure changes. Also in the first category, National Research Corporation Research Division is investigating the feasibility of a wide range (10^{-6} to 10^{-15} torr) absolute calibration system using an argon beam in a cryogenically pumped volume. The system incorporates a vycor purous plug which allows the absolute standard (a rotating piston gauge) to operate near atmospheric pressure.

In the second category, Micro-Erg Laboratories recently completed a feasability study of a gauge which determines pressure by measuring aerodynamic drag effects on a rotating body. The gauge was shown infeasible, and the program emphasis was shifted to an examination of a Knudsen gauge with a magnetic suspension and a radiation pressure restoring torque. The study showed that such a gauge can achieve 8% accuracy at 10^{-8} torr. However, since considerable developmental work is necessary to achieve this accuracy, the fabrication of this device is not contemplated.

PHYSICAL AND CHEMICAL PHENOMENA

The physical and chemical phenomena which occur in ionization gauges exposed to atmospheric gases are not completely understood. The chemical activity of atomic and molecular oxygen, hydrogen, and nitrogen complicate density measurements.

In-house experiments are presently under way to examine adsorption, desorption, gas production, and gas exchange phenomena occurring in both hot filament and cold cathode flight sensors in the presence of atmospheric gases. We are also investigating the pressure independent ion current in hot filament gauges operating in oxygen and/or carbon monoxide environments.

Under contract in this area GCA Corporation recently developed and built a system which produces a 20% concentration of atomic oxygen. In a follow-on contract they are now performing detailed studies of our sensor responses in this oxygen environment. Under a different contract GCA is conducting research with our model R5 cold cathode magnetron gauges in the areas of gas exchange, gauge memory, large amplitude pressure cycling effects, space charge, and ion energy distribution in the gauge discharge.

LOW PRESSURE MEASUREMENT

In our laboratory we have used cold cathode gauges, photocurrent suppressor gauges, reference 4, and magnetic mass spectrometers, reference 5, to measure pressures below 10^{-11} torr. We have, however, encountered difficulties in using each of these devices. Although we have several designs of cold cathode magnetron gauges which operate below 10^{-11} torr, their response characteristics are non-linear and are not well defined at these pressures, thus, our pressure measurement errors may be large. Our photocurrent suppressor gauges, which are reported to be capable of measuring 10^{-12} torr, create and measure their own local pressure below 10^{-11} torr. This is apparently due to

a materials outgassing problem. The current-pressure response of the Davis-Vanderslice type mass spectrometer has been reported to be linear to very low pressures. The instrument, however, because of voltage and electron multiplier gain instabilities, is difficult to use in a quantitative manner. We are currently modifying existing equipment to improve our spectrometer control systems, and are supporting a contract to study the gain stability of three commercially available electron multipliers. Consolidated Systems Corporation is performing this study as a function of composition exposure history, bakeout temperature, and time.

Also under contract we are obtaining warm cathode magnetron gauges, reference 6, from GE Research Laboratories. It is anticipated that the reported linear response of the Lafferty gauge below 10^{-8} torr, in combination with our continued work with photocurrent suppressor, cold cathode magnetron, and mass spectrometer gauges, will improve our low pressure measurement capability.

ADDITIONAL INFORMATION

Under contract in an area not previously mentioned, NRC Research Division is developing an in-flight calibrator. The calibrator is a small device that is attachable to a number of vacuum sensors. A known pressure is produced in the sensor volume by controlling the hydrogen permeation rate through a stainless steel tube by regulating the tube

temperature. A prototype unit has been built and is operational.

Details concerning any of the above contracts or further information on our in-house vacuum program may be obtained by contacting the authors.

REFERENCES

1. Horowitz, R., Advan. Astronautical Sci., 12, Western Periodicals Company, North Hollywood, California, 1963

2. Spencer, N.W., Planet. Space Sci., 13, p. 593, Pergamon Press Ltd., London, 1965

3. Newton, G.P., D.T. Pelz, G.E. Miller, and R. Horowitz, Trans. of the Tenth Nat. Vac. Symp., editor G.H. Bancroft, p. 208, The MacMillian Company, New York, 1963

4. Schuemann, W.C., Report R-156, Contract DA-36-039-SC-85122, Dept. of the Air Force (O.S.R.), 1962

5. Davis, W., and Vanderslice, T., Trans. of Seventh Vac. Symp., p. 47, Pergamon Press, New York, 1961

6. Lafferty, J.M., Journal App. Phys., Vol 32, No. 3, p. 424, Amer. Inst. Phys., 1961

FLIGHT INSTRUMATION RESEARCH

Carl A. Reber and Dan N. Harpold
Goddard Space Flight Center

An experimental study is being conducted to determine if the rhenium wire filaments as used in GSFC flight mass spectrometers generate carbon monoxide in an oxygen atmosphere. The current at mass 28 (CO and N_2) is monitored for various oxygen pressures and the contribution from N_2 contamination (known from the dissociated peak at mass 14) is subtracted. Initial results indicate no significant CO generation in the ion source of the flight mass spectrometer.

Due to several poorly timed burn-outs of rhenium filaments (0.007" and 0.005" diameter) a second program is under way to increase filament lifetimes and, at the same time, maintain a non-contaminating filament material. We are presently investigating lanthanum boride coatings on rhenium (to reduce the temperature required for electron emission) and various refractory metal alloys for their suitability as flight mass spectrometer filaments. Results are inconclusive at the present time. We are also attempting to obtain samples of small diameter, single crystal rhenium for evaluation, but have not as yet been successful in locating a reliable source.

In order to test the response of the mass spectrometers used on rockets and satellites to the relatively high velocity neutral particles (about 8 km/sec), a contract has been given to Physics Technology Labora-

tories, La Mesa, California, to study a method of generating a medium energy, mono velocity, dense neutral beam. The approach utilizes sputtering of condensed oxygen and nitrogen with a rotating disk velocity selector. According to the contractor, beam velocities have been produced between 10^5 and 10^6 cm/sec with a velocity spread of 2.5% while the flux densities are about 10^{15} cm^{-2} sec^{-1} over an area of 2 cm^2.

EXTENSION OF THE VOLUME-RATIO VACUUM GAGE CALIBRATION SYSTEM TO 10^{-6} TORR

by Raymond Holanda

Lewis Research Center

The volume-ratio technique for vacuum gage calibration consists of expanding a gas from a small volume at high pressure into a large volume which has been previously evacuated. The resulting pressure in the large volume is computed from a knowledge of the volumes and a measurement of the high pressure. Figure 1 shows pressure ranges and estimated errors of recent calibration work performed using the volume-ratio technique.

Figure 2 is a schematic diagram of the volume-ratio calibration system. A quantity of gas is expanded from the small-volume tank V_1 into the large test chamber V_2, which has been previously evacuated and closed by means of the gate valve. The volumes have been determined experimentally, and the pressure p_1 is high enough to be measured to high accuracies by means of a Bourdon-tube pressure gage. Then p_2 can be computed:

$$p_2 = \frac{V_1}{V_2}(p_{1,i} - p_{1,f}) \tag{1}$$

where

$p_{1,i}$ initial pressure in V_1 before gas expansion

$p_{1,f}$ final pressure in V_1 after gas expansion

with isothermal conditions and an initially perfect vacuum in V_2 assumed.

The test chamber is a 4-foot-diameter, 4-foot-long cylindrical stainless steel tank with a volume of 1500 liters. The use of a number of small-volume tanks resulted in a range of volume ratios from 1500 to 150, 000. The high-pressure gage is a fused-quartz Bourdon-tube gage with a 0 to 800 torr range. Six 8-inch gold-sealed flanges provide for mounting of ionization gages and mass spectrometers on the test chamber. A 10-inch

pneumatically operated gate valve is used to close the test chamber, and a 10-inch diffusion pump is used with a rated speed of 4200 liters per second.

The following equation is a modification of equation (1) that takes into account other effects of importance in the closed chamber; pressure is expressed as a function of time and an estimate is made of the effect of each term in the equation on the overall performance of the system:

$$p_{total} = \underbrace{\left\{\frac{V_1}{V_2}(p_{1,i} - p_{1,f}) + \left[-\frac{dp_p}{dt}(t)\right] + (-p_a)\right\}}_{\text{Test gas}} + \underbrace{\left\{\Sigma p_o + \Sigma\left[\frac{dp_g}{dt}(t)\right]\right\}}_{\text{Residual gases}}$$

Test gas sample	Ionization gage pumping	Adsorption	Initial background gas	Leaks permeation diffusion desorption (outgassing)
1×10^{-6} to 1×10^{-3} torr	(<1/2%/min)	None observed	2×10^{-8} torr	2×10^{-8} torr/min

It is assumed that the test gas is introduced into the test chamber at time $t = 0$ and that a datum can be obtained in approximately 1 minute. The lack of any adsorption effects by the walls of the test chamber on the test gas is probably due to the fact that these walls are already saturated with at least a stable monolayer of gas since the chamber has not been baked. The summation of residual gas effects results in less than 5 percent contamination of the test gas for any pressures encountered in the experiment.

Commercial hot-filament ionization gages were calibrated in the system. Large differences in calibration factors were observed between different gages along with various nonlinearity effects; however, the reproducibility (not the accuracy!) of a typical ionization gage calibration curve was found to be about ±3 percent.

RECENT HISTORY OF VOLUME–RATIO CALIBRATION SYSTEM PROGRESS

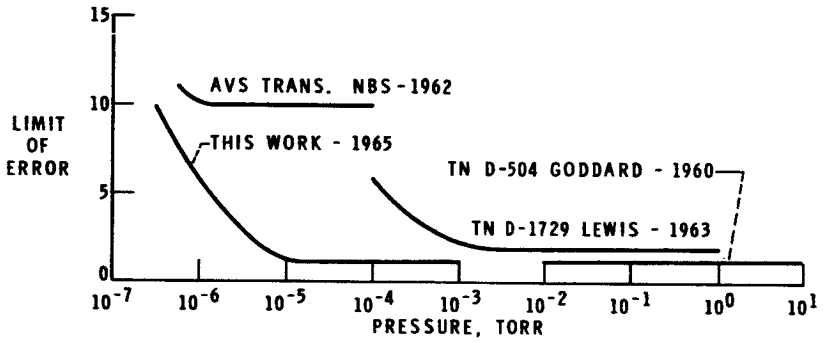

Figure 1

VOLUME–RATIO CALIBRATION SYSTEM

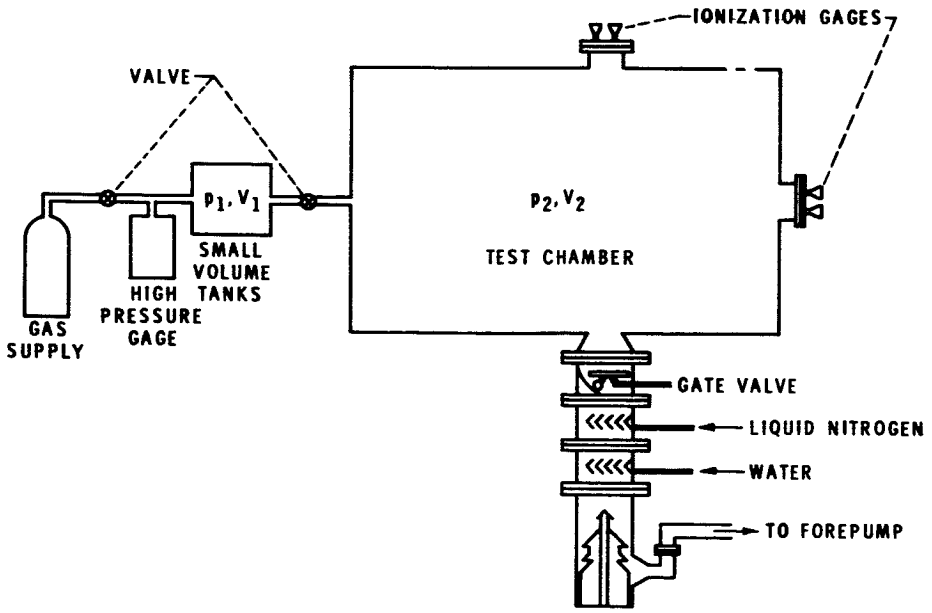

Figure 2

PERFORMANCE OF BAYARD-ALPERT GAGES IN ALKALI METAL VAPORS

by Robert L. Summers

Lewis Research Center

Measurements and observations of gage performance have been made in cesium and rubidium vapor. For the most part, these observations are restricted to commercial gages run under conditions specified by the manufacturer.

In the apparatus used, high-purity alkali metal was inserted into and sealed within an ionization gage under high-vacuum conditions. The pressure of the alkali metal within the sealed gage was controlled by varying the tubulation temperature, and in turn, the alkali metal vapor pressure within the tubulation. The procedures and techniques used are given in detail in reference 1, as well as the results obtained in the case of cesium.

No permanent gage damage was noted over several months of gage operation, although temporary gage failures were encountered because of the conductive plating of the alkali metals within the gages. This condition was easily corrected by the substitution of gages with suitable shielding of the element penetrations of the envelope.

The response of the gages to changes in alkali metal vapor pressure was inhibited because of condensation on the envelope walls. Pressure readings from the gage required periods of several hours to insure stability. The use of nude gages is the obvious solution to this problem.

Photoelectric currents were observed and measured. For a gage of the RG-75 type, the photoelectric currents were measured to be 2×10^{-8} ampere and less than 1×10^{-9} ampere, respectively, for cesium and rubidium.

Sensitivities for the RG-75 gage were measured to be 13.7 and 9.1 times the gage's nitrogen sensitivity for cesium and rubidium, respectively.

REFERENCE

1. Summers, Robert L.: Effects of Cesium Vapor on Bayard-Alpert Ionization Gages at Pressures Less Than 10^{-5} Torr. NASA TN D-2264, 1964.

ADHESION OF METALS IN ULTRAHIGH VACUUM

By John P. Mugler and James M. Bradford

NASA Langley Research Center

In this paper I will briefly review a Langley Research Center program on the effects of vacuum on the adhesion of metals in ultrahigh vacuum. It is the objective of this work to more fully define the parameters which influence the adhesion process and also provide some insight into the degree of adhesion that might be expected in certain space operations.

The literature on this subject indicates that the degree of surface contamination certainly would be expected to strongly influence the adhesion process. So in these studies the degree of surface contamination was included as a parameter along with temperature, contact pressure, time in contact, and material properties. Certainly a very interesting case to consider is the limiting case of the clean surface and that is the one that was investigated first.

Now there are only a few metals for which procedures have been established that will produce a clean surface. Currently two of these metals are being used in our experimental program; tungsten and nickel. Tungsten was studied first and the experimental apparatus is shown in figure 1.

The apparatus consists of a tungsten ribbon sample with each end connected to a terminal block. The sample is located between two movable anvils. For tungsten the cleaning procedure consists of flashing the ribbon several times to about 2300° K in ultrahigh vacuum. Figure 1 shows the sample ready to be flashed, that is, the apparatus is in the sample cleaning configuration. A potential difference is placed across the terminals and the sample is flashed. When the sample is cooled to the test temperature the anvils move together and exert a prescribed contact pressure for a predetermined period of time. Figure 2 shows this testing configuration. The anvils push the clean surfaces in contact with each other. One of the anvils has a ridge machined on it so the area in contact can be precisely defined. After the predetermined time in contact has elapsed the anvils are moved away and the terminal blocks, with strain gages mounted on the push-pull rods, pull the sample apart and measure the force required to break the adhesive bonds. Samples which adhered were examined by taking photomicrographs of the adhered region.

These photomicrographs indicate that the interface line has essentially disappeared which indicates a high degree of adhesion. Figure 3 summarizes the results of this study to date. With regard to the first result, we expected adhesion between clean surfaces at low contact pressures. It is suspected that the reason the tungsten did not adhere at low contact pressures is related to the compressive yield strength of the material. Tungsten, after flashing, is rather hard and brittle and when brought into contact tends to generate stresses in the local asperities rather than flowing plastically. When the contact pressure is removed the tungsten springs back apart because the elastic stresses are strong enough to break the small number of adhered points. At high contact

pressures enough plastic flow was induced to provide more area in contact while at the same time relieving some of the stored elastic stresses. The result is that the remaining stored elastic stresses cannot break the sample apart again.

More insight into whether or not this explanation is valid will be gained when we complete the experiments now in progress using nickel.

In any event it appears that surface cleanliness is not the only important parameter for adhesion, at least not for tungsten.

It was noted earlier that techniques to produce a clean surface have been established for only a few metals. For most metals of interest for spacecraft construction these techniques do not exist. Therefore, a contract effort to develop techniques to clean and monitor the degree of cleanliness of spacecraft metals has been initiated. This is being done under Contract NAS1-2691 with the National Research Corporation. At the present, abrasion and ion bombardment are being studied as cleaning techniques and a receiver work function technique is being studied to monitor the degree of cleanliness of the metal surfaces.

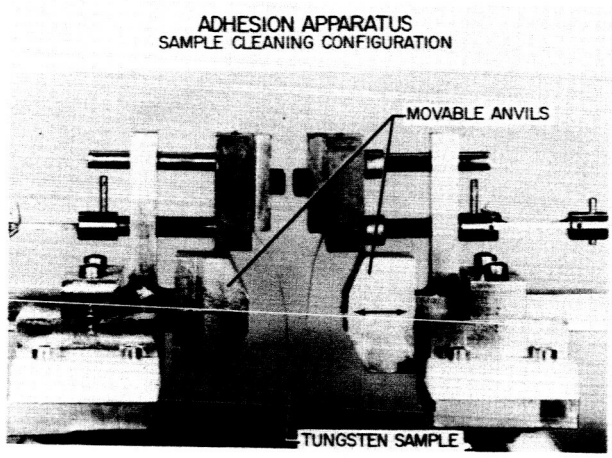

Figure 1

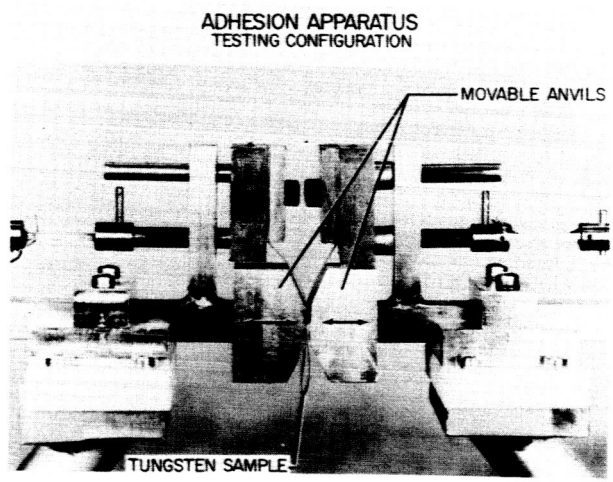

Figure 2

ADHESION TEST RESULTS

- CLEANED SAMPLES OF TUNGSTEN DID NOT ADHERE AT LOW CONTACT PRESSURE (APPROXIMATELY 1/3 YIELD) IN ULTRAHIGH VACUUM

- CLEANED SAMPLES OF TUNGSTEN DID ADHERE AT HIGH CONTACT PRESSURE (APPROXIMATE YIELD) IN ULTRAHIGH VACUUM

- CONTAMINATED SAMPLES OF TUNGSTEN DID NOT ADHERE AT ANY CONTACT PRESSURE TESTED

Figure 3

VACUUM EFFECTS ON SOLID-PROPELLANT ROCKET FUEL

By John P. Mugler and James M. Bradford

NASA Langley Research Center

In this paper I will briefly review a Langley Research Center program on the effects of vacuum on solid-propellant rocket fuel. This program includes measurement of outgassing rates for rocket fuels in vacuum, identification of the outgassed products, measurement of the changes in mechanical properties during vacuum storage, and measurement of the effects of vacuum storage on the ignitibility of the fuel. We are looking at fuels which are likely candidates for future space missions which includes fuels being considered for hybrid motors. To date in this program outgassing rates have been measured and the outgassed products identified for two fuels; Polyurethane and PBAA.

The outgassing rates were measured using the "Rate of Rise" technique in which the rate of pressure rise caused by the propellant sample in a known volume is measured.

Figure 1 shows the measured outgassing rate for Polyurethane as a function of exposure time. The exposure time ran to about 500 hours or 21 days. The outgassing rate is given in torr-liters per square centimeter per second. The outgassing rate decreases rather rapidly for the first 100 hours and then continues to decrease at a much lower rate for the remainder of the test. It is still decreasing after 21 days in vacuum. During this exposure period the outgassing rate decreased from about 3×10^{-7} torr-liters per square centimeter per second to about 3×10^{-8} torr-liters per square centimeter per second, i.e., about a factor of 10. These outgassing rates of around 10^{-7} torr-liters per square centimeter per second are about what would be expected from rubbery materials like this. There is some scatter in the measured rates which results from variations in the outgassing processes and is not inherent in the measuring technique.

Figure 2 shows the same variation but this time for the PBAA fuel. Again there seems to be a change in rate around 100 hours but the rate of decrease after 100 hours is much greater than for the Polyurethane. This increased rate coupled with the fact that the initial outgassing rate for the PBAA was somewhat higher resulted in a factor of 100 decrease in outgassing rate during the exposure as opposed to a factor of 10 for Polyurethane.

To get an idea of what pressure level might be experienced in a rocket motor in space, the measured outgassing rates were used to calculate the pressure-time profiles for several motors. Figure 3 presents the results for a 35-inch spherical motor with Polyurethane fuel. The conventional equation was used for the calculation and it is shown in figure 3. The pressure in the motor is "P" at any time "t." The pressure in the motor is "P_o" at $t = o$, "Q" is the outgassing rate of the propellant per unit area, "A" is the surface area of the propellant exposed, "F" is the nozzle conductance, and "V" is the volume inside the motor occupied by the gas. Using the measured outgassing

rates for Polyurethane the calculated pressure in this motor, without a nozzle closure, ranges from about 3×10^{-6} torr to about 3×10^{-7} torr after about 21 days. This pressure level is typical for many of the motors we examined.

As noted previously the outgassed products were identified. A time-of-flight mass spectrometer was installed in the chamber with the propellant sample. The time-of-flight mass spectrometer is briefly described in the paper "Comparison of Partial Pressure Analyzers" which is presented elsewhere in this volume. Figure 4 shows the experimental setup used for the identification of the outgassed products. A slab of propellant is suspended in the chamber on a thermocouple. The flight tube is mounted through the rear port of the chamber and the ionization or sampling portion is in the vicinity of the propellant sample. Using this setup the gases evolving from the fuel were identified as a function of storage time in vacuum.

Figure 5 shows a mass spectrogram of Polyurethane after 160 hours in vacuum. The mass-to-change ratio is shown on the abscissa and the peak height in amperes is shown on the ordinate. The 18 and 17 peaks, which are coming from water, are by far the largest peaks in the spectrogram. Many of the other peaks present indicate that there are some hydrocarbons evolving from the Polyurethane but they have not been identified as yet. The ratio of m/e 28, nitrogen, and m/e 32, oxygen, indicates that some air is also evolving from the Polyurethane. It was noted that this spectrogram was taken after 160 hours in vacuum. The spectrograms taken at the other times show that water was always the main outgassing constituent and accounted for about 60 percent of the total pressure throughout the entire exposure period.

Figure 6 shows a mass spectrogram for the PBAA after 180 hours in vacuum. In this case water is certainly not the main constituent evolving from the fuel. The main m/e peaks coming from the PBAA are hydrocarbons. Most of the peaks that are seen here are probably coming from the cracking pattern of some parent hydrocarbon that we have not yet identified. It is interesting to note that many of the peaks shown in this figure, and in the mass spectrogram for Polyurethane, can be accounted for if they had the chemical formula $C_XH_{2X\pm1}$ with X ranging from 2 to 8. One likely parent peak for the PBAA is the peak at m/e of 126. A comparison of four hydrocarbons with mass number 126 shows cracking patterns very similar to the pattern shown here but none of them matched well enough to identify the hydrocarbons evolving from the PBAA.

These data are being presented in more detail at the 21st Interagency Solid Propulsion Meeting in San Francisco on June 9, 10, and 11, 1965. Further analysis of these data is taking place along with some additional work to aid in the identification of the outgassed products. Tests to measure the effects of vacuum on the mechanical properties of the fuel are scheduled for later this year.

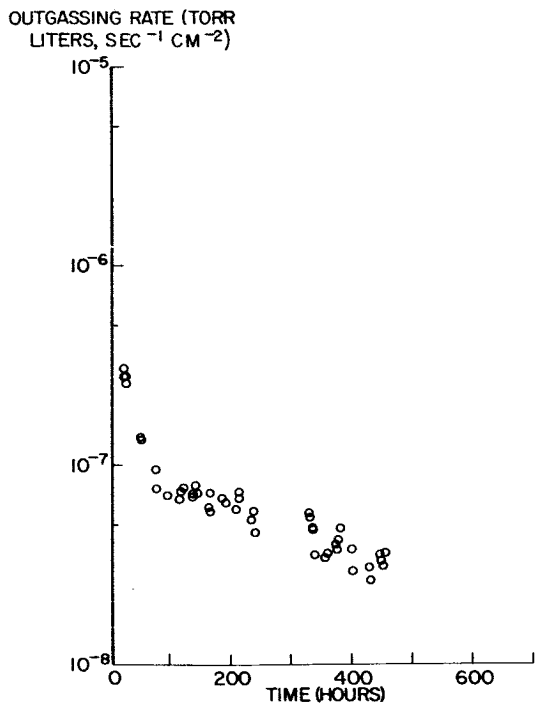

Figure 1.- Variation of the outgassing rate of polyurethane with time of exposure to vacuum.

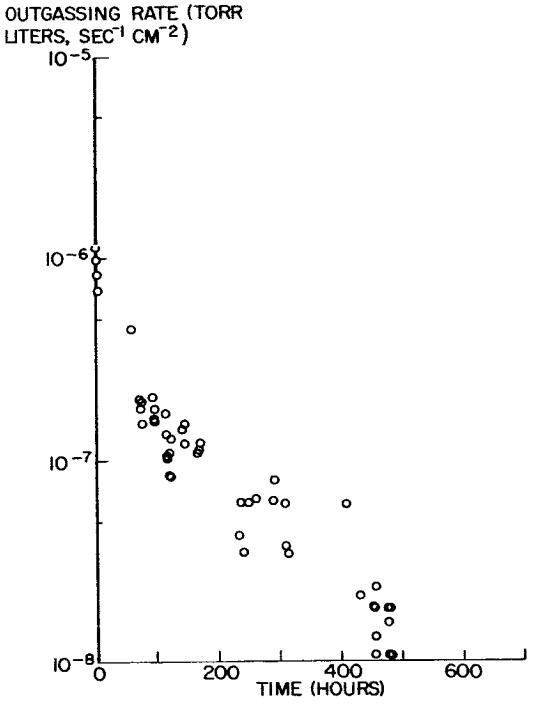

Figure 2.- Variation of the outgassing rate of PBAA with time of exposure to vacuum.

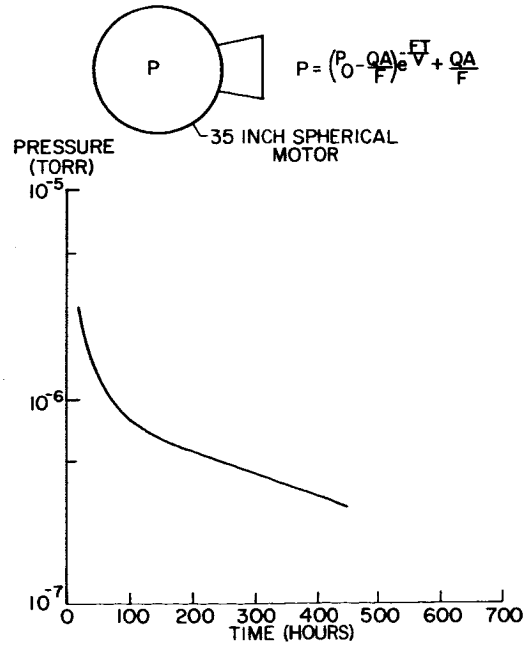

Figure 3.- Variation of pressure inside 35 inch spherical rocket motor with time of exposure to vacuum.

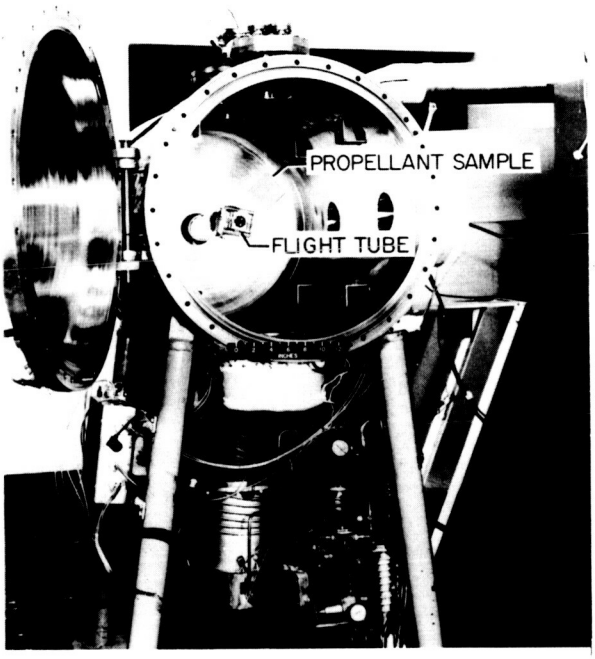

Figure 4.- Experimental Set-Up.

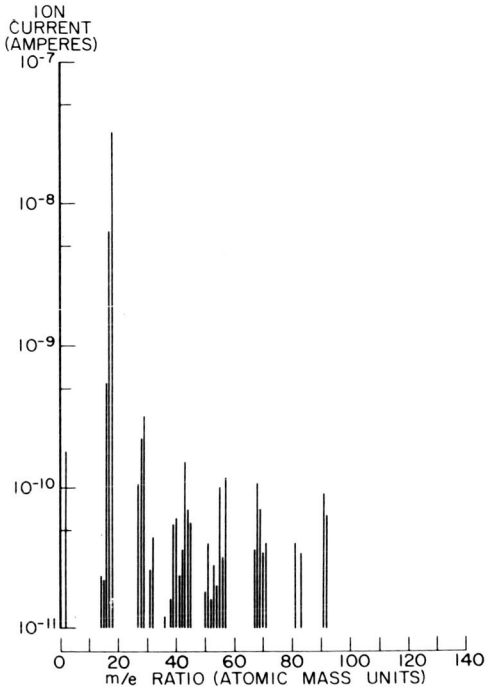

Figure 5.- Mass spectrogram of outgassing products from polyurethane.

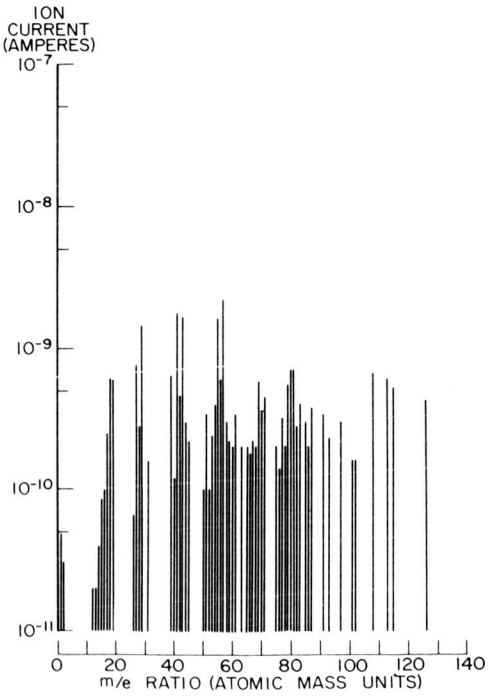

Figure 6.- Mass spectrogram of outgassing products from PBAA.

EXPERIMENTS ON ADHESION OF FINE CERAMIC POWDERS IN ULTRA-HIGH VACUUM

By Jonathan D. Klein and Guy V. Ferry

National Aeronautics and Space Administration
Space Sciences Division
Ames Research Center, Moffett Field, California

Knowledge of the behavior of thoroughly outgassed powders is of great importance in any consideration of the nature of the surface of the moon. The adhesion of fine ceramic powders in ultra-high vacuum is being studied at the Ames Research Center in order to gain insight into the state of fine powders on the surface of the moon, and the possible behavior of materials in a lunar environment.

Initial studies were made with a chain type balance which was built specifically for use in an ultra-high vacuum environment. This device had a sensitivity of the order of 1/10 g and could load specimens to about 100 g.

A standard 20 cu ft vacuum chamber manufactured by Ilikon Corp., Natick, Massachusetts, with additional electrical and mechanical feedthroughs and gaging was used. General Electric triggered cold cathode, G. C. A. Kreisman cold cathode, and Bayard Alpert type gages were also used. A General Electric magnetic focusing partial pressure analyzer was mounted on the system to monitor the residual gases. The chamber is of stainless steel and uses a 10-inch main diffusion pump with a Freon-cooled baffle and a liquid nitrogen trap to control oil backstreaming. There is a 2-inch oil diffusion pump to back the main pump, and finally a mechanical roughing and backing pump. The rubber O-ring seals are cooled by Freon to reduce diffusion and outgassing.

The samples used with this balance were glass lenses; the spherical surface of one being contacted to the flat surface of another after they were outgassed by heating and/or ultraviolet light irradiation. There was no sticking or adhesion seen during these experiments within the tenth gram sensitivity of the balance.

Adhesion of powders under similar conditions has been reported by Salisbury, et al. (refs. 1 and 2) and Halajian (ref. 3). In order to study the adhesive properties of powders, a pan was fabricated and placed in the vacuum system. The pan can be tilted about a horizontal axis to test the behavior of the powder, and can be vibrated from outside the vacuum system.

The first sample tested on the tilting pan was a garnet powder of 44 to 63 μ particle size. It was outgassed as thoroughly as possible by heating to approximately 150° C for 10 hr and by flooding it with ultraviolet light. The chamber pressure reached $2\text{-}3\times10^{-11}$ torr, but no adhesive behavior was seen. The powder behaved as it did in air.

The next sample used was a 3 μ alumina grinding powder. The chamber pressure reached about 1.5×10^{-11} torr after the same outgassing treatment as above. By this time, however, most of the powder had stuck to the pan. The rest of the powder moved in clumps when the pan was tilted or vibrated. When the pan was vibrated hard enough to break some of the powder from the pan, it broke off in clumps.

The powder was kept in the chamber, and after two days the pressure dropped (in a period of 2 hr) to $4\text{-}5 \times 10^{-12}$ torr; at the same time, some of the powder disaggregated and much more of the powder could be seen moving on the pan. This behavior was the opposite of what had been expected. It was tentatively concluded that there may have been an exchange of the gas on the surface of the particles to one which had more adhesion, and that with time this gas was being removed allowing the pressure to decrease and the particles to become unstuck. To test this hypothesis the liquid nitrogen trap was dumped; this increased the chamber pressure to the 10^{-9} or 10^{-8} torr range, the predominant gases being carbon dioxide and water vapor that had been condensed on the trap. After a period of hours at the higher pressure, the powder did indeed stick again. The effect could be repeated as often as desired. When the trap was refilled, the pressure would again drop into the 10^{-12} torr range after a period of several days, and the powder would then become looser again.

Since this vacuum system used oil diffusion pumps, the possibility of oil contamination of the sample by backstreaming diffusion pump oil is always present. The sample was checked for oil by washing it with spectro-chemically pure acetone, evaporating the acetone on a salt plate, and then looking at the infrared spectrum in transmission of the plate. This technique, even when used crudely with no great care taken to maximize the sensitivity, was sensitive to better than 0.1 microliters of oil. The alumina sample above appeared to have been contaminated by roughly 1 to 10 monolayers of oil, though there was no way of determining when the oil appeared. There is good reason to believe that most of the contamination occurs initially when the diffusion pump is started, but in this case some contamination was undoubtedly added when the trap was dumped.

The next sample studied was a 1 μ pure alumina powder. Great care was taken to minimize oil contamination during this experiment. No sticking was observed even after waiting several days by which time the pressure had reached $1\text{-}2 \times 10^{-11}$ torr. Even at this pressure the powder flowed back and forth across the pan as it did when it was in air. A check on oil contamination, when the sample was removed from the chamber, showed that there was perhaps 0.1 to 0.01 of a monolayer present.

One problem in these experiments is that there is no objective way of measuring the degree of cleanliness of the surface, and the extent of the outgassing. There is reason to believe that much more stringent techniques are required in order to remove the last few absorbed layers of gas. To remove this uncertainty, the next samples run were highly stressed glass drops made by dropping molten glass into water, thereby quenching in the thermal stresses. These so-called "Rupert drops" shatter when their tips are broken off, thus producing many fine particles.

In the next run six of these drops were broken after the chamber had been pumped down to $1\text{-}2\times10^{-11}$ torr. There was a momentary rise in pressure to the 10^{-9} torr range when the drops were broken, but this is no greater than the normal pressure rise whenever the mechanical feedthroughs are operated in this fashion. The pressure dropped back down in a few minutes and there was no adhesion observed in the resulting powder. This powder ran up and down the pan quite freely with no observable sticking. There was no detectable oil contamination on these particles and it is felt that their surfaces were quite likely free of adsorbed gases.

It is concluded that the adhesion of clean surfaces in ultra-high vacuum (i.e., cold welding) is small and that adhesive forces, if present, are smaller than can be observed on this scale. This is in agreement with the recent work of Ryan (ref. 4) on macroscopic samples. Earlier reported adhesion of brittle powders in ultra-high vacuum without the introduction of large enough forces to produce plastic flow are probably artifacts of the experiments, specifically diffusion pump oil in Salisbury's case, and not true cold welding of clean, identical surfaces.

REFERENCES

1. Salisbury, J. W.; Glaser, P. E.; Stein, B. A.; and Vonnegut, B.: Adhesive Behavior of Silicate Powders in Ultra-High Vacuum. Jour. Geophys. Res., vol. 69, no. 2, 1963, pp. 235-242.

2. Salisbury, J. W.; and Glaser, P. E., eds.: Studies of the Characteristics of Probable Lunar Surface Materials. Special Report No. 20, AFCRL-64-970, Air Force Cambridge Res. Lab., Jan. 1964.

3. Halajian, J. D.: Soil Behavior in a Low and Ultrahigh Vacuum. Presented at Annual Meeting of the Am. Soc. of Mech. Engr., Lunar Base Session, N. Y., RE-197J, Res. Dept., Grumman Aircraft Engr. Corp., Dec. 1964.

4. Ryan, J. A.: Experimental Investigation of Ultra-High Vacuum Adhesion as Related to the Lunar Surface. Progress report, Missiles and Space Systems Div., Douglas Aircraft Corp., Santa Monica. NASA Contract NAS7-307.

INFLUENCE OF A VACUUM ENVIRONMENT ON FRICTION AND LUBRICATION STUDIES

by Donald H. Buckley
Lewis Research Center

SUMMARY

The importance of a clean vacuum system on the friction characteristics of metals in sliding contact is discussed, and friction and mass spectrometer data are presented. Furthermore, the influence of vacuum system total and oxygen partial pressures is shown to affect markedly the friction behavior of metals in sliding contact. The relation of metal oxide stability to oxygen partial pressures and friction characteristics of metals is also discussed. The poor heat dissipation for materials in a vacuum is shown to affect the temperatures of sliding contact metals in friction studies. This poor heat dissipation is also related to the mechanism of degradation of materials such as polytetrafluoroethylene (PTFE) in friction experiments.

author

INTRODUCTION

Lubrication systems or devices depend heavily on the environment for their mechanisms of operation, or behavior characteristics. In developing devices for the study of lubrication systems intended for use in a space environment, all of those factors which influence the behavior of such complex systems in an air environment must be considered.

Factors in a space environment that differ from those at the surface of the Earth and can be expected to influence lubrication systems are ambient pressure, lack of oxygen, poor heat dissipation of mechanical components in contact, and radiation from advanced nuclear space powerplants. The effects of radiation from a space environment at the present time are not severe enough to cause concern, even with conventional oil- and grease-lubricated systems (ref. 1). This paper, therefore, does not include a discussion of this subject.

The objectives of this paper are to discuss (1) a vacuum system for friction and lubrication studies, (2) the effect of total system pressure on such studies, (3) the effect of the absence of oxygen, (4) the effect of poor heat dissipation, and (5) by way of an

example, the effect of these combined factors on the lubrication and degradation mechanism of a self-lubricating material, PTFE.

APPARATUS AND PROCEDURE

The apparatus used in this investigation for friction and lubrication studies of materials in sliding contact is shown in figure 1. The basic elements of the apparatus were the specimens (a $2\frac{1}{2}$-in. -diam. flat disk and a 3/16-in. -rad. rider) mounted in a vacuum chamber. The disk specimen was driven through a magnetic drive coupling. The coupling had two 20-pole magnets 0. 150 inch apart with a 0. 030-inch diaphragm between magnet faces. The driver magnet, which was outside the vacuum system, was coupled to a hydraulic motor. The second magnet was completely covered with a nickel-alloy housing and was mounted on one end of the shaft within the chamber (fig. 1). The end of the shaft that was opposite the magnet contained the disk specimen.

The rider specimen was supported in the specimen chamber by an arm that was mounted by gimbals and bellows to the chamber. A linkage at the end of the retaining arm, away from the rider specimen, was connected to a strain-gage assembly. The assembly was used to measure frictional force. Load was applied through a dead-weight loading system.

Attached to the lower end of the specimen chamber were a 400-liter-per-second ionization pump and a sorption pump. The pressure in the chamber was measured adjacent to the specimen with a cold-cathode ionization gage. In the same plane as the specimens and ionization gage was a diatron-type mass spectrometer (not shown in fig. 1) for determination of gases present in the vacuum system. A 20-foot-long stainless-steel coil of 5/16-inch-diameter tubing was used for liquid-nitrogen and liquid-helium cryopumping of the vacuum system.

In experiments where external heating of the specimens was required, a wire-wound tantalum heater was placed adjacent to the circumferential edge of the disk specimen (fig. 1). A thermocouple was inserted in the rider and the bulk specimen temperature recorded. No attempt was made to record interface temperatures.

The disk and the rider specimens used in friction and wear experiments were finished to a roughness of 4 to 8 microinches. Before each experiment, the disk and the rider were given the same preparatory treatment:

(1) Thorough rinsing with acetone to remove oil and grease

(2) Polishing with moist levigated alumina on a soft polishing cloth

(3) Thorough rinsing with tap water followed by distilled water

For each experiment, a new set of specimens was used.

RESULTS AND DISCUSSION

A number of years ago, when a vacuum apparatus was first constructed for friction and wear studies at the Lewis Research Center, an oil diffusion pump was installed on the apparatus. Numerous friction experiments with this device revealed the presence of contamination on the surface of the specimens. Evidence for surface contamination was detected by the friction values obtained and by a simple water wetting test which has been used for years to detect the presence of hydrocarbon on metal surfaces (ref. 2).

In friction experiments, friction coefficients of 0.2 and less were obtained for bearing steels sliding on themselves in vacuum. Data for 52100 bearing steel are shown in figure 2. Adhesion theory of friction would indicate very high coefficients of friction for such metals. A friction value of 0.2 or less is normally associated with effective boundary lubrication. Even in the presence of nothing more than residual surface oxides, in dry air friction coefficients of 0.5 are obtained for 52100 bearing steel sliding on itself. These friction coefficients would therefore indicate the presence of an organic film on the steel surfaces.

Further, if after cleaning specimens as described in the section APPARATUS AND PROCEDURE a drop of distilled water were placed on the specimen surface prior to sealing the vacuum chamber, it would wet the surface (because of a very low contact angle). After the experiment a drop of water would not wet the specimen surface (because of a high contact angle). This difference served as additional evidence for the presence of surface contamination.

Various devices, including cold traps, baffles, and heating grids, were used in an effort to stop the back-streaming of oil from the diffusion pump to the experimental chamber. Although some of these devices reduced the rate of back streaming, none was effective in stopping it completely. The oil diffusion pump was therefore replaced with an ion pumping system. Friction coefficients obtained with an ion pumped system are also presented in figure 2. The friction coefficient increased from 0.2 to 0.4 for 52100 bearing steel running dry in vacuum merely by changing pumping systems. The total pressure in both systems was approximately the same. Although the friction coefficient was still not what would be anticipated for a clean oxide-free surface, the value obtained with the ion pumped system will be shown to be related to residual oxygen partial pressure present at a total system pressure of 10^{-7} millimeter of mercury. When liquid helium was utilized to aid in pumping the vacuum system, complete welding of 52100 bearing steel was obtained (fig. 2). This welding resulted from a reduction in oxygen partial pressure in the system. These results differ markedly from those obtained with the oil diffusion pumped system.

The first criterion to have evolved from these studies was that the experimental chamber in which friction studies are to be conducted should be free of oil and organic

vapors. Although it may be possible to stop back-streaming from diffusion pumps, attempts with the system reported here were unsuccessful. Further experimental checks on a variety of diffusion pumped systems used at Lewis which are equipped with mass spectrometers have not revealed a system free of contamination.

The results of figure 2 indicated that a quantitative, as well as a qualitative, analysis of the gases present in a vacuum system for friction and lubrication studies was imperative; therefore, a mass spectrometer was installed. A residual gas analysis of the vacuum system shown in figure 1 is presented in figure 3, which indicates the influence of various pumping media and bakeout on the residual gases present. With liquid-helium cryopumping of an ion pumped vacuum system which has been baked out, the only gas detected within the sensitivity of the mass spectrometer was hydrogen (ref. 3). Liquid helium will not pump hydrogen at a total system pressure of 10^{-9} millimeter of mercury because of the high vapor pressure of hydrogen at liquid helium temperatures. Since the principal gaseous species present in outer space are hydrogen and helium, this system makes a useful environment for friction and lubrication studies.

Another factor to be considered is that of system total pressure. At what system pressure can a meaningful friction or lubrication experiment be conducted? A friction experiment was conducted in reference 4 at various ambient pressures with 52100 bearing steel sliding on itself, and the results presented in figure 4 were obtained. At an ambient pressure of 760 millimeters of mercury a friction coefficient of 0.5 was obtained. This friction coefficient reflected the friction characteristic of a film with a predominance of the high-oxygen oxide of iron, Fe_2O_3. When the ambient pressure was decreased, however, less oxygen became available for reaction at the metal to metal interface, and the lower-oxygen oxides of iron, Fe_3O_4 and FeO, became increasingly predominant. These oxides exhibited lower friction characteristics than Fe_2O_3, and as a consequence the friction coefficient decreased. With further decreases in ambient pressure, a point was reached where insufficient oxygen was available to provide a complete-protection oxide film and the friction again began to increase.

When the vacuum system was cryopumped with liquid helium to reduce total pressure and oxygen partial pressure further, the results shown in figure 5 were obtained. At the start of the experiment a relatively low friction coefficient was obtained because of the presence of residual surface oxides. As time progressed, however, this residual oxide was worn away and the friction began to increase markedly and ultimately reached a value of 5.0 with complete welding of the specimens (ref. 4). A photomicrograph of the type of weld obtained is shown in figure 6.

The marked difference in friction behavior for 52100 bearing steel in the presence and absence of surface oxides indicates their extreme importance. In order to gain some insight into the relative stabilities of various metal oxides in vacuum, the thermodynamic stability of various metal oxides at various oxygen partial pressures and temperatures is

plotted in figure 7. For points above the line the oxide is thermodynamically stable, and for those below the line the oxide is unstable. Oxides of metals such as copper and silver are relatively easily dissociated, while those of metals such as chromium are extremely stable.

From the data presented and those of more current investigations an ambient pressure of 10^{-9} millimeter of mercury or lower is believed necessary to obtain meaningful results in friction and lubrication studies. At higher pressures absorbed layers form too rapidly to allow for meaningful measurements to be made.

A problem which can be encountered in lubrication systems operating in a vacuum environment is poor heat dissipation. In air heat dissipation from such mechanical components as bearings, gears, and seals may be by conduction, convection, and radiation; but in vacuum only conduction and radiation operate. The differences in temperature which may be achieved in air and in vacuum are demonstrated by the data of figure 8. In simple sliding friction experiments with electrolytic silver sliding on 440-C stainless steel at various sliding velocities the effect of environment on the resultant temperature can be readily seen.

These results indicate that for such mechanical components as bearings in vacuum larger clearances may be required than when these same bearings are used in air. This potential problem for lubrication systems is extremely critical. It may not always be failure of a lubricant that results in objectional bearing torque but rather the cause may be the simple loss of internal clearance.

An example of the difference in behavior of materials in lubrication systems in air and vacuum may be obtained from a simple friction experiment conducted in vacuum with PTFE. Friction experiments were conducted with unfilled and filled PTFE sliding on 440-C stainless steel in vacuum (10^{-9} mm Hg) at various sliding velocities. The gases liberated from the sliding interface were analyzed with a mass spectrometer, and the data are presented in figures 9 to 11 (data from ref. 5).

In figure 9 increasing sliding velocity (interface temperature) with unfilled PTFE resulted in a decrease in ion concentration for decomposition products. This is the reverse of what would normally be expected. If, however, wear values at two sliding velocities are compared, an increase in wear occurs with an increase in sliding velocity. The PTFE wear particles are considered to carry away some of the heat generated at the sliding interface, which accounts for the decrease in ion concentration of decomposition products.

Similar experiments conducted with a 25-percent-glass-filled PTFE composition gave the results of figure 10. With an increase in sliding velocity (interface temperature) a marked increase in decomposition products occurred. Of particular interest is the increase in fluorine ion concentration. This increase coupled with the presence of carbon on the specimen of PTFE indicated carbon to fluorine bond scission at the sliding

interface. Such effects would not be expected in air since such decomposition products would be expected to react with oxygen from the atmosphere.

When copper metal is substituted for glass in the PTFE, mass spectrometer data such as those of figure 11 are obtained. Heat generated at the sliding interface is conducted to within the bulk of the polymer, and the rate of decomposition of PTFE at this sliding interface is reduced.

CONCLUSIONS

From the vacuum friction and lubrication studies discussed herein the following remarks are made:

1. When friction experiments are desired on nascent or clean metal surfaces, care should be taken to eliminate contaminants such as oil vapor and other hydrocarbons from vacuum systems.

2. Mass spectrometers on vacuum systems are extremely useful in determining the environmental effects on friction experiments.

3. Friction experiments should be conducted at an ambient pressure of 10^{-9} millimeter of mercury or lower.

4. Specimen or component temperatures of lubrication systems in a vacuum environment can be expected to be higher than in the same systems under the same conditions in air.

REFERENCES

1. Atkins, J. H. et al: Effects of Space Environment on Materials, National Research Corp., Ohio State University Research Foundation Project (RF)-920, August 15, 1960. WADD TR 60-721, 1960.

2. Hardy, W. B. Sir,: Collected Scientific Papers, Cambridge University Press, 1936.

3. Buckley, Donald H.; and Johnson, Robert L.: Influence of Microstructural Inclusions on Friction and Wear of Nickel and Iron in Vacuum to 10^{-9} Millimeter of Mercury. NASA TN D-1708, 1963.

4. Buckley, D. H.; Swikert, Max A.; and Johnson, R. L.: Friction, Wear, and Evaporation Rates of Various Materials in Vacuum to 10^{-7} mm Hg. ASLE Transactions, vol. 5, no. 1, April 1962, pp. 8-23.

5. Buckley, Donald H.; and Johnson, Robert L.: Friction, Wear, and Decomposition Mechanisms for Various Polymer Compositions in Vacuum to 10^{-9} Millimeter of Mercury. NASA TN D-2073, 1963.

VACUUM FRICTION AND WEAR APPARATUS

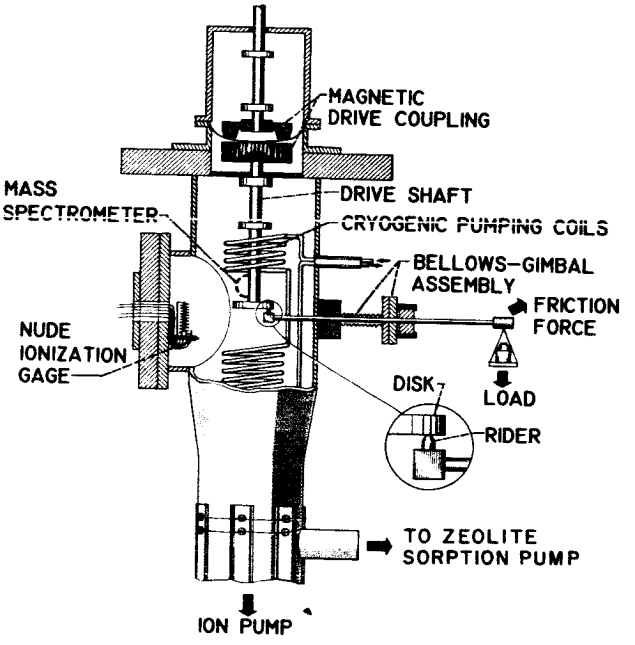

Figure 1

FRICTION FOR 52100 SLIDING ON 52100 IN VARIOUS VACUUM SYSTEMS

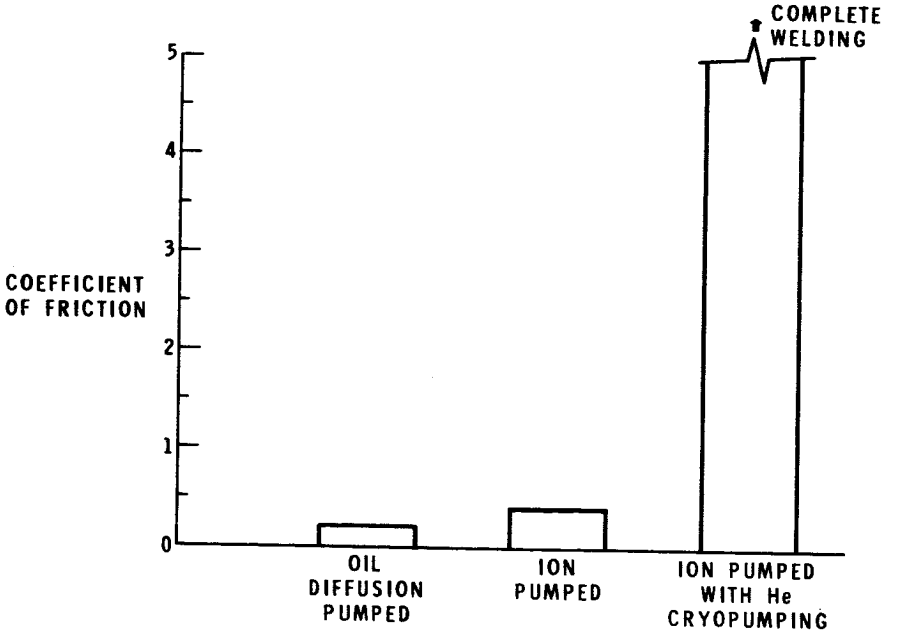

Figure 2

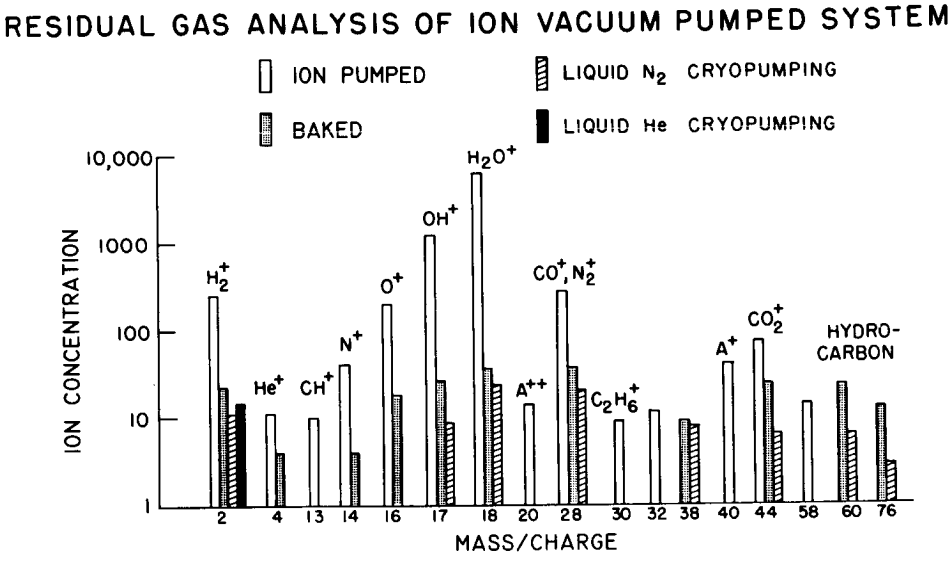

Figure 3

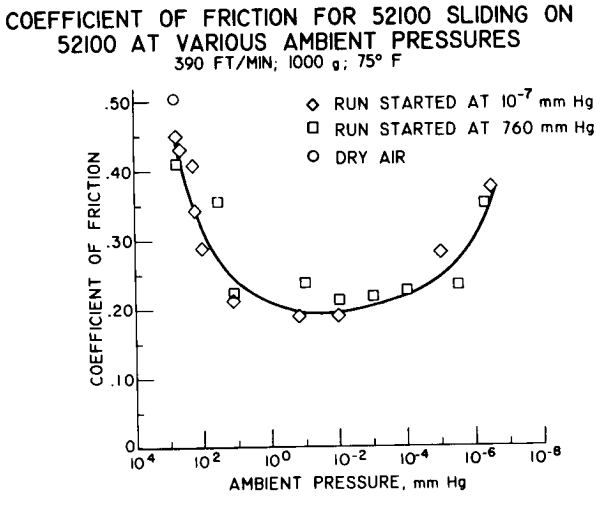

Figure 4

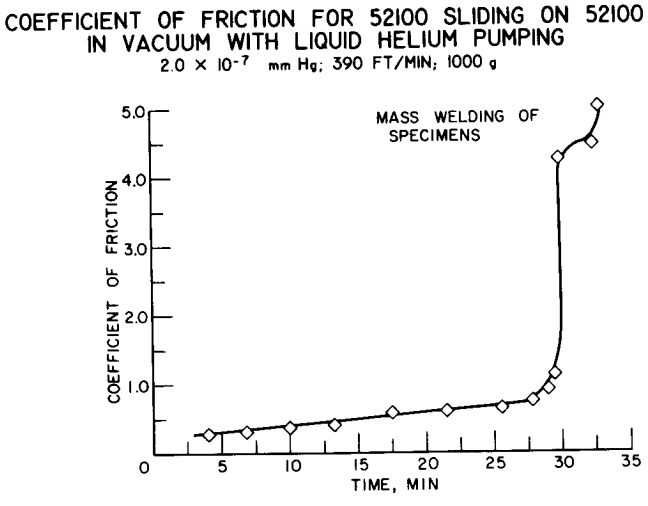

Figure 5

SEVERE SURFACE WELDING RESULTING FROM UNLUBRICATED SLIDING

(2% Al–Ni ALLOY FROM 10^{-9} mm Hg VACUUM EXPERIMENT)

Figure 6

OXYGEN PARTIAL PRESSURE NECESSARY FOR THE DISSOCIATION OF METAL OXIDES AT VARIOUS TEMPERATURES

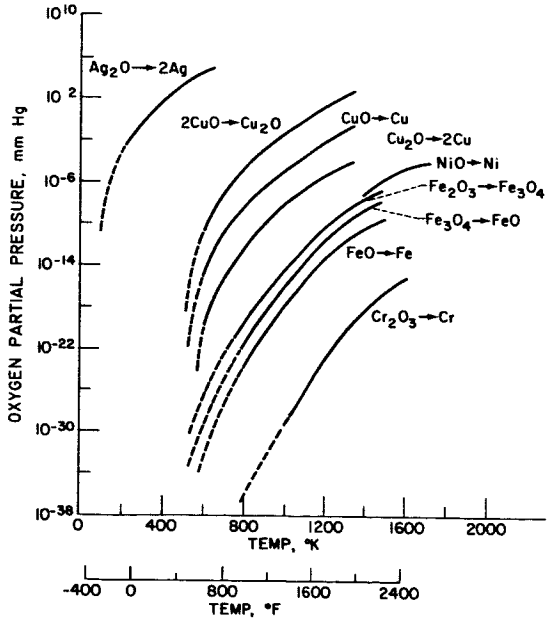

Figure 7

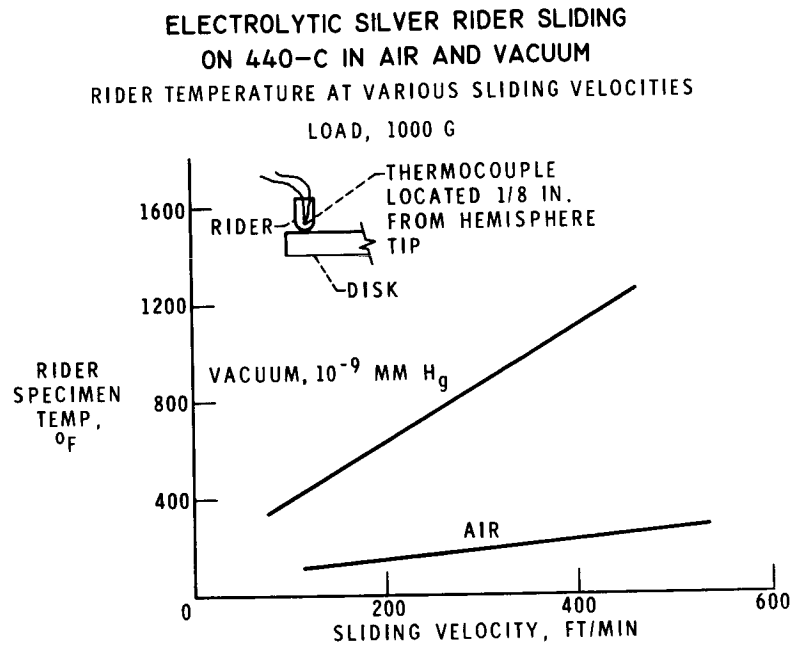

Figure 8

DECOMPOSITION PRODUCTS OF UNFILLED PTFE OBTAINED IN VACUUM FRICTION STUDIES

DISK, 440-C S.S.; 1000 G; 10^{-9} mm Hg; NO EXTERNAL SPECIMEN HEATING

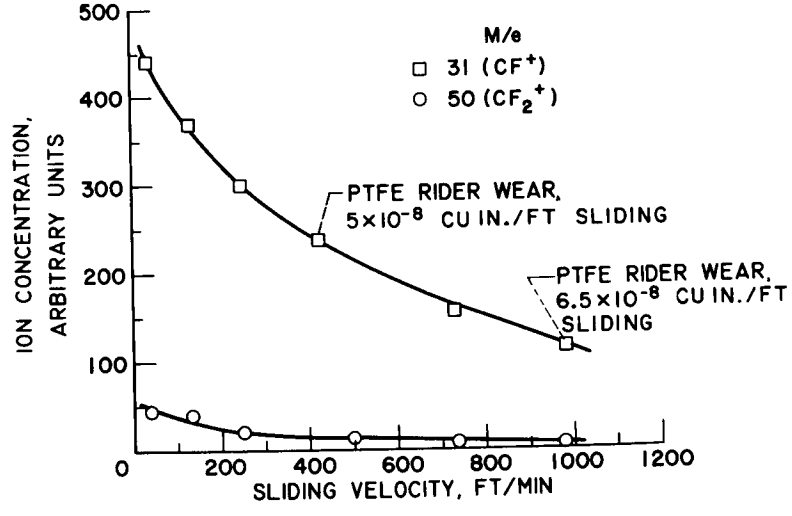

Figure 9

DECOMPOSITION PRODUCTS OF 25% GLASS–FILLED PTFE OBTAINED IN VACUUM FRICTION STUDIES

DISK, 440–C S.S.; 1000 G; 10^{-9} mm Hg; NO EXTERNAL SPECIMEN HEATING

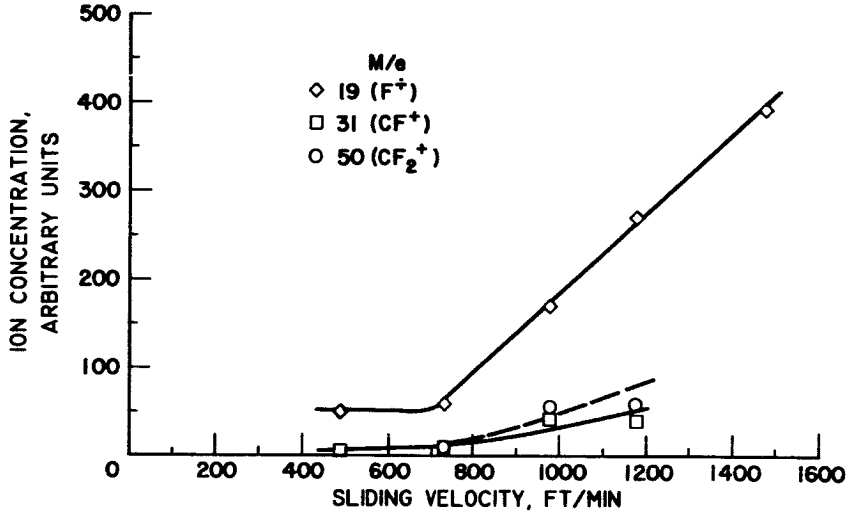

Figure 10

DECOMPOSITION PRODUCTS OF 25% COPPER–FILLED PTFE OBTAINED IN VACUUM FRICTION STUDIES

DISK, 440–C S.S.; 10^{-9} mm Hg; NO EXTERNAL SPECIMEN HEATING

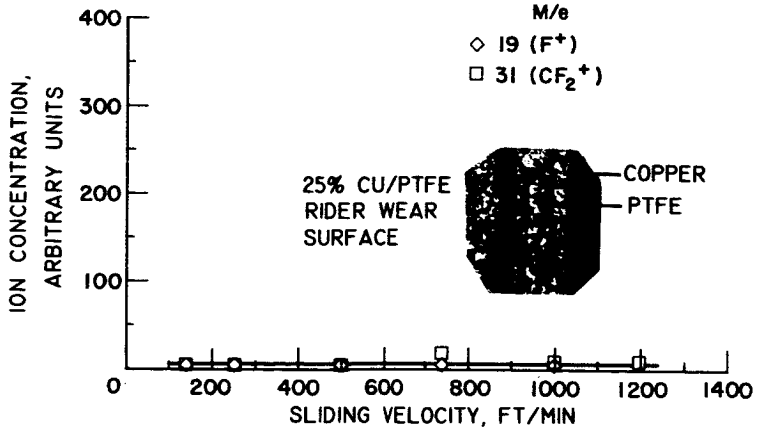

Figure 11

VACUUM REQUIREMENTS FOR HIGH-TEMPERATURE TESTING OF COLUMBIUM ALLOY SYSTEMS AND COMPONENTS

by Charles A. Barrett and Louis Rosenblum

Lewis Research Center

Several years ago, at the start of the Lewis space power system materials program, we became concerned with the effect of contamination of columbium at elevated temperatures in vacuum environments. Since most testing of space power systems would be performed on the ground rather than in space, a definition of environmental requirements was needed.

It is reasonable to assume that contamination of columbium by impurities in the environment involves two processes: (1) contaminants impinging and sticking to an exposed metal surface, and (2) diffusion of contaminants from the metal surface to the interior. Either one of these two processes could be rate controlling, depending on the partial pressure of impurity molecules, the temperature of the metal, and the concentration present in the metal of the particular impurity.[1] If, for example, the diffusion rate of oxygen (the most detrimental contaminant) into columbium is greater than the product of oxygen flux to the surface and the fraction of oxygen molecules sticking to the surface, no detectable surface columbium oxide layer should form. Conversely, when diffusion is rate controlling, a surface oxide layer should form and grow. Therefore, in the latter case, the weight gain of oxygen, essentially as surface oxide, should be proportional to the square root of the exposure time (ref. 1).

Calculations made using the diffusion rates of oxygen in columbium at 1000° C (refs. 2 and 3) indicate that at oxygen partial pressures less than 10^{-5} torr the influx of oxygen molecules that stick to the surface is the rate-controlling step. The oxygen flux that sticks to the surface is given by the Langmuir equation

$$F_L = 0.0583\, P\epsilon \left(\frac{M}{T}\right)^{1/2} \qquad (1)$$

[1] A third rate-controlling process can also be postulated to explain certain experimentally observed phenomena, namely, surface coverage control. Over the range of experimental conditions covered herein, this process is not believed to be significant.

where

F_L oxygen pickup of species, $g/(cm^2)(sec)$

P partial pressure of species, torr

ϵ sticking probability, or pumping efficiency,[2] of metal

M molecular weight of species

T absolute temperature, ^oK

The weight gain rate of the metal due to oxygen pickup $\dot{w}$ must be equal to F_L. Therefore $\dot{w}$ is directly proportional to P and the weight gain w is directly proportional to time.

From the practical aspect of predicting contamination rates, it is important to determine the validity of the above-postulated contamination processes, which specify that

(1) When the oxygen flux that sticks is rate determining, no surface oxide forms, $w \propto t$, and $\dot{w} \propto P$.

(2) When diffusion of oxygen in columbium is rate determining, surface oxide formation occurs, $w \propto t^{1/2}$, and $\dot{w}$ is independent of P.

Further, if process (1) is rate determining, it would be important to determine the pumping efficiency for a typical columbium alloy such as Cb-1Zr that might be used in an advanced space power system.

In 1961 the Lewis Research Center jointly with the General Electric Engineering Laboratory, Schenectady, New York, initiated an experimental program to determine the impurity weight gain as a function of time of Cb-1Zr specimens exposed at 980^o and 1100^o C to impurity gases at partial pressures of 10^{-5} to 10^{-7} torr. The GE Engineering Laboratory exposed the specimens in its high-vacuum facility. The Lewis Center analyzed the specimens chemically and metallurgically before and after exposure and reduced and analyzed the data.

The GE Engineering Laboratory obtained continuous (i.e., instantaneous) contamination rates by means of a novel technique capable of measuring weight changes in the order of 10^{-9} gram per second. Gravimetric methods, long used by experimenters to measure weight changes, are limited to detecting changes in the order of 10^{-6} gram per second.

A photograph and a schematic drawing of the test setup used by the GE Engineering Laboratory are shown in figure 1. The gas species of interest is continuously passed into the system through a controlled leak at the same time as two "pumps" - a diffusion

[2]Pumping efficiency is the preferred term to use here rather than sticking probability since steady-state rather than equilibrium conditions are of concern.

pump and the columbium alloy specimen - are working to remove it from the system. Measuring the difference in pressure between two stations separated by a length of tube of known conductance allows calculation of the pumping rate (i. e., weight gain rate) of the specimen for any set pressure and temperature condition in the sample chamber:

$$\text{Pumping rate} = \Delta P \times \text{Tube conductance} = \dot{w} \tag{2}$$

Of the 30 tests reported here, 8 were run for 236, 2 for 70, 18 for 24, and 2 for 5 hours. As a check on the above method, the specimen weight gain was measured by two additional methods: gravimetric and oxygen fusion analysis. The total weight gain as determined by (1) integrating the instantaneous weight-gain rates (eq. (2)) over the time of the test, (2) the weight gain determined from the difference in weight of the specimen before and after exposure, as well as (3) the weight gain determined by fusion analysis of the specimen before and after exposure were all in good agreement.

When the logarithm of oxygen contamination rate is plotted against the logarithm of oxygen partial pressure (fig. 2) and the logarithm of oxygen weight gain is plotted against the logarithm of time for any test pressure (not shown), the slopes of all the plots are 1, that is, $w \propto t$ and $\dot{w} \propto P$.

No surface oxide layer was detected on specimens exposed at pressures less than 10^{-6} torr. On a specimen run at 980° C and 3×10^{-6} torr, a thin discontinuous patch of black oxide, identified by X-ray diffraction as mainly columbium dioxide, was noted on the surface. Under the conditions of the test a crossover in the rate-controlling process of contamination from flux control to diffusion rate control probably occurred at some late time in the test. Additional credence can be given this conclusion by comparing the calculated time required to reach oxygen saturation at the surface of the specimen with the actual test time. The calculated time to reach oxygen saturation at the surface is 200 hours compared with the test exposure time of 236 hours.

The pumping efficiency ϵ of Cb-1Zr for oxygen, as calculated from the contamination-rate presented herein, has a value of 0. 15 for pressures from 10^{-7} to 10^{-5} torr and for temperatures from 1100° to 980° C. With this value of ϵ plots can be made which yield the exposure time to reach a given contamination level, as shown in figure 3. The exposure time is found at the intersection of the horizontal line - representing a 2000 ppm oxygen contamination level for a 0. 15-inch thickness of Cb-1Zr - and a weight-gain line. For example, an oxygen partial pressure of 1×10^{-7} torr will allow operation up to about 8000 hours before the 2000 ppm oxygen contamination level is exceeded.

Plainly, it is now possible to determine the maximum total oxygen contamination pickup of Cb-1Zr by means of the Langmuir equation and the value of ϵ determined in the experimental program reported herein.

REFERENCES

1. Kubaschewski, O., and Hopkins, B. E.: Oxidation of Metals and Alloys. Butterworths Scientific Publications, London, 1953.

2. Crank, J.: Mathematics of Diffusion. Oxford University Press, 1956.

3. Powers, R. W., and Doyle, Margaret V.: Diffusion of Interstitial Solutes in the Group V Transition Metals. J. Appl. Phys., vol. 30, no. 4, Apr. 1959, pp. 514-524.

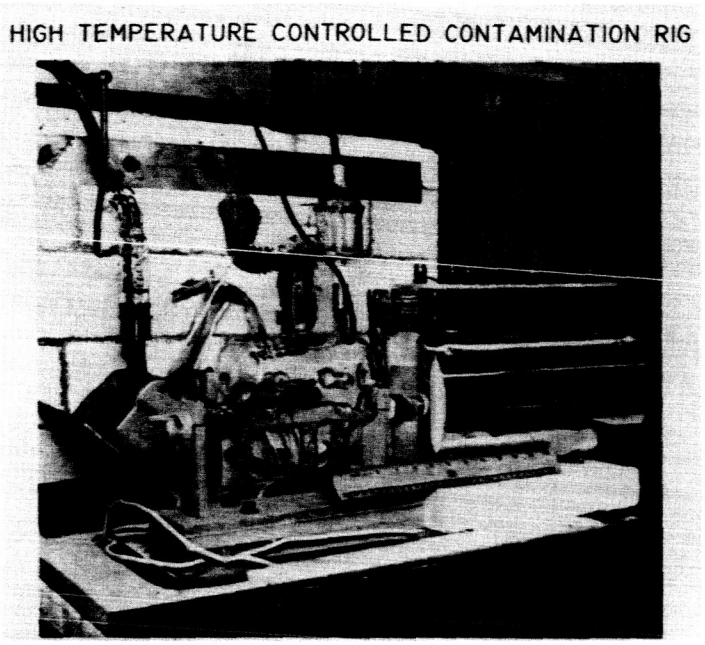

Figure 1. (a) Overall view.

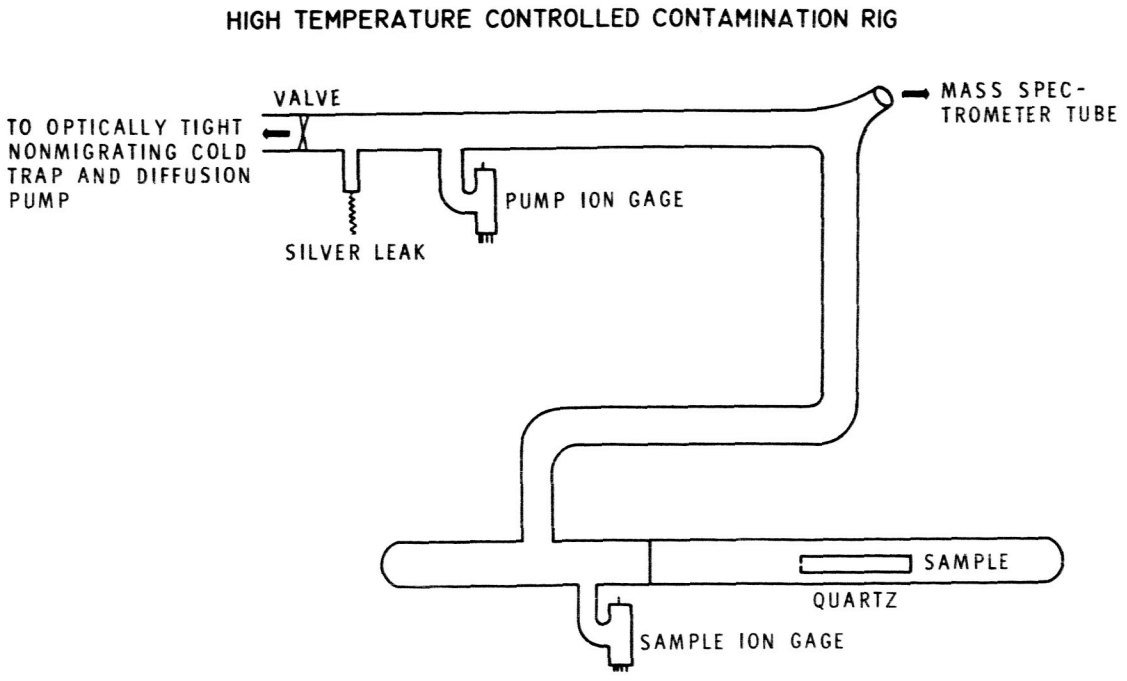

Figure 1. (b) Schematic diagram of system.

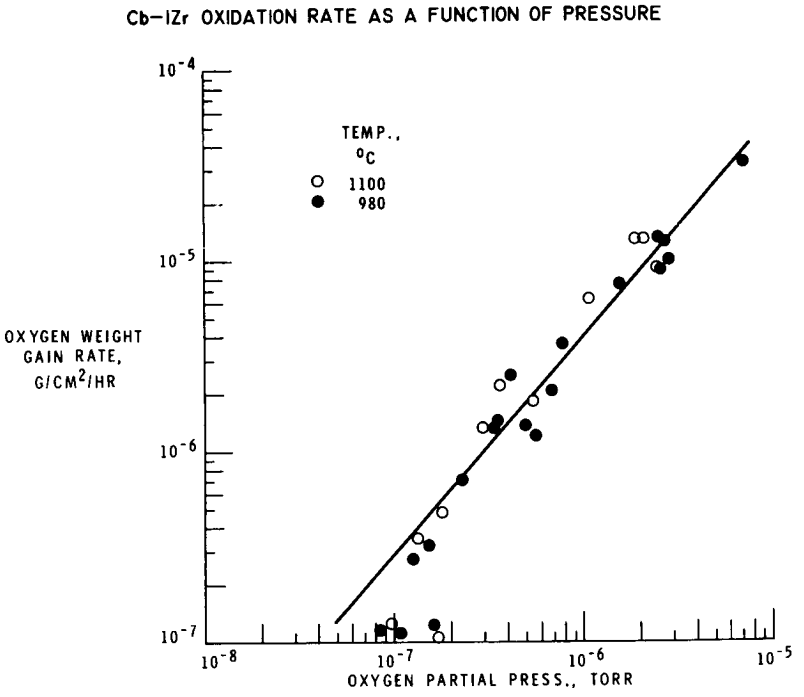

Figure 2

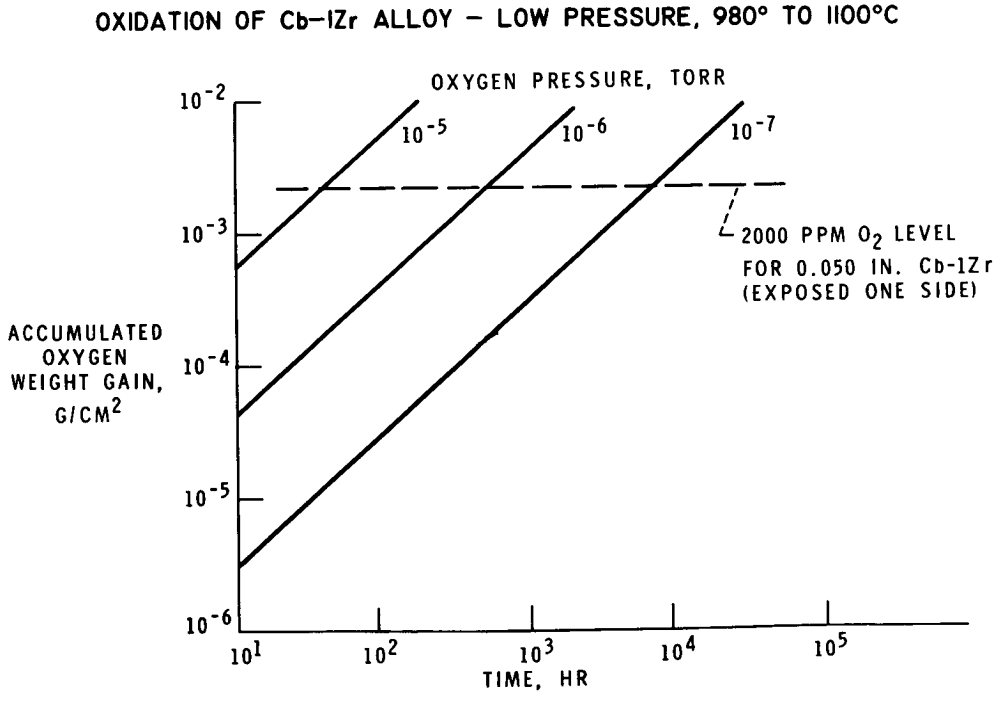

Figure 3

PARTICIPANTS

NASA High-Vacuum Technology, Testing, and Measurement Meeting
June 8-9, 1965
NASA Lewis Research Center
Cleveland, Ohio

Langley Research Center
James M. Bradford
Raymond M. Hansen
John P. Mugler, Jr.
Kaleb D. Osborn
Paul R. Yeager
Victor L. Vaughan, Jr.

Lewis Research Center
Charles A. Barrett
Daniel C. Briehl
Donald H. Buckley
James F. Connors
Ronald J. Cybulski
John Ferrante
Clifford V. Franks
Norman T. Grier
William A. Groesbeck
R. L. Grunes
Raymond Holanda
Arthur D. Holmes
W. W. Hultzman
Thomas A. Keller
Donald G. Kovach
Lloyd N. Krause
Joseph M. Lamberti
Herman Mark
Takuo Mimura
James W. Miser
Charles R. Nichols
Edward W. Otto
Daniel J. Peters
John H. Povolny
Louis Rosenblum
Ralph F. Schmiedlin
Ernest W. Spisz
Richard R. Steiner
Yale E. Strausser
Robert L. Summers
Robert H. Titran
Robert H. Vetrone
Isidore Warshawsky
Rayjor W. Webeler
George Wise

Goddard Space Flight Center
William F. Hardgrove
Russell T. Hollingsworth
George P. Newton
David T. Pelz
Carl A. Reber
Harold Shapiro

Jet Propulsion Laboratory
Roger M. Barnett
James R. Edberg
William R. Howard
James B. Stephens

Ames Research Center
Robert J. Debs
Guy V. Ferry
Jonathan D. Klein

Manned Spacecraft Center
William K. Roberts

Electronics Research Center
George W. Wagner

Marshall Space Flight Center
James O. Ballance
Ilmars Dalins
Jackson C. Horton
William R. Humphries

NASA Headquarters
Mason T. Charak
Edward T. C. Chao
Norman A. Crone
Jay A. Salmanson
John R. Wilhelm
George C. White, Jr.